THE UNIVERSITY OF CHICAGO

SPECIFICITY OF HOMEOSTATIC IGA

A DISSERTATION SUBMITTED TO

THE FACULTY OF THE DIVISION OF THE BIOLOGICAL SCIENCES

AND THE PRITZKER SCHOOL OF MEDICINE

IN CANDIDACY FOR THE DEGREE OF

DOCTOR OF PHILOSOPHY

INTERDISCIPLINARY SCIENTIST TRAINING PROGRAM:

IMMUNOLOGY

BY

JEFFREY J. BUNKER

CHICAGO, ILLINOIS

AUGUST 2018

TABLE OF CONTENTS

LIST OF FIGURES

LIST OF TABLES

ACKNOWLEDGMENTS

The past six years have been a time of tremendous intellectual and personal growth. The experience of completing a PhD is something that cannot be fully understood unless one has completed such a journey. Thus, I am thankful that my naïve interests and ambitions as a young undergraduate who decided to attend the MD/PhD program at the University of Chicago did not lead me astray. In academic research I have found a sense of purpose and a drive that surpasses any endeavor that I have experienced previously. I am fortunate to have had many successes as a graduate student. Some are attributable to chance, others attributable to a careful and broad reading of the literature, and others attributable to hours upon hours of hard work. Naturally, I also experienced many challenges during these years. The uncertainty of science can certainly take a toll on one's psyche from time to time. As I was tediously preparing my 500+ monoclonal antibodies or performing one of thousands of ELISA assays I often wondered whether it would all be worth it in the end. Time will be the judge of my work, but I am proud of what I have accomplished and would make the same choices I made over again in a heartbeat.

Many people have been involved directly or indirectly with the work presented here. Of them, my advisor and mentor Albert Bendelac has played the greatest role. Albert has been a tremendous mentor who has pushed me to realize my full potential. Albert has consistently set a high bar with high expectations, and this has left me feeling that there is always something more to accomplish. Most importantly, he has given me great freedom in taking ownership of my research as well as consistent, frank feedback. He and I found a certain synergy over the years and have often fed off of one another to come up with the next series of experiments. Albert has many qualities that I admire, of which his deep and broad understanding of biology, curiosity,

drive, and brevity are particularly notable. I am thankful that he accepted me into his laboratory and for his major role in fostering my growth as a scientist.

Numerous other faculty, students, and postdoctoral fellows have had a significant impact on my research and education. I am thankful for our longstanding collaboration with Dion Antonopoulos and Ted Flynn at Argonne National Laboratory – they took a chance to collaborate with me as a first year graduate student, and many of my findings would not have been possible without their enthusiastic participation and guidance. I also thank Patrick Wilson and numerous Wilson lab members including Carole Henry, Noel Pauli, Nai-Ying Zheng, and others for their collaborations and for teaching me how to clone monoclonal antibodies from single cells. Bana Jabri has several times facilitated important collaborations and she and members of her lab, particularly Marlies Meisel, have generously shared with me their supply of germ-free mice. I am also thankful for other members of my thesis committee including Alexander Chervonsky and Marcus Clark, who have been generous with their time and feedback. After years of responding to questions and challenges from the University of Chicago faculty, I feel that there is no situation or individual who I cannot stand in front of and explain and defend my ideas.

I am thankful for the many current and past members of the Bendelac lab who I have been with every day, from lab meetings to seminars to friendly discussions about science or life. In particular, I thank Ben McDonald, who generously taught me many skills when I was a young PhD student and served as a model student. Rebecca Mathew and Mike Constantinides both played a role in my early time in the lab, and I thank Rebecca especially for her observations in Cullin 3 knockout mice that led us to start thinking about IgA. I also thank those who I spent

much time with throughout my PhD, including Isabel Ishizuka, Aiping Mao, and Shan Kasal, as well as Steven Erickson, who played a major role in our studies of IgA antibodies reported here.

I am also thankful for many friends and family who have supported me throughout this journey. I thank my parents, Jim and Julie Bunker, for their constant support and for always encouraging me to follow my dreams. I thank my wonderful girlfriend Sofija Canavan for her love and support. Sofija was there for me every day of my journey, and together we have shared countless moments of joy and struggle, journeys around the world, and also many pleasant everyday moments. Sofija is an incredibly thoughtful and loving person, whose presence has brought a joy and inspiration to my life that has certainly been reflected in my professional work. I thank my many friends who have supported me, in particular Nicelio Sanchez-Luege and Ian Roundtree – my fellow MSTP classmates and the best of friends – for our constant banter about anything and everything and our many adventures in Chicago that have been highlights of my time here. I also thank my great friends Michael Stewart, Caleb Pickard, Eldon Summerson, and many others. I thank my Immunology PhD classmates Doug Kline, Toufic Mayassi, Isabel Ishizuka, and Kevin Lei for many hours of stimulating conversation as we learned the field together. I also thank my many MSTP classmates, who have been a source of support and have always been willing to collaborate and share thoughts.

Lastly, I thank the MSTP for giving me the opportunity to train at the University of Chicago. In particular, I thank Marcus Clark, Lucy Godley, Shanetha Thomas, Shay McAllister, Sarah Laloggia, Elise Covic, Alison Anastasio, and Kristin McCann for bringing me here and for supporting me throughout the journey. I have found a home here at the University of Chicago and have met many wonderful people who have supported and challenged me to be the best that I can be. For this, I am forever thankful.

ABSTRACT

A large fraction of the intestinal commensal microbiota is coated with IgA antibodies during homeostatic conditions, but the strategy and the mechanisms deployed to confront this immense diversity of bacterial antigens have remained elusive. Converging studies indicate that homeostatic IgA responses employ a highly polyreactive repertoire to bind broad but distinct subsets of microbiota. These antibody responses develop in the presence of limited T cell help, with low rates of somatic mutations and little affinity maturation. This new perspective contrasts with the classical paradigm of T cell-dependent, high-affinity antibody responses elicited by mucosal pathobionts, pathogens, and vaccines, and provides a simple immunological solution to the challenge of microbiota antigenic complexity. It also raises several fundamental issues, including how polyreactive specificities are generated and selected in the IgA repertoire, how these antibodies exert their effector functions, and how they coexist or overlap with other immune responses during homeostasis and disease.

CHAPTER 1

INTRODUCTION

The gastrointestinal environment presents a tremendous challenge for the immune system. Here, classical mechanisms of tolerance are challenged by the presence of a complex and dynamic mixture of largely innocuous foreign antigens from the diet and commensal microbiota as well as occasional harmful pathogens. As such, a number of unique immunological mechanisms have emerged to serve functions distinct to mucosal tissues (*1*). A homeostatic barrier consisting of mucus, antimicrobial peptides, and immunoglobulin A (IgA) antibodies maintains separation between luminal antigens and the underlying epithelium and serves as a first line of defense against both microbiota and pathogens. IgA antibodies are exceptionally abundant at mucosal surfaces: more than 80% of mammalian antibody-secreting plasma cells (PCs) reside in the gut and express the IgA isotype (*2*). IgA coats the cell surface of a subset of commensal bacteria and is also found free in solution (*3*-*7*). Notably, these antibodies arise prominently during homeostasis, in the absence of inflammation or immunization. Despite its abundance, the specificity, regulation, and functions of IgA in vivo have long remained enigmatic. Recently, significant advances have clarified our understanding of these processes during homeostasis and disease.

Evolution of mucosal antibodies

The IgM isotype is a defining feature of all B cell lineages and is ancient and highly conserved in all jawed vertebrates (*8*). By contrast, IgA arose relatively recently and is present only in reptiles, birds, and mammals. Whereas mice express a single IgA subtype, humans express two subtypes termed IgA1 and IgA2. Although IgA is absent in lower jawed vertebrates, many of these

organisms express specialized mucosal antibody isotypes that have arisen by convergent evolution. Bony fish express IgT in intestinal tissues, and these antibodies coat their gut microbiota (*9*). Amphibians express IgX intestinal antibodies (*10*). Interestingly, mucosal antibodies show a common multimeric structure: whereas IgA is typically dimeric, IgX is pentameric and IgT is tetrameric (*9, 10*). Notably, both IgT^+ and IgX^+ PCs appear to differentiate in the absence of T cell help, similar to a significant fraction of the IgA repertoire in mice and the IgA2 response in humans, as we discuss in detail later (*3, 4, 11, 12*). Together, these observations indicate that strong evolutionary pressure has driven the emergence of specialized mucosal antibodies.

Anatomy and organization of mucosal B cell responses

The largest population of IgA^+ PCs is found in the small intestinal (SI) lamina propria (LP), whereas the colonic LP harbors only a minor population (*4*). High levels of microbiota IgA coating and free IgA are also present in the SI, with lower levels in the colon (*4, 13, 14*). Additional minor populations of IgA^+ plasma cells are detectable in extraintestinal tissues including the salivary gland, lung, lactating mammary gland (LMG), liver, and bone marrow (BM) (*3, 15, 16*). Human IgA subtypes show distinct anatomical expression patterns, with IgA1 dominating in serum and IgA2 in the distal intestine (*12*).

Mucosa-associated lymphoid tissues (MALT) are the primary sites of IgA induction. These include Peyer's patches (PPs), mesenteric lymph nodes (mLNs), isolated lymphoid follicles (ILFs), and the cecal patch (*17-22*). IgA may also be induced in situ in the LP (*23*), and tertiary lymphoid structures have been observed in the LP in response to colonization with particular

commensal bacteria (*24*). Active germinal centers (GCs) are constitutively present in PPs and mLNs; these tissues therefore support both T cell-dependent (TD) and –independent (TI) pathways of IgA PC differentiation (*4, 11*). By contrast, ILFs are largely devoid of T cells and primarily support TI differentiation (*18, 21*). In vivo, there is likely considerable redundancy between these structures. Indeed, ablation of PPs or surgical removal of mLNs individually have little effect on IgA^+ PC abundance (*22, 25*). Mice lacking lymphotoxin signaling or the transcription factor retinoic acid-related orphan receptor γt (RORγt) lack all MALT tissues – these mice show a significant but incomplete reduction in IgA^+ PCs (*21, 26*). These MALT-independent PCs arise in lymphotoxin β-deficient mice via a TD mechanism that requires soluble lymphotoxin α3 expression by type 3 innate lymphoid cells (ILC3) (*27*), though the relevance of this pathway in wild-type (WT) mice remains unknown. Together these observations indicate that, while MALT are not strictly required for IgA PC differentiation, the vast majority of IgA PCs in vivo likely derive from these tissues.

IgA class-switch recombination, homing, maintenance, and secretion

The mechanisms that regulate class-switch recombination (CSR) to the IgA isotype, cellular migration and maintenance, and secretion of IgA antibodies have been extensively studied and reviewed – here, we discuss them only briefly (*28-31*). Naïve B cell precursors expressing IgM and IgD are induced to switch to the IgA isotype by cellular activation in the presence of certain factors that are constitutively present in the gut microenvironment, and the precise signals that direct class-switching differ during TD and TI pathways of activation. In all cases, BCR stimulation is necessary to induce expression of activation-induced cytidine deaminase (AID), which is essential for IgA class switching (*32*). Additional signals through TNF-superfamily

receptors promote CSR: CD40-CD40L interactions with T cells play a key role in TD responses; similar signaling in TI responses is achieved through BAFF/APRIL interactions with three potential receptors including transmembrane activator and calcium-modulating cyclophilin-ligand interactor (TACI), BAFF receptor (BAFFR), and B cell maturation antigen (BCMA) (*28, 33*). Class-switching to the IgA isotype requires induction of transcription in the Cα switch region (S_α), and this generates a substrate for AID activity and subsequent DNA recombination. Transcription at S_α can be initiated by a number of factors present in MALT tissues including transforming growth factor β1 (TGFβ1), IL-4, IL-6, IL-10, and retinoic acid (*28, 34-36*). Of these, TGFβ1 is likely the most important in vivo, although there may be considerable redundancy (*34, 35*). In humans, IgA1 or IgA2 CSR can occur in IgM^+ cells; alternatively, sequential IgA1-to-IgA2 CSR can be initiated in $IgA1^+$ cells (*12*). In vivo, many of the factors that regulate IgA CSR including BAFF and TGFβ1 activators are expressed by MALT follicular dendritic cells (fDCs), plasmacytoid DCs, and conventional DCs (*35, 37, 38*). Notably, the same signals that specify IgA CSR also imprint cells for homing to the intestinal LP by inducing expression of the integrin α4β7 and the chemokine receptors CCR9 and CCR10 (*39, 40*). After cellular activation, IgA CSR, and gut imprinting, lymphoblasts leave the MALT via lymphatics and reenter the bloodstream. Upon circulation through the intestinal vasculature, interactions between α4β7, CCR9, and CCR10 and their ligands mucosal vascular addressin cell adhesion molecule 1 (MAdCAM-1), CCL25, and CCL27 and CCL28, respectively, direct migration into the intestinal LP.

Murine SI IgA^+ PCs have an average half-life of 5 days and a maximum lifespan of 7-8 weeks (*41*). The IgA^+ PC population is heterogenous and contains both short-lived major

histocompatibility complex class II^{+} (MHCII^{+}) cells and longer-lived MHCII^{-} cells (*42*); some exceptionally long-lived PCs have been identified in humans (*43*). However, the factors that regulate intestinal PC maintenance and turnover are only partially understood. Interleukin-6 (IL-6) produced by intestinal epithelial cells and eosinophils contributes to PC maintenance (*44-46*). B cell activating factor (BAFF) and a proliferation-inducing ligand (APRIL) produced by eosinophils, dendritic cells (DCs), and plasmacytoid DCs similarly promote PC survival (*38, 44, 47*); additional unidentified factors are also likely to contribute. Notably, most intestinal PCs express B cell receptors (BCRs) on their cell surface (*48*), though it remains unknown whether PCs can signal or internalize antigen through their BCRs, and the role of surface BCR expression in PC maintenance remains unclear.

A key pathway for IgA secretion at mucosal surfaces involves the polymeric Ig receptor (pIgR) (*29, 30*). IgA in mucosal secretions predominantly exists as a dimer connected by a small polypetide called J chain, although monomers are also detectable (*49, 50*). pIgR is expressed on the basolateral surface of intestinal epithelial cells and binds selectively to polymeric IgA and IgM. Upon binding, antibodies are internalized and transported by transcytosis to the apical surface of the epithelial cell, where proteolytic cleavage releases the antibody bound to a highly glycosylated 80 kDa fragment of pIgR known as secretory component (SC). The complex of dimeric IgA, J chain, and SC is sometimes referred to as secretory IgA (sIgA). In numerous studies, pIgR-deficient mice have been used as models of sIgA-deficiency. However, analyses of these mice indicate only a 2-3-fold defect in SI IgA titers, a 5-10-fold decrease in fecal IgA, and no defect in breast milk IgA (*51, 52*). These data suggest that alternative pathways such as

paracellular transport can compensate for the loss of pIgR and may also contribute to steady-state IgA secretion (*53*).

Specificity of IgA

Despite decades of research, the specificity of homeostatic IgA antibodies has remained poorly understood. As I began my thesis research, we knew very little of what these antibodies might be targeting. What fraction of these antibodies are specific for microbiota, dietary antigens, or other intestinal antigens? Of those that bind microbiota, which microbial taxa are targeted? What are the immunological mechanisms that regulate these IgA responses? What are the molecular targets of IgA antibodies? In the subsequent chapters our published and unpublished work sheds light on these questions. A discussion then follows, which summarizes our findings and considers them in the context of the broader literature.

CHAPTER 2

INNATE AND ADAPTIVE HUMORAL RESPONSES COAT DISTINCT COMMENSAL BACTERIA WITH IMMUNOGLOBULIN A

Jeffrey J. Bunker[1,2], Theodore M. Flynn[3,4], Jason C. Koval[3], Dustin G. Shaw[5], Marlies Meisel[1,5], Benjamin D. McDonald[1,2], Isabel E. Ishizuka[1,2], Alexander L. Dent[6], Patrick C. Wilson[1,5], Bana Jabri[1,5], Dionysios A. Antonopoulos[3,4,5,7], and Albert Bendelac[1,2]

[1]Committee on Immunology, University of Chicago, Chicago, IL 60637, USA, [2]Department of Pathology, University of Chicago, Chicago, IL 60637, USA, [3]Biosciences Division, Argonne National Laboratory, Argonne, IL 60439, USA, [4]Computation Institute, University of Chicago, Chicago, IL 60637, USA, [5]Department of Medicine, University of Chicago, Chicago, IL 60637, USA, [6]Department of Microbiology and Immunology, Indiana University School of Medicine, Indianapolis, IN 46202, USA, [7]Institute for Genomics and Systems Biology, University of Chicago, Chicago, IL 60637, USA.

Contact: Albert Bendelac: abendela@bsd.uchicago.edu

Immunity. 2015 Sep 15;43(3):541-53. doi: 10.1016/j.immuni.2015.08.007.

SUMMARY

Immunoglobulin A (IgA) is prominently secreted at mucosal surfaces and coats a fraction of the intestinal microbiota. However, the commensal bacteria bound by IgA are poorly characterized and the type of humoral immunity they elicit remains elusive. We used bacterial flow cytometry coupled with 16S rRNA gene sequencing (IgA-Seq) in murine models of immunodeficiency to identify IgA-bound bacteria and elucidate mechanisms of commensal IgA targeting. We found that residence in the small intestine, rather than bacterial identity, dictated induction of specific IgA. Most commensals elicited strong T-independent (TI) responses that originated from the orphan B1b lineage and from B2 cells, but excluded natural antibacterial B1a specificities. Atypical commensals including segmented filamentous bacteria and *Mucispirillum* evaded TI responses but elicited T-dependent IgA. These data demonstrate exquisite targeting of distinct commensal bacteria by multiple layers of humoral immunity and reveal a specialized function of the B1b lineage in TI mucosal IgA responses.

INTRODUCTION

Host-commensal symbiosis is mediated at mucosal surfaces by secreted host-derived factors including mucus, antimicrobial peptides, and immunoglobulin A (IgA) (*54*). Mammals invest significant resources into IgA production: more than 80% of all human plasma cells secrete IgA and reside in the intestinal lamina propria. IgA can mediate protective immunity to enteric pathogens including viruses, bacteria, and toxins (*54*). However, IgA also contributes to intestinal homeostasis. Mice and humans with defective IgA secretion show increased susceptibility to inflammatory bowel disease, celiac disease, and allergy (*55, 56*). IgA may regulate commensal community composition, gene expression, and motility, which in turn influence host epithelial physiology and innate immunity (*5, 32, 57, 58*). Notably, IgA coating of commensal bacteria can be detected by flow cytometric and microscopic analysis of fecal samples from healthy mice and humans (*6, 7, 13, 14, 59, 60*). However, the commensal bacteria bound by IgA are poorly characterized and the mechanisms by which they induce specific IgA are unclear.

Mucosal IgA^+ plasma cells can be generated by both T-dependent (TD) and T-independent (TI) mechanisms. However, the relative contributions of each pathway remain unclear. TD responses are typically directed against protein antigens and occur in gut-associated lymphoid tissues including Peyer's patches (PPs) and mesenteric lymph nodes (mLNs), where germinal centers (GCs) are constitutively active. TD responses require signals from $CD4^+$ T follicular helper (Tfh) cells that direct the selection and differentiation of high affinity GC B cells into long-lived plasma cells. In contrast, TI responses may occur both in organized lymphoid tissues and in non-lymphoid tissues (*21, 38*). In both TD and TI pathways, factors in the intestinal microenvironment such as transforming growth factor β (TGF-β), interleukin 10

(IL-10), and retinoic acid direct class switch recombination to the IgA isotype (*54*). TI IgA responses may produce primarily 'natural,' polyreactive specificities with low affinity for commensal bacteria (*54, 61-63*), but have been demonstrated against a limited number of commensal model antigens (*11*). Thus, although protective immune responses to many enteric pathogens are TD (*54*), it is unclear whether IgA coating of commensal bacteria is more dependent on TD or TI responses.

While TI antigens can stimulate circulating follicular B2 B cells, they can also activate innate B1 B cells that reside primarily in the peritoneal cavity (*64*). In contrast, TD responses are thought to predominantly involve B2 B cells. Both B1 and B2 B cells can differentiate into intestinal IgA^+ plasma cells, although the relative contributions of these lineages remain controversial (*11, 65, 66*). Two subsets of B1 B cells, B1a and B1b, are present in the peritoneal cavity. Although limited data suggest differential capacity of B1a and B1b to undergo IgA class switch recombination (*67*), it is not known whether both subsets coat commensal bacteria *in vivo*. Peritoneal B1a secrete 'natural' antibodies that react with conserved microbial antigens and have been hypothesized to contribute to control of the microbiota (*54, 65*). In contrast, very little is known about the role of B1b except that they can generate protective TI responses against *Borrelia hermsii* and *Salmonella typhimurium* outer membrane proteins and *Streptococcus pneumoniae* capsular polysaccharides after systemic infection (*68-70*).

To characterize the commensal bacterial targets of IgA, we utilized bacterial flow cytometry coupled with 16S rRNA gene sequencing (IgA-Seq) (*5, 6, 59*). We found that IgA coated many but not all commensals in the homeostatic state and that dramatic differences were associated with bacterial localization along the gastrointestinal tract. Using murine genetic models of immunodeficiency, we found that most IgA-bound taxa were specifically targeted by

TI IgA. We further demonstrated that natural antibacterial B1a specificities did not contribute to IgA coating. In contrast, innate B1b - a phenotypically related but poorly understood, "orphan" lineage - and adaptive B2 B cells each contributed diverse commensal-reactive specificities. Finally, we identified an atypical subset of commensals that evaded TI responses but elicited TD IgA. Together, these data indicate that multiple layers of humoral immunity are elicited by distinct commensal bacteria in the small intestine and reveal a novel specialization for the B1b lineage in mucosal TI responses.

RESULTS

Distinct regulation of IgA synthesis in the small intestine and colon of mice and humans

To study the commensal bacteria targeted by IgA under homeostatic conditions, we established a flow cytometric assay to visualize IgA-bound (IgA^+) bacteria in murine feces. We found that approximately 20% of bacteria were IgA^+ in the feces of wild-type (WT) C57BL/6 mice and verified that this staining was specific and absent from *Rag2*$^{-/-}\gamma_c^{-/-}$ and *Aicda*$^{-/-}$ feces (Figure 1A), as reported previously (*5-7, 13, 14, 59, 60*). While the frequency of IgA^+ bacteria in the colon was relatively constant, we found substantial differences along the gastrointestinal tract. IgA coated a significantly greater fraction of bacteria in the small intestine than the colon (40-80% IgA^+ vs 10-30% IgA^+; Figure 1B), as reported previously (*13, 14*). This correlated with significantly higher titers of luminal free IgA in the small intestine (Figure 1B) and 10-15 fold more IgA^+ plasma cells in the small intestinal lamina propria relative to the colonic lamina propria (Figure 1B). Similar trends were apparent in WT BALB/c and C3H mice (data not shown). We also observed a higher frequency of IgA^+ bacteria in small intestinal aspirates of

healthy humans relative to colonic aspirates (Figure 1C). These data suggest that IgA responses against commensal bacteria are most prominent in the small intestine.

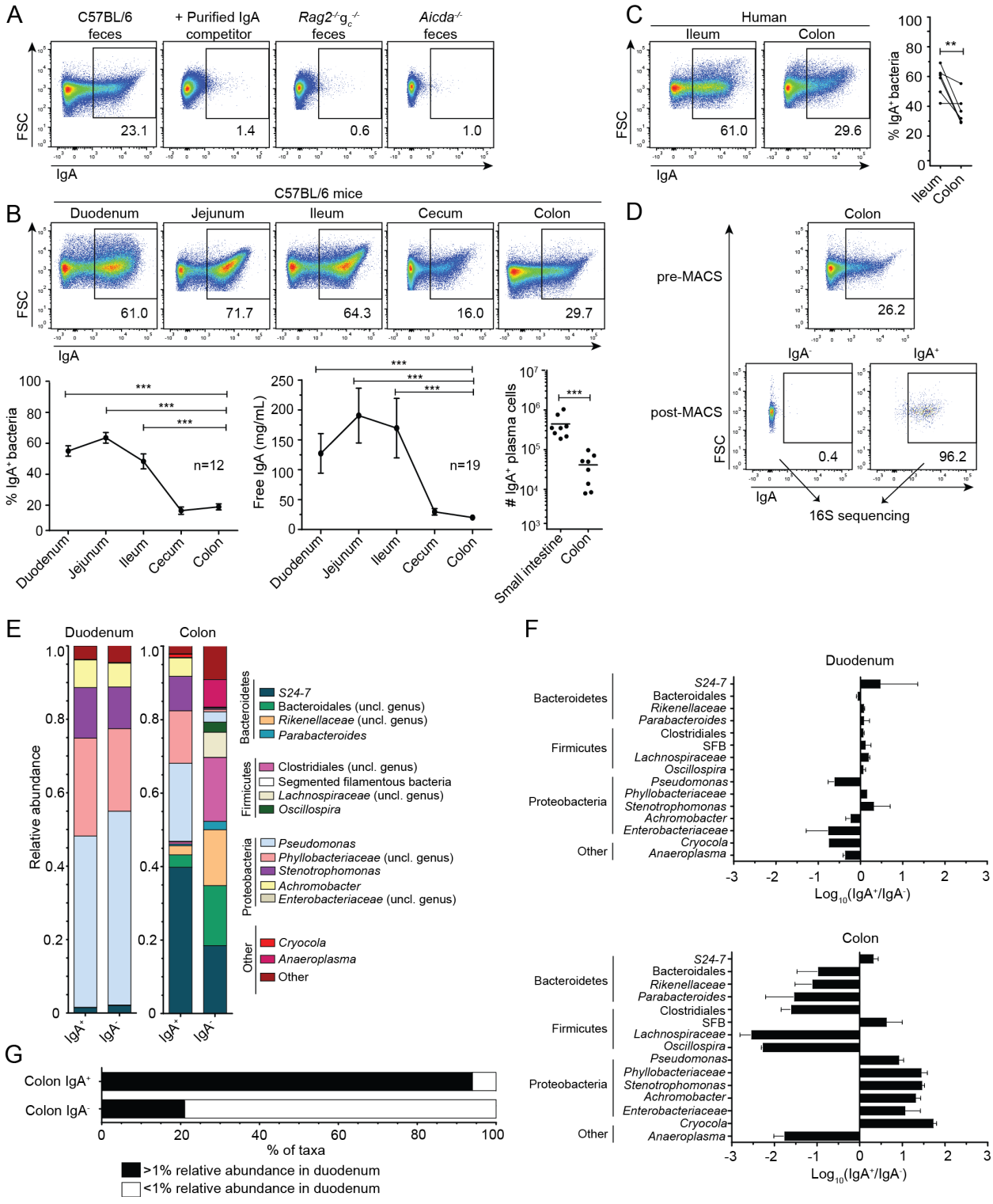

Figure 1. IgA responses predominantly target commensal bacteria of the small intestine. (A) Representative staining of C57BL/6 feces and negative controls showing staining in the presence of excess purified IgA and of *Rag2*$^{-/-}$*Il2rg*$^{-/-}$ mice lacking B cells or *Aicda*$^{-/-}$ mice lacking IgA. All bacterial flow cytometry plots were gated FSC^{+}SSC^{+}SYTO BC^{+}DAPI^{-}.

Figure 1, continued. (B) Representative staining and quantification of IgA^+ bacteria measured by flow cytometry (n=12) or free IgA measured by ELISA (n=19) or absolute numbers of IgA^+ plasma cells. Data compiled from five independent experiments. (C) Staining and quantification of IgA^+ bacteria in ileal or colonic aspirates from healthy humans. Lines connect samples from the same patient (n=6). (D) Representative pre- and post-MACS purity analysis of IgA^+ and IgA^- fractions. (E) Average relative abundance of taxa in indicated fractions as assessed by 16S sequencing. Duodenal and colonic samples were taken from the same mice, n=3. (F) Log_{10} relative abundance of each taxa in the IgA^+ divided by relative abundance in IgA^- from panel (E). (G) Quantification of average % of colonic IgA^+ or IgA^- taxa found at >1% relative abundance in the duodenum (black) or found at <1% relative abundance in the duodenum (white) in panel (E).

IgA predominantly targets commensal bacteria of the small intestine

To identify commensal bacteria targeted by IgA, we fractionated samples into highly pure IgA^+ and IgA^- fractions by stringent magnetic purification with an autoMACS separator (Figure 1D), and classified bacteria present in each fraction by IgA-Seq. We found that colonic bacteria markedly segregated into IgA^+ and IgA^- taxa (Figure 1E, F), as recently reported (*6, 59*). Numerous taxa were heavily enriched in the colonic IgA^+ fraction, suggesting specific targeting by IgA (Figure 1F). Conversely, numerous colonic taxa were not targeted by IgA and were instead enriched in the IgA^- fraction (Figure 1E, F). These trends were also apparent in human colonic samples (Figure 2). In stark contrast to the colon, duodenal bacteria did not segregate into IgA^+ and IgA^- taxa (Figure 1E, F). Instead, most duodenal taxa were found equally represented in both fractions. These data, as well as the high frequency of IgA^+ bacteria in the duodenum (Figure 1B), suggest that most duodenal commensals elicit specific IgA whereas many colonic commensals do not.

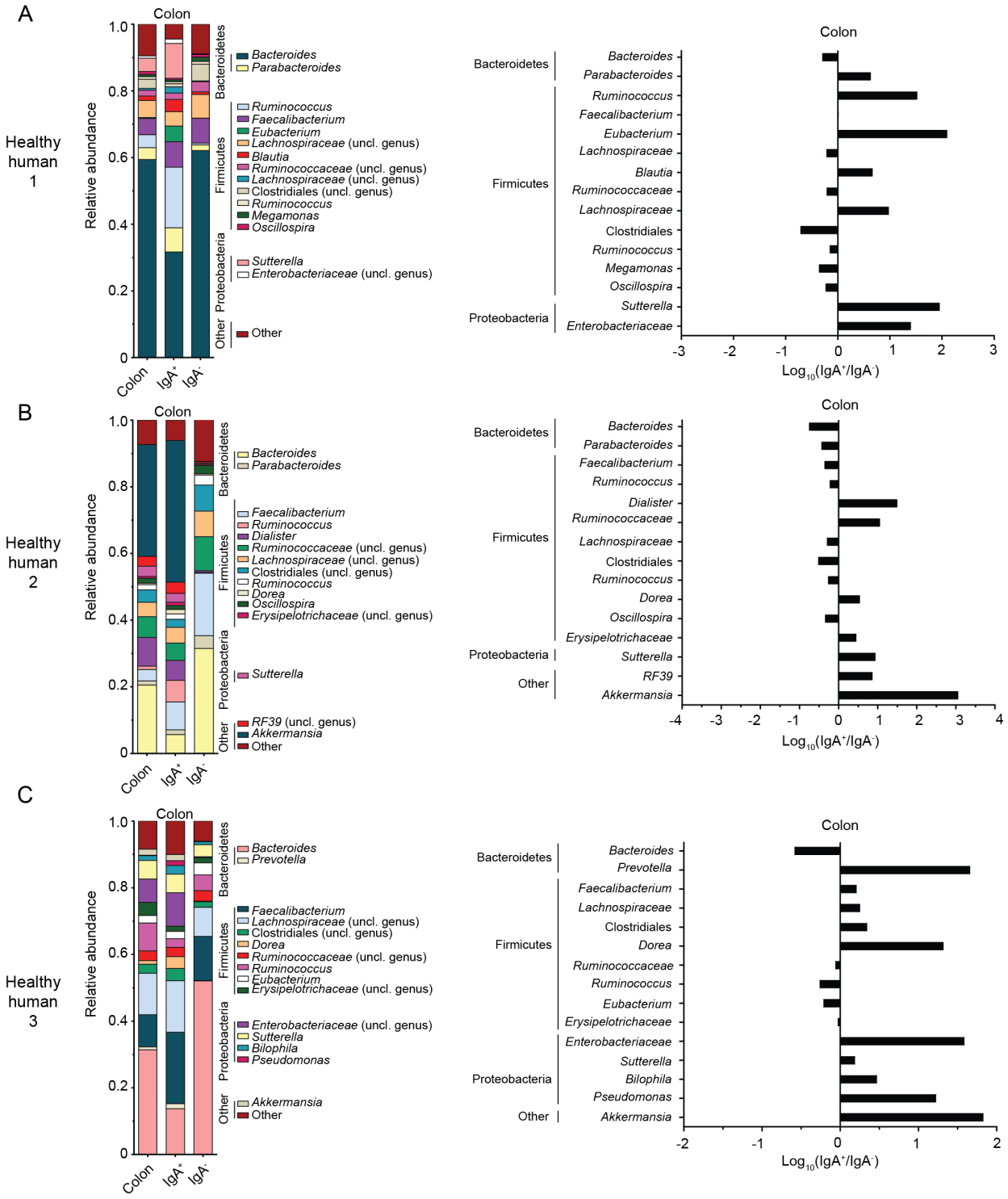

Figure 2. Colonic bacteria segregate into IgA$^+$ and IgA$^-$ fractions in healthy humans. (A-C) Relative abundance and Log_{10}(Relative abundance IgA$^+$/IgA$^-$) for indicated taxa recovered from healthy human donors. Each plot is representative of a single individual.

We reasoned that segregation of colonic bacteria into IgA^+ and IgA^- taxa could be explained if 1) Most bacteria indigenous to the colon were not targeted by IgA; and 2) Colonic IgA^+ bacteria also reside in the small intestine. In support of this, we found that the colonic IgA^+ fraction closely resembled the duodenal community whereas the colonic IgA^- fraction was mostly composed of taxa indigenous to the colon (Figure 1E). In total, more than 90% of colonic IgA^+ bacteria were present at >1% relative abundance in the duodenum (Figure 1G). A member of Bacteroidetes, *S24-7*, was the only taxon found appreciably in the colonic IgA^- fraction and at >1% relative abundance in the duodenum, but this taxon was also found enriched in the IgA^+ fraction in both locations (Figure 1E-G). Thus, nearly all colonic IgA^+ taxa were also abundant in the small intestine whereas most IgA^- taxa were abundant only in the colon.

To assess whether colonic IgA^+ bacteria could establish residence in the small intestine, we colonized germ free mice with either IgA^+ or IgA^- colonic fractions and analyzed small intestinal and colonic communities 28 days later. Consistent with origins in the small intestine, colonic IgA^+ bacteria stably colonized the jejunum of germ free mice and gave rise to a community that closely resembled the input community (Figure 3A). In contrast, the colonic community of these mice did not resemble the input community, likely representing outgrowth of minor contaminants in the input fraction (Figure 1D). Beta diversity-based analysis of bacterial communities further verified that small intestinal communities of recipient mice were more similar to the IgA^+ input than colonic communities (Figure 3B). Mice colonized with a colonic IgA^- inoculum showed an opposite pattern: IgA^- bacteria stably colonized the colon and gave rise to a colonic community that resembled the IgA^- inoculum (Figure 3A). In contrast, the small intestinal communities of these mice did not resemble the inoculum. Beta diversity-based analysis verified that colonic communities were more similar to the IgA^- inoculum than small

intestinal communities (Figure 3B). These data support the hypothesis that colonic IgA$^+$ bacteria also reside in the small intestine whereas colonic IgA$^-$ bacteria are indigenous to the colon.

In summary, we conclude that IgA predominantly targets small intestinal commensals and that most small intestinal bacteria elicit specific IgA. In contrast, bacteria found primarily in the colon are not major targets of IgA.

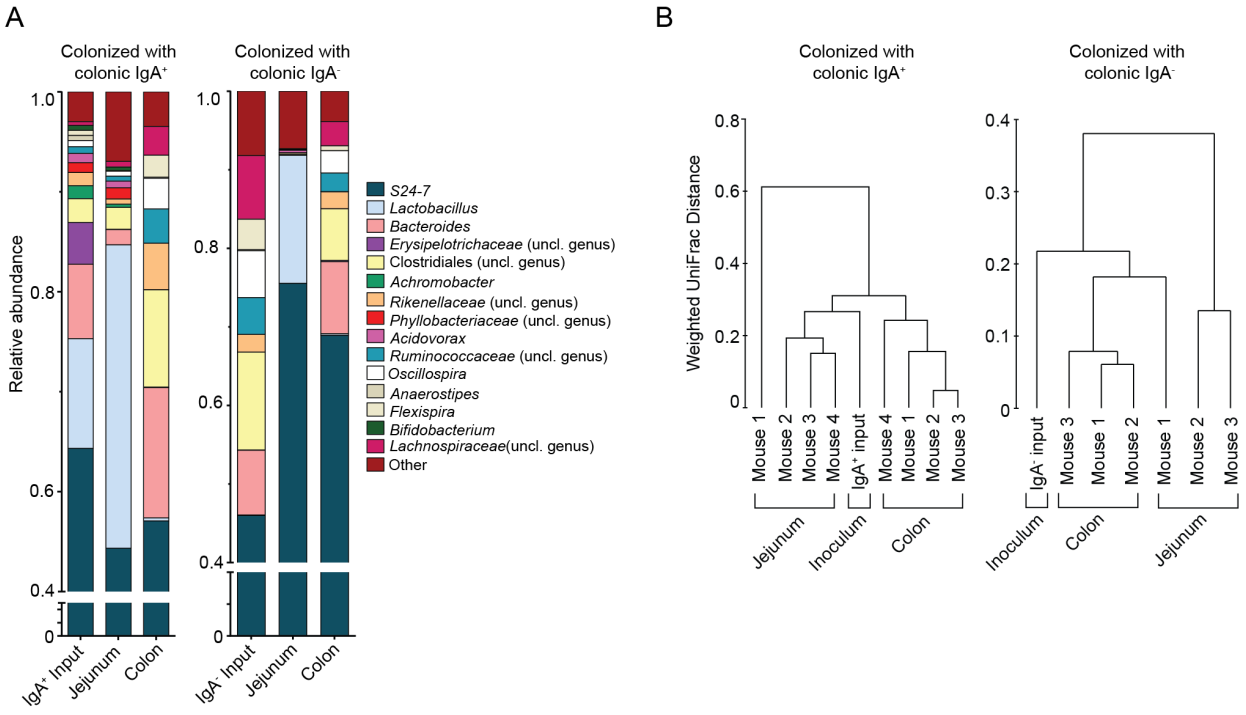

Figure 3. Colonic IgA$^+$ and IgA$^-$ bacteria differentially colonize the small intestine or colon. (A) Average relative abundance of indicated taxa in the jejunum or colon of germ free mice colonized with IgA$^+$ colonic bacteria (n=4) or mice colonized with IgA$^-$ colonic bacteria (n=3). Input fractions used to colonize recipient germ-free mice were from WT B6 mice. Recipients of IgA$^+$ or IgA$^-$ inocula were housed in separate gnotobiotic isolators and mice were analyzed 28 days after colonization. (B) Beta diversity analysis comparing intestinal microbial communities of mice colonized with IgA$^+$ colonic bacteria or IgA$^-$ colonic bacteria indicate similarity between samples shown in (A). Branch length is scaled to the weighted UniFrac distance.

T-independent and T-dependent IgAs coat distinct commensal bacteria

Commensal-specific IgAs have been posited to be largely TD (*6, 61, 63*). However, the specificity of TD IgA remains poorly understood and it is not clear whether GC reactions target all IgA^+ commensals or only a subset. Although mucosal GCs depend in part on signals from the microbiota (*63, 71*), we detected GC B cells, Tfh cells, and IgA in germ-free mice, suggesting that non-microbial antigens such as dietary antigens may also stimulate TD responses (data not shown). Seminal work by Macpherson and colleagues demonstrated that TI IgA could react with model antigens expressed by *E. coli* or with lysates from the model culturable commensal *Enterobacter cloacae* (*11*). However, it is unclear whether most commensal bacteria elicit TI responses *in vivo* and the commensals targeted by TI specificities have not been characterized.

To determine whether TI IgA is sufficient to coat commensal bacteria, we examined IgA responses in $Tcrb^{-/-}d^{-/-}$ mice and $Tcrb^{+/-}d^{+/-}$ littermate controls. $Tcrb^{-/-}d^{-/-}$ mice lack all αβ and γδ T cells and thus cannot mount TD antibody responses (*11*). $Tcrb^{-/-}d^{-/-}$ mice did not form GCs in mLNs and PPs but had normal numbers of $B220^+$ IgA^+ class-switched B cells (Figure 4A, B), as previously reported (*38, 71*). Despite this, small intestinal and colonic lamina propria $B220^-IgA^+$ plasma cells were reduced 10-fold in $Tcrb^{-/-}d^{-/-}$ mice (Figure 4C), consistent with previous reports (*11*). $Tcrb^{-/-}d^{-/-}$ IgA^+ small intestinal plasma cells displayed a mixed surface IgA^{hi} and IgA^{lo} phenotype while WT cells were largely IgA^{low}; colonic IgA^+ plasma cells were IgA^{hi} in both $Tcrb^{-/-}d^{-/-}$ mice and controls (Figure 4C). Surprisingly, we observed substantial commensal IgA coating in $Tcrb^{-/-}d^{-/-}$ mice (Figure 4D). Indeed, IgA^+ bacteria were found at identical frequencies to co-housed littermate controls and no appreciable differences in IgA staining intensity were apparent (Figure 4D). These observations suggest that TI IgA may account for most commensal bacterial coating.

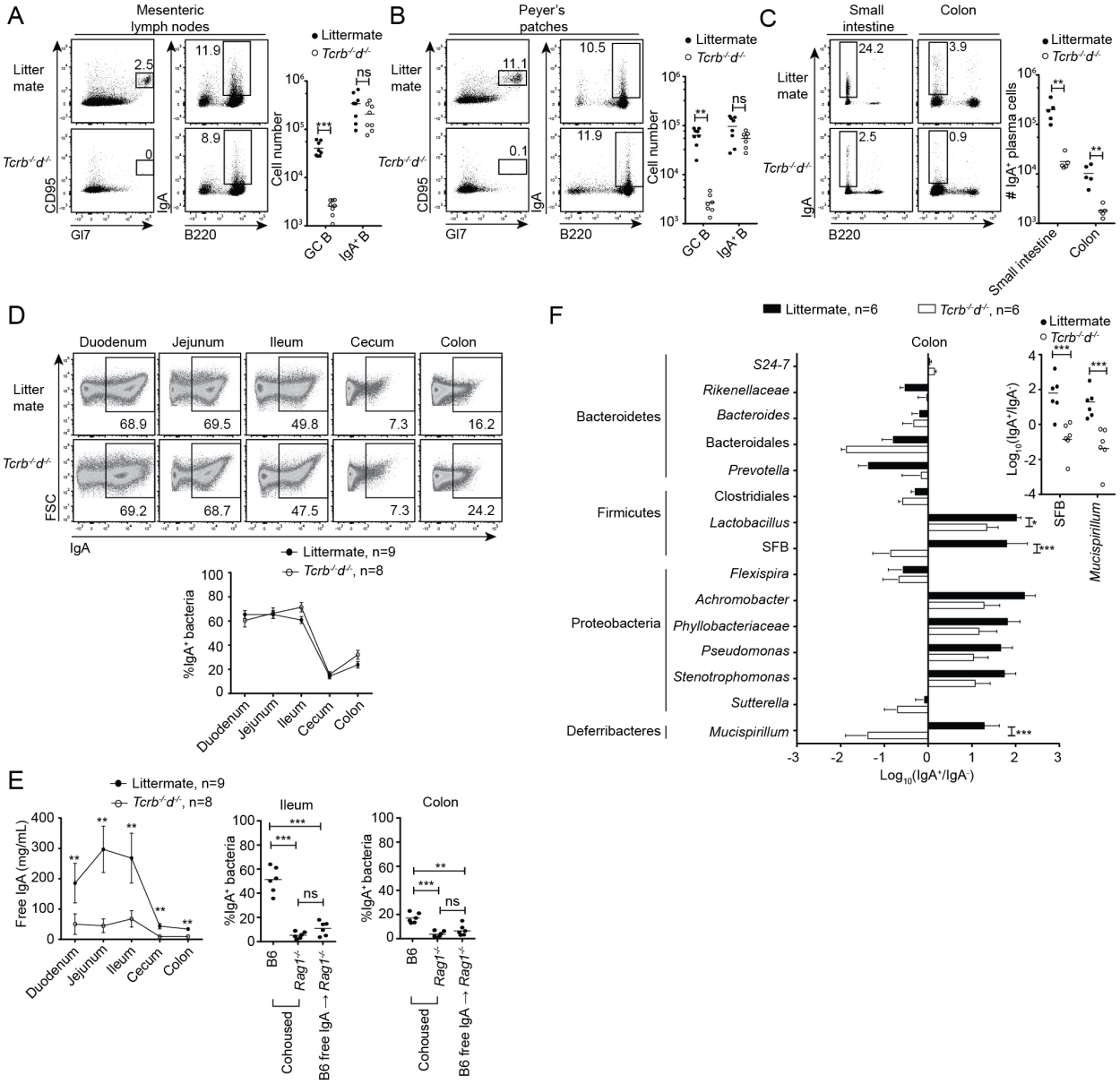

Figure 4. T-independent and T-dependent IgAs coat distinct commensal bacteria. (A) Representative staining and absolute numbers of indicated populations in the mLN, (B) PP, or (C) small intestinal and colonic lamina propria of *Tcrb*$^{-/-}$*d*$^{-/-}$ mice or *Tcrb*$^{+/-}$*d*$^{+/-}$ littermate controls. CD95 by Gl7 plots were gated CD19^{+}. B220 by IgA plots were gated Tcrb^{-}CD3^{-} in the mLN and PP and Lin^{-} (CD3, Tcrb, CD4, CD11c, NK1.1, F4/80) in the intestinal lamina propria. Data compiled from three independent experiments. (D) Representative staining and quantification of IgA^{+} bacteria in *Tcrb*$^{-/-}$*d*$^{-/-}$ mice (n=8) and littermate controls (n=9). Data compiled from four independent experiments. (E) (Left panel) Free IgA in *Tcrb*$^{-/-}$*d*$^{-/-}$ mice (n=8) and littermate controls (n=9) or (Right panels) Endogenous IgA coating in the ileum or colon of co-housed B6 and *Rag1*$^{-/-}$ mice and staining of *Rag1*$^{-/-}$ bacteria with B6 free IgA, as indicated.

Figure 4, continued. (F) Relative enrichment of taxa in the colonic IgA$^+$ fraction of controls (black) or knockouts (white). n=6 each genotype, representative of two independent experiments.

While commensal-specific IgA appeared largely intact in *Tcrb*$^{-/-}$*d*$^{-/-}$ mice, free IgA was significantly reduced (Figure 4E) (*11*). As this compartment was dramatically affected by the loss of T cells, we considered that it may contain TD specificities against non-microbial antigens and therefore assessed whether free IgA could bind commensal bacteria. We cohoused WT C57BL/6 mice with *Rag1*$^{-/-}$ mice for three weeks, which equilibrated microbial communities (Figure 5A). We then isolated ileal or colonic free IgA from WT mice and used it to stain *Rag1*$^{-/-}$ ileal or colonic bacteria, respectively. While some free IgA reacted with *Rag1*$^{-/-}$ bacteria, this staining was faint and insufficient to restore IgA coating to WT frequencies, even at high staining concentrations >100 μg/mL (Figure 4E). Thus, commensal-reactive specificities appear to be dilute in the free IgA and this compartment may contain primarily TD specificities against other luminal antigens.

To identify commensal bacteria targeted by TI IgA, we performed IgA-Seq on colonic and jejunal samples from *Tcrb*$^{-/-}$*d*$^{-/-}$ mice and co-housed littermate controls. Co-housed *Tcrb*$^{-/-}$*d*$^{-/-}$ mice and *Tcrb*$^{+/-}$*d*$^{+/-}$ littermates displayed largely overlapping small intestinal and colonic microbial communities (Figure 5B). Most IgA$^+$ bacteria found in controls were equally enriched in the IgA$^+$ fraction of *Tcrb*$^{-/-}$*d*$^{-/-}$ mice (Figure 4F, 5C). This trend was apparent in both the colon and jejunum (Figure 4F, 5C). These data suggest that most IgA$^+$ bacteria induce robust TI responses.

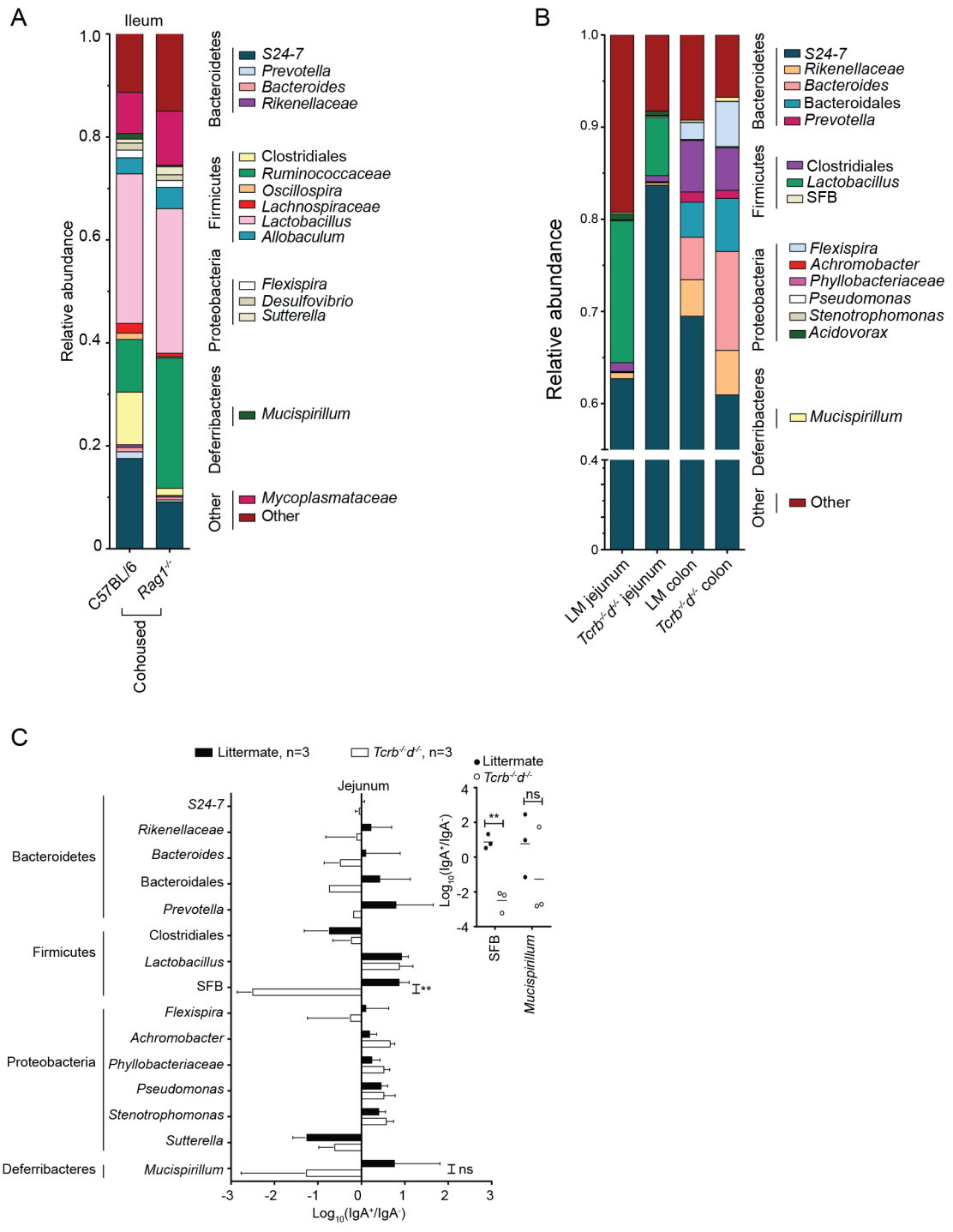

Figure 5. Cohousing normalizes microbiota of mice with diverse genotypes and *Tcrb*$^{-/-}$*d*$^{-/-}$ jejunal IgA-Seq. (A) Average relative abundance of indicated taxa in ileal samples of the co-housed C57Bl/6 mice or *Rag1*$^{-/-}$ mice used in Figure 4E, n=4 each genotype. (B) Average relative abundance of indicated taxa in unfractionated samples of the jejunum or colon of *Tcrb*$^{-/-}$*d*$^{-/-}$ mice or co-housed *Tcrb*$^{+/-}$*d*$^{+/-}$ litter mate controls, n=3 each genotype.

Figure 5, continued. (B) Relative enrichment of indicated taxa in the jejunal IgA^+ or IgA^- fractions of *Tcrb*$^{-/-}$*d*$^{-/-}$ mice (white) or littermate controls (black), n=3 each genotype.

We identified two taxa, segmented filamentous bacteria (SFB) and *Mucispirillum*, that were absent from the IgA^+ fraction of *Tcrb*$^{-/-}$*d*$^{-/-}$ mice but enriched in the IgA^+ fraction of *Tcrb*$^{+/-}$ *d*$^{+/-}$ littermate controls (Figure 4F, 5B). This pattern was observed in both colonic and jejunual samples (Figure 4F, 5B). Thus, TD specificities appear necessary for IgA coating of these taxa. Notably, both SFB and *Mucispirillum* interact closely with the intestinal epithelium in the terminal ileum (*24, 72*). We hypothesize that SFB and *Mucispirillum* may possess atypical cell wall structures that poorly stimulate TI responses and may therefore come into close contact with the mucosa, allowing sampling by antigen-presenting cells and priming of TD IgA responses.

Together, these data suggest that TD and TI responses may coat non-overlapping commensal bacterial taxa. While most IgA^+ bacteria induce strong TI responses, atypical commensals such as SFB and *Mucispirillum* exclusively elicit TD responses.

Germinal centers and somatic hypermutation are dispensable for commensal coating

We found prominent TI IgA coating in *Tcrb*$^{-/-}$*d*$^{-/-}$ mice, but it was possible that these mice had defects related to the absence of T cells but unrelated to TD IgA. Therefore, we sought to validate these observations by examining bacterial coating in two additional models.

We first examined IgA responses in *CD4-Cre Bcl-6*$^{fl/fl}$ (*Bcl-6*$^{\Delta T}$) mice, in which conditional deletion of the transcription factor BCL-6 in T cells prevents Tfh differentiation and GC formation (*73*). *Bcl-6*$^{\Delta T}$ mice lacked GCs and Tfh but had normal numbers of $B220^+IgA^+$ B cells in mLNs and PPs (Figure 6A). *Bcl-6*$^{\Delta T}$ small intestinal IgA^+ plasma cell numbers were reduced three-fold compared to controls (Figure 6A). Similar to *Tcrb*$^{-/-}$*d*$^{-/-}$ mice, bacterial IgA

coating in *Bcl-6*$^{\Delta T}$ mice was identical to controls and no differences in staining intensity were apparent (Figure 6B).

IgA-Seq revealed that all IgA^{+} commensal bacteria induced potent GC-independent IgA responses (Figure 6C) and that IgA^{+} bacteria in littermate controls were equally enriched in the IgA^{+} fraction of co-housed *Bcl-6*$^{\Delta T}$ mice. We found that SFB and *Mucispirillum* were IgA^{+} in *Bcl-6*$^{\Delta T}$ mice, suggesting that coating these bacteria is TD but GC-independent. These data support the conclusion that IgA^{+} commensal bacteria prominently induce TI responses.

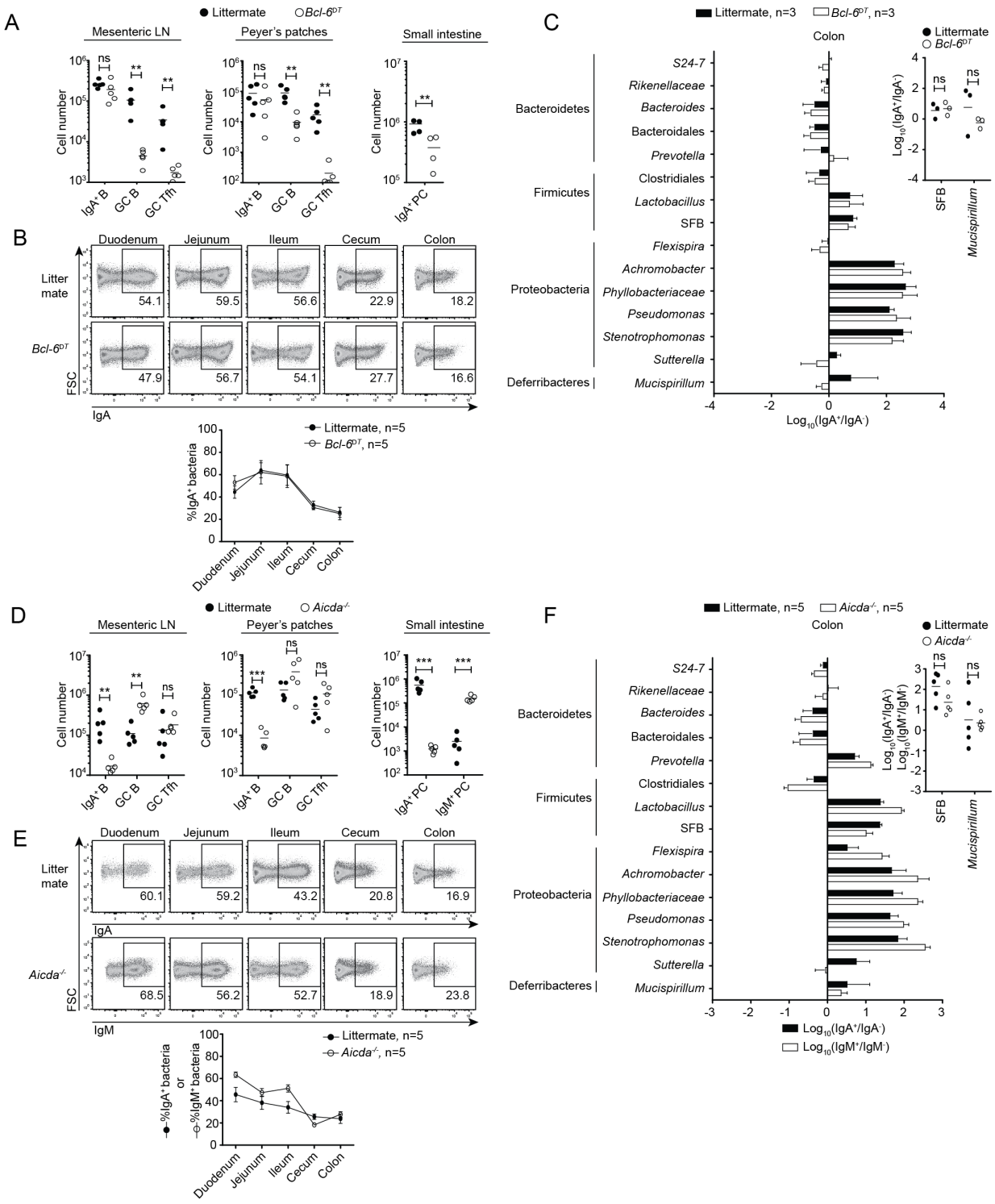

Figure 6. Germinal centers and somatic hypermutation are dispensable for commensal coating. (A) Absolute numbers of indicated populations in the mLN, PP, or small intestinal lamina propria of *CD4-Cre Bcl-6*$^{fl/fl}$ mice or littermate controls. Data compiled from three independent experiments. (B) IgA bacterial coating, compiled from two independent experiments. (C) Fold enrichment of indicated taxa in colonic IgA^{+} fraction of *Bcl-6*$^{\Delta T}$ mice or

Figure 6, continued. co-housed littermate controls. n=3 each genotype, representative of two independent experiments. (D) Absolute numbers of indicated populations in the mLN, PP, or small intestinal lamina propria of *Aicda*$^{-/-}$ mice or *Aicda*$^{+/-}$ littermate controls. Data compiled from two independent experiments. (E) IgM bacterial coating (*Aicda*$^{-/-}$ mice) or IgA bacterial coating (*Aicda*$^{+/-}$) mice. Data compiled from two independent experiments. (F) Fold enrichment of indicated taxa in colonic IgM^{+} fraction of *Aicda*$^{-/-}$ mice or IgA^{+} fraction of *Aicda*$^{+/-}$ mice. n=5 each genotype.

As a second approach, we examined bacterial coating in mice lacking activation-induced cytidine deaminase (AID; encoded by *Aicda*). AID is required for somatic hypermutation (SHM) and class-switch recombination and thus *Aicda*$^{-/-}$ mice produce unmutated antibodies of the IgM isotype (*32*). We observed Tfh and GCs in *Aicda*$^{-/-}$ mice (Figure 6D), and *Aicda*$^{-/-}$ mice had B220^{-}IgM^{+} but not B220^{-}IgA^{+} plasma cells in their small intestinal lamina propria (Figure 6D), as reported previously (*32*). As expected, we found no IgA^{+} bacteria in *Aicda*$^{-/-}$ mice (Figure 1A). Instead, we readily detected IgM^{+} bacteria in *Aicda*$^{-/-}$ mice but not in *Aicda*$^{+/-}$ or *Rag1*$^{-/-}$ controls (Figure 7A). The frequency of IgM^{+} bacteria in *Aicda*$^{-/-}$ mice was identical to the frequency of IgA^{+} bacteria in *Aicda*$^{+/-}$ littermate controls (Figure 6E).

To identify bacteria coated in the absence of SHM, we performed IgM-Seq on *Aicda*$^{-/-}$ mice and IgA-Seq on co-housed *Aicda*$^{+/-}$ littermate controls (Figure 7B). IgM^{+} bacteria in *Aicda*$^{-/-}$ mice were identical to IgA^{+} bacteria in controls and all taxa were equally enriched in the IgM^{+} fraction of *Aicda*$^{-/-}$ mice and the IgA^{+} fraction of controls (Figure 6F). SFB and *Mucispirillum* were both strongly IgM^{+} in *Aicda*$^{-/-}$ mice, further suggesting that coating of these taxa is TD but independent of SHM.

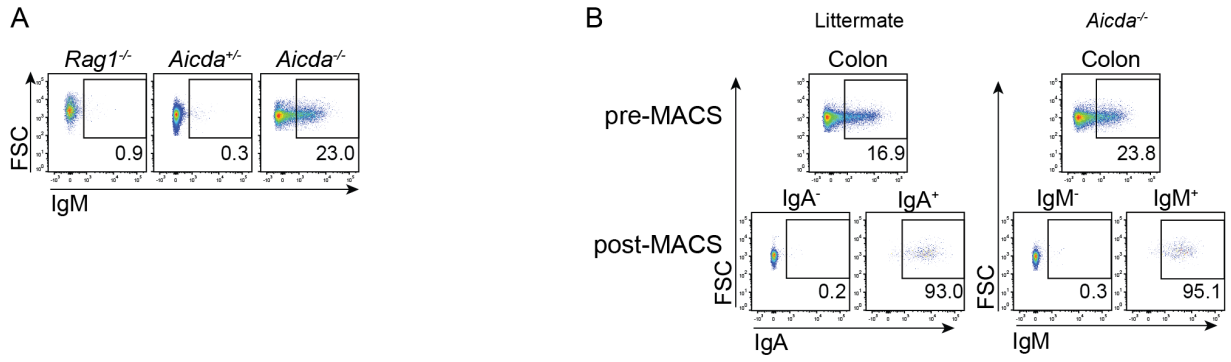

Figure 7. IgM staining of *Aicda*$^{-/-}$ bacteria is specific and allows purification for IgM-Seq. (A) Staining of IgM-bound colonic bacteria in *Rag1*$^{-/-}$, *Aicda*$^{+/-}$ co-housed litter mate controls or *Aicda*$^{-/-}$ mice. (B) Representative pre- and post-MACS purity checks verifying purity of IgA^{+} and IgA^{-} or IgM^{+} and IgM^{-} colonic bacterial fractions from *Aicda*$^{+/-}$ or co-housed *Aicda*$^{-/-}$ mice, respectively.

Together, these data indicate that GCs and SHM are dispensable for IgA coating of commensal bacteria and support the hypothesis that commensal-specific IgA is primarily TI.

Exaggerated coating of *S24-7* in a model of Tfh hyper-sufficiency

As a complementary approach, we analyzed IgA coating in a model of Tfh hyper-sufficiency. Our laboratory recently identified the E3 ubiquitin ligase Cullin-3 (CUL3) as a co-repressor that complexes with BCL-6 and limits Tfh differentiation (*74*). Conditional deletion of CUL3 in T cells (*CD4-Cre Cul3*$^{fl/fl}$*; Cul3*$^{\Delta T}$) results in mLN hyperplasia driven by spontaneous, cell-intrinsic, antigen-specific expansion of Tfh and T follicular regulatory (Tfr) cells in the absence of observable pathology (*74*). This expansion drove a 10-15-fold increase in mLN GC B cells and B220^{+}IgA^{+} B cells (Figure 8A) and a corresponding increase in B220^{-}IgA^{+} plasma cells in the proximal small intestinal lamina propria (Figure 8B). *Cul3*$^{\Delta T}$ mice had an increased frequency of IgA^{+} bacteria compared to co-housed littermate controls (Figure 8C). Increased IgA coating was clearly driven by exaggerated TD responses against a single taxon, *S24-7* (Figure 8D). *Cul3*$^{\Delta T}$ mice also showed a notable absence of *Mycoplasmataceae*, which were abundant in littermate

controls (Figure 8D). *S24-7* did not require T cells for IgA targeting, as its relative enrichment in the IgA$^+$ fraction was not altered in *Tcrb*$^{-/-}$*d*$^{-/-}$ mice (Figure 4F, 5B). These data suggest that *S24-7* can induce TD responses but, unlike SFB and *Mucispirillum*, does not require TD specificities to become IgA$^+$.

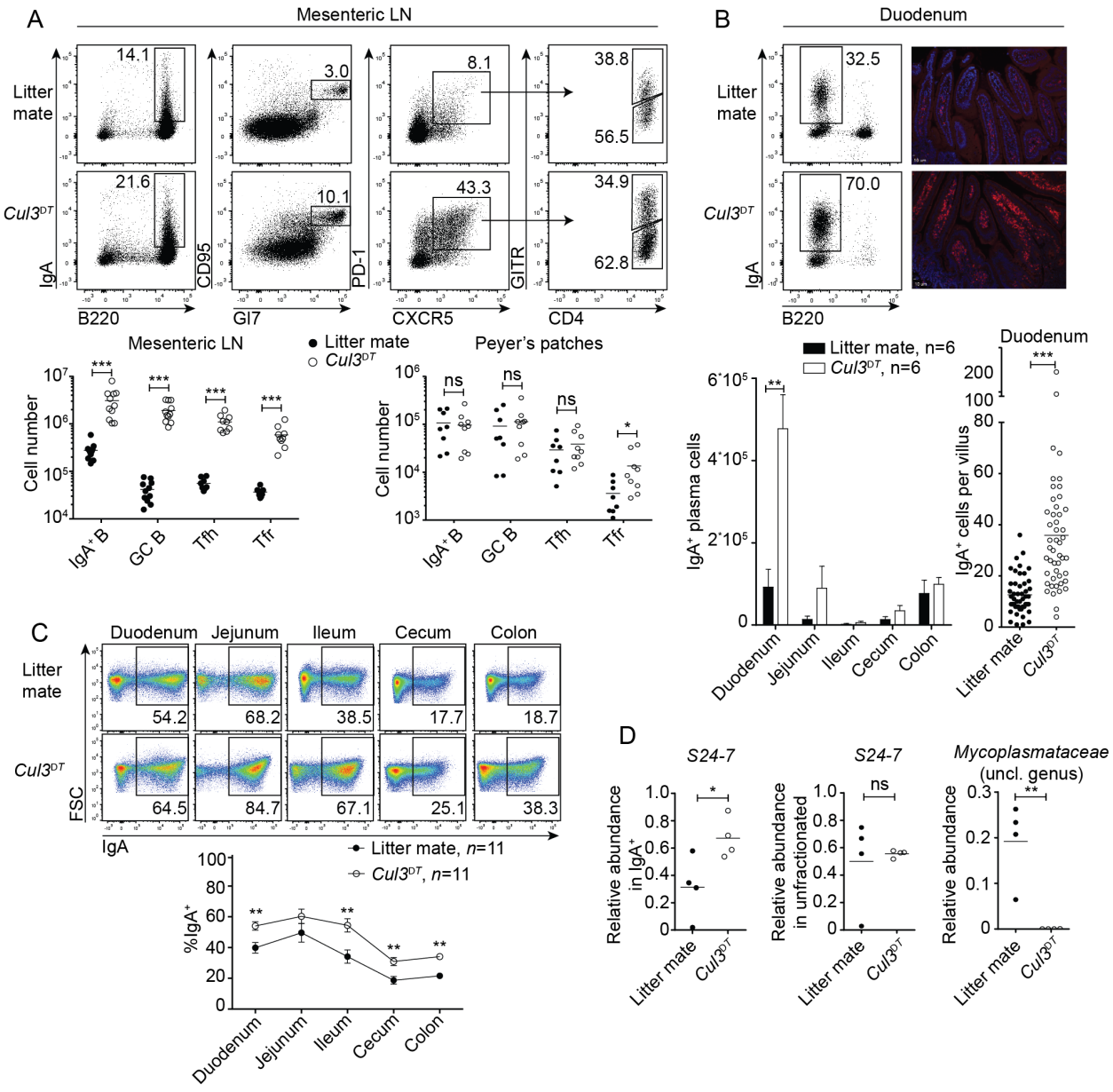

Figure 8. Enhanced IgA coating of *S24-7* in a model of Tfh hyper-sufficiency. (A) Representative flow cytometry plots and absolute numbers of indicated populations in the mesenteric lymph nodes or Peyer's patches of *CD4-Cre*$^+$ *Cul3*$^{fl/fl}$ (*Cul3* $^{\Delta T}$) mice or co-housed *CD4-Cre*$^-$ *Cul3*$^{fl/fl}$ litter mate controls. B220 by IgA plots were gated Tcrb$^-$CD3$^-$; CD95 by GI7

Figure 8, continued. plots were gated $B220^+$. PD-1 by CXCR5 plots were gated $Tcrb^+CD4^+$. GITR by CD4 plots were gated $Tcrb^+CD4^+CXCR5^+PD\text{-}1^+$, as indicated. (B) Left panels: Representative flow cytometry plots and absolute numbers of $B220^-$ IgA^+ plasma cells in the indicated intestinal segments. Plots were gated $Tcrb^-CD3^-DAPI^-$. n=6 each genotype, representative of two independent experiments. Right panels: Representative immunofluorescent staining and image quantification of paraffin-embedded sections from the duodenum of *Cul3* $^{\Delta T}$ mice and litter mate controls. n=3 each genotype, image quantification was performed on 2 duodenal sections from each mouse. (C) IgA coating of commensal bacteria at the indicated location in *Cul3* $^{\Delta T}$ mice and litter mate controls. n=11 each genotype. (D) Right panel: Relative abundance as determined by 16S sequencing of *S24-7* in the jejunal IgA^+ fraction. Middle panel: relative abundance of *S24-7* in unfractionated ileal samples. Right panel: Relative abundance of *Mycoplasmataceae* (unclassified genus) in unfractionated ileal samples of *Cul3* $^{\Delta T}$ mice and co-housed litter mate controls (n=4 each genotype).

Commensal-specific IgA^+ plasma cells differentiate from B1b and B2 B cell precursors

IgA^+ plasma cells can derive from both B1 and B2 B cell precursors, although the relative contributions of these lineages remain controversial (*11, 65, 66*). Limited evidence based on mixed bone marrow-peritoneal cell chimeric mice suggest that many IgA^+ plasma cells in *Tcrb* $^{-/-}$ *d* $^{-/-}$ mice may be of B1 origin (*11*). However, it is unclear whether both B1 and B2 B cells give rise to commensal-specific IgA and whether these lineages contribute differentially to IgA coating of certain commensal taxa.

Analysis of B1 B cells is complicated by a lack of genetic tools, such as fate-mapping models, to study these cells *in vivo*. Moreover, genetic alterations that disrupt B1 lineage development involve BCR signaling-related molecules that also disrupt the activation and function of B2 B cells (*64*). Therefore, to assess whether B1 or B2 B cells were sufficient to generate commensal-specific IgA, we reconstituted immunodeficient *Rag1* $^{-/-}$ mice with exclusively B1 or B2 B cells by transferring pure sorted populations. We initially established groups of *Rag1* $^{-/-}$ recipients reconstituted by: 1) Intraperitoneal (i.p.) transfer of B1 B cells; 2) i.p. B1 B cells + splenic $CD4^+$ and $CD8^+$ T cells (B1+T); 3) Intravenous (i.v.) transfer of B2 B cells;

and 4) i.v. B2 B cells + splenic $CD4^+$ and $CD8^+$ T cells (B2+T). We readily detected IgA^+ plasma cells and bacterial IgA coating in mice reconstituted with either B1 or B2 B cells (Figure 9A-C). Addition of T cells did not affect B1 differentiation into IgA^+ plasma cells but did induce free IgA, albeit at low titers (Figure 9A-C). In contrast, T cells markedly increased the number of B2 B cell-derived IgA^+ plasma cells and supported generation of high titers of free IgA (Figure 9A-C). Thus, TI B1 B cells and TI and TD B2 B cells can coat commensal bacteria while free IgA is predominantly derived from TD B2 B cells.

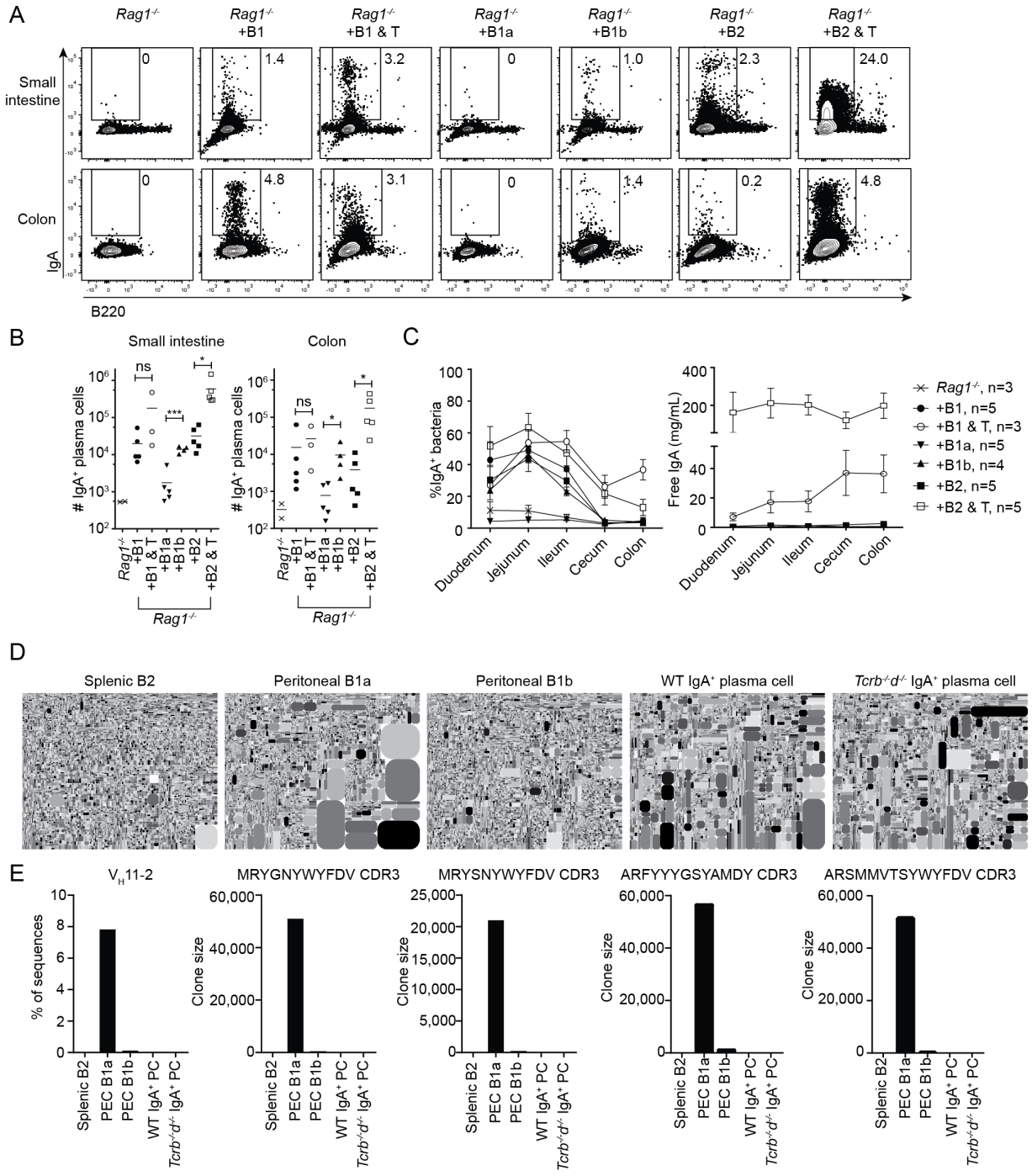

Figure 9. Commensal-specific IgA$^+$ plasma cells differentiate from B1b and B2 B cell precursors. (A)Representative staining and (B) absolute numbers of small intestinal or colonic IgA$^+$ plasma cells recovered from *Rag1*$^{-/-}$ mice that received the indicated sorted populations. B1 populations were transferred i.p. (500,000 B1, 1,000,000 CD4/CD8 T cells, or 250,000 B1a or B1b) and B2 populations were transferred i.v. (1,000,000 B2, 1,000,000 CD4/CD8 T cells). Mice were analyzed 5 weeks after transfer. Data compiled from six independent experiments and two separate sorts for each transferred population. (C) IgA bacterial coating or free IgA in indicated recipient mice. (D) Immunoglobulin heavy chain repertoire sequencing of indicated

Figure 9, continued. populations. Tree plots are shown - each shape indicates a unique IgH CDR3 and size is scaled to relative clonal abundance. (E) Frequency of V_H11 gene segments within the populations shown in (D) or number of sequences containing the indicated canonical B1a CDR3's.

We next assessed the ability of peritoneal B1a and B1b subsets to differentiate into IgA^+ plasma cells by i.p. transfer of sorted B1a or B1b into *Rag1*$^{-/-}$ recipients. While B1b B cells gave rise to a substantial population of IgA^+ plasma cells and coated commensal bacteria, B1a B cells did not differentiate into IgA^+ plasma cells (Figure 9A-C). We verified that both B1a and B1b B cells stably reconstituted the peritoneal cavity of recipient mice (Figure 10). To further assess whether B1a B cells contribute to the IgA^+ plasma cell pool, we performed immunoglobulin repertoire sequencing of peritoneal B1a and B1b B cells, splenic B2 B cells, WT IgA^+ plasma cells, and *Tcrb*$^{-/-}$*d*$^{-/-}$ IgA^+ plasma cells. The B1a B cell repertoire is enriched in canonical rearrangements of the V_H11 gene family that encode specificities toward conserved microbial antigens such as phosphorylcholine (*64*). Indeed, we found that the B1a repertoire was partially restricted and that approximately 8% of sequences were of the V_H11 gene family (Figure 9D, E). The B1a repertoire also contained prominent clonal populations with conserved CDR3 sequences representing the V_H11, V_H1-55, and V_H1-9 gene families (Figure 9D, E). In contrast, V_H11 gene segments made up a negligible fraction of the repertoires of splenic B2, peritoneal B1b, WT IgA^+ plasma cells, or *Tcrb*$^{-/-}$*d*$^{-/-}$ IgA^+ plasma cells and canonical B1a CDR3s were completely absent (Figure 9D, E). The peritoneal B1b repertoire was broad and of comparable diversity to that of splenic B2 B cells with little evidence of clonal expansion or conserved immunoglobulin rearrangements. Together, these data suggest that B1a B cells do not contribute to the IgA^+ plasma cell repertoire or IgA coating of commensals. We conclude that commensal-specific IgA is derived from B1b and B2 B cell precursor populations, although the precise contributions of

each subset remain unclear due to limitations in cell transfer studies and a lack of genetic tools to dissect these responses in intact mice.

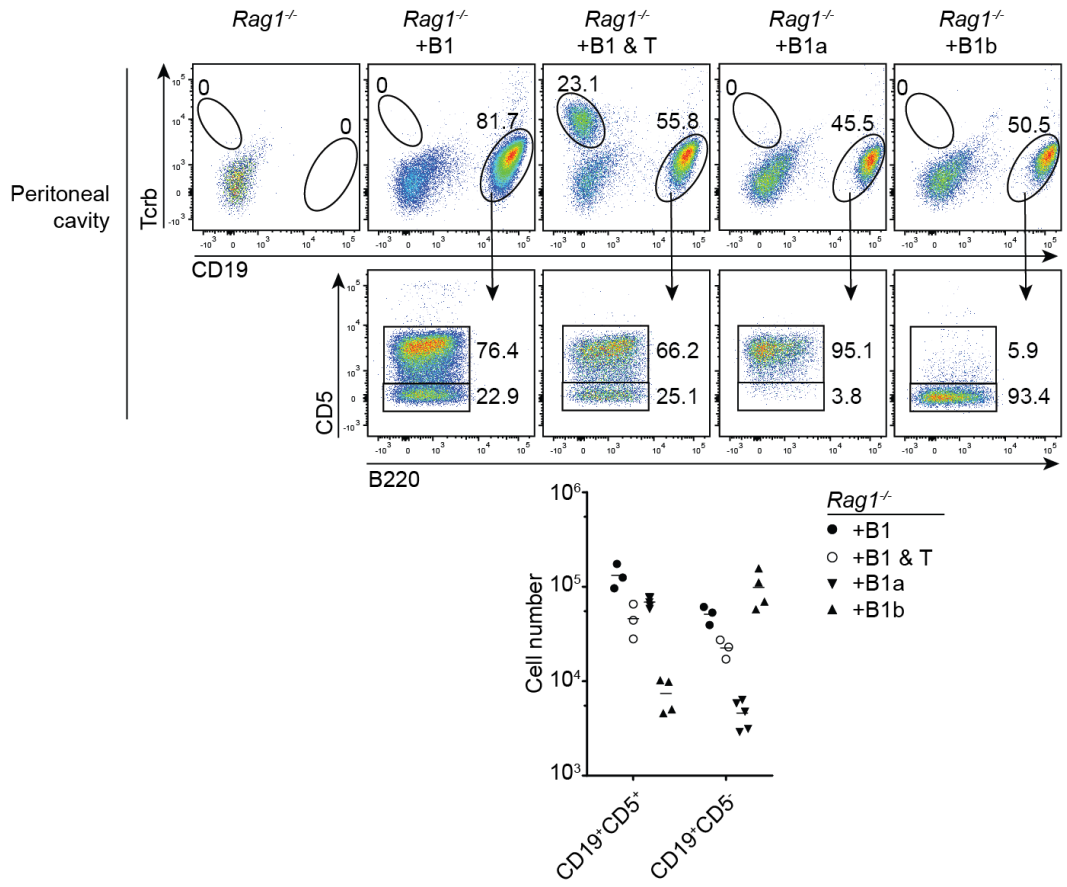

Figure 10. Transferred B cell populations reconstitute the peritoneal cavity of *Rag1*$^{-/-}$ recipients. (A) Representative flow cytometry plots and absolute numbers of indicated peritoneal cavity lymphocyte populations. Plots are gated on lymphocytes. n=3-5 each condition, as described in Figure 9 and Rag1$^{-/-}$ B cell Transfers below.

TI B1b and B2 B cells coat diverse and overlapping commensal bacterial taxa

To identify commensal bacteria bound by B1b or B2-derived IgA, we performed IgA-Seq on colonic samples from *Rag1*$^{-/-}$ mice reconstituted with B1 or B2 B cells. This analysis revealed that TI B1b and B2 B cells were each sufficient to coat a diverse array of commensal bacteria (Figure 11). B1b and B2 coated overlapping bacterial taxa and there were no apparent differences in efficacy of coating certain taxa by either subset (Figure 11). This is consistent

with the observation that both B1b and B2 B cells possess broad and diverse immunoglobulin repertoires (Figure 9D). Addition of T cells did not alter the taxa targeted by B1b or B2 B cells, further supporting the conclusion that most commensal bacteria primarily induce TI IgA (Figure 11).

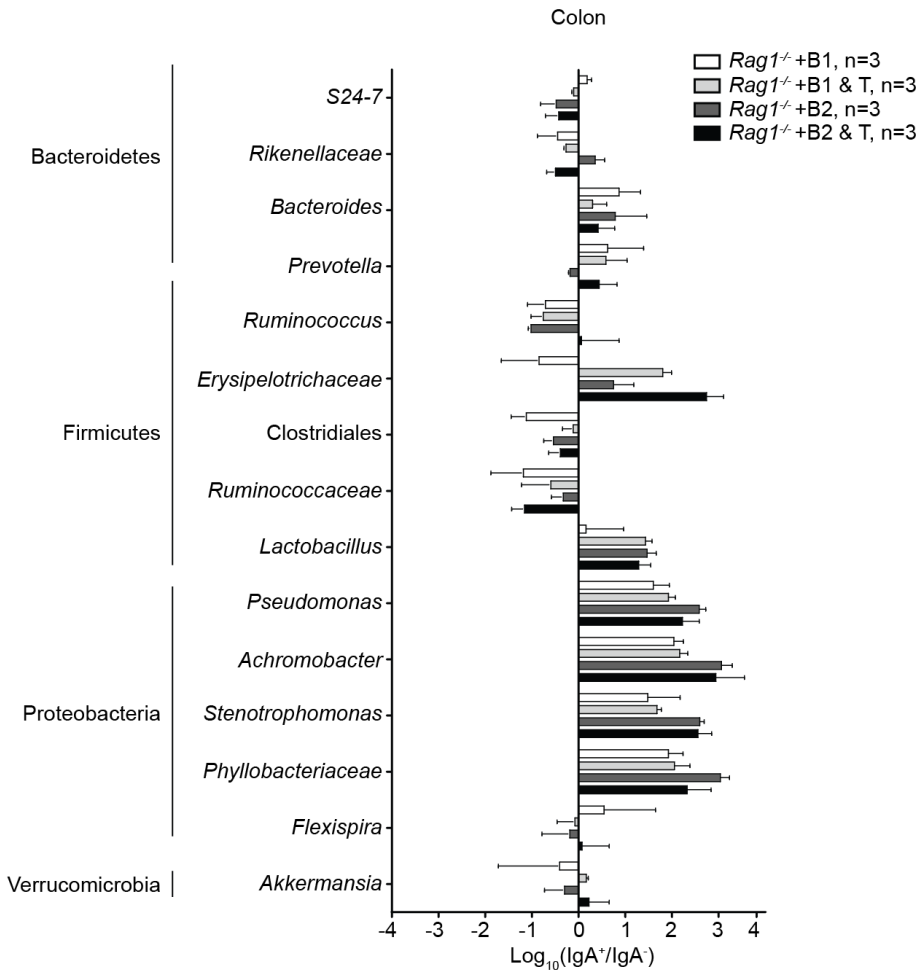

Figure 11. B1b and B2 B cells coat diverse and overlapping commensal bacterial taxa. Fold enrichment of indicated taxa in colonic IgA^+ fractions of *Rag1*$^{-/-}$ mice reconstituted with sorted B cell populations, as described in Figure 9. n=3 each group of mice, compiled from two independent experiments.

TI antibodies bind specifically to commensal bacteria

TI IgA responses may give rise to polyreactive specificities (*54, 75*). Further, IgA may interact with bacteria nonspecifically via the IgA fragment crystallizable (Fc) region or secretory component (*76*). We generated recombinant monoclonal antibodies from single *Tcrb*$^{-/-}$*d*$^{-/-}$ small intestinal IgA^{+} plasma cells and engineered them to express the human IgG1 Fc instead of mouse IgA Fc. Five out of five antibodies recognized *Rag1*$^{-/-}$ small intestinal or colonic commensal bacteria (Figure 12). Each antibody bound to a discrete bacterial subset and their mixture stained an even greater fraction of bacteria, revealing distinct specificities. Recognition was specific, as none of the antibodies reacted with the colonic commensal *Bacteroides fragilis* (Figure 12).

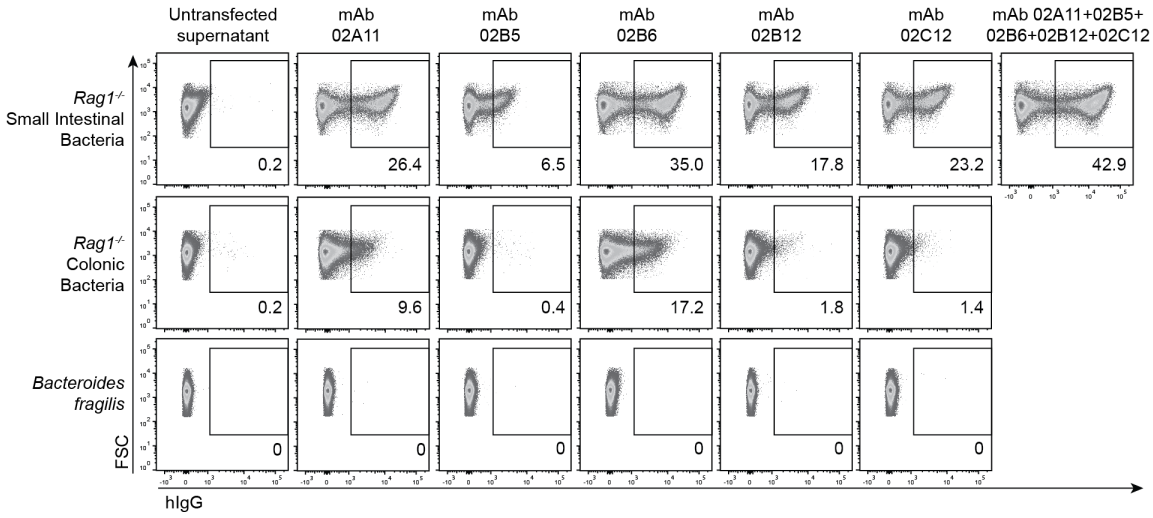

Figure 12. TI antibodies bind specifically to commensal bacteria. Staining of total small intestinal or colonic bacteria from *Rag1*$^{-/-}$ mice or pure cultures of *Bacteroides fragilis* with indicated recombinant monoclonal antibodies derived from single *Tcrb*$^{-/-}$*d*$^{-/-}$ small intestinal IgA^{+} plasma cells and engineered to express human IgG1 Fc instead of mouse IgA Fc Staining was performed using supernatants from transduced HEK293T cells expressing indicated antibody constructs. Untransfected supernatant was used as a negative control. Data representative of two independent experiments.

DISCUSSION

The commensal bacteria targeted by IgA have remained enigmatic. Recent studies suggest that IgA targets particularly immunogenic or invasive bacteria (*6, 59*). In contrast, we found that anatomical location was the primary factor that determined whether a particular taxon elicited an IgA response. Under homeostatic conditions, most small intestinal bacteria were IgA^+ and induced specific IgA. Although a fraction of colonic bacteria were IgA^+, colonic IgA^+ taxa were also abundant in the small intestine and homed to the small intestine upon transfer into germ free mice. It is possible that colonic IgA^+ bacteria represent small intestinal contaminants rather than indigenous colonic flora, and distinct physiological properties may contribute to the differential ability of colonic IgA^+ and IgA^- commensals to colonize the small intestine and colon. However, it seems unlikely that small intestinal bacteria are more immunogenic than colonic bacteria. Instead, this anatomical regulation is likely due to extensive priming of commensal-specific IgA^+ plasma cells in secondary lymphoid tissues accompanying the small intestine. PPs and isolated lymphoid follicles are predominantly associated with the small intestine and possess a specialized epithelium that allows sampling of luminal antigens (*21*). Our data suggest that these tissues prime IgA against nearly all bacteria present in the small intestinal lumen.

Previous work has suggested that TI IgA responses generate low affinity antibodies that react poorly with commensal bacteria (*32, 54, 61-63*). Further, recent studies of dysbiotic mice suggested that many commensals may elicit TD responses (*6*). In contrast, we found strong commensal Ig coating in mice lacking T cells, GCs, or SHM. These data indicate that most commensals elicit strong TI responses and that TI IgA is completely sufficient to coat most commensal bacteria at frequencies and staining intensities found in WT mice. This conclusion was also strongly supported by our finding that five out of five antibodies generated from *Tcrb*$^{-/-}$

$d^{-/-}$ small intestinal IgA^+ plasma cells recognized commensal bacteria. Although we did not directly measure their affinity, these TI antibodies were clearly sufficient to brightly stain commensal bacteria. TI responses generate short-lived plasma cells, and active turnover of commensal-specific plasma cells may facilitate rapid, dynamic IgA responses upon exposure to novel commensal antigens. TI responses may also prevent pathological activation of commensal-specific T cells by sequestering bacteria away from antigen-presenting cells in the intestinal epithelium.

TI responses may promote the generation of polyreactive specificities (*54, 75*), and IgA may bind nonspecifically to bacteria via the Fc region or secretory component (*76*). However, by generating recombinant monoclonal antibodies from single $Tcrb^{-/-}d^{-/-}$ IgA^+ plasma cells engineered to express the human IgG1 Fc region instead of mouse IgA Fc, we demonstrated Fab-dependent binding to discrete subsets of commensal bacteria but not to cultured *B. fragilis*. Ongoing work in our laboratory is focused on characterizing the commensal bacteria and specific antigens recognized by these antibodies.

B1a cells constitute the most abundant peritoneal B cell lineage and have been extensively investigated and shown to produce natural IgM antibodies with antimicrobial and self reactivities. However, the minor "sister" B1b lineage has remained largely elusive and has only been reported to participate in humoral responses against *B. hermsii*, *S. typhimurium*, and *S. pneumoniae* (*68-70*). Our results extend these early reports and reveal a specialization of the B1b lineage in TI IgA responses against intestinal commensal bacteria. Future work should address the development of B1b cells and the sites at which they encounter intestinal antigens and undergo class-switch recombination *in vivo.*

Previous work has suggested that TI B1a B cells may give rise to 'natural' IgA in the form of intestinal free IgA, which resembles 'natural' low-affinity IgM found in circulation in the absence of immunization (*54, 62, 64, 75*). However, we found that the IgA^+ plasma cell immunoglobulin repertoire did not include canonical 'natural' B1a specificities and that B1a B cells did not differentiate into IgA^+ plasma cells, consistent with a previous study (*67*). IgA plasma cells contributing to the free IgA compartment appeared to be predominantly derived from TD B2 B cells. Thus, although many potential antigens may stimulate free IgA, this compartment does not represent 'natural' IgA and appeared largely specific for non-microbial antigens.

Interestingly, SFB and *Mucispirillum* evaded TI IgA and instead elicited TD specificities to become IgA coated. Yet, IgA coating of these taxa was independent of GCs and SHM and thus these organisms may induce IgA by atypical mechanisms that are dependent on T cells or T cell-derived factors. SFB is known to be particularly immunogenic and can induce formation of GCs and tertiary lymphoid structures as well as effector T cell differentiation (*24*). SFB also induces large quantities of free IgA that is not SFB-specific (*24*). In contrast to SFB, the immunogenicity of *Mucispirillum* remains uncharacterized. Ongoing work in our laboratory is focused on culturing and characterizing the properties of this organism. Notably, SFB and *Mucispirillum* both closely associate with the intestinal epithelium in the terminal ileum (*24, 72*). Thus, these organisms may inhabit similar niches and possess atypical immunogenic properties, allowing them to evade TI responses and come into close contact with the mucosa where they can be sampled by antigen-presenting cells and elicit TD responses.

We consistently observed that most small intestinal commensal bacteria were IgA^+, however we found no instances in which 100% were IgA^+. As small intestinal IgA^- bacteria

appeared taxonomically similar to IgA^+ bacteria, a fraction of bacteria may escape coating. This may result from phase variation of surface capsular polysaccharide antigens (*57*). Alternatively, commensal-specific IgA may be limiting or may be actively degraded by bacterial IgA proteases (*56*). Understanding the specificity of individual IgA antibodies will shed light on this important issue.

We found that ~20% of colonic bacteria were typically IgA^+, similar to reports by Kroese, de Waard and Bos (*13*) and Tsuruta, Inoue, Nojima, Tsukahara, Hara and Yajima (*14*) ENREF 15, but higher than the ~8% reported by Palm, de Zoete, Cullen, Barry, Stefanowski, Hao, Degnan, Hu, Peter, Zhang, Ruggiero, Cho, Goodman and Flavell (*6*). These differences may be technical, as we used a polyclonal anti-IgA antibody whereas Palm et al. (2014) used a monoclonal antibody. Palm, de Zoete, Cullen, Barry, Stefanowski, Hao, Degnan, Hu, Peter, Zhang, Ruggiero, Cho, Goodman and Flavell (*6*) also described a population of IgA^{hi} bacteria that was enriched in commensals with pathogenic properties and largely targeted by TD IgA. This observation may be limited to a dysbiotic flora, as we did not observe an IgA^{hi} population in healthy mouse microbiota.

In summary, our data reveal the prominent role of the enigmatic B1b lineage in control of the microbiota, and suggest a model whereby multiple layers of humoral immunity contribute to homeostatic IgA coating of microbiota in the small intestine. Most commensals induce TI responses from B1b and B2 B cells and these responses sequester bacteria away from the intestinal epithelium, preventing T cell activation. However, atypical commensals including SFB and *Mucispirillum* evade TI responses and penetrate the mucus layer, where they interact with antigen presenting cells and prime T cell responses. Humoral regulation of commensal bacteria may have represented a substantial evolutionary force promoting the diversification and

maintenance of peripheral B cell lineages, including the elusive B1b lineage. While these data clarify the homeostatic regulation of commensal-specific IgA, a further understanding of the antigens targeted by IgA may shed light on the regulation of IgA responses and allow opportunities for therapeutic intervention in microbiota-associated pathologies such as inflammatory bowel disease, obesity, diabetes, and celiac disease.

EXPERIMENTAL PROCEDURES

Mice

8-12 week old knockout mice were compared to co-housed littermate controls and maintained under strict SPF conditions. Germ-free C57BL/6 mice were housed at the University of Chicago gnotobiotic facility and experimental groups were housed in separate gnotobiotic isolators. See also Supplemental Experimental Procedures.

Antibodies and Flow Cytometry

Conjugated antibodies purchased from commercial vendors were used to stain samples prior to analysis on a LSRII flow cytometer (Becton Dickinson), sorting on a FACSAria (Becton Dickinson), or separation with an autoMACS (Miltenyi). Data were analyzed using FlowJo (TreeStar). See also Supplemental Experimental Procedures.

Analysis of IgA^+ bacteria, IgM^+ bacteria and free IgA

Homogenized intestinal contents were resuspended at 0.1 mg/μL in PBS with protease inhibitors (Sigma), homogenized, and centrifuged at 400g to remove large debris. Supernatant was filtered through a sterile 70 μm strainer and centrifuged at 8000g to pellet bacteria. This supernatant was collected and assayed for free Ig by ELISA. The bacterial pellet was resuspended in PBS 0.25% BSA with SYTO BC (Life Technologies) and 5% goat serum and then stained with biotinylated goat anti-mouse IgA, goat anti-human IgA, or goat anti-mouse IgM (Southern Biotech). After

washing, bacteria were stained with streptavidin-APC (BioLegend). Bacteria were washed and resuspended in PBS 0.25% BSA with DAPI (Life Technologies) prior to flow cytometry using a low FSC and SSC threshold to allow bacterial detection. See also Supplemental Experimental Procedures.

Human Samples

Human study was approved by the Institutional Review Board at the University of Chicago. Healthy subjects undergoing routine colonoscopy were recruited at their procedure and informed consent was obtained from all subjects. See also Supplemental Experimental Procedures.

16S rRNA Gene Sequencing and Microbial Community Analysis

Bacterial DNA was extracted and16S rRNA gene amplicons were generated and sequenced on an Illumina MiSeq. Sequence data was processed and analyzed using QIIME (*77*) and Primer-6 (Primer-E Ltd). Sequence data is publicly available through MG-RAST (*78*) under project 14533. See also Supplemental Experimental Procedures.

***Rag1*$^{-/-}$ Cell Transfers**

Indicated populations were sorted on a FACSAria cell sorter (Becton Dickinson) and post-sort samples were verified for purity. Combinations of 500,000 peritoneal B1, 250,000 B1a, 250,000 B1b, and 1,000,000 splenic T cells were injected intraperitoneally into *Rag1*$^{-/-}$ mice. Combinations of 1,000,000 splenic B2 and 1,000,000 splenic T cells were injected intravenously. Recipients were analyzed 5 weeks after transfer. See also Supplemental Experimental Procedures.

Immunoglobulin Repertoire Analysis

RNA was extracted from sorted samples using an RNeasy kit (Qiagen) and sent on dry ice to iRepertoire, Inc. for cDNA synthesis, PCR amplification, and sequencing on an Illumina MiSeq. See also Supplemental Experimental Procedures.

Monoclonal Antibody Generation

Recombinant monoclonal antibodies were generated from sorted single IgA^+ plasma cells and expressed as chimeric human IgG1 constructs. Culture supernatants from transfected 293T cell cultures were sterile filtered and used for staining of intestinal bacteria at 2 μg/mL. See also Supplemental Experimental Procedures.

Statistical Analysis

Unpaired or paired student's t test was performed with Prism (Graph Pad). *$p<0.05$, **$p<0.01$, ***$p<0.001$.

AUTHOR CONTRIBUTIONS

J.J.B. designed research, performed experiments, and analyzed data. T.M.F. analyzed 16S rRNA sequencing data. J.C.K. performed bacterial DNA extractions and generated 16S rRNA amplicon libraries. D.G.S. obtained patient samples. M.M., B.D.M., and I.E.I. assisted with experiments shown in Figure 3. A.L.D. contributed reagents. P.C.W. contributed methods, reagents and advice in generating monoclonal antibodies from single plasma cells. B.J., D.A.A., and A.B. designed and supervised research. J.J.B. and A.B. wrote the paper. All authors reviewed and approved the final manuscript.

ACKNOWLEDGMENTS

We thank the University of Chicago Flow Cytometry Core for assistance with cell sorting, S. Owens and S. Greenwald in the Next Generation Sequencing Core at Argonne National Laboratory for assistance with amplicon sequencing, and B. Casterline for providing *B. fragilis* cultures. J.J.B and B.D.M. were supported by an NIH Medical Scientist Training Program grant T32GM007281 and M.M. by FWF Austrian Science Fund grant J3418-B19. This work was supported by NIH grants R01AI038339, R01AI108643, R01GM106173, and R01HL118092 to A.B., NIH grant 1R21AI099825 to A.L.D., NIH grants to R01DK067180 and R01DK098435 to B.J., and support to D.A.A. from the University of Chicago DDRCC, NIDDK P30DK42086.

MATERIALS AND METHODS

Mice

C57BL/6J, *Aicda*$^{-/-}$ (B6;129P2-*Aicda*$^{tm1(cre)Mnz}$/J), *Tcrb*$^{-/-}$*d*$^{-/-}$ (B6.129P2-*Tcrb*^{tm1Mom} *Tcrd*^{tm1Mom}/J), *Rag1*$^{-/-}$ (B6.129S7-*Rag1*^{tm1Mom}/J), and *Bcl-6*$^{fl/fl}$ (B6.129S(FVB)-*Bcl6*$^{tm1.1Dent}$/J) were purchased from Jackson Laboratories. C57BL/6NTac, *Rag2*$^{-/-}$*Il2rg*$^{-/-}$ (B10;B6-*Rag2*^{tm1Fwa} *Il2rg*^{tm1Wjl}), and CD4-Cre (B6.Cg-Tg(CD4-cre)1Cwi) were purchased from Taconic. *CD4-Cre Cul3*$^{fl/fl}$ mice were bred in our colony. Fecal samples were obtained from *CD4Cre Bcl-6*$^{fl/fl}$ mice bred at the University of Indiana School of Medicine for one replicate of the experiment shown in Figure 6C. To establish litter mate controls, mice were bred to C57BL/6 mice in our colony and heterozygous mice were bred to homozygous knockouts. *Aicda*$^{-/-}$ mice were compared to *Aicda*$^{+/-}$ litter mate controls. *Tcrb*$^{-/-}$*d*$^{-/-}$ mice were compared to *Tcrb*$^{+/-}$*d*$^{+/-}$ litter mate controls. *CD4-Cre*$^{+}$ *Bcl-6*$^{fl/fl}$ mice were compared to *CD4-Cre*$^{-}$ *Bcl-6*$^{fl/+}$ litter mate controls. *CD4-Cre*$^{+}$ *Cul3*$^{fl/fl}$ mice were compared to *CD4-Cre*$^{-}$ *Cul3*$^{fl/fl}$ litter mate controls. For all experiments, mice

were analyzed at 8-12 weeks of age. All mice were maintained in a specific pathogen-free environment at the University of Chicago and experimental guidelines were approved by the Institutional Animal Care and Use Committee (IACUC).

Germ free C57BL/6 mice were housed at the University of Chicago gnotobiotic facility under strict germ-free conditions. Mice colonized with an IgA^+ or IgA^- inoculum were housed in separate gnotobiotic isolators for the duration of the experiment and analyzed 28 days after colonization.

Bacterial Flow Cytometry and Antibodies

The small intestine was divided into three equal length sections corresponding to the duodenum, jejunum, or ileum. The colon was divided into two sections corresponding to the cecum and colon. Intestinal contents were removed by running forceps along a given intestinal segment and placed in a 1.5 mL Eppendorf tube on ice. Contents were then weighed and resuspended at 0.1 mg/μL in phosphate-buffered saline (PBS; Corning) with protease inhibitors (SIGMAFAST Protease Inhibitor Tablets). Contents were homogenized by taping the Eppendorf tube horizontally on a vortex and vortexing vigorously for 5 minutes. Tubes were centrifuged at 400g for 5 minutes to pellet large debris and the supernatant was filtered through a sterile 70 μm cell strainer (Fisher) and transferred to a new tube. This tube was spun at 8000g for 5 minutes to pellet bacteria. Supernatant was saved and frozen at -20 ºC for free IgA analysis by ELISA. Bacterial pellets were resuspended in PBS 5% goat serum (Jackson Immunoresearch) with SYTO BC (Life Technologies) for 15 minutes on ice. Biotinylated goat anti-mouse IgA (Southern Biotech) was added for 20 minutes on ice. Samples were washed and resuspended in PBS with streptavidin-APC (BioLegend) for 20 minutes on ice. Samples were washed and resuspended in PBS with DAPI (Life Technologies) for flow cytometry analysis. Flow

cytometry was performed on an LSRII Flow Cytometer (Becton Dickinson) with a low FSC and SSC threshold to allow bacterial detection. FSC and SSC were set to a Log scale and samples were gated FSC^+SSC^+SYTO BC^+ $DAPI^-$ and then assessed for IgA staining. In experiments involving *Aicda*$^{-/-}$ mice, bacteria were stained with biotinylated goat anti-mouse IgM (Southern Biotech) followed by streptavidin-APC. In human experiments, bacteria were stained with biotinylated goat anti-human IgA (Southern Biotech) followed by streptavidin-APC.

Lymphocyte Flow Cytometry and Antibodies

Cell suspensions were incubated with Fc Block (BD) prior to staining with the following fluorophore or biotin conjugated monoclonal antibodies (clone in parentheses) against CD4 (GK1.5 or RM4-5), CD5 (53-7.3), CD8 (53-6.7), CD11c (HL3), CD19 (6D5), CD21 (7G6), CD23 (B3B4), CD45.2 (104), CD138 (281-2), B220 (RA3-6B2), CXCR5 (L138D7), F4/80 (BM8), gdTCR (GL3), GITR (YGITR765), Gl7 (GL7), GR1 (RB6-8C5), IgD (11-26c.2a), IgM (Il/41), NK1.1 (PK136), PD-1 (29F.1A12), TER-119 (TER-119), TCRb (H57-597) or goat anti-mouse IgA(Southern Biotech). All antibodies were purchased from Biolegend, eBioscience, or BD Biosciences unless otherwise indicated. Doublet exclusion and DAPI staining to remove dead cells were used when possible. Cell numbers were calculated by flow cytometry with counting beads (Spherotech).

Microbial Community Analyses

DNA was extracted from all samples using the PowerSoil®-htp 96 Well Soil DNA Isolation Kit (MO BIO Laboratories, Inc.) and following the manufacturer's instructions. Amplicons of the V4 region of 16S rRNA genes from domains Bacteria and Archaea were generated using the polymerase chain reaction (PCR) using the 515F-806R primer set (*79, 80*). The primers were Golay-barcoded to allow for multiplexing on the Illumina MiSeq platform (*81*). PCR reactions

were carried out in triplicate for each sample using sterile, DNase-free 96 well plates with appropriate (DNA template-free) negative controls using the 5 PRIME MasterMix (Gaithersburg, MD). No significant amplification was observed in the template-free control reactions, and negative control reactions processed through the sequencing pipeline did not produce any valid sequences. PCR reactions were heated to 95 ºC for 3 min for initial denaturation, followed by 35 cycles of 95 ºC for 30 s, 55 ºC for 45 s, then 72 ºC for 1.5 min. PCR was finalized by a single extension step at 72 ºC for 10 min.

Triplicate PCR reactions were then pooled together and the total amount of DNA was quantified using the PicoGreen® dsDNA Assay (Life Technologies). Primer dimers were removed from the pooled product using the UltraClean® PCR Clean-Up Kit (MoBio Laboratories, Inc.) and the amount of amplicon in each pooled sample was normalized to a final concentration of 2 ng μL^{-1}. Amplicons were sequenced on an Illumina MiSeq using 151×151 base pair paired-end sequencing at the Next-Generation Sequencing Core at Argonne National Laboratory following procedures described by Caporaso et al. (*81*).

2.53×10^7 total sequences were generated for 364 samples giving an average sequencing depth of 69,445±39,468 per sample. Raw sequence data was processed using the QIIME analysis pipeline (*77*) and other bioinformatics toolkits. Paired-end reads were joined together using PEAR (*82*), and any reads of insufficient quality that prevented joining were discarded (< 5% of total reads). Sequences were then aligned to a database of reference sequences using PyNAST (*83*) and clustered into operational taxonomic units (OTUs) using UCLUST at 97% similarity (*84*). For beta diversity calculations, any OTUs containing only a single sequence (singletons) were discarded and samples were rarefied to even sequencing depth. A consensus taxonomy from the Greengenes reference database (*85*) was assigned to each sequence using the UCLUST

taxonomy assigner. Beta diversity comparisons between samples were made using the weighted UniFrac algorithm (*86-88*) and visualized using dendrograms created in Primer-6 (Primer-E Ltd., Plymouth, UK). Data are publically available via MG-RAST (Meyer et al., 2008) under project ID 14533.

Free IgA Measurement and ELISA's

Intestinal supernatants containing free IgA were isolated as described above in Bacterial Flow Cytometry and Antibodies. ELISA's were performed according to the protocol included in the Bethyl Mouse IgA or IgM Quantitation Set. Briefly, ELISA plates (Bethyl) were coated with goat anti-mouse IgA (Bethyl) or goat anti-mouse IgM (Bethyl) and washed with an ELISA plate washer. Plates were then blocked and washed. Experimental samples and standards were added to wells and incubated for one hour at room temperature. All samples were run in duplicate and were serially diluted along the plate. Plates were then washed and incubated with goat anti-mouse IgA or IgM-HRP (Bethyl). Plates were washed again and developed in the dark using TMB substrate (Bethyl) and 0.18M H_2SO_4 to stop the reaction. Plates were read using an ELISA plate reader (Bio-Tek) and sample values quantified by comparison to standards fit to a four-parameter logistic curve.

MACS Purification of Bacteria

Bacteria were stained with biotinylated goat anti-mouse IgA and streptavidin-APC as described above under Bacterial Flow Cytometry and Antibodies. After streptavidin-APC staining, cells were washed and resuspended in 1 mL PBS with anti-APC MACS beads (1:10 dilution, Miltenyi) for 20 minutes on ice. Cells were then washed and resuspended in 2 mL PBS prior to MACS separation. At this point an aliquot was saved for DNA exraction and 16S rRNA gene sequencing (Unfractionated Control) and an aliquot was saved for flow cytometric analysis.

Samples were separated using an autoMACS separator (Miltenyi) using the posselds program. Positive and negative fractions were collected and the negative fraction was saved for DNA extraction and16S rRNA gene sequencing (IgA^- fraction). The positive fraction was further purified by running a second time on the autoMACS using the posseld2 program and the positive fraction was collected and saved for DNA extraction and 16S rRNA gene sequencing (IgA^+ fraction). Post-MACS fractions were analyzed for purity by flow cytometry. Positive fractions were typically >95% IgA^+ and negative fractions were typically <0.5% IgA^+.

Lamina Propria Cell Isolation

Small intestines or colons (excluding the cecum) were excised and fat, Peyer's patches, and intestinal contents were removed. Intestines were opened longitudinally and cut into ~1 cm pieces. Intestinal pieces were placed into RPMI 1% FCS 1 mM EDTA and shaken at 37C for 15 minutes. Pieces were collected on a 100 μm cell strainer (Fisher) and placed in fresh RPMI 1% FCS 1 mM EDTA at 37C for 15 minutes with shaking. These fractions contain predominantly intraepithelial lymphocytes and were discarded. Intestinal pieces were collected on a 100 μm cell strainer and placed in RPMI 20% FCS with 0.5 mg/mL collagenase A (Roche) and 0.1 mg/mL DNase I (Roche) for 30 minutes at 37C with shaking. Intestinal pieces were again collected on a 100 μm cell strainer and placed in fresh RPMI 20% FCS with collagenase and DNase for an additional 30 mins at 37C with shaking. Supernatant was again collected by filtering through a 100 μm cell strainer and the strainer was washed with 30 mL RPMI. The two lamina propria lymphocyte fractions were combined and subjected to centrifugation in 40% percoll (Sigma) to further remove epithelial cells and debris.

Assessment of Free IgA Commensal Reactivity

6 *Rag1*$^{-/-}$ and 6 C57BL/6 females were co-housed for 3 weeks to allow equilibration of microbial communities. Each B6 mouse was paired with a co-housed *Rag1*$^{-/-}$ mouse. B6 ileal or colonic contents were processed as described above in Bacterial Flow Cytometry and Antibodies. B6 bacterial pellets were assayed for endogenous bacterial coating and free IgA was isolated. A bacterial aliquot was saved for 16S sequencing. *Rag1*$^{-/-}$ ileal or colonic contents were isolated by the same manner and aliquots were saved for 16S sequencing. *Rag1*$^{-/-}$ ileal or colonic bacteria were split into two samples: one that was stained as a negative control and a second that was resuspended in 100 uL of 1X intestinal supernatant from the ileum or cecum of their co-housed B6 mouse. Intestinal supernatants were filtered through a 0.45 μm syringe filter (Fisher) prior to staining to eliminate any residual bacteria from the supernatant. Ileal supernatants contained 100-400 μg/mL free IgA and colonic supernatants contained 20-70 μg/mL free IgA. *Rag1*$^{-/-}$ bacteria were stained with free IgA on ice for 20 minutes and then washed and stained with anti-mouse IgA as described above in Bacterial Flow Cytometry and Antibodies.

Rag1$^{-/-}$ B cell transfers

4-7 week old *Rag1*$^{-/-}$ mice were used as recipients and mice were analyzed 5 weeks after transfer of indicated populations. Data are representative of 3 separate experiments sorted separately. *Rag1*$^{-/-}$ mice received the following sorted populations: 1) 500,000 peritoneal B1 ($CD19^+CD23^-F4/80^-$; in one experiment cells were additionally sorted $IgM^{hi}IgD^{lo}$) i.p.; 2) 500,000 peritoneal B1 plus 1,000,000 splenic CD4 and CD8 T cells (sorted $CD4^+$ or $CD8^+$) i.p.; 3) 250,000 peritoneal B1a ($CD19^+CD23^-F4/80^-CD5^+B220^{lo}$) i.p.; 4) 250,000 peritoneal B1b ($CD19^+CD23^-F4/80^-CD5^-B220^{lo}$) i.p.; 5) 1,000,000 splenic B2 ($CD19^+B220^+CD23^+CD21^+$) i.v.; 6) 1,000,000 splenic B2 + 1,000,000 splenic CD4 and CD8 T cells i.v. All populations were verified for purity after sorting prior to injection.

Human Samples

Human study was approved by the University of Chicago Institutional Review Board. Subjects were recruited from University of Chicago Medical Center patients undergoing routine screening colonoscopies. The patient's medical records were reviewed before consenting to ensure that patients were eligible for this study. Exclusion criteria included being above 75 years in age, below 18 years of age, status-post organ transplant, pregnancy, positive screening and confirmatory tests for HIV or Hepatitis B or C, history of *C. difficile*, history of GI resection, history of colorectal cancer, history of inflammatory bowel disease or celiac disease, history of autoimmune disorders, and other co-morbidities including chronic kidney disease or cardiovascular disease requiring anticoagulants. The collection of lavages was at the endoscopist's discretion. Patients were approached the morning of their procedures in the prep area and informed consent was acquired before the administration of the IV. 50mL of sterile water used for irrigation was injected through the endoscope into either the terminal ileum or the ascending colon (doctors were instructed to flush with water at 10cm distal to the ileocecal valve). Ileal lavages were collected first. The doctors aspirated into a fluid trap until 20-30mL of water was recovered. The lavage was immediately transferred to a 50mL conical tube and placed on ice until processing. The lavages were completed before brushings or biopsies were taken. Samples were processed and stained by flow cytometry the same day they were collected (see Bacterial Flow Cytometry and Antibodies above).

Immunofluorescent microscopy and Image Quantification

Slides were fixed using Carnoy solution (Ricca) and embedded in paraffin at the University of Chicago Surgical Pathology Laboratory. To deparaffinize tissue, slides were warmed at 50C for 60 minutess in a slide oven and then subjected to 4 x 3 minute incubations in xylenes (Sigma)

and 4 x 3 minute incubations in absolute EtOH (Sigma) at room temperature. Slides were warmed for an additional 25 minutes at 50 ºC. A Dako pen was used to create a hydrophobic barrier around the staining area and slides were briefly air dried. Slides were then placed in TBS-T for 20 minutes at RT with gentle shaking in a slide beaker. Slides were blocked by incubation in TBS-T supplemented with 10% normal goat serum (Jackson Immunoresearch) 5% BSA (Fisher) and 1:400 Fc block (BD) for 30 minutes in a humidified chamber. Slides were rinsed in TBS-T. Texas-Red conjugated goat anti-mouse IgA (Southern Bitoech) was added at a 1:200 dilution in TBS-T for 45 minutes in the dark in a humidified chamber. Slides were washed three times for 10 minutes in TBS-T followed by 10 minutes in TBS and 10 minutes in PBS in a slide beaker with gentle shaking at room temperature. Sections were stained with DAPI for 5 minutes at room temperature and then rinsed three times in PBS. Fluoromount anti-fade mountant (Southern Biotech) and a cover slip were applied and slides were imaged within 24 hours of staining on an Axiovert 200M fluorescent microscope at the University of Chicago Microscopy Core. Images were further analyzed using SlideBook (Intelligent Imaging). Images were quantified manually by counting IgA^+ cells per villus.

Immunoglobulin Repertoire Sequencing

RNA was extracted from 200,000 sorted peritoneal B1a (pooled from 5 mice), peritoneal B1b (pooled from 5 mice),, splenic B2 (pooled from 2 mice), WT IgA^+ plasma cells (pooled from 4 mice), or *Tcrb*$^{-/-}$*d*$^{-/-}$ IgA^+ plasma cells (pooled from 8 mice) using an RNeasy mini kit (Qiagen). RNA was sent on dry ice to iRepertoire, Inc where cDNA synthesis and PCR followed by analysis on an Illumina MiSeq were performed using primers and reagents proprietary to iRepertoire, Inc. Approximately 1,300,000 unique reads were obtained for each sample. Data were analyzed using iRWeb (iRepertoire, Inc.).

Monoclonal Antibody Generation and Bacterial Staining

Small intestinal lamina propria lymphocytes were isolated and pooled from three *Tcrb*$^{-/-}$*d*$^{-/-}$ mice and single IgA^{+} plasma cells were sorted into 96 well PCR plates (BioRad) using a FACSAria (Becton Dickinson). Recombinant monoclonal antibodies were generated using methods and primers described in Tiller, Busse and Wardemann (*89*). cDNA was generated using SuperScript III First Strand cDNA Synthesis System (Invitrogen) and nested PCR was performed using DreamTaq Green 2X Master Mix (Life Technologies). After sequencing of products from the second PCR reaction, antibodies were cloned using gene-specific primers and Q5 DNA Polymerase (New England Biolabs), restriction digested, and ligated into digested human IgG1, human IgK, or human IgL expression vectors, transformed into *E. coli* (Agilent XL10 Gold Ultracompetent Cells), and plated on LB + carbenicillin agar. Construct minipreps were sequenced to confirm identity with second PCR product and correct constructs were transformed into *E. coli* (Invitrogen OneShot Top 10) and midiprepped (Qiagen HiSpeed Midi Kit). Paired IgH and IgK or IgL were then transfected into HEK293T cells and culture supernatants were harvested, sterile filtered, and stored at 4ºC with 0.05% sodium azide (Sigma). Supernatants from untransfected cultures prepared at the same time were harvested for use as a negative control. Antibody concentrations were assessed by sandwich ELISA using mouse anti-human Kappa or mouse anti-human Lambda (Southern Biotech) as a capture reagent and mouse anti-Human IgG1 Fc-HRP as a detection reagent. mAbs 02A11, 02B6, 02B12, and 02C12 have an IgK light chain and mAb 02B5 has an IgL light chain.

Total small intestinal or colonic bacteria (isolated as described above) were pooled from two *Rag1*$^{-/-}$ littermates and filtered through a 70 μm cell strainer. Bacteria were resuspended in PBS with SYTO BC (Life Technologies) and culture supernatants were added at a 1:10 dilution

(representing a final staining concentration of ~2 μg/mL recombinant antibody). Cells were washed and resuspended in PBS with anti-human IgG-APC (Biolegend; clone HP6017). Cells were washed again and resuspended in PBS with DAPI for analysis by flow cytometry. Pure saturated cultures of *Bacteroides fragilis* were stained by the same procedure.

CHAPTER 3

REFINED PROTOCOL FOR GENERATING MONOCLONAL ANTIBODIES FROM SINGLE HUMAN AND MURINE B CELLS

Irvin Y. Ho[*,a], Jeffrey J. Bunker[*,b,c], Steven A. Erickson[b,c], Karlynn E. Neu[a,c], Min Huang[a], Mario Cortese[d], Bali Pulendran[d,e], Patrick C. Wilson[‡,a,c]

[a]Department of Medicine, Section of Rheumatology, Gwen Knapp Center for Lupus and Immunology Research, University of Chicago, 924 E 57th Street R422, Chicago, Illinois, 60637, USA

[b]Department of Pathology, University of Chicago, 929 E 57th Street W503S, Chicago, Illinois, 60637, USA

[c]Committee on Immunology, University of Chicago

[d]Emory Vaccine Center, Yerkes National Primate Research Center, Atlanta, GA, 30329, USA

[e]Department of Pathology, Emory University School of Medicine, Atlanta, GA, 30322, USA

[*]Irvin Y. Ho and Jeffrey J. Bunker made equal contributions to this work.

[‡]Corresponding author

J. Immunol. Methods. 2016 Nov;438:67-70. doi: 10.1016/j.jim.2016.09.001.

Abstract

Generating monoclonal antibodies from single B cells is a valuable tool for characterizing the specificity and functional properties of humoral responses. We and others developed protocols that have facilitated major advances in our understanding of B cell development, tolerance, and effector responses to HIV and influenza. Here, we demonstrate various refinements and dramatically reduce the time required to produce recombinant antibodies. Further, we present new methods for cloning and isolating antibodies from cells with lower immunoglobulin mRNA levels that may be resistant to traditional techniques. Together, these refinements significantly increase single-cell antibody expression efficiency and are easily integrated into established and novel pipelines.

Keywords

monoclonal antibodies; single-cell PCR; human antibodies; gibson assembly; antibody expression

Technical Note

Antibodies are the primary mediator of humoral immunity, so they are a recurrent focus of scientific inquiry and medical discovery. In recent years, characterization of humoral responses by production of monoclonal antibodies from single cells has enabled rapid advances in B cell biology due to the high throughput and efficiency of these methods (*90-92*). These include the isolation of large numbers of broadly neutralizing antibodies against diverse pathogens like HIV and influenza, which are revolutionizing vaccine and therapeutic design. Single cells from a population of interest are isolated using flow cytometry then immunoglobulin genes from each cell are cloned into a vector for protein expression. The resulting antibodies are used for downstream assays to study their specificity, function, and repertoire characteristics.

A popular use for this involves screening panels of monoclonal antibodies, allowing a clonal assessment of the specificities present in a population of interest. Antibodies derived from plasmablasts, the temporary effector cells that peak 7 days after an immune response, present an opportunity to study acute infection and vaccination (*93, 94*). Memory B cells give access to affinity-matured antibodies, especially those formed during chronic or repeated infections (*95, 96*). An advantage of this method over traditional serum or hybridoma methods is that rare single cells with desirable antibodies can be isolated. Characterization of individual monoclonal antibodies yields data on specificity, binding conformation, reactivity breadth and potency, and protective capacity. Studies using these methods have shed light on potential targets for universal vaccine development and provide benchmarks for evaluating future therapeutics.

Here, we show several refinements for single-cell cloning and antibody expression that eliminate bottlenecks by replacing various single-sample manipulations with high-throughput alternatives. For large-scale projects, these changes are easily implemented and noticeably increase the pace at which antibodies can be generated. Further, our methods enable high-throughput isolation and characterization of antibodies from cells with relatively low immunoglobulin expression levels such as naïve or memory B cells. Limitations that are inherent to generating antibodies from single cells remain, including cell fragility (plasmablasts cannot be frozen and thawed) and the time-consuming nature of sorting cells and transfecting individual antibodies. Additionally, the lack of PCR error correcting mechanisms necessitate redundancy measures and the occasional redo. Instructions and primers for creating both fully human and chimeric (murine variable region and human constant region) antibodies are included.

Methods

This section describes the steps that are substantially different from our previously published protocol (*90*). A complete protocol, which includes other modifications and quality-of-life changes, is included as supplementary material. **Table 1** compares the bench time required for each step for our old protocol and this new protocol.

Table 1. Comparison of the bench time required to perform the steps in the protocol.

SMITH, NATURE METHODS, 2009	STEP	NEW PROTOCOL
Unchanged	Blood draw and flow cytometry	Unchanged
Unchanged	cDNA prep	Unchanged (RNA bead purification: add 45 minutes/plate)
Unchanged	PCR	Unchanged
1 day, 100 sequences	Prepare expression vector	**15 minutes, 96 sequences**
1 hour, 24 sequences	Transformation	**1 hour, 96 sequences**
Unchanged	Plasmid DNA preparation	Unchanged
Unchanged	Cell culture and transfection	Unchanged
1 day, 24 antibodies	Antibody purification	**45 minutes, 24 antibodies**

We applied this procedure to human plasmablasts isolated seven days after seasonal influenza vaccination and pneumococcal vaccination. We validated the cloning efficiency of the new protocol **(Figure 13a)** and confirmed the production of vaccine-specific antibodies by ELISA (**Figures 13b, 13c**).

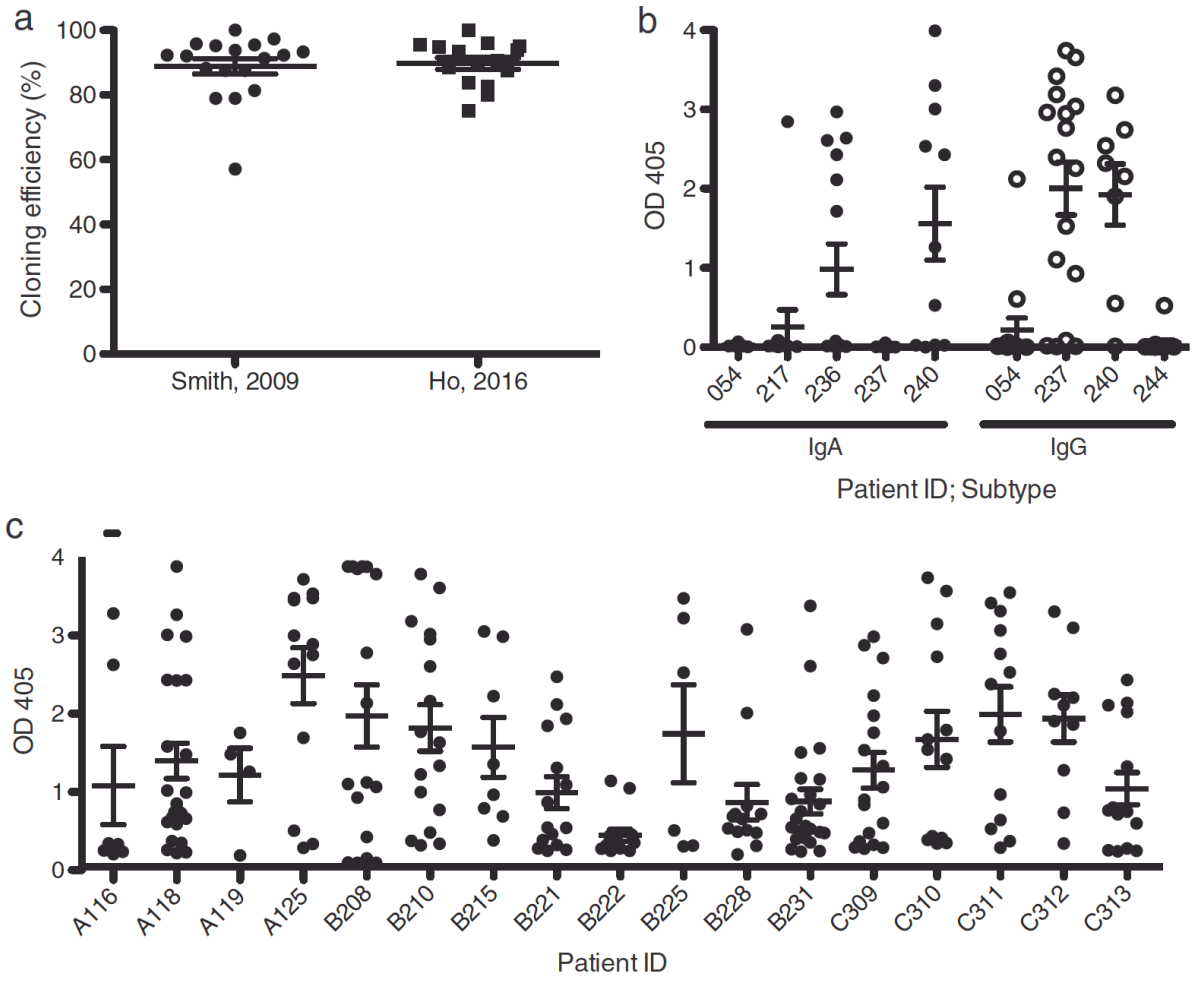

Figure 13. A) Comparison of cloning efficiency (the proportion of sequences with a consensus miniprep sequence after one attempt) for old and new protocols; each data point represents a separate plate. **B)** ELISA vaccine binding data for 115 influenza vaccine-induced IgG and IgA monoclonal antibodies, grouped by subtype and subject ID. **C)** ELISA vaccine binding data for 231 pneumococcal vaccine-induced IgG monoclonal antibodies, grouped by subject ID.

Peripheral blood samples were collected in accordance with the University of Chicago Institutional Review Board (#09-043-A) and informed consent was obtained from all subjects.

cDNA preparation

To prepare template cDNA from lysed cells, a non-specific cDNA synthesis kit is used rather than immunoglobulin-specific primers. With specific primers, for each sample plate only one of

the light chain genes (lambda or kappa) can be reverse transcribed, and antibodies that use the other gene are lost. With non-specific primers, both lambda and kappa chain DNA can be recovered from the same plate.

Important: use RNase-free precautions.

Direct cDNA synthesis from sorted and lysed cells

This is efficient for most cell types, especially plasmablasts. Non-plasmablast human cells may experience slightly diminished PCR efficiency.

Note: Sort cells into 10 µl/well of catch buffer (for ten half-plates: 5 ml RNase-free water, 50 µl 1M Tris pH 8.0, 125 µl RNasin; make fresh each time)

1. Create the master mix.

Table 2. cDNA synthesis master mix.

cDNA reaction	**1 well**
5x Buffer Mix	3 µl
Maxima Enzyme Mix	1.5 µl
5% IGEPAL	1.5 µl

2. Aliquot 6 µl master mix into each well with catch buffer, for a total reaction volume of 16 µl. Run the following program. Store plates at -20°C.

25°C for 10 min
50°C for 30 min
85°C for 5 min
4°C forever

cDNA synthesis after RNA purification

Purification with SPRI beads removes debris and other contaminants, increasing the efficiency of cDNA synthesis and subsequent PCRs (*97*). A variety of murine non-plasmablast cells amplify very inefficiently; SPRI purification increases the yield of naïve cells, small intestinal IgA

plasma cells, and colonic IgA plasma cells by 41%, 17%, and 127% respectively (**Figure 14**). However, this technique may be useful for all plates that have low PCR efficiency.

Note: Do not sort cells into catch buffer. Instead, use 5 µl/well of TCL buffer and 1% beta-mercaptoethanol (vol/vol). Plates can be flash-frozen on dry ice and stored at -80°C.

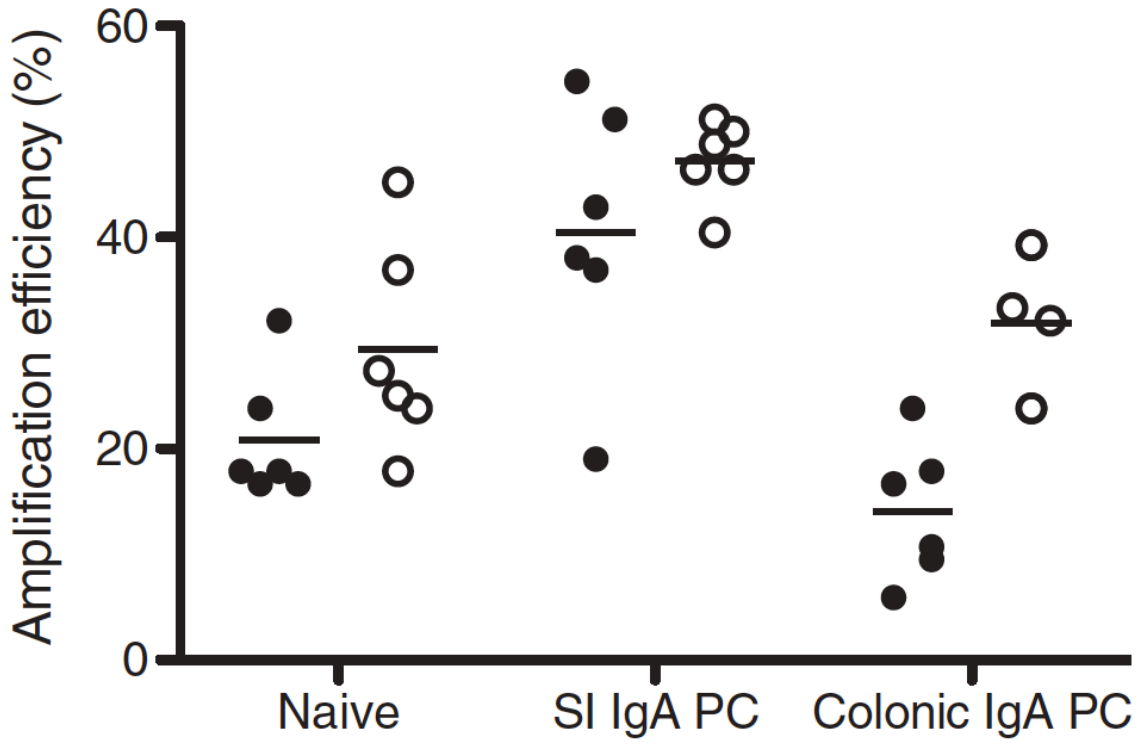

Figure 14. PCR amplification efficiency of various murine cell types, expressed as the percentage of wells that have a successfully amplified heavy and light chain; each data point represents a plate.

1. Warm RNase-free SPRI beads to room temperature.

2. Add 10 µl nuclease-free water to each sample, then add 33 µl SPRI beads to each sample. Cover plate to prevent contamination and incubate at room temperature for 10 min.

3. Place the plate on top of the magnetic plate and incubate, covered, at room temperature for 5 minutes.

4. Wash the plate 3x with 75 µl 80% EtOH, incubating 30 sec each cycle. Upon final aspiration, air dry for 8 min and remove from the magnetic plate.

5. Begin cDNA synthesis by resuspending beads in 10 µl/well reverse transcription mix #1, and thermocycle.

Table 3. cDNA reaction #1 master mix.

cDNA reaction #1	**1 well**
10mM dNTPs	1.25 µl
Oligo $d(T)_{18}V$	1 µl
Template RNA pellet	-
Nuclease-free water	to 10 µl

65°C for 5 min
4°C forever

6. Incubate on ice for 1 min, then add reverse transcription mix #2; aliquot 10 µl/well and cycle. Store plates at -20°C.

Table 3, continued. cDNA reaction #2 master mix.

cDNA reaction #2	**1 well**
5x SuperScript IV RT Buffer	4 µl
100 mM DTT	1 µl
RNaseOUT	0.5 µl
SuperScript IV Reverse Transcriptase	0.25 µl
Nuclease-free water	to 10 µl

50°C for 1 hr

80°C for 10 min
4°C forever

Cloning

After cDNA preparation, two rounds of PCR are performed to amplify immunoglobulin genes for sequencing. The products of the first round are used as templates in a cloning PCR reaction to generate DNA for insertion into expression vectors. We designed sequence-specific primers that each contain an overhanging region that overlaps with the proper expression vector. To join the insert with the vector, we use Gibson assembly, a rapid procedure for assembling DNA fragments with overlapping ends (*98*) (**Figure 15**). Overall, this process is much quicker than the traditional digest-ligation method and slightly more reliable, reducing the number of sequences that must be redone (data not shown).

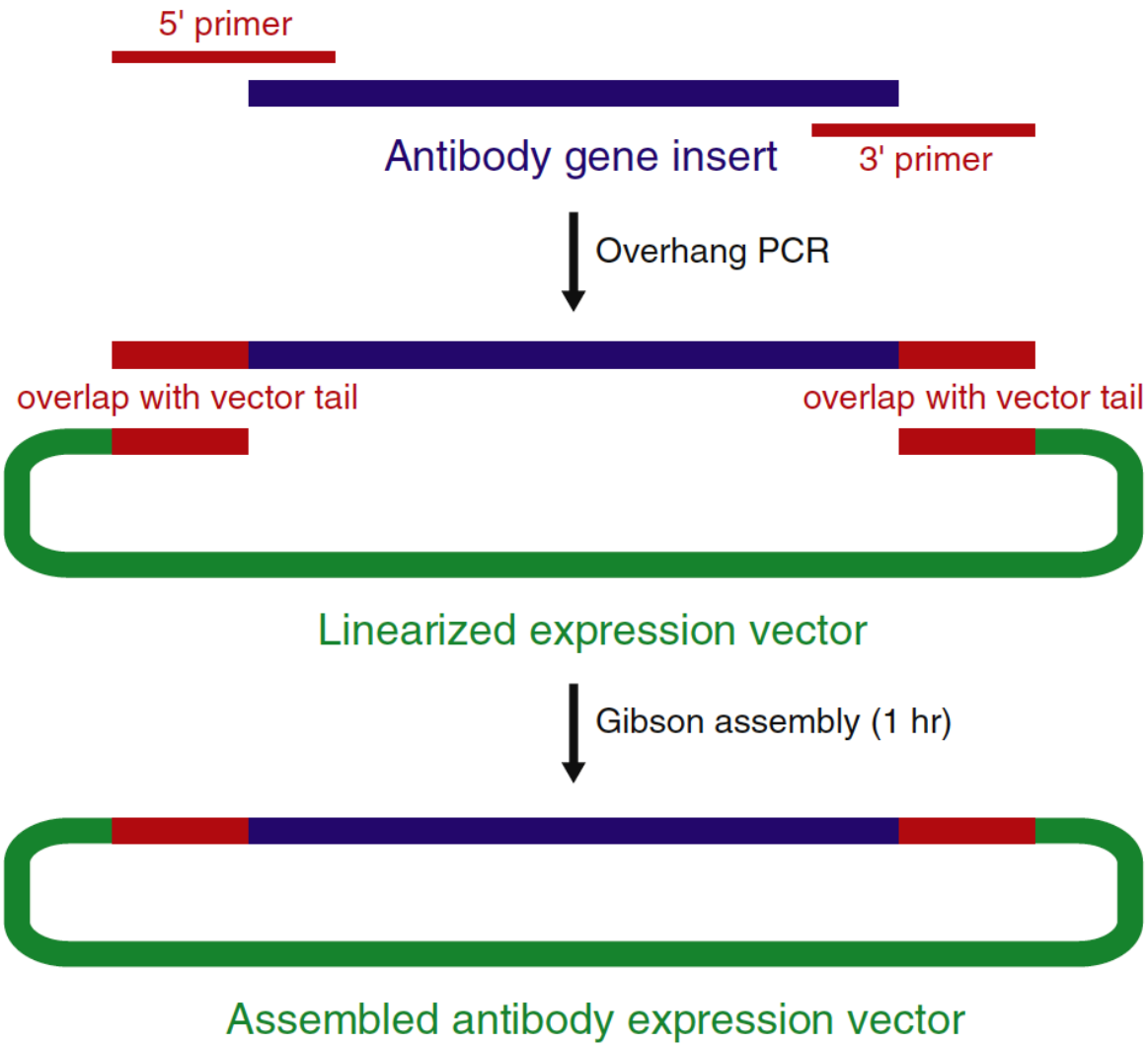

Figure 15. Schematic for cloning antibody genes into expression vectors. PCR with gene-specific overhang primers frames the antibody gene on both sides with approximately 20-25 bp of overlap with the expression vector. Gibson assembly is then used to join the two fragments.

Linearize plasmids to prepare expression vectors for assembly

(Vector sequences can be found on NCBI GenBank: accession numbers **FJ475055**, **FJ475056** and **FJ517647** for heavy, kappa, and lambda, respectively; the vectors are available upon request)

1. Reaction setup

Note: 25 ng gel-purified vector is needed per assembly reaction

Table 4. Vector digest master mix.

Vector digest	
Plasmid with heavy, kappa, or lambda vector	5 µg
10x FastDigest buffer	5 µl
Chain-specific restriction enzyme	2.5 µl
BshTI (AgeI)	2.5 µl
H_2O	to 50 µl

Chain-specific restriction enzymes:

Heavy: SalI
Kappa: Pfl23II (BsiWI)
Lambda: Xho1

2. Incubate at 37°C for 15 minutes, then add 2.5 µl FastAP. Repeat.

3. Incubate at 37°C for 10 minutes.

4. Heat-inactivate at 80°C for 10 minutes.

5. Run on a 1.2% agarose gel (100V for 5 min, then 75V for 75 min) and cut bands with the digested vectors from the gel for extraction.

6. Purify by following the protocol outlined in the GeneJET Gel Extraction Kit with one exception: elute the final product in 40 µl EB.

Perform overlap PCR with Gibson assembly primers

Important: to avoid contamination, avoid contact with the interior of Eppendorf tubes and limit airflow over open racks. Wipe pipettes and surfaces with DNA off before use.

1. Create a master mix for each combination of 5' and 3' primers (for details on choosing primers, refer to the Supplementary Methods). The template is the unpurified product of the 1st PCR step. Include a template-less negative control for each master mix of primers to ensure there is no contamination.

Table 5. Human cloning PCR master mix.

Human cloning PCR	**1 well**
5' primer (10 µM)	1 µl
3' primer (10 µM)	1 µl
2X Green DreamTaq MasterMix	12.5 µl
Nuclease-free H_2O	9 µl
1st PCR product	1.5 µl

Thermocycle:

94°C for 4 min
Repeat 40x:
    94°C for 30 sec
    58°C for 30 sec
    72°C for 45 sec
72°C for 8 min
4°C forever

The above PCR details are optimized for human primers; see the supplementary methods for mouse cloning PCR instructions.

2. Run 2 µl PCR product directly on a 1% agarose gel to confirm a successful reaction and to check for contamination in the negative control wells.

Perform Gibson assembly

1. Reaction setup (it is not necessary to purify the cloning PCR products: Gibson assembly and bacterial transformation are equally effective when using unpurified PCR products)

Table 6. Gibson assembly master mix.

Gibson assembly	**1 well**
NEBuilder 2X MasterMix	5 µl
Linearized heavy, kappa, or lambda vector	25 ng
Cloning PCR product	1 µl
H_2O	to 10 µl

2. Incubate the reaction in a thermocycler at 50°C for 1 hr. The assembled product can be stored at -20°C before transformation.

Acknowledgments

The authors thank Carole Henry for technical discussions and assistance.

This project was funded in parts with federal funds from the National Institute of Allergy and Infectious Diseases, National Institutes of Health, Department of Health and Human Services, under CEIRS contract HHSN272201400006C (P.C.W.) and NIH grants U19AI109946, P01AI097092, U19AI057266, U19AI05766-11, U19AI082724, and U19AI090023. J.J.B. was supported by NIH grant F30AI124476, NIH Medical Scientist Training Program grant T32GM007281, and the University of Chicago Digestive Diseases Research Core Center grant P30DK42086.

Supplementary Methods – Full Protocol

This full protocol is similar to the protocol presented in our previous paper (*90*). It incorporates several altered or updated procedures in addition to the modifications introduced in the methods section.

Sample collection and B cell enrichment (Step 1)

For best results, begin processing blood immediately after collection. If necessary, samples may be stored overnight at 4°C, but processing should begin within 18 hr of collection. Depending on the B cell subset, PBMCs frozen in appropriate tissue culture freeze-down media can also be used, albeit with reduced efficiency.

If ASCs are the cells of interest: ASCs become unstable and begin to die after removal from whole blood, so cells should be used immediately in ELISPOT and flow cytometry.

Materials:

RosetteSep (STEMCELL, 15064)
Lymphocyte Separation Media (Mediatech, 25072CV)

1.1. Collect 40 ml blood in citric acid dextrose tubes 7 days post-vaccination. Typically, one tube is for ELISPOT and three tubes are for sorting.

1.2. Pool the whole blood in a 50 ml conical tube and add 100 µl RosetteSep. Mix well by inverting. Incubate at room temperature for 20 min.

1.3. Aliquot the blood into three separate conical tubes, then dilute each with an equal volume of 0.02% BSA/PBS.

1.4. Set up three new 50 ml conical tubes with 15 ml lymphocyte separation media. To each tube, carefully overlay the diluted blood (no more than 30 ml blood per tube). Centrifuge at room temperature and 800g for 30 min with no brake.

1.5. Collect the PBMC layer, which is sandwiched between the serum and the lymphocyte separation media, and transfer to a new conical tube. Rinse the PBMCs by adding 0.02% BSA/PBS to 50 ml. Centrifuge at room temperature and 800g for 5-10 min with no brake. Remove the supernatant.

1.6. Combine cells from different tubes by filtering through a 40 μm cell strainer into a new conical tube. Add 0.02% BSA/PBS to 50 ml. Centrifuge at room temperature and 360 g for 5-10 min (brake can be used).

ELISPOT (Step 2)

Materials:

Filter plate with hydrophilic MCE membrane (Millipore, MSHAN4B50)
Goat anti-human IgA, IgG, IgM (KPL, 01-10-07)
Goat anti-human IgA-biotin (Southern Biotech, 2050-08)
Goat anti-human IgG-biotin (Southern Biotech, 2040-08)
Goat anti-human IgM-biotin (Southern Biotech, 2020-08)
Goat anti-mouse IgA, IgG, IgM (KPL, 01-18-07)

Goat anti-mouse IgA-biotin (Southern Biotech, 1040-08)
Goat anti-mouse IgG-biotin (Southern Biotech, 1030-08)
Goat anti-mouse IgM-biotin (Southern Biotech, 1021-08)
Streptavidin-AP (Southern Biotech, 7100-04)
Tween 20 (Sigma, P9416)
RPMI (Invitrogen, 11875135)
Penicillin-Streptomycin (Gibco, 15140)
L-Glutamine (Gibco, 25030)
FBS (Gibco, 16000)
Beta-mercaptoethanol (Pierce, 35602)
HEPES (Invitrogen, 15630)
Sodium pyruvate (Invitrogen, 11360)
1-Step NBT/BCIP (Thermo, 34042)

Reagents:

Cell media:

RPMI
1% P/S
1% HEPES
1% sodium pyruvate
1% L-glutamine
20% FBS
50 mM beta-mercaptoethanol

Complete media:

RPMI
1% P/S
1% HEPES
1% L-glutamine
10% FBS

Blocking media:

RPMI
10% FBS

2.1. Coat individual columns of filter plates with 100 µl/well of coating antibody (10 µg/ml goat species-specific IgA, IgG, and IgM in PBS) and virus, vaccine (dilute approximately 1:20 in PBS), or other desired antigen. Determine exact coating protein concentrations

experimentally to ensure adequate spot size. Spots should be large enough to be counted clearly. Incubate plates at 4°C for at least 18 hr and up to 7 days.

2.2. Wash 3x with 200 µl/well PBS/0.05% Tween (vol/vol) using a multichannel pipette.

Important: when washing, do not touch the membrane with pipette tips, and pipette with the plate at an angle. To remove liquid between washes, pour quickly. Refrain from tapping plates on paper towels to dry them unless necessary.

2.3. Wash 4x with 200 µl PBS using a multichannel pipette.

2.4. Block with 200 µl/well blocking media. Incubate at 37°C for 2 hr.

2.5. Aliquot 0.5-1 million PBMCs per condition (each coated column on the filter plate). Wash cells with cell media and centrifuge at room temperature and 360g for 5-10 min. Repeat twice. Resuspend PBMCs in complete media (200 µl per condition).

2.6. In a U-bottom plate, add 200 µl cells to row 1. Add 100 µl complete media to rows 2-7.

2.7. Make 1:2 serial dilutions of cells in rows 1-7 by progressively transferring and mixing 100 µl from each row to the next. Add 100 µl cell media to row 8.

2.8. Remove blocking media from ELISPOT plates by pouring.

2.9. Transfer 100 µl/well cell dilutions to the ELISPOT plate. Incubate overnight at 37°C and 5% CO_2.

2.10. Wash 4x with 200 µl/well PBS/0.05% Tween (vol/vol) using a multichannel pipette.

2.11. Wash 4x with 200 µl/well PBS using a multichannel pipette.

2.12. Make the species-specific, isotype-specific, biotin-conjugated goat antibody mixture for cell detection. Add each at 1:1000 to PBS/0.05% Tween/1% FBS.

2.13. Add 100 µl/well revealing solution and incubate at room temperature for 2 hr.

2.14. Wash 4x with 200 µl/well PBS/0.05% Tween (vol/vol) using a multichannel pipette.

2.15. Prepare the secondary antibody by adding 1:500 streptavidin-AP to PBS/0.05% Tween/1% FBS.

2.16. Add 100 µl/well secondary antibody and incubate at room temperature for 2 hr.

2.17. Wash 3x with 200 µl/well PBS/0.05% Tween (vol/vol) using a multichannel pipette.

2.18. Wash 2x with 200 µl/well PBS using a multichannel pipette. Let the PBS sit for 5 min during each wash cycle.

2.19. Add 100 µl/well NBT/BCIP to reveal the substrate. Incubate under a paper towel for 1-5 min at room temperature, or until dark spots appear.

2.20. Stop the revealing reaction by washing the plate under a faucet. Pat dry the inverted plate on a paper towel, then air dry in a drawer before reading spots with an ELISPOT analyzer. Spots are stable for several years at room temperature.

Flow cytometry (Step 3)

Begin with 4-8 million enriched PBMCs. This flow strategy is designed to isolate human plasmablasts, but can be modified to suit different requirements.

Materials:

CD3 FITC (Invitrogen, MHCD0301)
CD19 Pacific Blue (Biolegend, 302224)
CD27 PE (Biolegend, 302808)
CD38 AlexaFluor 647 (Biolegend, 303514)
DMEM (Gibco, 11965)
FBS (Gibco, 16000)
Penicillin-Streptomycin (Gibco, 15140)
L-Glutamine (Gibco, 25030)
RNasin (Promega, N2515)
TCL buffer (Qiagen, 1031576)
Beta-mercaptoethanol (Pierce, 35602)

Reagents:

Catch buffer (for ten half-plates; made fresh)
5 ml RNase-free water
50 µl 1M Tris pH 8.0
125 µl RNasin

TCL buffer
TCL buffer
1% beta-mercaptoethanol (vol/vol)

Staining buffer
PBS
2% FCS

3.1. As controls, for each fluorophore, prepare an aliquot of 0.5 x 10^6 cells in 100 µl staining buffer. Prepare an additional aliquot of 0.5 x 10^6 cells in 100 µl staining buffer that will remain unstained. Prepare the remaining cells for sorting in 500 µl staining buffer.

3.2. Add fluorophores (CD3 FITC, anti-CD27 PE, anti-CD38 APC-Cy5.5, anti-CD19 Pacific Blue) to the sorting aliquot and also individually to the aliquots designated as compensation controls. Incubate cells at 4°C for 30 min.

Note: Each fluorophore should be titrated to distinguish single color populations before beginning the experiment.

3.3. Wash twice with 200 µl 0.2% BSA/PBS (vol/vol) and filter through a 40 µm cell strainer to prevent clogging.

3.4. Gate $CD19^+/CD3^-/CD27^{high}/CD38^{high}$ cells. Bulk sort the cells into tubes that contain complete DMEM (DMEM with 10% FBS, 1% P/S, 1% L-Glutamine).

3.5. Sort plasmablasts on forward vs side scatter using a live cell gate with doublet discrimination into 96-well PCR plates containing the desired buffer (catch buffer or TCL buffer, depending on whether RNA purification will be performed).

Sort cells from each sample into half-plates (columns 1-6 or 7-12). Reserve row H for buffer-only controls, which will be used to detect PCR contamination.

Use RNase-free precautions. Immediately seal plates and put on dry ice, then store at -80°C (for several years if necessary).

cDNA preparation (Step 4)

Refer to the technical methods section in the main paper.

Materials:

RNasin (Promega, N2515)
TCL buffer (Qiagen, 1031576)
SPRI beads (Beckman, A63987)
Ring Super Magnet Plate (Beckman, A32782)
RNase away (Thermo, 7003)
DNA off (Takara, 9036)
Maxima cDNA Synthesis Kit (Thermo, K1642)
IGEPAL CA-630 (Sigma, I8896)
SuperScript IV Synthesis System (Thermo, 18091200)
Hard-Shell Low-Profile Thin-Wall 96-Well Skirted PCR Plates (Bio-Rad, HSP9601)
Microseal “F” foil seals (Bio-Rad, MSF1001)

PCR (Step 5A /5B)

Important: to avoid contamination, avoid contact with the interior of Eppendorf tubes and limit airflow over open racks. Wipe pipettes and surfaces with DNA off before use.

Human 1st and 2nd PCR (Step 5A)

Three rounds of PCR are performed: 1st PCR, 2nd PCR, and Cloning PCR.

The template for the 1st PCR is the reverse transcription product from step 4A or 4B. The product of the 1st PCR is used as template DNA for both the 2nd PCR and the Cloning PCR. The 2nd PCR's product is sent for sequencing and the Cloning PCR's product is used in Gibson assembly and further cloning.

Materials:

DreamTaq Green PCR 2X MasterMix (Thermo, K1082)
NEBuffer 3 (NEB, B7003S)
CIP (NEB, M0290L)
ExoI (NEB, M0293L)

Table 7. Human single cell amplification PCR primers.

1st PCR heavy

5' L-VH 1	ACAGGTGCCCACTCCCAGGTGCAG
5' L-VH 3	AAGGTGTCCAGTGTGARGTGCAG
5' L-VH 4/6	CCCAGATGGGTCCTGTCCCAGGTGCAG
5' L-VH 5	CAAGGAGTCTGTTCCGAGGTGCAG
3' HuIgG-const-anti	TCTTGTCCACCTTGGTGTTGCT
3' Cm CH1 (IgM)	GGGAATTCTCACAGGAGACGA
3' IgA1-RT	CCTGGCTGGGTGGGAAGTTT

Table 7, continued.

1st PCR kappa

5' L Vk 1/2	ATGAGGSTCCCYGCTCAGCTGCTGG
5' L Vk 3	CTCTTCCTCCTGCTACTCTGGCTCCCAG
5' L Vk 4	ATTTCTCTGTTGCTCTGGATCTCTG
3' Ck 543–566	GTTTCTCGTAGTCTGCTTTGCTCA

1st PCR lambda

5' L Vl 1	GGTCCTGGGCCCAGTCTGTGCTG
5' L Vl 2	GGTCCTGGGCCCAGTCTGCCCTG
5' L Vl 3	GCTCTGTGACCTCCTATGAGCTG
5' L Vl 4/5/9	GGTCTCTCTCSCAGCYTGTGCTG
5' L Vl 6	GTTCTTGGGCCAATTTTATGCTG
5' L Vl 7	GGTCCAATTCYCAGGCTGTGGTG
5' L Vl 8	GAGTGGATTCTCAGACTGTGGTG
3' Cl	CACCAGTGTGGCCTTGTTGGCTTG

2nd PCR heavy

5' VH3a-sense	SARGTGCAGCTGGTGGAG
5' VH3b-sense	GAGGTGCAGCTGTTGGAG
5' VH1/5/7-sense	CTGCAACCGGTGTACATTCCGAGGTGCAGCTGGTGCAG
5' VH4-sense	CTGCAACCGGTGTACATTCCCAGGTGCAGCTGCAGGAG
3' Cgamma (IgG)	AGTAGTCCTTGACCAGGCAGCCCAG
3' MuD (IgM)	GGAATTCTCACAGGAGACGA
3' IgA1	CAGAGGCTCAGCGGGAAGACC

2nd PCR kappa

5' Pan Vk	ATGACCCAGWCTCCABYCWCCCTG
3' Ck 494–516	GTGCTGTCCTTGCTGTCCTGCT

2nd PCR lambda

5' AgeI Vl1	CTGCTACCGGTTCCTGGGCCCAGTCTGTGCTGACKCAG
5' AgeI Vl2	CTGCTACCGGTTCCTGGGCCCAGTCTGCCCTGACTCAG
5' AgeI Vl3	CTGCTACCGGTTCTGTGACCTCCTATGAGCTGACWCAG
5' AgeI Vl4/5	CTGCTACCGGTTCTCTCTCSCAGCYTGTGCTGACTCA
5' AgeI Vl6	CTGCTACCGGTTCTTGGGCCAATTTTATGCTGACTCAG
5' AgeI Vl7/8	CTGCTACCGGTTCCAATTCYCAGRCTGTGGTGACYCAG
5' XhoI Cl	CTCCTCACTCGAGGGYGGGAACAGAGTG

Vector sequencing

Ab-vec-sense	GCTTCGTTAGAACGCGGCTAC

5A.1. Prepare heavy, kappa, and lambda 1st PCR master mixes. Each half-plate of cDNA requires a total of three half-plate PCR setups (one for each chain).

Table 8. Human single cell 1st PCR master mix.

1st PCR (for 1 half-plate)	VH	VK	VL
2X Green DreamTaq MasterMix	500 µl	500 µl	500 µl
5' primers (60 µM)	8 µl (x4)	8 µl (x3)	8 µl (x7)
3' primers (60 µM)	8 µl (x3)	8 µl (x1)	8 µl (x1)
Nuclease-free H_2O	to 900 µl	to 900 µl	to 900 µl
cDNA template	2 µl	2 µl	2 µl

Aliquot 18 µl master mix to each half-plate, then use a multichannel pipette to add 2 µl cDNA template for a total reaction volume of 20 µl.

5A.2. Thermocycler instructions, 1st PCR:

94°C for 4 min
Repeat 15x:
    94°C for 30 sec
    51°C for 30 sec
    72°C for 55 sec
Repeat 30x:
    94°C for 30 sec
    56°C for 30 sec
    72°C for 55 sec
72°C for 8 min
4°C forever

5A.3. Prepare heavy, kappa, and lambda 2nd PCR master mixes. Plate layouts remain the same from the 1st PCR.

Typically, VH3 primers (VH3a and VH3b) are sufficient to amplify all heavy chain gene segments. However, for repertoire studies, separate VH1/5 and VH4 reactions should be run to ensure complete coverage.

Table 9. Human single cell 2nd PCR master mix.

2nd PCR (for 1 half-plate)	VH3	VH1/5, 4	VK	VL
2X Green DreamTaq MM	625 µl	625 µl	625 µl	625 µl
5' primers, 60 µM	8 µl (x2)	8 µl (x1)	8 µl (x1)	8 µl (x6)
3' primers, 60 µM	8 µl (x3)	8 µl (x3)	8 µl (x1)	8 µl (x1)
Nuclease-free H_2O	to 1125 µl	to 1125 µl	to 1125 µl	to 1125 µl
1st PCR product	2.5 µl	2.5 µl	2.5 µl	2.5 µl

Aliquot 22.5 µl master mix to each half-plate, then use a multichannel pipette to add 2.5 µl 1st PCR product for a total reaction volume of 25 µl.

5A.4. Thermocycler instructions, 2nd PCR:

94°C for 4 min
Repeat 50x:
    94°C for 30 sec
    57°C for 30 sec
    72°C for 45 sec
72°C for 10 min
4°C forever

5A.5. Run 2 µl of product directly on a 1.2% Agarose gel (130V, 25 min). Successful reactions are identified by a band at approximately 400 bp. Ensure there are no bands of this size in the negative control wells (row H). Generate a list of wells that have a heavy chain amplicon and at least one light chain amplicon (infrequently, the kappa and lambda PCRs will both produce a positive result).

5A.6. Run a PCR clean-up with 5 µl of these desirable PCR products to prepare them for sequencing.

Table 10. PCR clean-up master mix.

PCR clean-up	1 well (7 µl)	200 wells
dH_2O	0.7 µl	140 µl
NEBuffer	0.7 µl	140 µl
CIP (10 units/ul)	0.1 µl	20 µl
ExoI	0.5 µl	100 µl

2nd PCR product	5 µl	

Run at 37°C for 30 min then 80°C for 20 min.

5A.7. Sequence with the 5' primers used in the 2nd PCR (VH3a/b-sense, VH1/5-sense, VH4-sense, Pan Vk, and XhoI Cl primers).

Mouse 1st and 2nd PCR (Step 5B)

For heavy chain DNA, perform two PCR steps (nested PCR and cloning PCR). For kappa chain DNA, perform three PCR steps (1st PCR, 2nd PCR, and cloning PCR).

Materials:

Q5 Hot Start High-Fidelity Polymerase (NEB, M0493L)
dNTPs, PCR Grade (Qiagen, 201901)
One-Taq Hot Start Quick-Load 2X Master Mix (NEB, M0488L)
ExoSAP-IT (Affymetrix, 78202 4X1 ML)

Table 11. Mouse single cell amplification PCR primers.

Heavy PCR

5' MsVHE	GGGAATTCGAGGTGCAGCTGCAGGAGTCTGG
3' Cy1 outer (IgG1)	GGAAGGTGTGCACACCGCTGGAC
3' Cy2b outer (IgG2b)	GGAAGGTGTGCACACTGGAC
3' Cy2c outer (IgG2c)	GGAAGGTGTGCACACTGCTGGAC
3' Ca outer (IgA)	GAGGCGAGGGCAGGTGGAAAGTTCACGG
3' Cm outer (IgM)	AGGGGGCTCTCGCAGGAGACGAGG

Table 11, continued.

Kappa 1st PCR

5' VK3	TGCTGCTGCTCTGGGTTCCAG
5' VK4	ATTWTCAGCTTCCTGCTAATC
5' VK5	TTTTGCTTTTCTGGATTYCAG
5' VK6	TCGTGTTKCTSTGGTTGTCTG
5' VK689	ATGGAATCACAGRCYCWGGT
5' VK14	TCTTGTTGCTCTGGTTYCCAG
5' VK19	CAGTTCCTGGGGCTCTTGTTGTTC
5' VK20	CTCACTAGCTCTTCTCCTC
3' MCK	GATGGTGGGAAGATGGATACAGTT

Kappa 2nd PCR

5' mVkappa	GAYATTGTGMTSACMCARWCTMCA
3' BsiWI P-mJK01	GCCACCGTACGTTTGATTTCCAGCTTGGTG
3' BsiWI P-mJK02	GCCACCGTACGTTTTATTTCCAGCTTGGTC
3' BsiWI P-mJK03	GCCACCGTACGTTTTATTTCCAACTTTGTC
3' BsiWI P-mJK04	GCCACCGTACGTTTCAGCTCCAGCTTGGTC

5B.1. Set up wells for heavy chain amplification:

Table 12. Mouse single cell 1st PCR master mix.

Heavy PCR (1 well)	**IgG (40 µl)**	**IgA (40 µl)**	**IgM (40 µl)**
Q5 polymerase	0.4 µl	0.4 µl	0.4 µl
5X Q5 buffer	8 µl	8 µl	8 µl
5X Q5 high GC enhancer	8 µl	8 µl	8 µl
dNTPs (10 mM)	0.8 µl	0.8 µl	0.8 µl
5' MsVHE (100 µM)	0.2 µl	0.2 µl	0.2 µl
3' primers (100 µM)	0.2 µl (x3)	0.2 µl (x1)	0.2 µl (x1)
Nuclease-free H_2O	17 µl	17.4 µl	17.4 µl
cDNA template	5 µl	5 µl	5 µl

Transfer 35 µl master mix to each well then add 5 µl of cDNA template for a total reaction volume of 40 µl.

5B.2. Thermocycler instructions:

98°C for 30 sec
Repeat 10x:
    98°C for 10 sec
    60°C for 20 sec
    72°C for 45 sec
Repeat 50x:
    98°C for 10 sec
    72°C for 60 sec
72°C for 10 min
4°C forever

5B.3. Set up wells for the 1st PCR for kappa chain amplification:

Table 13. Mouse kappa 1st PCR master mix.

Kappa 1st PCR	**1 well (40 µl)**
Q5 polymerase	0.4 µl
5X Q5 buffer	8 µl
dNTPs (10 mM)	0.8 µl
5' primers (100 µM)	0.2 µl (x8)
3' mCK (100 µM)	0.2 µl
Nuclease-free H_2O	23.9 µl

cDNA template	5 µl

Transfer 35 µl master mix to each well then add 5 µl of cDNA template for a total reaction volume of 40 µl.

5B.4. Thermocycler instructions, 1st PCR:

98°C for 30 sec
Repeat 50x:
    98°C for 10 sec
    62°C for 30 sec
    72°C for 45 sec
72°C for 10 min
4°C forever

5B.5. Set up wells for the 2nd PCR for kappa chain amplification:

Table 14. Mouse kappa 2nd PCR master mix.

Kappa 2nd PCR	**1 well (40 µl)**
One-Taq 2X Master Mix	20 µl
5' mVkappa (10 µM)	0.8 µl
3' primers (10 µM)	0.8 µl (x3)
Nuclease-free H_2O	14.8 µl

1st PCR product	2 µl

Transfer 38 µl master mix to each well then add 2 µl of 1st PCR product for a total reaction volume of 40 µl.

5B.6. Thermocycler instructions, 2nd PCR:

94°C for 3 min
Repeat 50x:
    94°C for 30 sec
    45°C for 30 sec
    72°C for 45 sec
72°C for 10 min
4°C forever

5B.7. Run 2 µl of product from the heavy PCR and the 2nd kappa PCR on a 1.2% Agarose gel (130V, 25 min). Generate a list of wells that have amplicons for both chains.

5B.8. Run a PCR clean-up with ExoSAP-IT, following the manufacturer's protocol.

5B.9. Sequence the heavy chain sequences with 5' MsVHE and the kappa chain sequences with 3' mCK.

Cloning PCR (Step 6)

Prior to setting up the cloning PCR, use NCBI's IgBLAST or the IMGT database to determine the exact V and J gene composition for each antibody's heavy and light chains. V gene identity determines the forward primer for the cloning PCR and J gene identity determines the reverse primer. Many primers target conserved sequences so they can be used for more than one gene segment. For example, the human VH1/5/7 primer is used for any gene from the VH1, VH5, or VH7 families. The human VH3 primer is used for any gene from the VH3 family, except VH3-23, which instead uses the VH3-23 primer.

Typically, for a cloning PCR setup for all the antibodies derived from a half-plate of single cells, up to a few dozen master mixes (pairs of V/J primers) are required.

For details on running the human cloning PCR, refer to the technical methods section in the main paper.

Materials:

DreamTaq Green PCR 2X MasterMix (Thermo, K1082)
NEBuilder DNA Assembly 2X MasterMix (New England Biolabs, E2621)

Table 15. Human gene specific cloning primers.

VH1/5/7	ATCCTTTTTCTAGTAGCAACTGCAACCGGTGTACATTCCGAGGTGCAGCTGGTGCAG
VH3	ATCCTTTTTCTAGTAGCAACTGCAACCGGTGTACATTCTGAGGTGCAGCTGGTGGAG
VH3–23	ATCCTTTTTCTAGTAGCAACTGCAACCGGTGTACATTCTGAGGTGCAGCTGTTGGAG
VH4	ATCCTTTTTCTAGTAGCAACTGCAACCGGTGTACATTCCCAGGTGCAGCTGCAGGAG
VH4–34	ATCCTTTTTCTAGTAGCAACTGCAACCGGTGTACATTCCCAGGTGCAGCTACAGCAGTG

Table 15, continued

VH3–9/30/33	ATCCTTTTTCTAGTAGCAACTGCAACCGGTGTACATTCTGAAGTGCAGCT GGTGGAG
VH6–1	ATCCTTTTTCTAGTAGCAACTGCAACCGGTGTACATTCCCAGGTACAGCT GCAGCAG
Vk1	ATCCTTTTTCTAGTAGCAACTGCAACCGGTGTACATTCTGACATCCAGAT GACCCAGTC
Vk1–9/1–13	ATCCTTTTTCTAGTAGCAACTGCAACCGGTGTACATTCAGACATCCAGTT GACCCAGTCT
Vk1D–43/1–8	ATCCTTTTTCTAGTAGCAACTGCAACCGGTGTACATTGTGCCATCCGGAT GACCCAGTC
Vk2	ATCCTTTTTCTAGTAGCAACTGCAACCGGTGTACATGGGGATATTGTGAT GACCCAGAC
Vk2–28/2–30	ATCCTTTTTCTAGTAGCAACTGCAACCGGTGTACATGGGGATATTGTGAT GACTCAGTC
Vk3–11/3D-11	ATCCTTTTTCTAGTAGCAACTGCAACCGGTGTACATTCAGAAATTGTGTT GACACAGTC
Vk3–15/3D-15	ATCCTTTTTCTAGTAGCAACTGCAACCGGTGTACATTCAGAAATAGTGAT GACGCAGTC
Vk3–20/3D-20	ATCCTTTTTCTAGTAGCAACTGCAACCGGTGTACATTCAGAAATTGTGTT GACGCAGTCT
Vk4–1	ATCCTTTTTCTAGTAGCAACTGCAACCGGTGTACATTCGGACATCGTGAT GACCCAGTC
Vl1	ATCCTTTTTCTAGTAGCAACTGCAACCGGTTCCTGGGCCCAGTCTGTGCT GACKCAG
Vl2	ATCCTTTTTCTAGTAGCAACTGCAACCGGTTCCTGGGCCCAGTCTGCCCT GACTCAG
Vl3	ATCCTTTTTCTAGTAGCAACTGCAACCGGTTCTGTGACCTCCTATGAGCT GACWCAG
Vl4/5	ATCCTTTTTCTAGTAGCAACTGCAACCGGTTCTCTCTCSCAGCYTGTGCTG ACTCA
Vl6	ATCCTTTTTCTAGTAGCAACTGCAACCGGTTCTTGGGCCAATTTTATGCT GACTCAG
Vl7/8	ATCCTTTTTCTAGTAGCAACTGCAACCGGTTCCAATTCYCAGRCTGTGGT GACYCAG
JH1/2	GGAAGACCGATGGGCCCTTGGTCGACGCCTGAGGAGACGGTGACCAG
JH4/5	GGAAGACCGATGGGCCCTTGGTCGACGCTGAGGAGACGGTGACCAG
JH3	GGAAGACCGATGGGCCCTTGGTCGACGCTGAAGAGACGGTGACCATTG
JH6	GGAAGACCGATGGGCCCTTGGTCGACGCTGAGGAGACGGTGACCGTG
Jk1/2/4	AAGACAGATGGTGCAGCCACCGTACGTTTGATYTCCACCTTGGTC
Jk3	AAGACAGATGGTGCAGCCACCGTACGTTTGATATCCACTTTGGTC
Jk5	AAGACAGATGGTGCAGCCACCGTACGTTTAATCTCCAGTCGTGTC
Cl	TGTTGGCTTGAAGCTCCTCACTCGAGGGYGGGAACAGAGTG

Use the following instructions for mouse cloning PCR.

Materials:

Q5 Hot Start High-Fidelity Polymerase (NEB, M0493L)
dNTPs, PCR Grade (Qiagen, 201901)

Table 16. Mouse gene specific cloning primers.

mVH01	CCTTTTTCTAGTAGCAACTGCAACCGGTGTACATTCCCAGGTGCAGGCAGCCTGG
mVH02	CCTTTTTCTAGTAGCAACTGCAACCGGTGTACATTCCCAGGTGCAGGCAGTCTGG
mVH03	CCTTTTTCTAGTAGCAACTGCAACCGGTGTACATTCCCAGGTGCAGCTGAAGCAGTCTGG
mVH04	CCTTTTTCTAGTAGCAACTGCAACCGGTGTACATTCCCAGGTGCAGCTGAAGGAGTCTGG
mVH05	CCTTTTTCTAGTAGCAACTGCAACCGGTGTACATTCCGAGGTGAAGCTGGAGGAGTCTGG
mVH06	CCTTTTTCTAGTAGCAACTGCAACCGGTGTACATTCCGAGGTGCAGCTGGTGGAGTCTGG
mVH07	CCTTTTTCTAGTAGCAACTGCAACCGGTGTACATTCCGAAGTGCAGCTGTTGGAGACTGG
mVH08	CCTTTTTCTAGTAGCAACTGCAACCGGTGTACATTCCGAGGTGCAGGCAGTCTGG
mVH09	CCTTTTTCTAGTAGCAACTGCAACCGGTGTACATTCCGAGGTGCAGGGAGTCTGG
mVH10	CCTTTTTCTAGTAGCAACTGCAACCGGTGTACATTCCGAGGTGCAGGCAGTCTGTG
mVH11	CCTTTTTCTAGTAGCAACTGCAACCGGTGTACATTCCGAGGTGAAGCTGGTGGAGTCTGG
mVH12	CCTTTTTCTAGTAGCAACTGCAACCGGTGTACATTCCCAGATCCAGGCAGTCTGG
mVH13	CCTTTTTCTAGTAGCAACTGCAACCGGTGTACATTCCCAGGTTCAGACAGTCTGA
mVH14	CCTTTTTCTAGTAGCAACTGCAACCGGTGTACATTCCGAGTTCCAGGCAGTCTGG
mVH15	CCTTTTTCTAGTAGCAACTGCAACCGGTGTACATTCCGATGTACAGCTTCAGGAGTCAGG
mVH16	CCTTTTTCTAGTAGCAACTGCAACCGGTGTACATTCCGAGGTGCAGCTTGTTGAGTCTGGTGGAGG
mVH17	CCTTTTTCTAGTAGCAACTGCAACCGGTGTACATTCCCAGCGTGAGGCAGTCTGG
mVH18	CCTTTTTCTAGTAGCAACTGCAACCGGTGTACATTCCGACGTGAAGCTGGTGGAGTCTGG
mVH19	CCTTTTTCTAGTAGCAACTGCAACCGGTGTACATTCCGAAGTGATGCTGGTGGAGTCTGG
mVH20	CCTTTTTCTAGTAGCAACTGCAACCGGTGTACATTCCCAGGTGCAGCTTGTAGAGACCGG
mVH21	CCTTTTTCTAGTAGCAACTGCAACCGGTGTACATTCCCAGATGCAGCTTCAGGAGTCAGG
mVH22	CCTTTTTCTAGTAGCAACTGCAACCGGTGTACATTCCCAGGCTTATCTACAGCAGTCTGG
mVH23	CCTTTTTCTAGTAGCAACTGCAACCGGTGTACATTCCGAGTTCCAGGCAGTCTGG
mJH01	GAAGACCGATGGGCCCTTGGTCGACGCTGAGGAGACGGTGACCGTGG
mJH02	GAAGACCGATGGGCCCTTGGTCGACGCTGAGGAGACTGTGAGAGTGG
fmJH03	GAAGACCGATGGGCCCTTGGTCGACGGAGACAGTGACCAGAG
mJH04	GAAGACCGATGGGCCCTTGGTCGACGCTGAGGAGACGGTGACTGAGG

Table 17. Mouse cloning PCR master mix.

Mouse cloning PCR	**1 well (50 µl)**
5' primer (10 µM)	2.5 µl
3' primer (10 µM)	2.5 µl
Q5 polymerase	0.5 µl
5X Q5 buffer	10 µl
5X Q5 high GC enhancer	10 µl
dNTPs (10 mM)	1 µl
Nuclease-free H_2O	21.5 µl

1st PCR product	2 µl

Thermocycle:

94°C for 3 min
Repeat 10x:
    94°C for 30 sec
    45°C for 30 sec
    72°C for 60 sec
Repeat 30x:
    94°C for 30 sec
    72°C for 90 sec
72°C for 10 min
4°C forever

DNA assembly (Step 7)

Refer to the technical methods section in the main paper.

Materials:

QIAquick gel extraction kit (Qiagen, 28706)
FastDigest BshTI (AgeI) (Thermo, FD1464)
FastDigest SalI (Thermo, FD0644)
FastDigest Pfl23II (BsiWI) (Thermo, FD0854)
FastDigest Xho1 (Thermo, FD0694)
FastAP (Thermo, EF0654)
GeneJET Gel Extraction Kit (Thermo, K0692)

Transformation (Step 8)

Materials:

5-alpha competent E. coli (NEB; C2988 for individual samples, C2987P for 96-well format)
SOC media
LB agar (+ ampicillin)

8.1. Follow the transformation protocol given for the desired comptent cell line (the protocol can be performed with indivdual samples or in a 96-well format). Use 2 ul of assembled vector.

8.2. Plate on selection plates pre-warmed to 37°C (LB agar, 100 µg/ml ampicillin) and incubate overnight at 37°C. Successful transformations typically have 50-200 colonies per plate, but may have as few as 20.

Plasmid DNA preparation (Step 9)

Materials:

QIAprep 96 Plus Kit (Qiagen, 27291)
Genepure Plasmid Maxi Kit (Roche, 03143422001)
LB broth (+ ampicillin)
Glycerol (autoclaved)

9.1. Prepare a 96-well flat-bottom block for cell cultivation by adding 1.3 ml LB broth with 100 µg/ml ampicillin to each well. Pick four colonies from each transformation plate and individually inoculate wells in the flat-bottom block. Incubate cultures at 37°C for 20-24 hr with vigorous shaking.

9.2. Make glycerol stocks for each sample by transferring 700 µl from each well to 300 µl of a 1:1 mixture of LB:glycerol (without ampicillin). Store at -80°C; these stocks are viable for several years.

9.3. Follow instructions for preparing minipreps with the QIAprep 96 Plus Kit using the QIAvac vacuum manifold.

9.4. Sequence the plasmid DNA with the AbVec primer.

9.5. Compare the four miniprep sequences with sequence alignment to determine the consensus sequence. PCR error may introduce random errors in some sequences, but typically one or more of the sequences represents the consensus. Use this sequence for the following maxiprep steps.

In the rare cases where there is no consensus (even when adding the 1st PCR sequences and germline sequences to the alignment), pick four new colonies and repeat the miniprep process.

9.6. Prepare 14 ml round-bottom tubes with 5 ml of LB broth/ampicillin. Inoculate with the desired minipreps by scraping a small amount of bacteria from frozen glycerol stocks. Incubate at 37°C and 225 rpm for 4-5 hours.

9.7. Transfer the cultures to 500 ml flasks containing 250 ml LB broth/ampicillin. Incubate at 37°C and 225 rpm overnight.

9.8. Prepare plasmid DNA: follow instructions for the Genepure Plasmid Maxi Kit.

Note: for projects without the need for large amounts of DNA, a midiprep can be substituted for the maxiprep.

Transfection and cell culture (Step 10)

Materials:

293A cells (Invitrogen, R70507)
Advanced DMEM (Gibco, 12491)
L-glutamine (Gibco, 25030)
FBS ultra-low IgG (Gibco, 16250)
Antibiotic/Antimycotic (Gibco, 15240)
PEI (Polysciences, 23966)
DMEM (Gibco, 11965)
PFHM-II (Gibco, 12040)
150 mm x 25 mm tissue culture plates (Falcon, 087726)
Protein A agarose beads (Pierce, 20334)

Reagents:

293A culture media
- Advanced DMEM
- 1% L-glutamine
- 1% Antibiotic/Antimycotic
- 2% ultra-low IgG FBS

10.1. Maintain 293A cells in 150 mm x 25 mm tissue culture plates, following the instructions on the product sheet. Transfection-ready plates are 80-90% confluent. Keep track

of the passage number of the cells; cells with more than 30 passages may exhibit lowered transfection efficiency (and simultaneously, lowered day-to-day growth rate).

10.2. Warm DMEM to room temperature. Set up transfections in 5 ml conical tubes.

Table 18. 293T transfection master mix.

Transfection	**1 plate**
DMEM	2.4 ml
Heavy chain DNA	9 µg
Light chain DNA	9 µg
Polyethylenimine (1 mg/ml)	100 µl

Vortex immediately after addition of polyethylenimine (PEI). Incubate at room temperature for 15 min.

10.3. Remove all but 18 ml of media from each plate to be transfected. Add the transfection mixture, gently tilting plates to mix. Incubate at 37°C and 5% CO_2.

10.4. After 12-18 hr, carefully remove the cell culture media, then gently add 25 ml PFHM-II media. Avoid physically disturbing adherent cells.

Warning: PEI is cytotoxic. Avoid longer incubation periods.

10.5. At day 3, collect the culture supernatants in a 50 ml conical tube and re-add 25 ml PFHM-II media.

10.6. At day 6, collect the culture supernatants again for a total of 50 ml from each plate.

10.7. Spin supernatants at 3000 rpm for 15 min to pellet cells, then transfer the supernatants to new 50 ml conical tubes.

10.8. Prepare protein A agarose beads by rinsing twice with PBS. Centrifuge in 50 ml conical tubes at 3000 rpm and 4°C for 10 min with no brake.

Important: Do not use a centrifuge brake on any steps involving agarose beads; braking can damage the beads.

10.9. Add 75 µl protein A agarose beads to each tube containing supernatants, then incubate overnight at 4°C on a slowly-agitating rocker. Place tubes horizontally to maximize bead binding surface area.

Protein purification (Step 11)

Materials:

Mini Bio-Spin Chromatography Column (Biorad, 732-6207)

Reagents:

10x Preservative
- dH_2O
- 5% BSA
- 1.5M NaCl
- 0.5% NaN_3

11.1. Move the beads to a room temperature rocker for 1-2 hr. Centrifuge at 3000 rpm and 4°C for 10 min with no brake.

11.2. Aspirate the supernatant, then resuspend beads in 400 µl 1M NaCl.

11.3. Transfer to a chromatography column. Place columns on a vacuum manifold (such as Qiagen's QIAvac 24) and apply vacuum, releasing upon completion.

11.4. Wash twice with 200 µl PBS, applying vacuum after each wash.

11.5. Prepare clean 1.5 ml Eppendorf tubes with 40 µl Tris pH 9.0 and transfer columns.

11.6. Add 200 µl glycine, then centrifuge at 500g for 1 min. Repeat once. Ensure that the pH of the solution is roughly 7.

11.7. Antibodies can be preserved by adding 50 µl of a 10x preservative (5% BSA, 1.5M NaCl, 0.5% sodium azide). Alternatively, buffer exchange to PBS and preserve with 0.05% sodium azide. Note that *in vivo* assays are sensitive to the addition of azide.

CHAPTER 4

NATURAL POLYREACTIVE IGA ANTIBODIES COAT THE INTESTINAL MICROBIOTA

Jeffrey J. Bunker[1,2], Steven A. Erickson[1,2], Theodore M. Flynn[3], Carole Henry[1,4], Jason C. Koval[3], Marlies Meisel[1,4], Bana Jabri[1,4], Dionysios A. Antonopoulos[3,4,5], Patrick C. Wilson[1,4], and Albert Bendelac[1,2 *]

Affiliations:

[1]Committee on Immunology, University of Chicago, Chicago, IL 60637, USA.

[2]Department of Pathology, University of Chicago, Chicago, IL 60637, USA.

[3]Biosciences Division, Argonne National Laboratory, Argonne, IL 60439, USA.

[4]Department of Medicine, University of Chicago, Chicago, IL 60637, USA.

[5]Institute for Genomics and Systems Biology, University of Chicago, Chicago, IL 60637, USA.

***Correspondence to:** Albert Bendelac abendela@bsd.uchicago.edu

Science. 2017 Oct 20;358(6361). pii: eaan6619. doi: 10.1126/science.aan6619.

Abstract:

Large quantities of immunoglobulin A (IgA) are constitutively secreted by intestinal plasma cells to coat and contain the commensal microbiota, yet the specificity of these antibodies remains elusive. Here, we profiled the reactivities of single murine IgA plasma cells by cloning and characterizing large numbers of monoclonal antibodies. IgAs were not specific to individual bacterial taxa but rather polyreactive, with broad reactivity to a diverse but defined subset of microbiota. These antibodies arose at low frequencies among naïve B cells, and were selected into the IgA repertoire upon recirculation in Peyer's patches. This selection process occurred independent of microbiota or dietary antigens. Furthermore, while some IgAs acquired somatic mutations, these did not substantially influence their reactivity. These findings reveal an endogenous mechanism driving homeostatic production of polyreactive IgAs with innate specificity to microbiota.

One Sentence Summary:

Intestinal IgAs are natural polyreactive antibodies with innate specificity to microbiota.

Main Text:

An innate barrier of mucus, antimicrobial peptides, and immunoglobulin A (IgA) serves as a first line of defense at mucosal surfaces (*1, 22, 99*). Of these components, IgAs uniquely derive from plasma cells (PCs) of the adaptive immune system, yet the specificity of these antibodies has long remained enigmatic. IgA responses occur constitutively under normal homeostatic conditions through both T-dependent (TD) and T-independent (TI) pathways in mucosal lymphoid tissues such as Peyer's patches (PPs) (*4, 11, 35*). While some studies have suggested that IgAs may be highly specific to individual components of the commensal microbiota (*5, 32, 42, 100*), continuous generation of high-affinity responses against the vast and dynamic array of exogenous antigens encountered daily could be overwhelmingly complex in practice. Instead, others have suggested that IgAs may be polyreactive, with individual antibodies able to naturally bind and neutralize multiple targets with low affinity (*101-103*). In support of the latter hypothesis, we recently found that T cells, germinal centers (GCs), and somatic hypermutation were largely dispensable for polyclonal IgA coating of microbiota (*4*). Previous studies of IgA-derived monoclonal antibodies (mAbs) have generally failed to assess reactivity to microbiota (*57, 104, 105*), leaving open the central question of their specificity. Here, we interrogated at the single-cell level the specificity and origins of IgA responses with an unbiased, large-scale analysis of mAbs derived from murine IgA PC populations and other B cell subsets.

Microbiota-reactivity and polyreactivity of mAbs from IgA PCs or naïve B cell subsets

We first sought to establish the frequency of microbiota-reactive specificities within the repertoire of murine small intestinal lamina propria (SI) IgA PCs compared with naïve B cell populations that express IgM and IgD. To allow direct comparison of specificities across

different isotypes, all mAbs were cloned from sorted single cells and expressed as monomeric human IgG1/Igκ chimeras (*106*). mAb panels were derived from pools of mice in multiple independent sorting experiments, and their microbiota-reactivity was assessed by staining and bacterial flow cytometry of SI microbiota taken directly ex vivo from *Rag1*$^{-/-}$ mice to avoid potential epitope saturation by endogenous IgA (Fig. 16A)(*4*). Initial experiments indicated that most IgA-derived mAbs bound microbiota, consistent with their intestinal PC origin, whereas most mAbs from naïve splenic B2 cells, peritoneal B1b, or anti-influenza human plasmablasts did not (Fig. 17A). Surprisingly, some mAbs from naïve B cells or anti-influenza plasmablasts also bound microbiota and resembled IgA mAbs, though these were found more rarely at a frequency of ~30%. Dose titration suggested that microbiota-reactive mAbs, regardless of origin, were moderate to low affinity (Fig. 17A). We did not find mAbs that bound a small fraction of microbiota brightly; instead, staining intensity correlated with percent of bacteria bound (Fig. 17B). Though absolute staining values of individual mAbs showed minor variation across independent experiments, presumably due to differences in microbiota composition, mAb rank order was well-preserved (Fig. 17C). Based on these observations, and to facilitate screening of large numbers of mAbs, we established standardized scoring and inclusion criteria for microbiota staining experiments (Materials and Methods). mAbs were assigned a microbiota-reactivity percentile score according to a control splenic B2 or anti-influenza distribution assayed side-by-side. Scores of ≥70 were considered high microbiota-reactivity, and <70 low microbiota-reactivity; details of threshold selection and scoring are described under Materials and Methods.

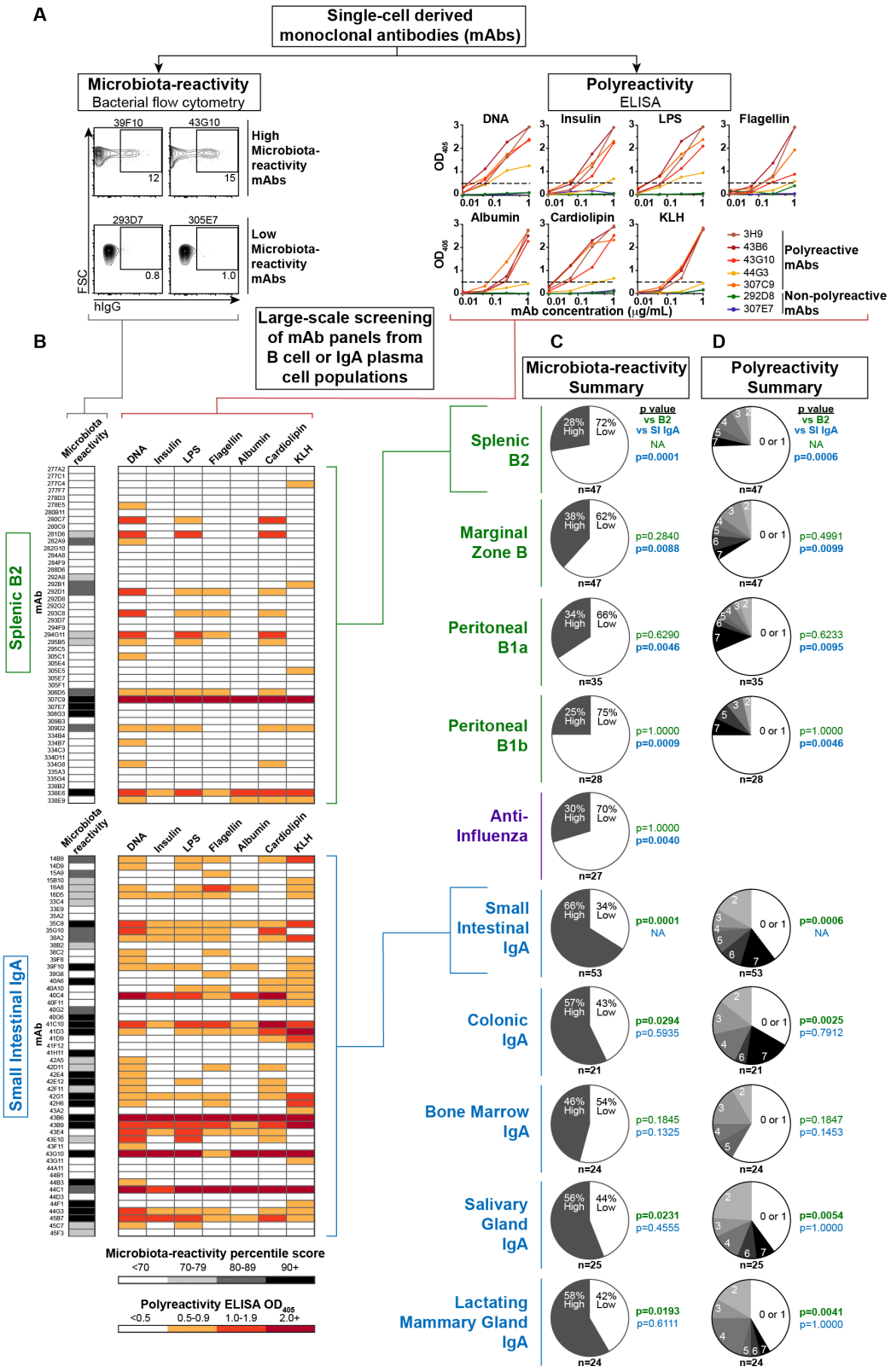

Figure 16. Microbiota-reactivity and polyreactivity of monoclonal antibodies from IgA plasma cell populations and naïve B cell subsets. (A) Workflow for characterizing

Figure 16, continued. monoclonal antibodies (mAbs) cloned from sorted single cells. All mAbs were expressed as monomers with murine variable regions and human IgG1/Igκ constant regions except anti-influenza mAbs, which had fully human variable regions. mAbs were scored for microbiota-reactivity by bacterial flow cytometry against *Rag1*$^{-/-}$ SI microbiota or polyreactivity by ELISA against indicated antigens. **(B)** Microbiota-reactivity percentile scores and polyreactivity ELISA OD_{405} values for individual mAbs from indicated panels. **(C)** Summaries of indicated panels scored for microbiota-reactivity, indicating percent of mAbs that scored either high or low microbiota-reactivity; or **(D)** Polyreactivity summaries, indicating percent of mAbs with indicated number of positive reactivities. Numbers of mAbs analyzed in each panel are indicated below each chart. P values calculated by Fisher's exact test against B2 (green) or SI IgA (blue) panels. Data compiled from >30 independent experiments.

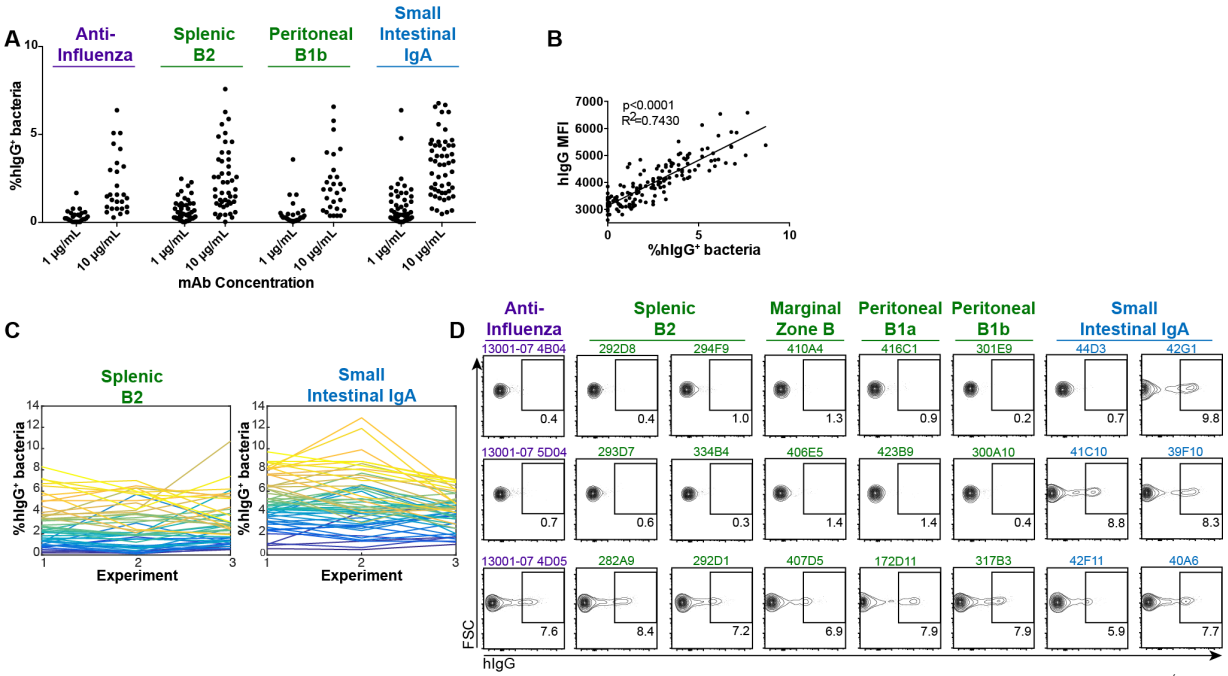

Figure 17. Reproducibility of mAb staining of microbiota. (A) Percent hIgG^{+} of *Rag1*$^{-/-}$ SI microbiota stained with mAbs from indicated panels at indicated concentrations. Representative of multiple independent experiments. **(B)** Correlation of %hIgG^{+} bacteria and median fluorescence intensity (MFI) within the positive gate. P and R^2 values calculated by linear regression. **(C)** Reproducibility of microbiota staining. Percent hIgG^{+} bacteria of *Rag1*$^{-/-}$ SI microbiota stained with mAbs from indicated panels in three independent experiments. Independent preparations of SI microbiota were isolated from three distinct cohorts of *Rag1*$^{-/-}$ mice from our colony and stained on three separate days. The average standard deviation across experiments was 1.00% hIgG^{+}. Lines connect individual mAbs across experiments. Each mAb was assigned a unique color according to its rank order within its panel in experiment 1, with purple being the lowest rank and yellow the highest; color assignment was performed separately for B2 and IgA panels. **(D)** Representative flow cytometry plots depicting staining of *Rag1*$^{-/-}$ SI microbiota by indicated mAbs and panels. Gated on FSC^{+}SSC^{+}SYTO BC^{+}DAPI^{-} cells. Plots are representative of multiple independent experiments.

We extended this analysis to 157 mAbs from all known naïve B cell subsets (Fig. 16B-C, 17D, 18A-D, Table 20). While B2 and B1b cells are the predominant precursors to IgA PCs (*4, 11*), peritoneal B1a and splenic marginal zone (MZ) B cells were also examined, as they have been suggested to encode natural antibacterial and polyreactive antibodies (*107*). We found that a similar frequency of 25-38% of mAbs showed natural, germline-encoded high microbiota-reactivity across all naïve B cell subsets, as did 30% of anti-influenza controls (Fig. 16C, 18A-D). In contrast, 66% of SI IgA mAbs (35 of 53) showed high microbiota-reactivity (Fig. 16B-C, Table 20), demonstrating that microbiota-reactive specificities occur naturally in all naïve B cell populations but are considerably enriched in the IgA repertoire.

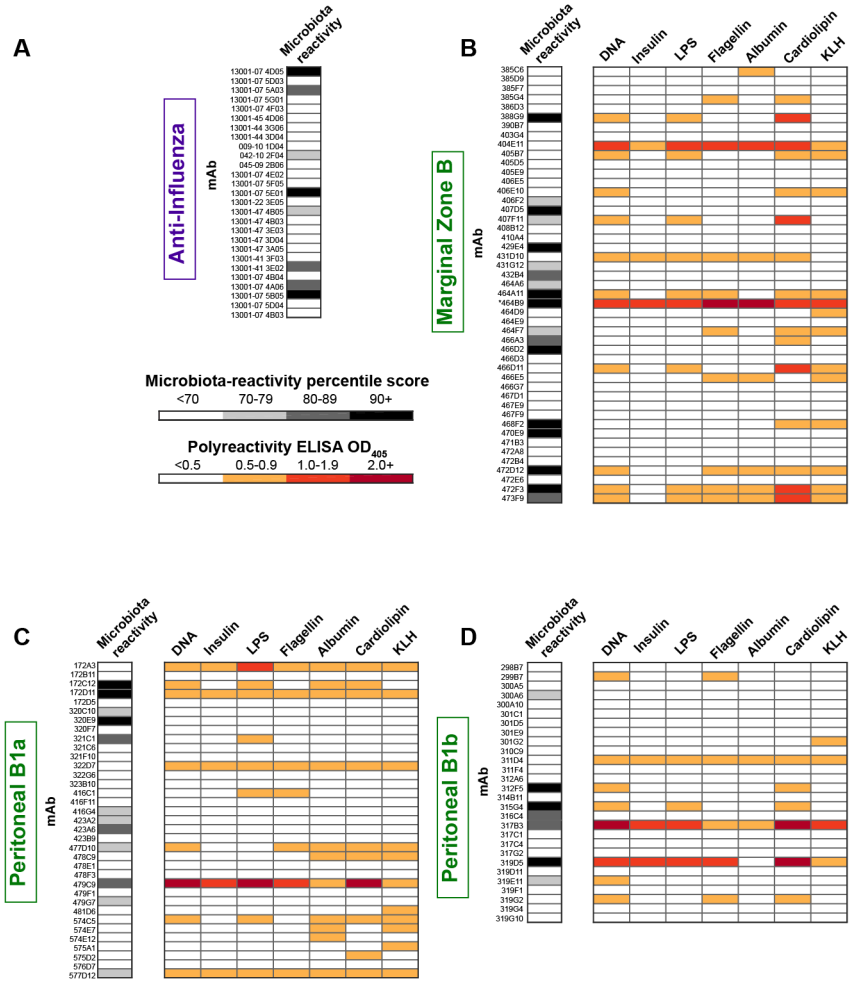

Figure 18. Reactivities of individual mAbs from naïve B cell subsets or anti-influenza panels. (A-D) Microbiota-reactivity percentile scores and polyreactivity ELISA OD_{405} values for individual mAbs from indicated panels. Data are summarized in Fig. 16C-D.

As microbiota-reactivity could be a consequence of a broader pattern of polyreactivity, we next assessed the frequency of polyreactive specificities within the naïve B cell or IgA repertoires by screening mAbs against a panel of seven structurally diverse antigens including DNA, insulin, lipopolysaccharide (LPS), flagellin, albumin, cardiolipin, and keyhole limpet hemocyanin (KLH) by enzyme-linked immunosorbent assay (ELISA) (Fig. 16A). mAbs that bound two or more antigens with an OD_{405} of ≥0.5 at a concentration of ≤1 μg/mL were considered polyreactive, in accordance with prior studies (*92, 108, 109*). We found that 25-34% of naïve B cell mAbs were polyreactive, consistent with previous estimates (*110*), with no major differences between naïve

B cell subsets (Fig. 16B, D, 18B-D). In contrast, 60% of IgA-derived mAbs were polyreactive (Fig. 16B, D), indicating that polyreactive specificities arise naturally in all naïve B cell subsets but are enriched in the IgA repertoire.

Flagellin and LPS are proposed antigenic targets of IgA (*58, 111-114*). Although 43% of IgAs bound each of these antigens, these antibodies were consistently polyreactive and low affinity (Fig. 16B). While polyreactive mAbs lacked the anti-nuclear reactivity of disease-associated autoantibodies (Fig. 19A), they exhibited a pattern of self-reactivity in vivo, as suggested by their reduced retention in serum after injection into mice (Fig. 19B-C)(*115*). Furthermore, polyreactivity persisted after purification of mAbs by size exclusion chromatography, excluding potential artifacts of recombinant protein expression such as abnormal folding or aggregation (Fig. 19D).

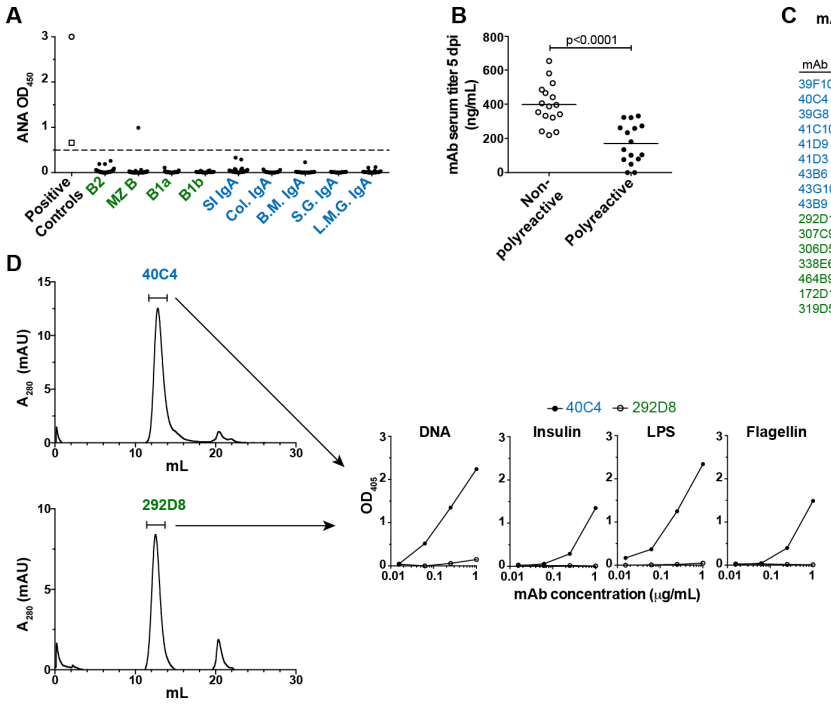

Figure 19. Anti-nuclear reactivities of individual mAbs, serum retention in vivo, and protein quality validation of polyreactive mAbs. (A) HEp2 lysate anti-nuclear antibody (ANA) ELISA. Filled circles indicate individual mAbs and all mAbs shown in Fig. 16 were

Figure 19, continued. assayed. Open circle in positive control column indicates 3H9 high positive control mAb; open square indicates low positive control serum provided by the manufacturer; these controls were included on all plates assayed. * in Fig 18 indicates the single HEp2-reactive MZ B mAb. Data compiled from five independent experiments. **(B)** Serum concentration of mAbs at 5 days-post-injection (dpi) of 2 μg into *Rag1*$^{-/-}$ mice. Data compiled from three independent experiments. P value calculated by unpaired t test. **(C)** List of mAbs used for in vivo serum retention measurements. **(D)** Size exclusion chromatography A_{280} trace of indicated mAbs. Brackets indicate monomeric fractions purified and immediately used in polyreactivity ELISAs against indicated antigens (right).

Polyreactivity and microbiota-reactivity were significantly but not systematically associated in our assays (Fig. 16B, 18B-D), and average polyreactivity of individual mAbs correlated with their microbiota-reactivity (Fig. 20A). Neither polyreactivity nor microbiota-reactivity were significantly correlated with antibody features such as length, charge, or hydrophobicity (Fig. 20B), nor with particular variable gene usage (Fig. 20C), consistent with several previous studies (*109, 110*). Altogether, microbiota-reactive and polyreactive specificities accounted for 83% of SI IgAs versus only 45% of naïve B cell mAbs, underscoring the fundamental differences between these repertoires ($p<0.0001$, Fisher's exact test).

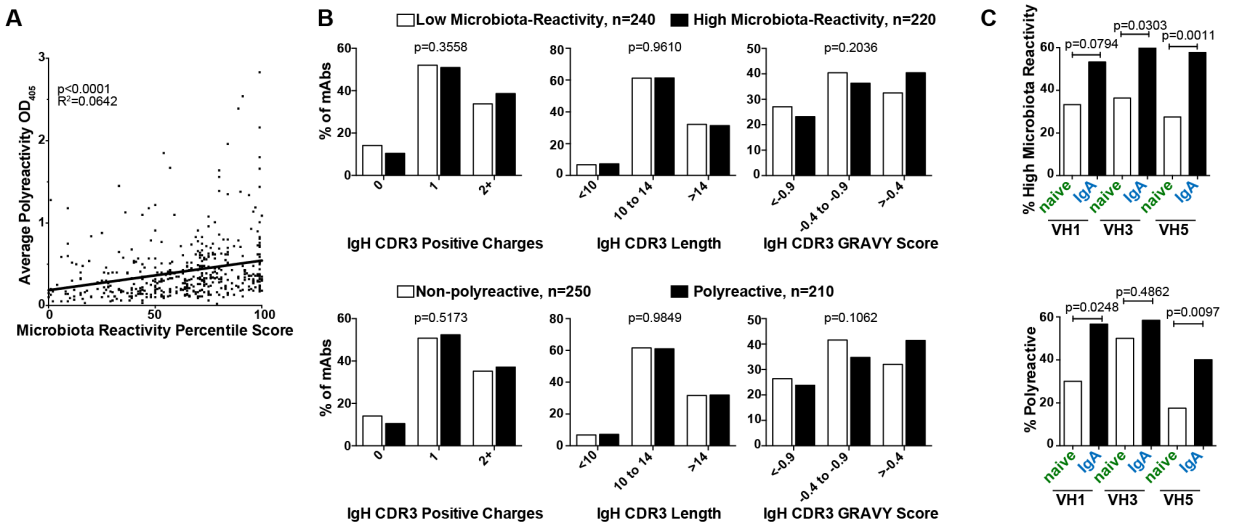

Figure 20. Correlates of microbiota-reactivity and polyreactivity. (A) Correlation of average polyreactivity ELISA OD_{405} across all seven antigens for individual mAbs with their microbiota reactivity percentile score. Plot includes all mAbs in this study except germline reverted mAbs

Figure 20, continued. and anti-influenza panels. P and R^2 values calculated by linear regression. **(B)** Percent of mAbs among low microbiota-reactivity and high microbiota-reactivity classifications (upper panels) or polyreactive and non-polyreactive classifications (lower panels) with indicated repertoire features. Plots include all mAbs in this study except germline reverted mAbs and anti-influenza panels. P values calculated by chi-square test. **(C)** Percent high microbiota reactivity (upper panel) or polyreactive mAbs (lower panel) among all naïve B cell or IgA-derived antibodies in this study, grouped according to VH gene usage. V genes other than 1, 3, and 5 were not included as sample numbers were inadequate for statistical comparison due to low or absent representation in many panels. P values calculated by 2x2 Fisher's exact test.

While the SI harbored the most abundant population of IgA PCs, smaller populations were also apparent in the colonic lamina propria, bone marrow (BM), lung, salivary gland (SG), and lactating mammary gland (LMG) (Fig. 21A). Analysis of somatic mutation distribution and T-cell-deficient *Tcrb*$^{-/-}$*d*$^{-/-}$ mice indicated that SI, colonic, and SG IgA PCs were mixtures of TD and TI specificities, whereas BM and LMG IgAs were largely TD (Fig. 21A-C). To assess the specificity of these IgAs, we cloned 94 mAbs from colonic, BM, SG, or LMG PCs (Table 20). These mAb panels bore striking resemblance to SI IgAs and showed similar enrichment for both microbiota-reactive and polyreactive specificities, with the possible exception of BM IgAs, which displayed a somewhat lower frequency of such reactivities (Fig. 16C-D, 22A-D). Therefore, regardless of their tissue of origin, IgA PC populations predominantly expressed microbiota-reactive and polyreactive antibodies.

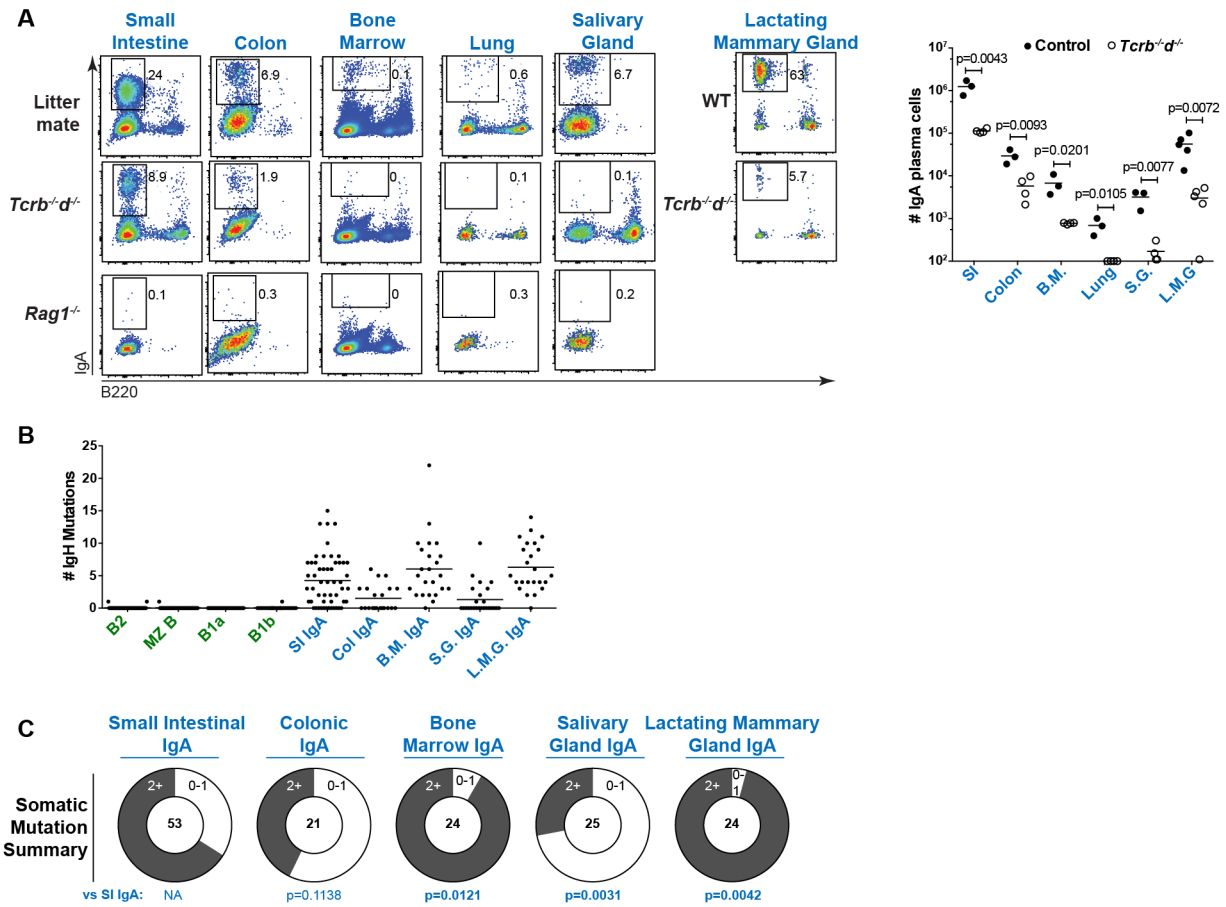

Figure 21. Contributions of TI or TD pathways to intestinal and extraintestinal IgA populations. **(A)** Representative staining and cell number summary of IgA plasma cells in indicated tissues of *Tcrb*$^{-/-}$*d*$^{-/-}$ mice, controls, or *Rag1*$^{-/-}$ mice. Mice were compared to co-housed *Tcrb*$^{+/-}$*d*$^{+/-}$ littermates for all tissues except for the lactating mammary gland; this analysis consisted of a separate cohort of 3-7d post-partum *Tcrb*$^{-/-}$*d*$^{-/-}$ females compared to age-matched and co-housed WT B6 females. P values calculated by unpaired t test. Data compiled from two independent experiments. **(B)** Number of IgH somatic mutations for individual mAbs of indicated cellular origin. **(C)** Summary of somatic mutations for indicated panels. P values calculated by Fisher's exact test.

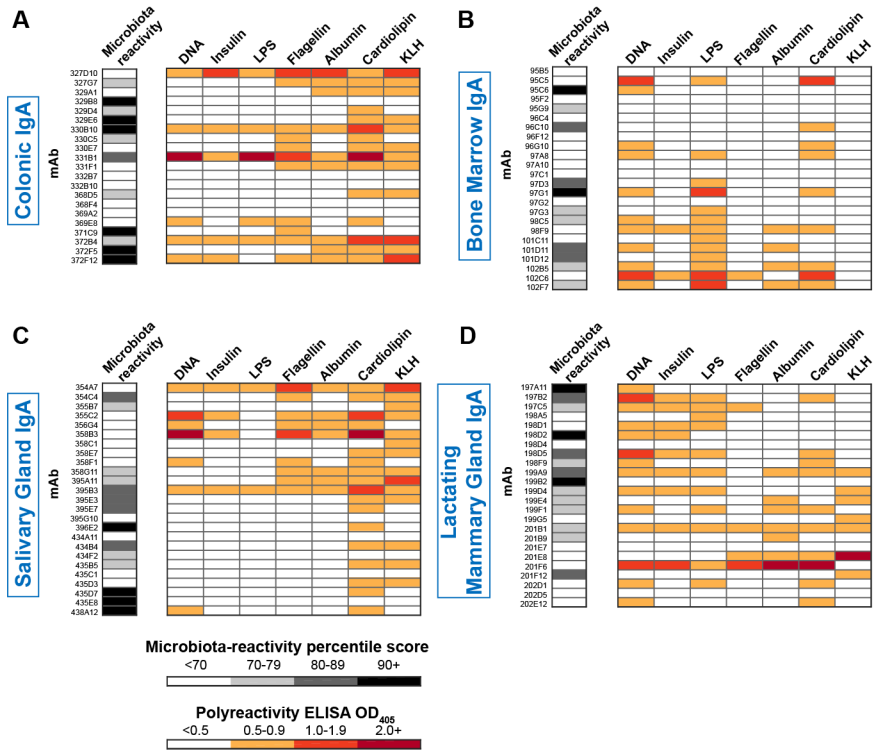

Figure 22. Reactivities of individual mAbs from colonic and extraintestinal IgA PC populations. (A-D) Microbiota-reactivity percentile scores and polyreactivity ELISA OD_{405} values for individual mAbs from indicated panels. Data are summarized in Fig. 16C-D.

Microbiota-reactive antibodies bind a diverse subset of commensal bacteria

Polyclonal IgA coats a distinct subset of microbiota in vivo (*4-6, 59, 63, 116, 117*). To identify the targets of individual microbiota-reactive IgA-derived mAbs, we purified and characterized mAb^+ and mAb^- bacteria by 16S rRNA gene-targeted (16S) amplicon sequencing (Fig. 23A)(*4*). IgA-derived mAbs showed a variety of binding patterns but typically bound multiple distinct microbial taxa with frequent reactivity to Proteobacteria; however, most Bacteroidetes and Firmicutes were not bound (Fig. 23B, 24A-B). Importantly, the 16S microbiota-binding patterns of many individual mAbs closely resembled previously published patterns of binding by endogenous polyclonal IgA (*4*). Furthermore, co-purification of polyclonal IgA^+ or mAb^+ fractions from colonic microbiota of wild-type (WT) B6 mice demonstrated strongly overlapping patterns of microbial targeting (Fig. 24A). Several Proteobacteria-reactive mAbs also bound

segmented filamentous bacteria (SFB), a member of the Firmicutes and known stimulator of IgA responses (Fig. 24A)(*4, 6, 24, 118, 119*). Additionally, in double-staining experiments on WT colonic microbiota, mAbs selectively bound to bacteria that were endogenously coated by IgA in vivo (Fig. 23C). Together, these data indicate that IgA-derived mAbs recapitulate the binding patterns of endogenous IgAs that coat the microbiota.

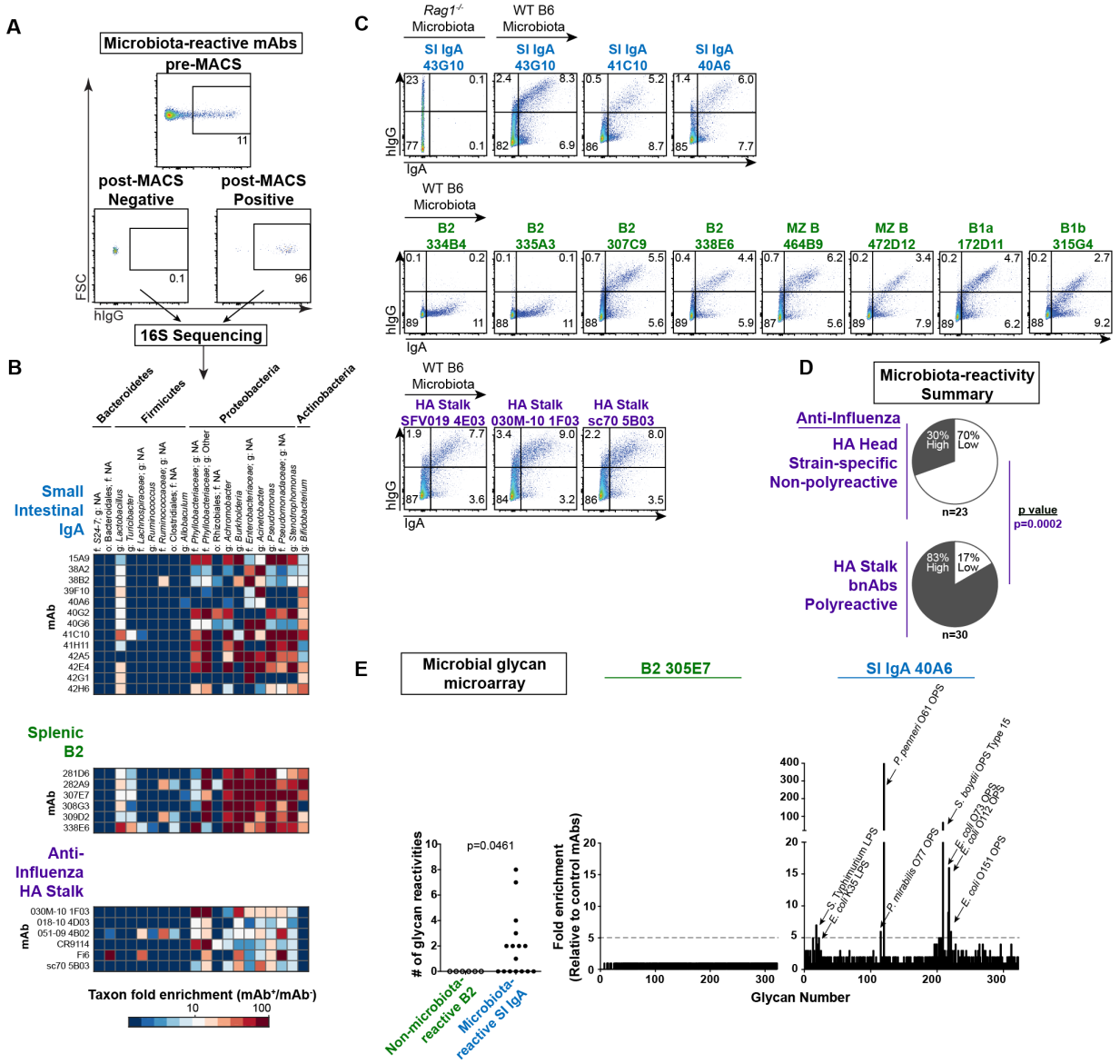

Figure 23. Microbiota-reactive antibodies bind a broad but defined subset of commensal bacteria. (A) Representative plots depicting pre-MACS and post-MACS positive or negative fractions used for 16S sequencing analysis of mAb-bound or –unbound bacteria purified from *Rag1*$^{-/-}$ SI microbiota. **(B)** Microbial taxa bound by individual mAbs from indicated panels;

Figure 23, continued. enrichment in 16S sequencing data calculated by relative abundance in mAb^+/mAb^- fractions. All mAbs in a given panel were co-purified in the same experiment. Data compiled from three independent experiments. Taxonomy abbreviations: o= order; f=family; g=genus. **(C)** Flow cytometry of *Rag1*$^{-/-}$ or WT B6 colonic microbiota comparing bacteria stained by indicated mAbs with those endogenously coated by polyclonal IgA. Data compiled from three independent experiments. **(D)** Summary of microbiota-reactivity for panels of non-polyreactive strain-specific mAbs against the HA head or polyreactive bnAbs against the HA stalk. Numbers of mAbs analyzed in each panel are indicated below each chart. P value calculated by Fisher's exact test. **(E)** Summary of microbial glycan microarray reactivities for microbiota-reactive IgA mAbs or non-microbiota-reactive B2 mAbs (left), and representative reactivities of individual mAbs (right). P value calculated by Fisher's exact test. Data expressed as enrichment over average background of six B2 negative control mAbs. Annotated peaks showed >5-fold enrichment. Data compiled from two independent experiments.

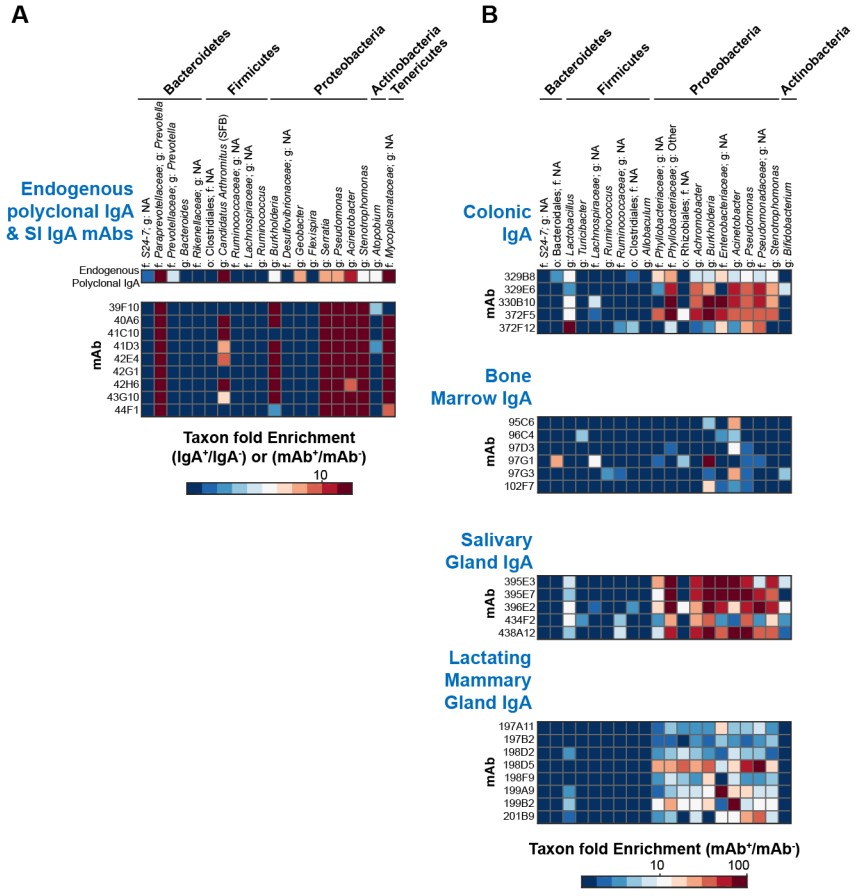

Figure 24. Microbial targets of individual microbiota-reactive IgA-derived mAbs. (A-B) Microbial taxa bound by individual mAbs from indicated panels. Enrichment calculated from 16S sequencing data as relative abundance in mAb^+/mAb^- or endogenous polyclonal IgA^+/IgA^- samples purified from WT B6 colonic microbiota in A or *Rag1*$^{-/-}$ SI microbiota in B. All mAbs in a given panel were co-purified in the same experiment.

Notably, naturally microbiota-reactive mAbs from naïve B cells showed the same patterns of microbiota-binding by 16S sequencing as those derived from IgAs, and also selectively stained endogenously IgA-coated microbiota (Fig. 23B-C, 25A) suggesting that, although less frequent, they and IgAs both belong to the same category of natural polyreactive antibodies. To test whether this property of microbiota-reactivity extended to other unrelated polyreactive antibodies, we examined a panel of 30 human broadly neutralizing antibodies (bnAbs) to influenza that recognize the conserved hemagglutinin (HA) stalk region (Table 20). These bnAbs were previously reported to show extensive polyreactivity to the same DNA, insulin, and LPS antigens used in our study (*108*). Strikingly, we found that a majority of bnAbs showed high microbiota-reactivity with similar binding patterns to IgA-derived mAbs, including selective staining of endogenously IgA-coated microbiota (Fig. 23C-D, 26A). In contrast, 23 non-polyreactive strain-specific mAbs against the influenza HA head typically showed little reactivity (Fig. 23D, 26A, Table 20), similar to a previous independent panel (Fig. 16C, 18A). Interestingly, bacteria naturally coated with the highest levels of endogenous IgA were usually the most brightly stained by mAbs (Fig. 23C). Together, these data show that polyreactive antibodies of various origins, whether derived from IgA PCs, naïve B cells, or anti-influenza responses, exhibit similar patterns of reactivity to a broad yet defined subset of microbiota, reminiscent of pattern recognition by innate immune receptors.

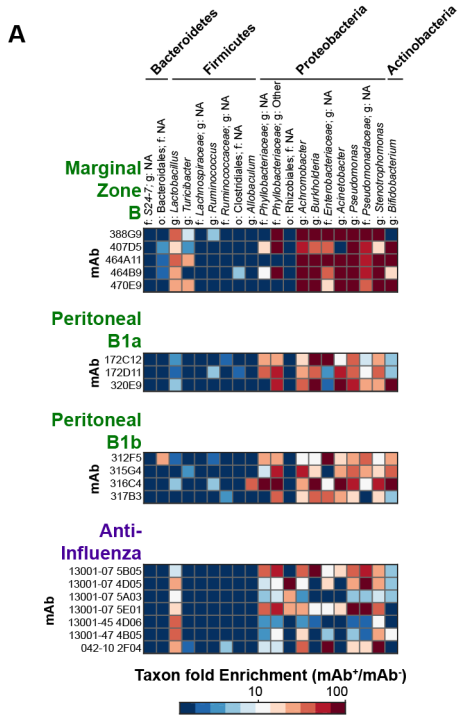

Figure 25. Microbial targets of individual microbiota-reactive naïve B cell-derived mAbs or anti-influenza controls. (A) Microbial taxa bound by individual mAbs from indicated panels. Enrichment calculated from 16S sequencing data as relative abundance in mAb^{+}/mAb^{-} samples purified from *Rag1*$^{-/-}$ SI microbiota. All mAbs in a given panel were co-purified in the same experiment.

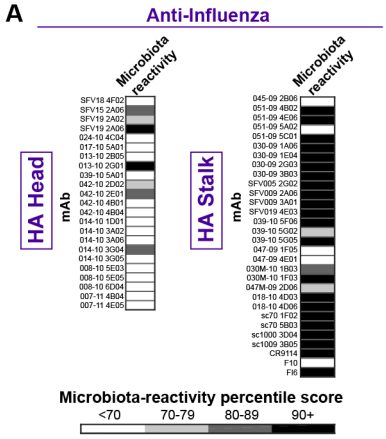

Figure 26. Microbiota-reactivity of individual mAbs from anti-influenza HA head strain-specific or HA stalk bnAb panels. (A) Microbiota-reactivity percentile scores assigned according to the HA head distribution and polyreactivity ELISA OD_{405} values for individual mAbs from indicated panels. Data are summarized in Fig. 23D.

While we observed robust mAb staining of microbiota ex vivo, we did not detect binding to a series of bacterial strains cultured in vitro from the mAb^+ fraction (Fig. 27A-B), suggesting that relevant surface antigen expression was dependent upon the in vivo niche. Indeed, numerous reports have documented modulation of bacterial surface antigens including capsular polysaccharides, LPS, flagella, and adhesion factors in response to different growth or environmental conditions (*120-126*), and additional biochemical modifications by host- or microbiota-derived factors are also possible (*127-129*). Moreover, ex vivo mAb staining of microbiota was unaltered by pre-treatment with nuclease or pre-washing with low pH glycine buffer (Fig. 27C), indicating that the observed reactivity was not due to bacterial adsorption of free nucleic acids nor non-covalently-associated factors from the host or other microbes.

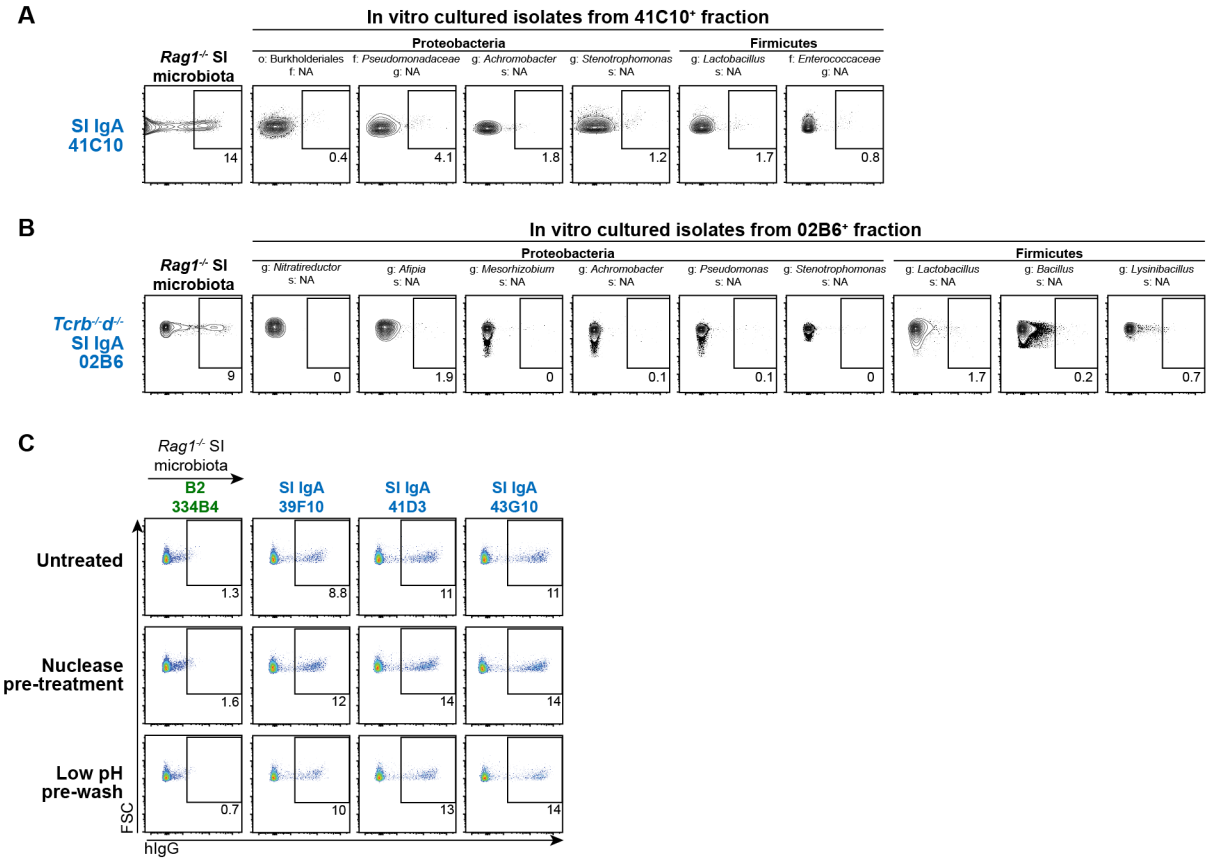

Figure 27. Reactivity of mAbs to in vitro cultured bacterial strains and ex vivo staining after nuclease pre-treatment or low pH pre-washing. (A) Flow cytometry staining with SI IgA mAb 41C10 of ex vivo *Rag1*$^{-/-}$ SI microbiota or individual strains cultured in vitro from the 41C10 mAb^{+} fraction. All staining was performed at 10 μg/mL. Taxonomy abbreviations: o= order; f=family; g=genus; s=species. Similar negative staining of these in vitro cultured isolates was obtained with an additional 27 microbiota-reactive SI IgA mAbs. **(B)** Flow cytometry staining with mAb 02B6 of ex vivo *Rag1*$^{-/-}$ SI microbiota or individual strains cultured in vitro from the 02B6 mAb^{+} fraction. All staining was performed at 10 μg/mL. **(C)** mAb staining of ex vivo *Rag1*$^{-/-}$ SI microbiota that was untreated, pre-treated with nuclease, or pre-washed with glycine-HCl pH 3.0.

To further understand the molecular basis for microbiota surface-reactivity, we asked whether IgAs might bind microbial glycans by screening mAbs against a microbial glycan microarray (*130*). Numerous glycan reactivities were observed among microbiota-reactive mAbs from IgA PCs (Fig. 23E, 28A-B), whereas non-microbiota-reactive mAbs from B2 cells showed little reactivity. Significantly, microbiota-reactive IgA mAbs typically bound multiple distinct microbial glycans, often at low to moderate affinity. For example, mAb 40A6 showed both high-

binding and low-binding interactions with glycans from *Proteus penneri, Proteus mirabilis, Shigella boydii*, *Salmonella* Typhimurium, and various strains of *Escherichia coli*. These findings support the conclusion that microbial surface glycans are common targets of microbiota-reactive IgAs (*57, 131*).

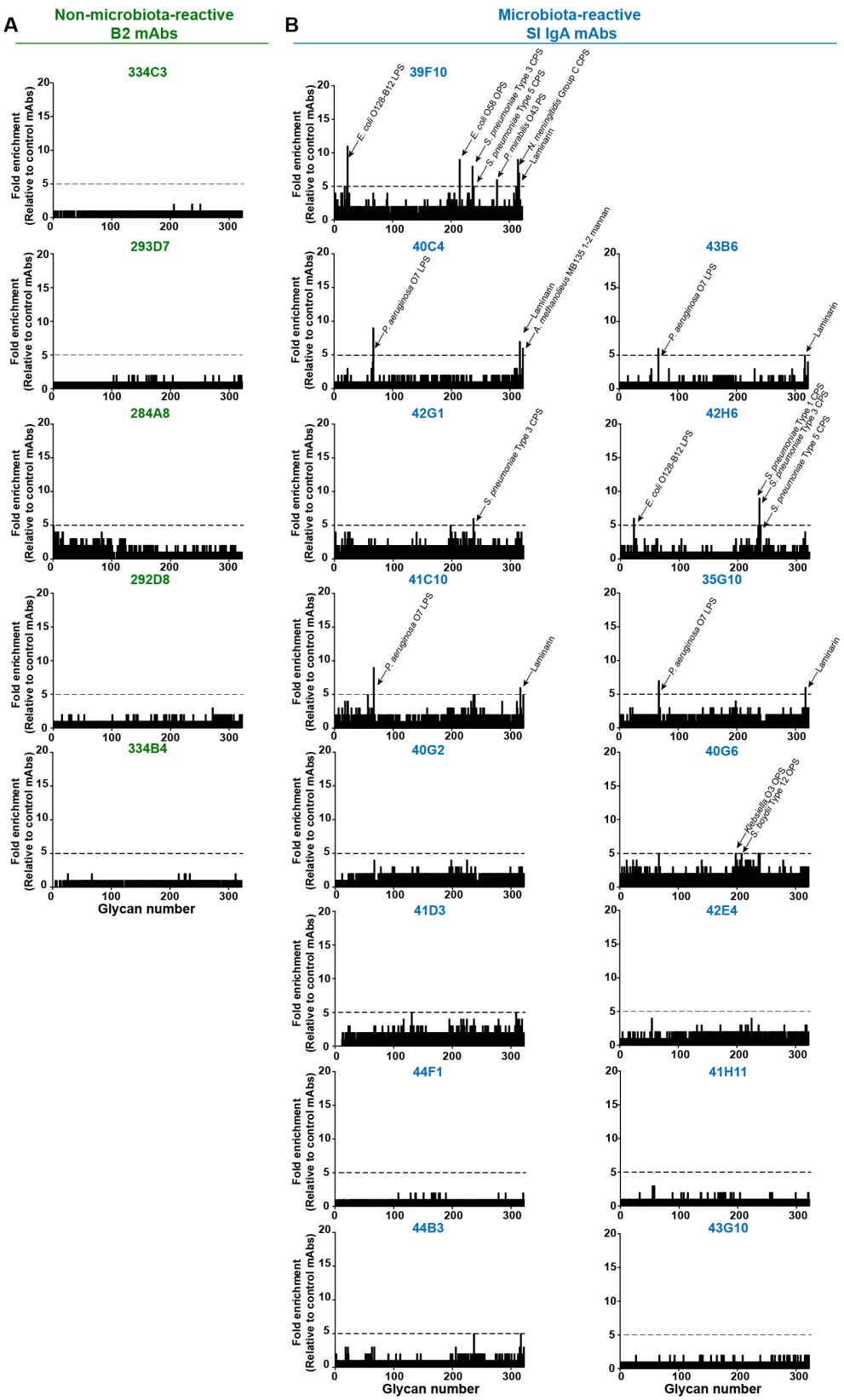

Figure 28. Microbial glycan microarray analysis of individual mAbs. Microbial glycan microarray data for **(A)** Indicated negative control B2 mAbs selected based on lack of

Figure 28, continued. microbiota-reactivity or **(B)** microbiota-reactive SI IgA mAbs. Data expressed as enrichment over average background of six B2 mAb negative controls. Annotated peaks showed >5-fold enrichment. Data compiled from two independent experiments.

Naturally microbiota-reactive recirculating naïve B cells are selected into the IgA repertoire in PPs

To determine the mechanisms by which microbiota-reactive and polyreactive specificities are selected into the IgA repertoire, we first considered whether selection might preferentially occur through either TD or TI pathways. Some hypotheses suggest TI IgA responses may favor generation of polyreactive specificities (*54, 100*), whereas others suggest polyreactivity may be acquired in GCs (*109, 132*). In our SI IgA mAb panel, which derived from 8-to-15-week-old mice, about two-thirds of sequences harbored somatic mutations (Fig. 29A, 30A). However, there was no association between microbiota-reactivity or polyreactivity and the presence or extent of somatic mutation (Fig. 29A). Furthermore, a panel of 24 TI mAbs cloned from *Tcrb*$^{-/-}$*d*$^{-/-}$ SI IgAs showed similar frequencies and patterns of microbiota-reactivity and polyreactivity to WT SI IgAs, despite a near absence of mutations (Fig. 29B, 30A-C, Table 20). Conversely, a panel of 22 mAbs cloned from SI IgA PCs of one-year-old WT mice displayed an even greater frequency of mutated sequences than 8-to-15-week-old mice, as reported (*133*), but showed comparable microbiota-reactivity and polyreactivity to younger mice (Fig. 29C, 30A, D-E, Table 20). To directly test the contribution of somatic mutations to mAb reactivity, we reverted 21 highly mutated SI IgAs to germline configuration (Fig. 31A, Table 20). Reverted mAbs showed no significant differences in overall microbiota-reactivity or polyreactivity (Fig. 29D-E), although there were a few examples of either gain or loss of polyreactivity and/or microbiota-reactivity (Fig. 31B-C). These results are consistent with the observation that only ~70% of IgA mutations were nonsynonymous, a rate that does not support affinity selection (Fig.

31D), and with a recent report suggesting that PP GCs lack evidence of antigen-driven selection (*134*). While T cells did not substantially modulate the specificity of IgA, they did promote an increase in IgA PC numbers and were largely required for the generation of extraintestinal IgA PC populations (Fig. 21A). We conclude that selection of microbiota-reactive and polyreactive IgAs occurs independent of GCs and that these specificities can differentiate via either TI or TD pathways.

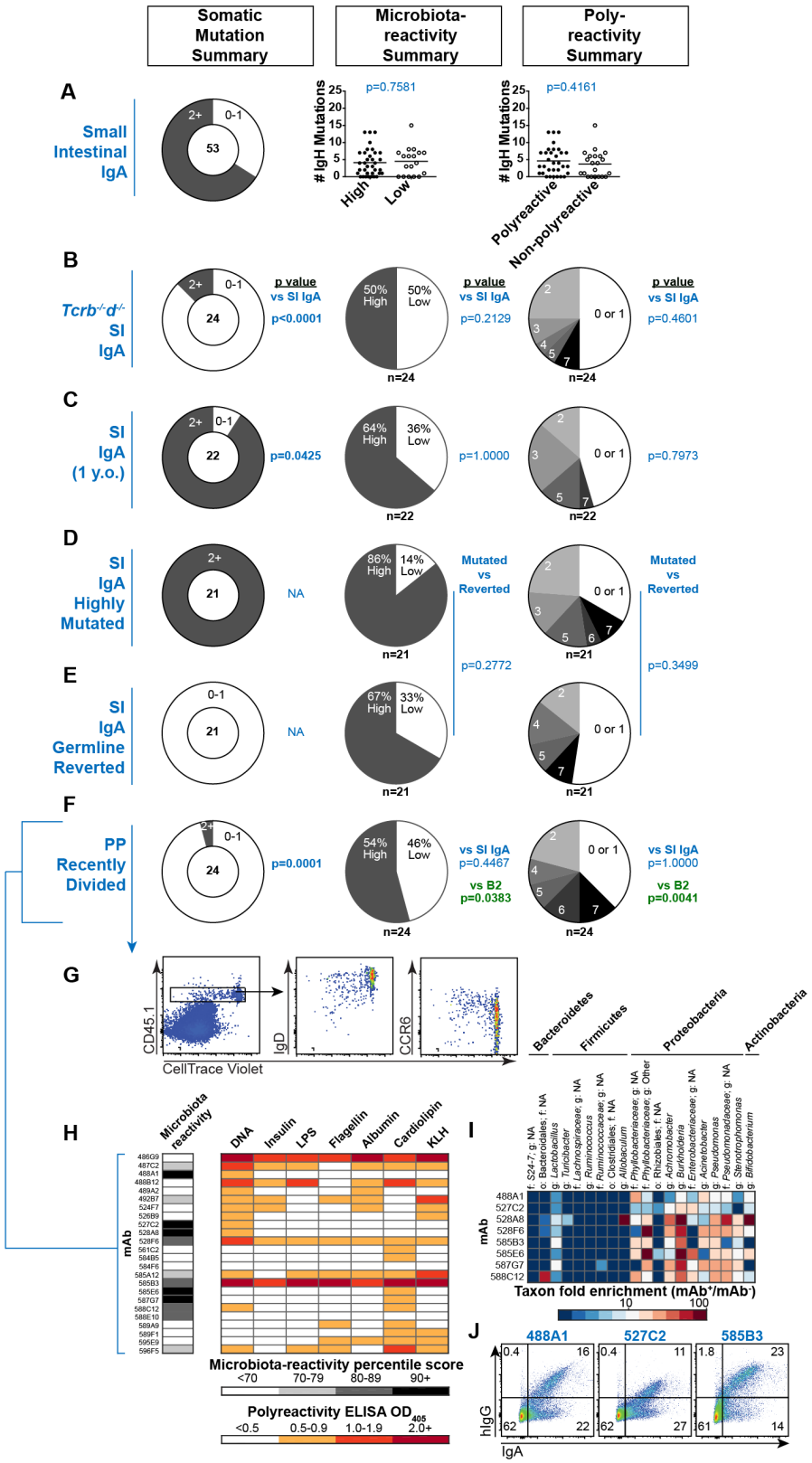

Figure 29. Mechanisms of IgA selection. Summary of somatic mutations, microbiota-reactivity, and polyreactivity of mAb panels derived from **(A)** SI IgA PCs from 8-15 week old

Figure 29, continued. WT B6 mice, **(B)** *Tcrb*$^{-/-}$*d*$^{-/-}$ SI IgA PCs, or **(C)** SI IgA PCs from one-year-old WT B6 mice. Data compiled from >5 independent experiments. **(D-E)** Summary of 21 highly mutated SI IgAs and their engineered germline revertants, or **(F)** recently divided CD45.1^{+} donor-derived cells in PPs 7d after transfer to MD4Tg recipients, isolated as indicated in **(G)**. **(H)** Microbiota-reactivity percentile scores and polyreactivity ELISA OD_{405} values of individual mAbs from recently divided cells in PPs, compiled from three independent experiments, **(I)** Microbial taxa binding patterns of individual mAbs as determined by 16S sequencing, or **(J)** double staining of colonic microbiota comparing individual mAbs with endogenously IgA-coated bacteria. Numbers of mAbs analyzed in each panel are indicated below each chart. P values calculated by unpaired t test in panel A and Fisher's exact test in panels B-F.

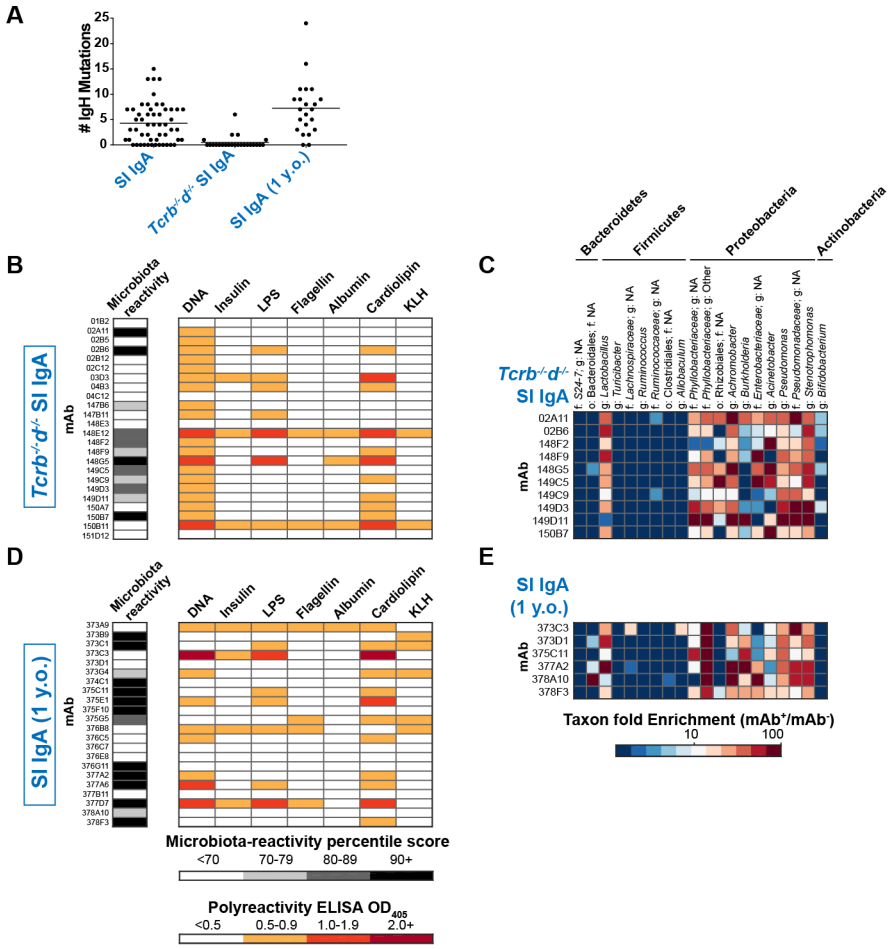

Figure 30. Reactivities of individual T-dependent or T-independent SI IgA mAbs. (A) Number of IgH somatic mutations for individual mAbs from indicated SI IgA panels. **(B, D)** Microbiota-reactivity percentile scores and polyreactivity ELISA OD_{405} values for indicated mAbs and panels. Data summarized in Fig. 29B-C. **(C, E)** Microbial taxa bound by indicated mAbs and panels. Enrichment calculated from 16S sequencing data as relative abundance in mAb^{+}/mAb^{-} samples purified from *Rag1*$^{-/-}$ SI microbiota. All mAbs in a given panel were co-purified in the same experiment.

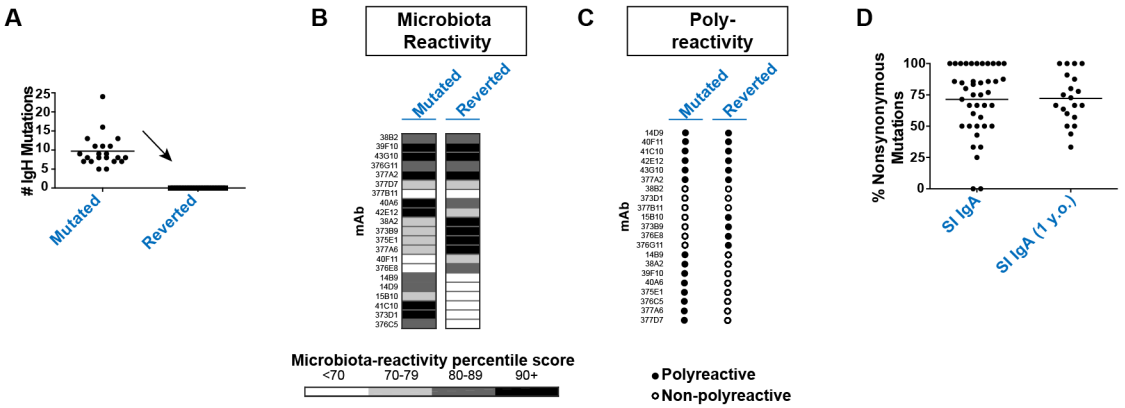

Figure 31. Reactivities of individual mutated or germline reverted SI IgA mAbs. (A) IgH somatic mutations in mAbs selected for reversion to germline. IgK chains were similarly reverted. **(B)** Microbiota-reactivity percentile scores and **(C)** polyreactivity ELISA scoring of indicated mutated or germline reverted mAbs. **(D)** Percent nonsynonymous mutations among individual mutated mAbs in indicated panels.

Searching for an early post-selection progenitor to intestinal IgA, we asked whether the recently identified $IgM^{+}IgD^{+}CCR6^{+}$ dividing B cell population in PPs, which originates from recirculating naïve B cells (*35*), might exhibit signs of selection for microbiota-reactivity. We transferred fluorescently-labeled $CD45.1^{+}$ polyclonal splenic B cells into $CD45.2^{+}$ MD4 Ig-transgenic (MD4Tg) recipients that have little endogenous PP B cell activation (*35*), and isolated 24 mAbs from recently-divided $CD45.1^{+}$ $IgD^{+/lo}$ $CCR6^{+}$ cells in PPs (Fig. 29F-G, Table 20). While these mAbs were largely unmutated, as expected, they exhibited a striking enrichment in microbiota-reactivity and polyreactivity (Fig. 29F-H), and displayed 16S microbiota-binding patterns that resembled SI IgAs (Fig. 29I, 23B) as well as selective binding to bacteria endogenously coated with polyclonal IgA (Fig. 29J). Such specificities accounted for 88% of mAbs and were significantly enriched relative to naïve B cell panels ($p=0.0001$, Fisher's exact test). These data indicate that naturally microbiota-reactive and polyreactive naïve B cells are extracted from circulation to become intestinal IgA precursors in PPs. Expression of CCR6 then

guides their migration to the PP subepithelial dome, where they receive signals that direct class-switch recombination to the IgA isotype and imprinting for gut homing (*28, 33, 35, 39*).

An endogenous mechanism driving natural IgA selection

These observations prompted us to examine the role of exogenous microbiota or dietary antigens in IgA selection. IgA production is thought to be microbiota-dependent, as titers are diminished in germ-free (GF) relative to specific-pathogen-free (SPF) mice (*135*). Consistent with this notion, we found that IgA PCs were severely reduced or absent from most tissues in GF mice, including the colon, BM, lung, SG, and LMG (Fig. 32A). However, in the SI, the predominant site of IgA production, IgA PCs were largely preserved and showed only a minor decrease (Fig. 32A). Differentiation of SI IgAs in GF mice might represent a response to dietary antigens. To explore this possibility, we weaned three-week-old GF mice onto either a standard chow (SC) or chemically-defined antigen-free (AF) diet (Table 19) (*136, 137*). Remarkably, a dramatic expansion of SI IgA PCs and luminal free IgA titers was apparent after weaning of GF mice fed both SC and AF diets, indicating that neither microbiota nor dietary antigens were required for the post-weaning IgA response (Fig. 32B-C). Notably, as previously reported, SI $Nrp1^{lo}$ T regulatory cells failed to accumulate in GF/AF compared to GF/SC mice, confirming the major impact of the AF diet on other aspects of intestinal immunity (Fig. 32D)(*136*).

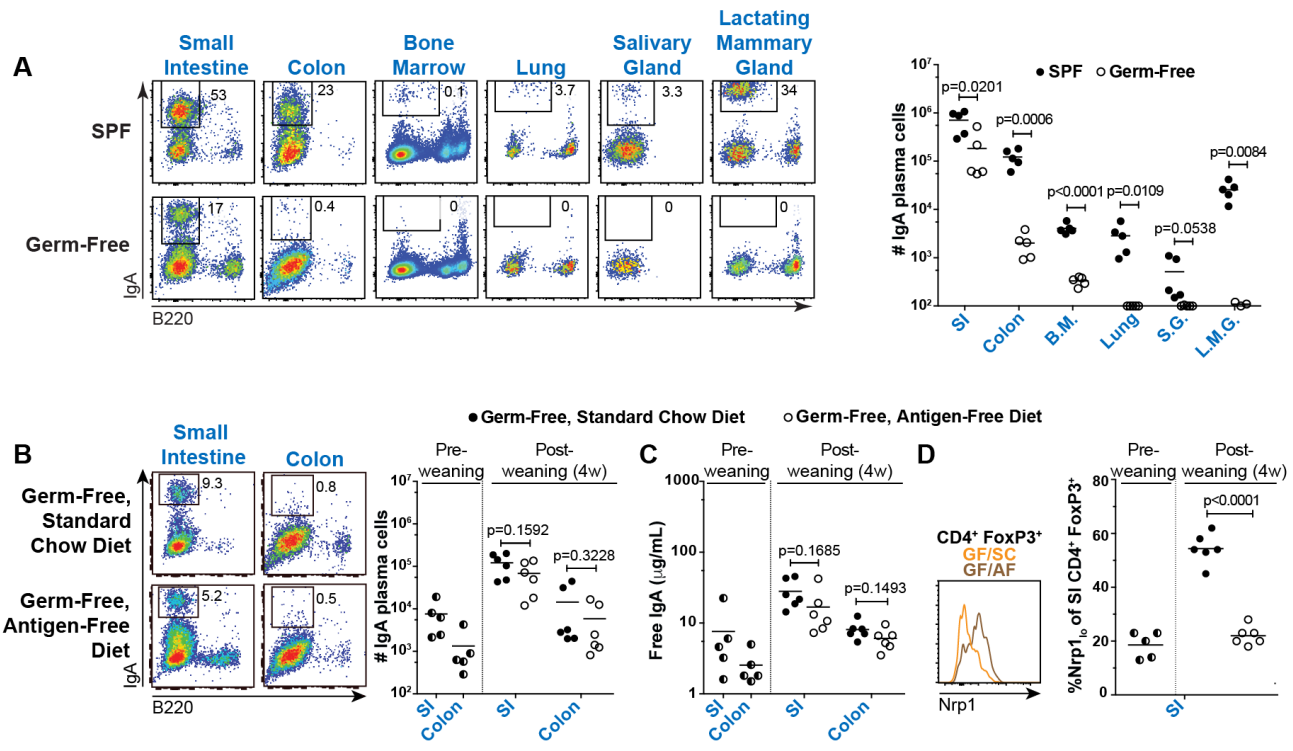

Figure 32. Small intestinal IgA plasma cell differentiation does not require exogenous microbiota or dietary antigens. (A) Representative flow cytometry plots and cell number summary of IgA PCs in SPF or GF B6 mice. Plots gated on lineage$^-$ lymphocytes. L.M.G. were obtained from females 3-7d post-partum; all other tissues were from males. P values calculated by unpaired t test. **(B)** Representative flow cytometry plots and cell number summary of IgA PCs or **(C)** Luminal free IgA titers determined by ELISA in indicated mice, and **(D)** Representative flow cytometry of SI CD4$^+$ FoxP3$^+$ cells and summary of percent Nrp1^{lo} among CD4$^+$ FoxP3$^+$ cells in indicated mice. P values calculated by unpaired t test. Data compiled from four independent experiments.

Table 19. Recipe for antigen-free diet.

Aqueous Solution 1	
Add to sterile nanopure water at 70 ºC	g/L
0.36 L H_2O	
Dextrose (Sigma D9434)	220
Aqueous Solution 2	
Add to sterile nanopure water at 70 ºC	
0.64 L H_20	
Leucine (Sigma L8000)	5.775
Phenylalanine (Sigma P2126)	2.25

Table 19, continued.

Isoleucine (Sigma I2752)	3.3
Methionine (Sigma M9625)	4.8
Tryptophan (Sigma T0254)	1.125
Valine (Sigma V0500)	4.1
Asparagine (Sigma A0884)	3.75
Arginine-HCl (Sigma A5131)	2.775
Threonine (Sigma T8625)	2.25
Lysine-HCl (Sigma L5626)	5.4
Histidine-HCl*H2O (Sigma H5659)	2.25
Cool to 45C, add the following:	
Glycine (Sigma G7126)	1.8
Proline (Sigma P0380)	4.5
Serine (Sigma A0884)	4.05
Alanine (Sigma A7627)	1.8
Na-Glutamate (Sigma G1626)	10.35
Ethyl L-tyrosinate HCl (Sigma T4879)	1.875
Ferrous gluconate (Sigma 344427)	0.15
Mn acetate tetrahydrate (Sigma 229776)	0.1662
ZnSO4*H2O (Sigma 96495)	0.1218
Cu acetate*H2O (Sigma 217557)	1.11E-02
Cr acetate*H2O (Santa Cruz sc-227648)	7.50E-03
NaF (Sigma 201154)	6.30E-03
SnSO4*2H2O (Sigma 244635)	1.11E-03
Ammonium molybdate tetrahydrate (Sigma 09880)	1.11E-03
NiCl2 hydrate (Sigma 364304)	1.11E-03
Cobalt acetate tetrahydrate (Sigma 403024)	3.30E-04
Sodium orthovanadate (Sigma 450243)	6.60E-04
Sodium selenate (Sigma S5261)	2.88E-04
Cool to 4 ºC, add the following:	
Ca glycerophosphate (Sigma G6626)	15.9
Mg glycerophosphate (Sigma 17766)	4.35
CaCl2*2H2O (Sigma 3881)	0.5625
NaCl (Sigma S9888)	0.1778
KI (Sigma 207969)	1.42E-03
K acetate (Sigma P1190)	5.625

Table 19, continued.

Choline HCl (Sigma C1879)	0.95
Vitamin B12 (Sigma V2876)	4.72E-03
Biotin (Sigma B4501)	8.20E-04
Folic acid (Sigma 7876)	1.23E-03
Thiamine HCl (Sigma T4625)	4.10E-03
Pyridoxine HCl (Sigma 9755)	5.13E-03
Riboflavin (Sigma R4500)	6.15E-03
Niacinamide (Sigma N5535)	3.08E-02
D-Pantothenic acid (Sigma 21210)	4.10E-02
myo-Inositol (Sigma I5125)	2.05E-01
Combine both solutions at 4 ºC *& sterile filter*	
Lipid Solution	
Soybean oil (Sigma S7381)	
Retinyl palmitate (Sigma R3375)	1.87E-01
Cholecalciferol (Sigma C9756)	5.00E-04
Vitamin K (Sigma V3501)	0.675
DL-tocopherol acetate (Sigma T3376)	20
DL-tocopherol (Sigma 258024)	10
Warm to 50 ºC prior to sterile filtration	

We assessed the specificities of 31 GF/SC and 55 GF/AF SI IgA-derived mAbs (Table 20). Despite their selection in the absence of exogenous antigens, both panels showed frequent microbiota-reactivity and polyreactivity (Fig. 33A-D) with similar 16S binding profiles to SPF SI IgAs (Fig. 33E, 23B), and selectively bound bacteria endogenously coated with IgA in vivo (Fig. 33F). Together, microbiota-reactive and polyreactive specificities accounted for 69% of GF/SC and GF/AF SI IgA mAbs, a significant enrichment relative to naïve B cell panels ($p=0.0005$, Fisher's exact test). GF/SC and GF/AF SI IgAs were largely unmutated (Fig. 33A-B) and resembled IgAs from SPF *Tcrb*$^{-/-}$*d*$^{-/-}$ mice in mutation frequency, mAb reactivity, and

intestinal/extraintestinal PC distribution (Fig. 21A, 29B, 30A-C), consistent with a requirement for T cell-intrinsic sensing of microbiota through Toll-like receptors for T cell help (*63*), and with the observation that individual IgA clones in GF mice persist and progressively acquire somatic mutations after colonization with microbiota (*133*). As $IgD^{+}CCR6^{+}$ cells were readily observed in GF/SC and GF/AF PPs (Fig. 33G), natural IgA selection presumably occurred through the same pathway described in SPF mice (Fig. 29). We conclude that a natural IgA response occurs in PPs that is largely independent of exogenous antigens or T cell help, and may instead result from autoreactive stimulation by endogenous antigens. This innate response preferentially recruits naturally polyreactive and microbiota-reactive recirculating naïve B cells to enter the intestinal IgA PC repertoire and secrete the IgA that coats the commensal microbiota.

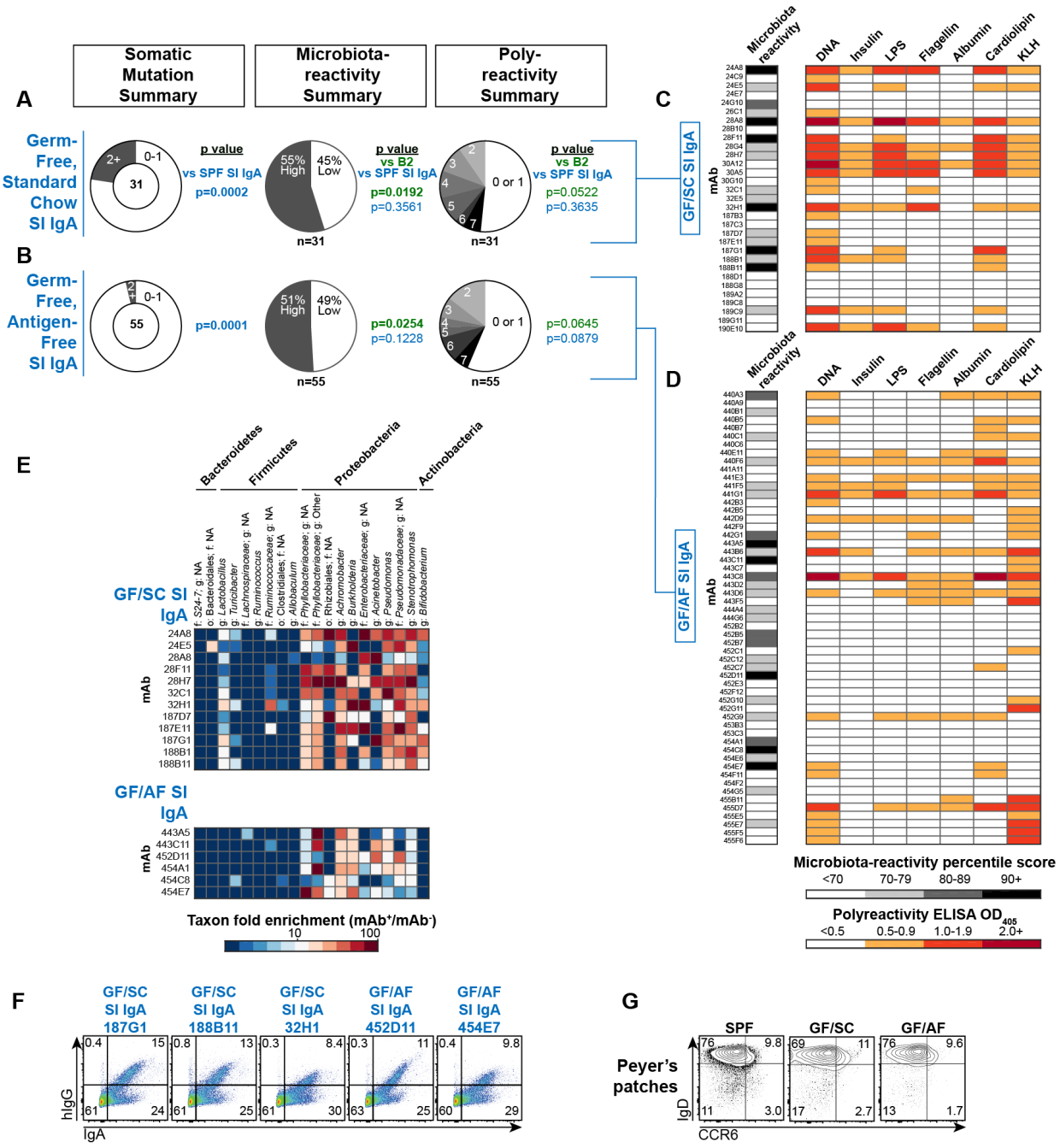

Figure 33. Natural IgA selection. Summary of somatic mutations, microbiota-reactivity, and polyreactivity of mAb panels derived from **(A)** GF/SC SI IgA PCs or **(B)** GF/AF SI IgA PCs. Numbers of mAbs analyzed in each panel are indicated below each chart. P values calculated by Fisher's exact test. **(C-D)** Microbiota-reactivity percentile scores and polyreactivity ELISA OD_{405} values of individual mAbs from GF/SC and GF/AF SI IgA panels. Data compiled from >6 independent experiments. **(E)** Microbial taxa binding patterns of individual mAbs as determined by 16S sequencing, or **(F)** double staining of colonic microbiota comparing individual mAbs with endogenously IgA-coated bacteria. **(G)** Flow cytometry of $CD19^{+}IgD^{+}CCR6^{+}$ cells in PPs of SPF, GF/SC, or GF/AF mice. Representative of two independent experiments.

Discussion

Our studies have elucidated the specificity of homeostatic intestinal IgA and demonstrate its natural origins. They also define an endogenous mechanism of selection in PPs that enriches microbiota-reactive and polyreactive specificities into the IgA repertoire (Fig. 34). Of note, this response appears distinct from natural serum IgM responses that derive from peritoneal B1a cells (*138*) as canonical B1a rearrangements were not observed in the SI IgA PC repertoire (*4*), and these specificities were not conspicuously enriched in microbiota-reactivity.

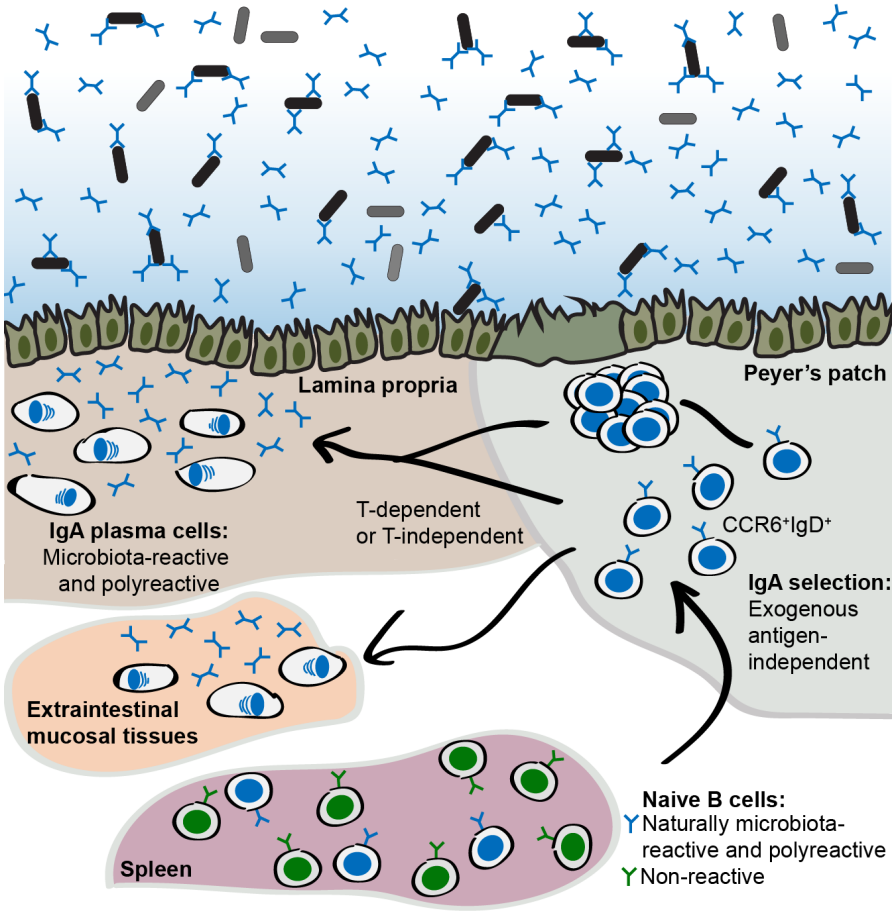

Figure 34. Summary model for selection of microbiota-reactive and polyreactive IgAs. Microbiota-reactive and polyreactive specificities occur naturally at frequencies of ~30% in the repertoires of all naïve B cell subsets. Upon trafficking through Peyer's patches, cells expressing

Figure 34, continued. these specificities are selected to divide via a natural, exogenous antigen-independent mechanism. Cells that undergo IgA selection upregulate CCR6, which facilitates receipt of local factors that direct IgA class-switch recombination and gut imprinting. Cells then proceed through either T-dependent or T-independent pathways that instruct differentiation to IgA plasma cells. Cells migrate to the intestinal lamina propria or to extraintestinal tissues and secrete specificities that naturally bind a diverse but defined subset of commensal microbiota.

We found that IgA PCs from a diverse array of intestinal and extraintestinal tissues typically expressed microbiota-reactive and polyreactive specificities. These data suggest a common mechanism by which IgAs found in serum, intestinal, salivary, and mammary secretions promote homeostasis in various tissue contexts and in nursing offspring (*139-141*). Notably, IgA PCs in tissues other than the SI were severely reduced in the absence of microbiota and T cells; this may reflect defects in cell trafficking, proliferation, or maintenance in the absence of the TD response, which requires T cell-intrinsic innate immune signals from the microbiota (*63*). In contrast to these sites, SI IgA PCs were readily detected in GF mice and showed a four-fold reduction, comparable to previous reports (*11, 24, 118, 142*). Two-thirds of SI IgA PCs were somatically mutated in WT mice, and we previously reported a three-fold reduction in in CD4-cre *Bcl-6*$^{fl/fl}$ mice, which lack T follicular helper cells (T_{fh}) and germinal centers but otherwise retain an intact T cell compartment (*4*). As T cell-deficient *Tcrb*$^{-/-}$*d*$^{-/-}$ mice showed a more significant ten-fold reduction, T cells appear to have additional effects on IgA PCs outside the canonical T_{fh} pathway, potentially by regulating plasma cell maintenance, trafficking, or proliferation, cytokine production, and/or mucosal barrier integrity.

We identified a broad but distinct subset of microbiota that was bound by IgA antibodies in vivo. Yet, it remains unclear whether this binding has functional effects on commensal fitness or

physiology; it is possible that IgA binding either enhances or diminishes fitness. These effects could include alterations in microbial gene expression, motility, and/or spatial localization and may be mediated by mechanisms such as agglutination, enchained growth, neutralization, and immune exclusion (*57, 58, 143-145*). While we observed numerous IgA reactivities to bacterially-derived antigens including flagellin, LPS, and various glycans, the relevant targets of these natural antibodies in vivo remain unclear as relevant culture conditions, biochemistry, and genetics have not been established for the targeted commensal organisms. However, we hypothesize that recognition may involve low-affinity interactions with numerous antigens on the bacterial surface. It is also possible that polyreactivity enhances binding to entropically unfavorable targets such as carbohydrates, reminiscent of its role in increasing the apparent affinity of broadly neutralizing antibodies against the HIV envelope spike (*109*). The structural basis for antibody polyreactivity remains enigmatic; in particular, it is unclear whether similar or distinct binding mechanisms are utilized for different antigens. As we did not discern clear repertoire features associated with polyreactivity or microbiota-reactivity, it is probable that individual antibodies can achieve this type of recognition via a variety of structural mechanisms. One previous study identified the heavy-chain complementarity determining region 3 (CDR3) as a key determinant of polyreactivity, though this analysis was limited to a single antibody (*146*) , and silencing of heavy chain polyreactivity by light chains has been described (*147*). Detailed structural studies including crystallography of these antibodies in complex with various ligands are warranted.

Our analysis of GF/AF mice demonstrated that IgA plasma cells with microbiota-reactive specificities can arise in the absence of exogenous microbiota or dietary antigens. While

exogenous antigen exposure was dramatically reduced in these mice, as exemplified by a lack of SI regulatory T cell induction (*136*), it is possible that they encountered trace quantities of dietary antigen during the first few weeks of life, potentially transmitted via lactation. Long-term maintenance on the AF diet results in emergence of micronutrient insufficiencies – notably deficiency of vitamin A, a known regulator of IgA class-switch recombination and gut trafficking, and thus new caveats emerge in mice fed this diet for several generations (*28, 39, 136*). Nonetheless, our ontogenetic analysis revealed a dramatic expansion of IgA plasma cells and luminal titers after weaning of mice onto the AF diet, comparable to mice weaned onto SC, supporting our conclusion that these plasma cells can differentiate in the absence of exogenous antigen. While our studies focused on the C57BL/6 strain, GF BALB/c mice were reported to produce significantly higher titers of intestinal IgA than GF C57BL/6 and these antibodies appeared to be polyreactive, suggesting that the polyreactive and microbiota-reactive nature of IgAs extends to different strain backgrounds (*102, 105*).

Natural IgA secretion may represent an innate-like mechanism for mucosal defense and may be evolutionarily ancient; indeed, specialized mucosal antibodies of TI origin have been described in a wide variety of jawed vertebrates (*9, 10*), suggesting evolutionary benefit to antibody coating of microbiota. Curiously, natural IgAs bind a broad but defined subset of microbiota; thus, evolutionary pressure may have led certain bacterial taxa to express a cell surface that either attracts or evades these antibodies. IgA responses are amplified in inflammatory bowel diseases (*6*) and enteric infections (*148*), yet the extent to which these responses differ from homeostatic mechanisms remains unclear. Notably, recruitment of new, antigen-specific clones into the SI IgA repertoire was observed after infection with *S.* Typhimurium *(133)*, suggesting

that more specific responses may be induced in response to particularly strong inflammatory stimuli. B cells expressing polyreactive specificities have been implicated in lymphomas of mucosal origin (*149*), are counterselected during central tolerance (*92, 150*), and are elevated in systemic autoimmune disease (*151*), which had suggested a detrimental role for these antibodies. However, recent reports that inherently polyreactive antibodies constitute the bulk of broadly neutralizing antibody responses to influenza virus and HIV (*108, 109, 152, 153*), and our finding that these bnAbs are of the same type that fuels the homeostatic intestinal IgA response, provide concrete examples demonstrating the protective value of polyreactive antibodies in a variety of homeostatic as well as pathological contexts; exploiting the naturally polyreactive IgA response may provide novel opportunities to elicit bnAbs by mucosal vaccination.

Materials and Methods

Mice

C57BL/6J, one-year-old C57BL/6J, *Tcrb*$^{-/-}$*d*$^{-/-}$ (B6.129P2-*Tcrb*^{tm1Mom} *Tcrd*^{tm1Mom}/J), CD45.1^{+} (B6.SJL-*Ptprc*^{a} *Pepc*^{b}/BoyJ), *Rag1*$^{-/-}$ (B6.129S7-*Rag1*^{tm1Mom}/J), and MD4Tg (C57BL/6-Tg(IghelMD4)4Ccg/J) mice were purchased from Jackson Laboratories. For most experiments, mice were analyzed at 6-12 weeks of age and compared to littermate controls unless otherwise indicated. Mice were maintained in a specific pathogen-free environment at the University of Chicago. Germ free C57BL/6 mice were housed in isolators at the University of Chicago gnotobiotic facility under carefully monitored germ-free conditions; germ free cages contained sterile pine shavings as bedding material. Experimental guidelines were approved by the Institutional Animal Care and Use Committee (IACUC).

Single-cell cloning and production of monoclonal antibodies

Single cells were sorted from the following populations using the indicated markers in parentheses: Splenic B2 ($CD19^+$ $B220^+$ $CD21^+$ $CD23^+$); Splenic MZ B ($CD19^+$ $B220^+$ $CD21^{hi}$ $CD23^-$); Peritoneal B1a ($CD19^+$ $CD23^-$ $CD5^+$); Peritoneal B1b ($CD19^+$ $CD23^-$ $CD5^-$); dividing donor-derived cells in MD4Tg recipients ($CD45.1^+$ $CD19^+$ CellTrace $Violet^{diluted}$); or IgA plasma cells ($Lineage^-$ $B220^-$ IgA^+).

Detailed protocols for single-cell cloning and mAb production have been published separately (*89, 90, 106*). Briefly, single cells were sorted into 96-well plates (Biorad) using a BD AriaII cell sorter. In all plates, one row was left empty as a negative control. For most plasma cell populations, cells were sorted into 10 μL/well nuclease-free 10 mM Tris-HCl with 1 U/ μL SUPERase-In RNase inhibitor (Ambion) and immediately frozen on dry ice. Single-cell cDNA synthesis and paired amplification of rearranged immunoglobulin VH and Vκ genes was then performed using a cocktail of primers as described (*106*). Non-plasma cell populations amplified inefficiently with this method and were instead sorted into 5 μL/well TCL buffer (Qiagen) with 1% beta-mercaptoethanol (v/v). RNA was purified using RNase-free SPRI beads (Beckman Coulter) as described (*106*), and cDNA synthesis and paired amplification were performed as described above. PCR products from single cells were sequenced and cloned using gene-specific primers into human IgG1/Igκ expression vectors as described (*106*); plasmid midipreps were performed with a Qiagen HiSpeed Midi Kit. All sequences were identified and processed using IMGT's default settings (www.imgt.org)(*154, 155*). Somatic mutations were identified and quantified using IMGT's default settings. In some cases, mutations introduced at the beginning or end of the sequence by degenerate primers were discarded from analysis. For germline

reverted mAbs, heavy and light chain sequences were reverted to inferred germline as determined using IMGT, synthesized, and cloned into expression vectors using the same methods described above. If identical mAbs were obtained from multiple cells, only a single copy was retained. mAbs were expressed by transient PEI transfection of 293T cells as described (*106*). Culture supernatants were harvested 6-7d after transfection, cleared of cells by centrifugation at 900g for 10 mins, and mAbs purified with Protein A agarose (Thermo) as described (*106*). mAbs were stored at 4 ºC in TBS pH 8.0 with 0.5% BSA, 150 mM NaCl, and 0.05% sodium azide.

Protein expression and concentration were determined by ELISA performed as follows: ELISA plates (Thermo) were coated with 100 μL/well goat anti-human kappa capture antibodies (Southern Biotech) at 10 μg/mL in carbonate buffer (Bethyl) for 1 hour, washed 4x with TBS-T, and blocked with 200 μL/well TBS 1% BSA (Sigma) for 1 hour. Plates were washed 4X with TBS-T, incubated for 1 hour with 100 μL/well mAbs or purified human IgG1-kappa standard (Sigma) each run in duplicate and serially diluted, washed 4X with TBS-T, incubated for 1 hour with goat anti-human IgG HRP detection antibodies (Southern Biotech, 1:20,000 in TBS-T 1% BSA), washed 4X with TBS-T, revealed with TMB HRP substrate (Bethyl), and quenched with 0.18M H_2SO_4. OD_{450} was read using an ELISA plate reader (BioTek) and concentration was determined by comparison to standards fit to a four-parameter logistic curve.

Lymphocyte flow cytometry and antibodies

Cells were incubated with anti-CD16/32 (Fc block) prior to staining with the following fluorophore or biotin conjugated monoclonal antibodies purchased from Biolegend, eBioscience,

or BD unless otherwise indicated (clone in parentheses): B220 (RA3-6B2), CCR6 (29-2L17), CD4 (GK1.5 or RM4-5), CD5 (53-7.3), CD8 (53-6.7), CD11c (HL3), CD19 (6D5), CD21 (7G6), CD23 (B3B4), CD45.1 (A20), CD45.2 (104), F4/80 (BM8), FoxP3 (FJK-16s), Gl7 (GL7), GR1 (RB6-8C5), IgD (11-26c.2a), IgM (Il/41), NK1.1 (PK136), TER-119 (TER-119), Tcrb (H57-597), goat anti-mouse IgA(Southern Biotech), and goat anti-mouse Nrp1 (RD Systems). Lineage cocktail for plasma cell staining included CD3, CD4, CD11c, F4/80, NK1.1, Tcrb, and TER-119. Doublet exclusion was used when possible. FoxP3 intracellular staining was performed using a FoxP3 staining kit (eBioscience). Cell numbers were calculated by flow cytometry with counting beads (Spherotech).

Lymphocyte isolation from tissues

Small intestinal or colonic (excluding the cecum) lamina propria isolation was performed as follows: tissues were excised and fat, Peyer's patches, and intestinal contents removed. Tissues were opened longitudinally, cut into ~1 cm pieces, and placed into a 50 mL tube with 10 mL RPMI 1% FCS 1 mM EDTA. Small intestines were processed as two halves in separate tubes and combined after lamina propria lymphocyte isolation as noted below; colons were processed in a single tube. Samples were incubated at 37 ºC with shaking for 15 mins. Pieces were collected on a 100 μm cell strainer (Fisher) and placed in fresh RPMI 1% FCS 1mM EDTA for another 15 mins with shaking at 37 ºC. Pieces were again collected on a 100 μm cell strainer and flow-through was discarded as it predominantly contained epithelial cells and intraepithelial lymphocytes. Intestinal pieces were then placed into 10 mL RPMI 20% FCS with 0.5 mg/mL collagenase A (Roche) and 0.1 mg/mL DNase I (Roche) at 37 ºC with shaking for 30 mins. Supernatant was collected by filtering through a fresh 100 μm cell strainer and intestinal pieces

were placed in fresh RPMI 20% FCS with collagenase and DNase for another 30 mins with shaking at 37 ºC. Supernatant was again collected, remaining tissues was mashed, and the cell strainer was washed with 30 mL RPMI. The two lamina propria lymphocyte fractions were combined after centrifugation and further enriched by centrifugation in 40% percoll (Sigma) to remove epithelial cells and debris, washed in flow cytometry buffer, and resuspended for cell staining.

Salivary gland, lactating mammary gland, and lung isolations were performed as follows: after excision, fat was removed and tissues were chopped into small pieces and placed into a 50 mL tube containing 5 mL RPMI 4% BSA (Fisher), 2 mg/mL collagenase type I (Gibco), and 0.1 mg/mL DNase (Roche). Samples were incubated for 45 mins at 37 ºC with shaking, then filtered through a 100 μm cell strainer. Remaining tissue was mashed and the strainer was washed with 30 mL RPMI. After centrifugation, lymphocytes were enriched by centrifugation in 40% percoll (Sigma), washed in flow cytometry buffer, and resuspended for cell staining.

Bacterial flow cytometry and antibodies

Small intestinal contents from two or more 6-to-20-week-old *Rag1*$^{-/-}$ mice were isolated by running forceps along the length of the intestinal tissue, pooled, and placed into a 2 mL Eppendorf Biopur tube on ice. 1 mL PBS (Corning) was added and samples were homogenized by taping the Eppendorf tube horizontally on a vortex and vortexing vigorously for 5 mins. Samples were centrifuged for 5 min at 400g to pellet large debris, and supernatant was filtered through a sterile 70 μm cell strainer (Fisher) and transferred to a new 2 mL tube. Samples were centrifuged at 8000g for 5 min and supernatant was removed by aspiration. The bacterial pellet

was resuspended in ~3 mL per mouse PBS 0.25% BSA with SYTO BC (1:7500, Life Technologies) and incubated ~30 mins on ice. 50 μL/well of bacterial suspension was added to a 96-well V bottom plate (Fisher) and cells pelleted by centrifugation at 4700g for 15 mins. Supernatant was removed and bacteria were resuspended in 100 μL mAb pre-diluted to 10 μg/mL (or desired concentration) in PBS 0.25% BSA and incubated for 20 mins on ice. Suspensions were washed once with 100 uL PBS 0.25% BSA and cells pelleted by centrifugation at 4700g for 15 mins. Supernatant was removed and pellets were resuspended in 100 μL PBS 0.25% BSA 5% normal mouse serum (Jackson Immunoresearch) with mouse anti-human IgG-APC (1:800; HP6017, Biolegend) and incubated for 20 mins on ice. Suspensions were washed once with 100 uL PBS 0.25% BSA and cells pelleted by centrifugation at 4700g for 15 mins, then resuspended in PBS 0.25% BSA with DAPI (Life Technologies) prior to flow cytometry. Staining of live bacteria was visualized by gating on $FSC^{+}SSC^{+}$SYTO $BC^{+}DAPI^{-}$ cells. In most experiments, samples were run using an LSRII flow cytometer (BD) equipped with a high throughput sampler (HTS).

For pre-treatment of microbiota with nuclease, SI microbiota were isolated as described above and incubated with 1 U/mL nuclease (Benzonase, Sigma) for 10 mins at room temperature in PBS 0.25% BSA. Cells were washed twice with 1 mL PBS 0.25% BSA, and resuspended in PBS 0.25% BSA with SYTO BC for 15 mins on ice and stained as described above. For pre-washing of microbiota with low pH buffer, SI microbiota were resuspended in 0.1M glycine-HCl pH 3.0 (Boston Bioproducts) and incubated for 1 min at room temperature. Cells were centrifuged for 1 min at 8000g, and supernatant was aspirated. Cells were washed once with 1 mL PBS 0.25% BSA, centrifuged 5 mins at 8000g, and resuspended in PBS 0.25% BSA with

SYTO BC for 15 mins on ice and stained as described above. Untreated controls were processed side by side and washed twice with PBS 0.25% BSA prior to resuspension in PBS 0.25% BSA with SYTO BC and staining as described above.

For co-staining of mAbs and endogenous polyclonal IgA, intestinal contents from WT B6 mice were processed as described above and resuspended in PBS 0.25% BSA with SYTO BC for 30 mins on ice. 50 μL bacterial suspension was stained with 50 μL 2X mAb master mix at a final concentration of 10 μg/mL for 20 mins on ice. Cells were washed once with 1 mL PBS 0.25% BSA, centrifuged 5 mins at 8000g, and resuspended in 50 μL PBS 0.25% BSA with 10% normal goat serum for 10 mins on ice. 50 μL 2X goat anti-human IgG biotin (1:400 final concentration, Southern Biotech) and goat anti-mouse IgA PE (1:800 final concentration, Southern Biotech) were added and incubated 20 mins on ice. Cells were washed once with 1 mL PBS 0.25% BSA, centrifuged 5 mins at 8000g, and resuspended in 100 μL PBS 0.25% BSA with streptavidin-APC (1:800, Biolegend) for 20 mins on ice. Cells were washed once with 1 mL 0.25% BSA, centrifuged 5 mins at 8000g, and resuspended in PBS 0.25% BSA with DAPI prior to flow cytometry on an LSRII flow cytometer (BD).

Microbiota-reactivity scoring and inclusion criteria

Standardized scoring and inclusion criteria for microbiota-reactivity were used to score all mAbs in this study unless otherwise noted; these were as follows: 1) All experiments were performed using *Rag1*$^{-/-}$ small intestinal microbiota. 2) Scores were assigned based on the percent hIgG^{+} bacteria at a mAb staining concentration of 10 μg/mL. 3) mAbs were assigned a microbiota-reactivity percentile score based on a control distribution of the 47 splenic B2 or 27 anti-

influenza mAbs shown in Fig. 16, assayed side-by-side in the same experiment. Percentile scores were assigned using the Microsoft Excel PERCENTRANK.INC function. 4) Experiments were considered invalid and repeated if high positive SI IgA mAb 39F10 stained less than 6% of microbiota, and this mAb was included in all experiments. This cutoff was selected arbitrarily to avert incorrect scoring of low-positive clones if staining fell to low levels, thus impairing signal detection. 5) mAbs were classified categorically as high microbiota-reactivity if their percentile score was ≥70 and low microbiota-reactivity if their percentile score was <70. This cutoff was selected based on the observation that mAbs with scores of ≥70 showed reactivity that was reproducibly above background.

Purification of mAb-bound or unbound microbiota

Small intestinal contents from two or more 6-to-20-week-old *Rag1*$^{-/-}$ mice were isolated by running forceps along the length of the intestinal tissue, pooled, and placed into a 2 mL Eppendorf Biopur tube on ice. 1 mL sterile PBS (Corning) was added and samples were homogenized by taping the Eppendorf tube horizontally on a vortex and vortexing vigorously for 5 mins. Samples were centrifuged for 5 min at 400g to pellet large debris, and supernatant was filtered through a sterile 70 μm cell strainer (Fisher) and transferred to a new 2 mL tube. Samples were centrifuged at 8000g for 5 min and supernatant was removed by aspiration. The bacterial pellet was resuspended in 3 mL per mouse sterile PBS 0.25% BSA with SYTO BC (1:7500, Life Technologies) and incubated ~30 mins on ice. An unfractionated control sample was archived for all experiments. 250 μL bacterial suspension was added to a 1.5 mL Eppendor tube and 250 μL 2X mAb master mix diluted in PBS 0.25% BSA was added for a final staining concentration of 10 μg/mL. Samples were incubated 20 mins on ice then washed once with 1

mL PBS 0.25% BSA and pelleted by centrifugation at 8000g for 5 min. Pellets were resuspended in 500 μL PBS 0.25% BSA 5% normal goat serum (Jackson Immunoresearch) 1:400 goat anti-human IgG-biotin (Southern Biotech) and incubated for 20 mins on ice. Samples were washed once with 1 mL PBS 0.25% BSA and centrifuged 5 mins at 8000g. Pellets were then resuspended in 500 μL PBS 0.25% BSA 1:800 streptavidin-APC (Biolegend) and incubated 20 mins on ice. Samples were washed once with 1 mL PBS 0.25% BSA and centrifuged 5 mins at 8000g. Pellets were resuspended in in 500 μL PBS 0.25% BSA 1:50 anti-APC magnetic beads (Miltenyi) and incubated 20 mins on ice. Samples were washed once with 1 mL PBS 0.25% BSA and centrifuged 5 mins at 8000g then resuspended in 500 μL PBS 0.25% BSA. Samples were separated using an autoMACS separator (Miltenyi) and the posselds program. Negative samples were saved, and positive samples were further purified by running again using the posseld2 program. Samples were centrifuged at 8000g and frozen at -70 ºC until DNA extraction for 16S sequencing. Aliquots of pre- and post-MACS fractions from all samples were analyzed to verify separation and purity, and negative controls were included in all experiments. In some experiments, colonic contents excluding cecal contents were removed from WT C57BL/6 mice as described above and resuspended in 6 mL PBS 0.25% BSA with SYTO BC (1:7500, Life Technologies) and incubated ~30 mins on ice, then stained with mAbs and separated as described above. For analysis of endogenous polyclonal IgA coating, bacteria were resuspended in 250 μL PBS 0.25% BSA with SYTO BC and 5% normal goat serum and incubated 20 mins on ice. 250 μL of PBS 0.25% BSA 2X goat anti-mouse IgA-biotin (1:1600 final concentration, Southern Biotech) was added and cells incubated 20 mins on ice. Samples were then processed and separated as described above using streptavidin-APC, anti-APC beads, and separation by autoMACS.

For bacterial culture after purification, the mAb^+ fraction was prepared as described above, serially diluted, and plated on Schaedler's Blood Agar (BD) or EMB Agar (BD) under either aerobic or anaerobic conditions and grown for two days at 37 ºC. In a second experiment, bacteria were plated on either blood agar or MacConkey agar (Thermo) and grown for two days at 37 ºC. Individual colonies were restreaked and DNA was extracted using the PureLink Microbiome DNA Extraction Kit (Invitrogen). 16S sequences were amplified using forward primer ACTCCTACGGGAGGCAGCAGT and reverse primer ATTACCGCGGCTGCTGGC using Q5 Hot Start Polymerase Master Mix (New England Biolabs) and the following PCR program: Initial denaturation at 98 ºC for 30s, followed by 35 cycles of 98 ºC for 10s and 72 ºC for 20s, with a final cycle of 72 ºC for 2 mins. PCR products were cleaned up using ExoSAP-IT (Thermo) according to the manufacturer's protocol and subjected to Sanger sequencing. Bacterial taxonomy was assigned from sequences using the Michigan State University Ribosomal Database Project Classifer (*156*). For flow cytometry staining, bacteria were washed from agar plates with 5 mL sterile PBS 0.25% BSA and centrifuged for 5 min at 400g to pellet debris. Supernatant was filtered through a 70 um cell strainer, transferred to a new tube, and pelleted at 8000g for 5 mins. Bacterial pellets were resuspended in PBS 0.25% BSA with SYTO BC (1:7500) and incubated for 15 mins on ice, then stained as described above.

16S rRNA gene sequencing and analysis

DNA was extracted using the PowerSoil®-htp 96 Well Soil DNA Isolation Kit (MO BIO Laboratories, Inc.) according to the manufacturer's instructions. Amplicons of the V4 region of 16S rRNA genes were generated using the polymerase chain reaction (PCR) using the modified

515F-806R primer set (*157*). The primers were Golay-barcoded to allow for multiplexing on the Illumina MiSeq platform (*158*). PCR reactions were carried out in triplicate for each sample using sterile, DNase-free 96 well plates with appropriate (DNA template-free) negative controls using the 5 PRIME MasterMix (Gaithersburg, MD). No significant amplification was observed in the template-free control reactions, and negative control reactions processed through the sequencing pipeline did not produce any valid sequences. PCR reactions began with an initial denaturation step of 95 ºC for 3 minutes, followed by 35 cycles of the following: 95 ºC for 30 seconds, 55 ºC for 45 seconds, then 72 ºC for 1.5 minutes. The PCR reaction was finalized using a single extension step at 72 ºC for 10 minutes.

Triplicate PCR reactions were then pooled together and total DNA was quantified using the PicoGreen® dsDNA Assay (Life Technologies). Primer dimers were removed from the pooled product using the UltraClean® PCR Clean-Up Kit (MoBio Laboratories, Inc.) and the amount of amplicon in each pooled sample was normalized to a final concentration of 2 ng μL^{-1}. Amplicons were sequenced on an Illumina MiSeq using 151×151 base pair paired-end sequencing at the Environmental Sample Preparation and Sequencing Facility at Argonne National Laboratory.

Raw sequence data was processed using the QIIME analysis pipeline (*159*) and other bioinformatics toolkits. Paired-end reads were joined together using PEAR (*160*), and any reads of insufficient quality that prevented joining were discarded (< 5% of total reads). From a total of 270 samples, 1.24×10^7 paired-end reads were generated (46,065±24,747 reads per sample). Sequences were then aligned to a database of reference sequences using PyNAST (*161*) and clustered into operational taxonomic units (OTUs) using UCLUST at 97% similarity (*162*). A

consensus taxonomy from the Greengenes reference database (*163*) was assigned to each sequence using the UCLUST taxonomy assigner. Sequencing data are publicly available to download via MG-RAST (*78*).

Polyreactivity ELISAs

Polyreactivity assays were performed as described (*92, 108, 109*). ELISA plates (Thermo) were coated overnight with 50 μL/well antigen diluted in carbonate buffer (Bethyl) with the exception of cardiolipin, which was coated overnight in 100% ethanol left uncovered to allow evaporation. The following antigens and concentrations were used for coating: calf thymus DNA (Life Technologies), 10 μg/mL; human insulin (Fitzgerald), 5 μg/mL; LPS from *E. coli* (Sigma), 10 μg/mL; flagellin from *S. typhimurium* (InvivoGen), 2 μg/mL; cardiolipin (Sigma), 10 μg/mL; albumin from human serum, low endotoxin (Sigma), 10 μg/mL; and KLH, endotoxin free (Millipore), 10 μg/mL. Plates were washed 4x with nanopure H_2O with an ELISA plate washer (BioTek) and blocked with 150 μL/well blocking buffer [1X TBS-T (Thermo), 1mM EDTA (Boston BioProducts)] for 1 hour at 37 ºC. Plates were washed 4x with H_2O using an ELISA plate washer (BioTek) and 50 μL/well of mAbs pre-diluted in TBS pH 7.4 were added. mAbs were assayed at 1 μg/mL and three additional 1:4 dilutions. Strongly polyreactive positive control mAb 3H9 and four TBS-only wells were included on each plate. Plates were incubated at 37 ºC for one hour then washed 4x with H_2O. 75 μL/well of goat anti-human IgG HRP (Southern Biotech) diluted in blocking buffer were added and plates were incubated one hour at 37 ºC then washed 4x with H_2O. 150 μL/well of blocking buffer was added and plates incubated 5 mins at room temperature. Plates were washed 4x with H_2O and 100 μL/well of developing reagent was added (Super AquaBlue ELISA Substrate, eBioscience). Plates were monitored at

OD_{405} using an ELISA plate reader (BioTek) and reading was stopped when the 3H9 positive control reached an OD_{405} of ~3.0. Average OD_{405} of TBS-only wells was subtracted from mAb-containing wells for analysis. mAbs were considered polyreactive if they bound two or more antigens with an OD_{405} of ≥0.5 at a concentration of ≤ 1 μg/mL.

HEp2 ANA ELISAs

mAbs were assayed at 10 μg/mL and 3 additional 1:4 dilutions using the QUANTAlite ANA ELISA kit (INOVA Diagnostics) using the manufacturer's protocol and provided reagents. High positive control mAb 3H9 was included on each plate, as were low positive and negative control serum provided by the manufacturer.

Free IgA ELISAs

Intestinal contents were resuspended at 0.1 mg/μL in PBS (Corning) with protease inhibitors (SIGMAFAST Protease Inhibitor Tablets, Sigma) and homogenized by taping the Eppendorf tube horizontally on a vortex and vortexing vigorously for 5 mins. Samples were centrifuged 5 mins at 400g and supernatants were filtered through a 70 μm sterile strainer (Fisher) and transferred to a new tube. This tube was centrifuged at 8000g for 5 mins. Supernatant was collected and assayed for free IgA by ELISA using the Bethyl Mouse IgA Quantitation Set according to the manufacturer's protocol. Plates were read using an ELISA plate reader (BioTek) and samples values quantified by comparison to mouse IgA standards fit to a four-parameter logistic curve.

mAb in vivo serum retention experiments

mAbs were buffer exchanged into sterile HBSS using an Amicon 30K centrifugal filter and 2 μg was injected intravenously into *Rag1*$^{-/-}$ recipients. Blood was collected 5d after injection and serum isolated using serum separator tubes (BD). mAb concentration was measured by ELISA using goat anti-human IgK capture antibodies (Southern Biotech) and goat anti-human IgG HRP detection antibodies (Southern Biotech) and concentration determined by comparison to a standard curve as described above under 'Single cell cloning and production of monoclonal antibodies.' Polyreactive and non-polyreactive mAbs were randomly distributed among mice of similar age and gender.

Size exclusion chromatography

mAbs were purified from several pooled 293T culture supernatants with protein A agarose, eluted in Gly-HCl pH 3.0, and neutralized with 1M Tris-HCl pH 8.0 as described above. No BSA or additional preservatives were added. Samples were analyzed and monomers purified by fast protein liquid chromatography (FPLC) using a Superdex 200 column (GE). Purified monomers were immediately used in assays as indicated.

Microbial glycan microarrays

mAbs were diluted to 10 μg/mL or 1 μg/mL in 20 mM Tris-HCl pH 7.4 150mm NaCl 2mM CaCl 2mM MgCl 0.05% Tween 20 1% BSA and assayed against the microbial glycan microarray by the Consortium for Functional Glycomics at the Protein-Glycan Interaction Core (CFG) and National Center for Functional Glycomics at Beth Israel Deaconess Medical Center in Boston, MA. Raw data are publicly available under accession numbers CFG_3246, CFG_3329, and CFG_3402 (www.functionalglycomics.org).

MD4Tg cell transfers

Spleens from multiple CD45.1$^+$ donors were pooled and depleted of non-B cells with biotinylated anti-CD4, CD8, CD3, NK1.1, CD11c, GR1, and TER119 antibodies and streptavidin magnetic beads (Miltenyi) using an autoMACS separator (Miltenyi). Depleted samples were counted and resuspended in PBS at 20 million cells per mL. 0.0312 μL of 5mM CellTrace Violet stock solution (Life Technologies) was added per mL and cells were incubated at 37 ºC for 20 mins. Reaction was quenched by adding PBS 10% FCS and incubating at 37 ºC for 5 mins. Cells were centrifuged 5 min at 500g, washed with HBSS 0.25% BSA, centrifuged again at 500g, washed with PBS, and resuspended in sterile HBSS. Small aliquots were taken for counting and staining to verify purity and fluorescent labeling (anti-CD19 and CD45.1). 20-30 million B cells were injected intravenously into 6-to-10-week-old MD4Tg recipients and analyzed 7d later. For single cell cloning, Peyer's patches from multiple recipients were pooled and MACS-enriched for CD45.1$^+$ cells and single CD19$^+$CD45.1$^+$ cells that had diluted CellTrace Violet were sorted.

Antigen-free diet experiments

Three-week-old germ-free mice were weaned onto either standard chow or antigen-free diets. The antigen-free diet consisted of an aqueous solution of vitamins and minerals administered ad libitum as well as a lipid supplement administered by daily oral gavage (0.25 mL/d). Aqueous diet was refilled as needed and fresh stock solutions were introduced into the isolator every two weeks. Both components were sterilized by filtration through a 0.22 μm sterile filter (Millipore).

Mice were kept on the diet for four weeks and then analyzed. Diet was prepared as described (*136, 137*) according to the recipe in Table 19.

Statistical analysis

Paired or unpaired t test, chi-square test, or 2x2 Fisher's exact test were performed as indicated in figure legends using GraphPad Prism.

Acknowledgements: We thank the University of Chicago Flow Cytometry Core for assistance with cell sorting, S. Owens and S. Greenwald at the Argonne National Laboratory Environmental Sample Preparation and Sequencing Facility for assistance with 16S sequencing, the University of Chicago DNA Sequencing Core for assistance with plasmid minipreps and sequencing, B. Theriault and the University of Chicago Gnotobiotic Facility for assistance with germ-free and antigen-free experiments, the Consortium for Functional Glycomics for microbial glycan microarray screening, G. Salzman for assistance with FPLC, and S. Canavan for assistance with figure preparation. This work was supported by NIH grants T32GM007281 and F30AI124476 (to J.J.B), grants U01AI125250, R01AI038339, R01AI108643, R01GM106173, and R01HL118092 (to A.B.), grant P41GM103694 to the National Center for Functional Glycomics at Beth Israel Deaconess Medical Center, and grant P30DK042086 to the University of Chicago Digestive Diseases Research Core Center (to A.B., B.J., and D.A.A.).

All data to understand and assess the conclusions of this research are available in the main text, supplementary materials, and via the following repositories: antibody sequences are available

via GenBank accession numbers MF466210-MF467203 and 16S rRNA sequencing data are available via MG-RAST accession number MGP80334.

Author Contributions: J.J.B. and A.B. conceived the study; J.J.B., S.A.E., and A.B. designed research; A.B. supervised research; J.J.B. and S.A.E. performed experiments and analyzed data; C.H. and P.C.W. contributed anti-influenza mAbs and advice regarding mAb production and characterization; T.M.F., J.C.K., and D.A.A. processed samples for 16S sequencing and analyzed associated data; M.M. and B.J. provided mice and assistance with gnotobiotic experiments; J.J.B. and A.B. wrote the paper and all authors approved the final manuscript.

Table 20. List of mAbs used in this study. Supplementary Excel file listing name, cellular origin, microbiota-reactivity, polyreactivity, heavy and light chain variable gene usage and CDR3 sequence, somatic mutation, and additional notes for all mAbs used in this study. Variable gene usage, somatic mutation, and CDR3 sequence were determined using IMGT (www.imgt.org).

CHAPTER 5

STRUCTURAL BASIS OF ANTIBODY POLYREACTIVITY

Jeffrey J. Bunker and Albert Bendelac

Unpublished.

Summary

Emerging studies indicate that polyreactivity is an important property that is strongly associated with broadly neutralizing antibody responses to HIV and influenza (*108, 109*) and IgA-mediated homeostasis with the intestinal microbiota (*3*). However, the structural basis for antibody polyreactivity remains enigmatic. Here we used serial alanine mutagenesis of heavy and light chain CDR1/2/3 regions to assess the contribution of individual amino acid residues to antibody polyreactivity. These results reveal that individual residues commonly participate in reactivity to a variety of antigens. Further, different antibodies utilized a variety of structural mechanisms to achieve polyreactivity. Aromatic amino acids such as tyrosine and phenylalanine were commonly involved in polyreactivity, as were positively charged arginine residues. These data suggest that a wide variety of structural mechanisms can be used by individual antibodies to achieve polyreactivity, and highlight the contribution of individual amino acids to this peculiar type of recognition.

Introduction

In contrast to the highly specific antibodies typically associated with adaptive immune responses, polyreactive antibodies possess the ability to bind a wide variety of structurally diverse antigens, typically at relatively low affinity. Numerous studies have associated these antibodies with negative selection during B cell central tolerance (*92*), with autoimmune disorders such as systemic lupus erythematosus (*151*), or with receptors cloned from B cell lymphomas (*149*). Together, these data had suggested a detrimental role for polyreactivity and raised questions about why these antibodies would arise in the B cell repertoire under normal conditions.

Contrary to these suggestions, recent reports have demonstrated that polyreactivity is associated with broadly neutralizing antibody (bnAb) responses to HIV and influenza (*108, 109*) and in homeostatic IgA responses to the intestinal microbiota (*3*). HIV virions express envelope (Env) protein spikes at very low densities on the viral surface such that bivalent binding of a single antibody to two spikes is largely prevented. To increase relative binding affinity, HIV Env-specific bnAbs utilize polyeactivity, which allows low-affinity binding to other antigens on the virions and facilitates an increase in apparent antibody affinity for the virus (*109*). Similarly, targeting of the conserved influenza hemagluttinin (HA) stalk region is sterically hindered in intact virions (*108*), and thus polyreactivity has been suggested to enhance apparent affinity by a similar mechanism. In the intestine, polyreactivity facilitates binding to a broad but defined array of commensal bacteria (*3*). This property allows a simple immunological solution to the dynamic and complex nature of antigens encountered in the gut from various microbial and dietary sources.

While these studies provide concrete examples of the physiological relevance of antibody polyreactivity, the biochemical and structural mechanisms that mediate this curious type of reactivity remain poorly understood. While some studies have identified associations between polyreactivity and the net charge of antibody variable regions (*92*), this has not been observed in other studies (*3, 109*). One study utilizing two similar antibodies, one polyreactive and one non-polyreactive, demonstrated that polyreactivity could be transferred by the heavy chain CDR3 (*146*). However, other observations suggest that heavy chain polyreactivity can be silenced by light chains (*147*), suggesting that multiple mechanisms likely contribute to this type of reactivity.

To begin to understand the molecular basis for antibody polyreactivity, we performed serial alanine scanning mutagenesis on six polyreactive and microbiota-reactive antibodies from IgA plasma cells or naïve B cells. Our data identify individual residues that participate in polyreactive recognition of diverse antigens, and highlight a number of unique mechanisms used by antibodies to achieve this type of reactivity. Future studies focused on crystallization of these antibodies alone or in complex with various antigens are in progress.

Results

We selected six polyreactive monoclonal antibodies (mAbs) for detailed structural analysis. These antibodies were isolated in our previous work documenting the specificity of intestinal IgA antibodies (*3*). Three of these antibodies were isolated from small intestinal (SI) IgA plasma cells (PCs) of wild-type SPF mice, one was isolated from SI IgA PCs of germ-free (GF) mice, and two were isolated from naïve splenic B2 cells. As measured by ELISA, all six antibodies are strongly polyreactive against seven structurally diverse antigens including DNA,

insulin, LPS, flagellin, cardiolipin, albumin, and KLH. Further, all antibodies are reactive against intestinal microbiota and target multiple microbial taxa, with prominent reactivity to the phylum Proteobacteria.

To investigate the amino acids responsible for antibody polyreactivity and microbiota reactivity, we serially mutated each amino acid in the heavy and light chain complementarity determining region (CDR) 1, 2, and 3, resulting in 40-50 single acid mutant variants of each wild-type antibody. Each variant was assayed for polyreactivity and microbiota-reactivity and compared to the unmutated wild-type parental antibody.

Analysis of SI IgA antibody 41C10 identified several amino acids involved in polyreactivity. In particular, two tyrosine (Y) residues in the CDR1 region, a tyrosine and serine (S) in the CDR2, and a stretch of four amino acids, phenylalanine-leucine-leucine-argine, in the CDR3 appeared to be major contributors (Fig. 35). Of note, mutations that disrupted binding to on antigen typically affected reactivity to all the antigens assayed, suggesting a common mechanism of recognition. By contrast, few if any mutations in the antibody light chain affected polyreactivity. Several of the heavy chain mutants that affected polyreactivity also reduced antibody microbiota-reactivity. However, many mutants in the light chain had a strong negative effect on microbiota-reactivity. Thus, mAb 41C10 appears to utilize several residues in the heavy chain CDR1/2/3 to achieve polyreactivity, whereas the light chain appears to predominate in conferring its microbiota-reactivity.

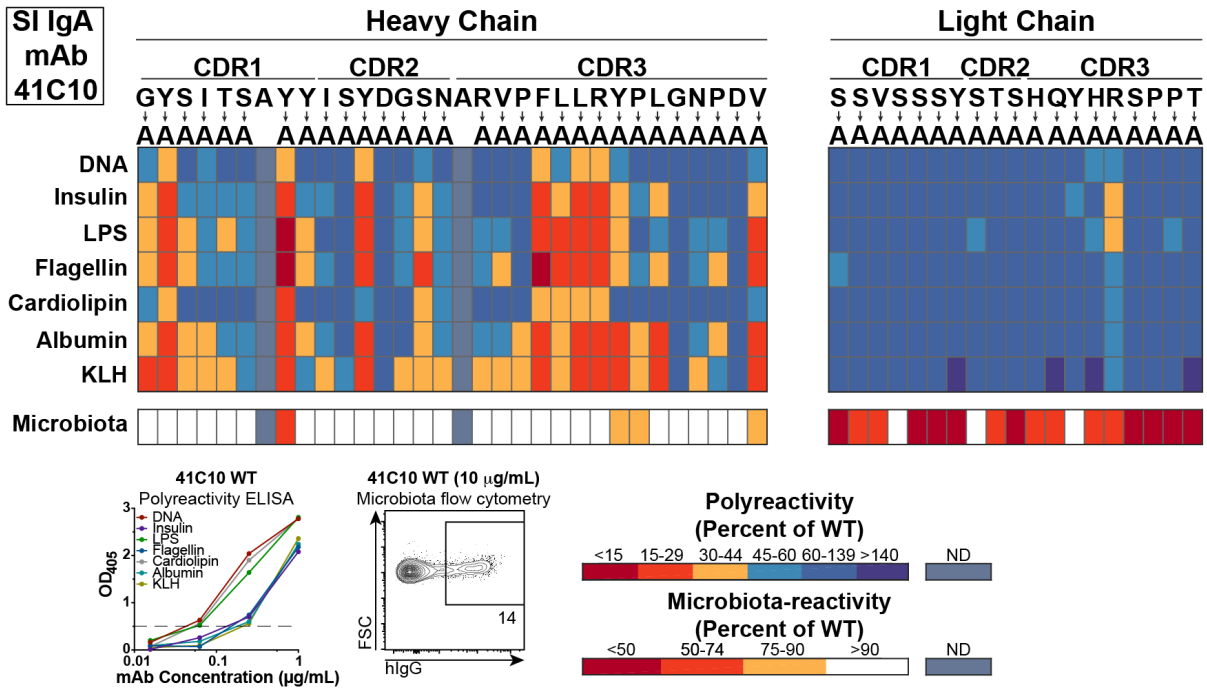

Figure 35. Polyreactivity and microbiota-reactivity of SI IgA mAb 41C10 alanine mutants. Indicated alanine mutants were assayed for polyreactivity by ELISA or microbiota by bacterial flow cytometry. Displayed is the reactivity for each mutant as a percent of wild-type according to the color scheme indicated.

Analysis of SI IgA mAb 43G10 indicated that an arginine residue in the heavy chain CDR3 as well as tyrosine and lysine (K) residues in the light chain CDR1 were important for recognition of all seven antigens assayed (Fig. 36). Interestingly, several heavy chain residues including a glycine (G), isoleucine (I), tyrosine, and phenylalanine in the heavy chain CDR1 as well as isoleucine in the heavy chain CDR2 appeared to be important for recognition of the protein antigens (insulin, flagellin, albumin, and KLH) but largely dispensable for non-protein antigens. A variety of mutations in the heavy and light chains affected microbiota-reactivity. These were partially overlapping with mutations that confer polyreactivity, but also highlighted a prominent contribution of multiple residues in the light chain CDR3 to microbiota-reactivity.

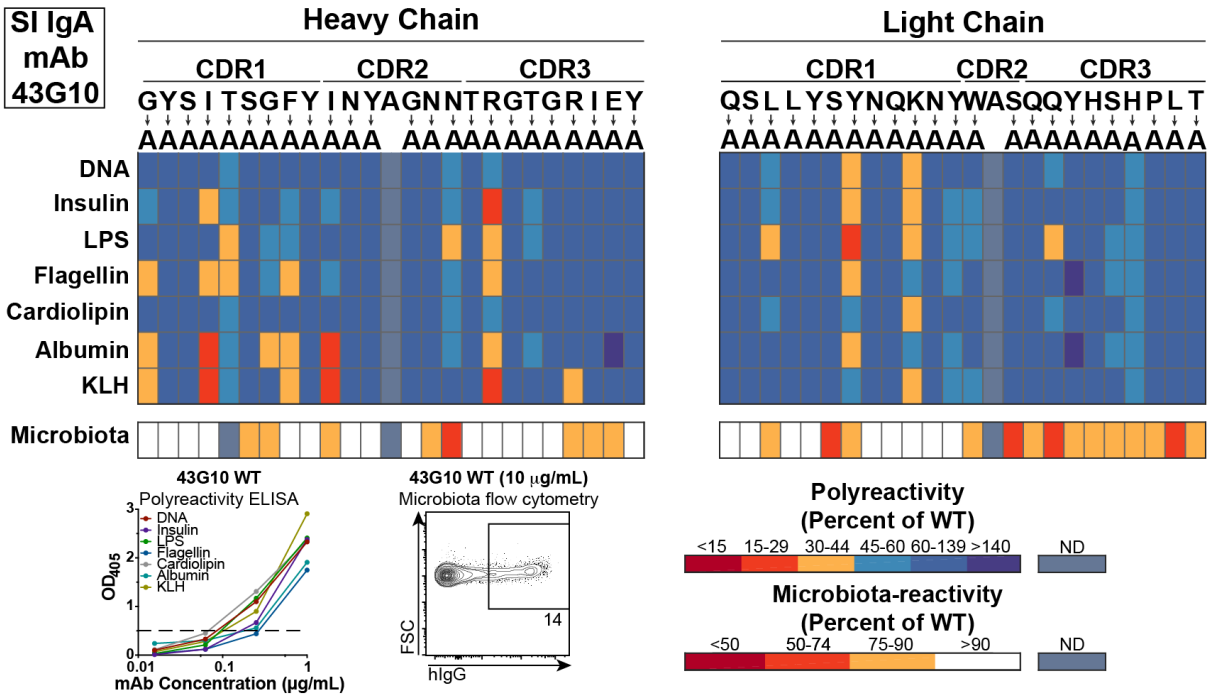

Figure 36. Polyreactivity and microbiota-reactivity of SI IgA mAb 43G10 alanine mutants. Indicated alanine mutants were assayed for polyreactivity by ELISA or microbiota by bacterial flow cytometry. Displayed is the reactivity for each mutant as a percent of wild-type according to the color scheme indicated.

Mutants of SI IgA mAb 45B7 indicated a role for a glycine and two phenylalanine residues in the heavy chain CDR1, an arginine in the heavy chain CDR3, and a tryptophan and tyrosine in the light chain CDR3 in polyreactivity (Fig. 37). Thus, the pattern of amino acid dependence for this antibody differs from the previous antibodies but resembles them in its common involvement of aromatic amino acids and arginine. Microbiota-reactivity again showed a partially-overlapping amino acid dependence with polyreactivity, and involved numerous amino acids in the heavy and light chain CDR1,2, and 3.

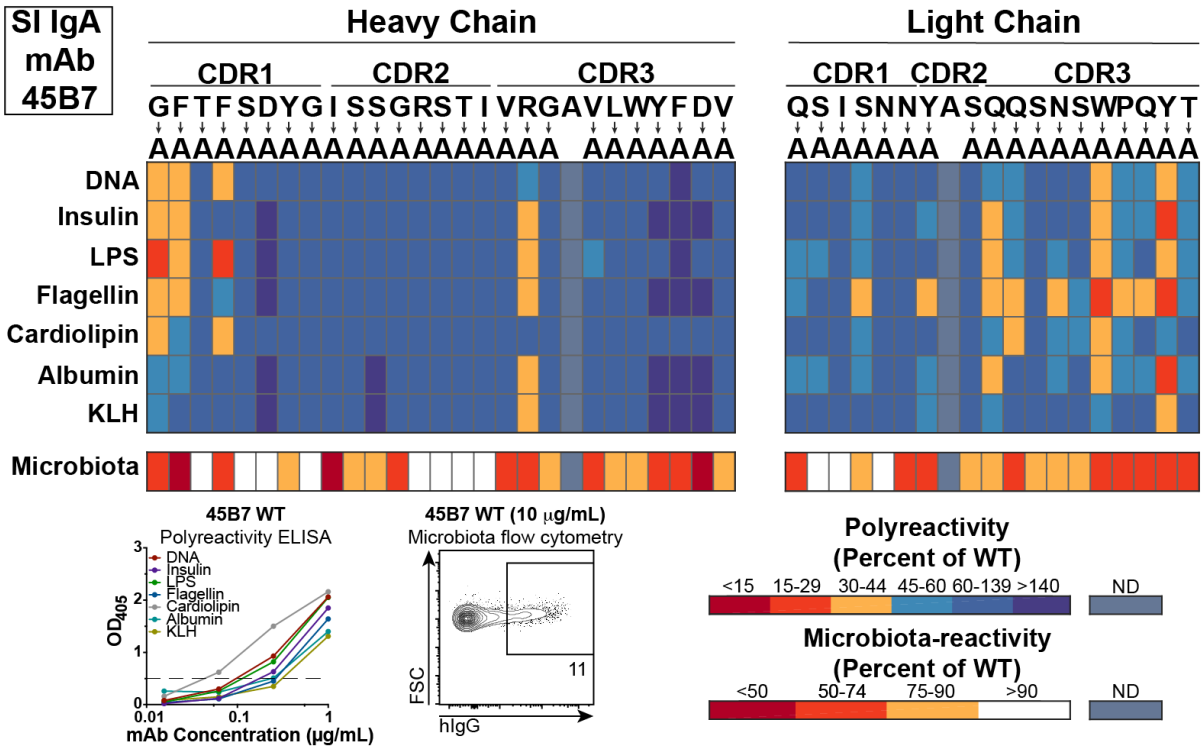

Figure 37. Polyreactivity and microbiota-reactivity of SI IgA mAb 45B7 alanine mutants. Indicated alanine mutants were assayed for polyreactivity by ELISA or microbiota by bacterial flow cytometry. Displayed is the reactivity for each mutant as a percent of wild-type according to the color scheme indicated.

Alanine scanning mutagenesis of GF SI IgA mAb 28A8 highlighted involvement of a phenylalanine residue in the heavy chain CDR1 and arginine in the heavy chain CDR2 in antibody polyreactivity (Fig. 38). In addition, similar to SI IgA mAb 43G10, this antibody appeared to use certain residues for recognition of protein but not non-protein antigens, including a tyrosine in the heavy chain CDR1, phenylalanine in the heavy chain CDR3, and arginine in the light chain CDR3. Microbiota-reactivity was largely overlapping with polyreactivity, although some mutations showed defects in one type of reactivity but not the other.

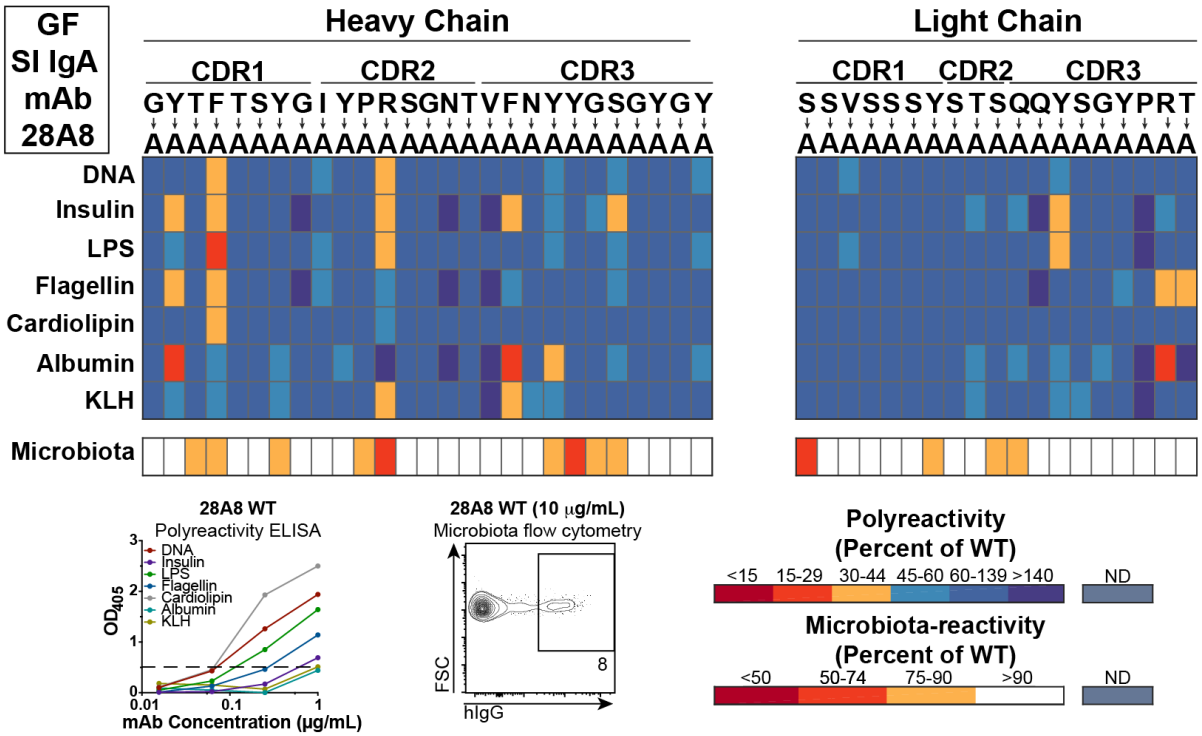

Figure 38. Polyreactivity and microbiota-reactivity of GF SI IgA mAb 28A8 alanine mutants.
Indicated alanine mutants were assayed for polyreactivity by ELISA or microbiota by bacterial flow cytometry. Displayed is the reactivity for each mutant as a percent of wild-type according to the color scheme indicated.

Analysis of B2 mAb 338E6 indicated a pattern that differed from the previously analyzed mAbs (Fig. 39). In particular, many residues in the light chain CDR1, 2, and 3 showed moderate reductions in polyreactivity. Additionally, heavy chain mutants in glycine and phenylalanine in the CDR1, isoleucine in the CDR2, and aspartate in the CDR3 showed reductions in polyreactivity. Residues affecting microbiota-reactivity were largely overlapping with those involved in polyreactivity.

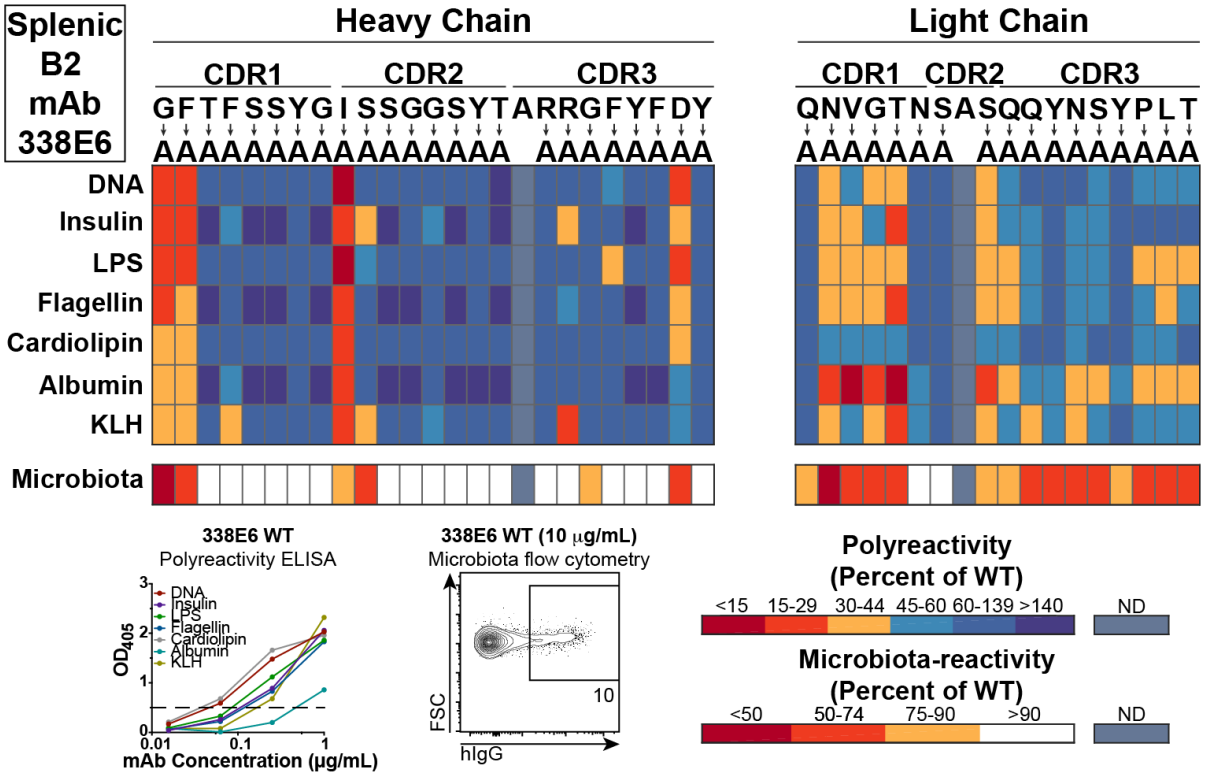

Figure 39. Polyreactivity and microbiota-reactivity of B2 mAb 338E6 alanine mutants. Indicated alanine mutants were assayed for polyreactivity by ELISA or microbiota by bacterial flow cytometry. Displayed is the reactivity for each mutant as a percent of wild-type according to the color scheme indicated.

Finally, mutational analysis of B2 mAb 307C9 revealed a pattern that again differed from any other antibody examined. We identified only a single residue – a proline in the light chain CDR3 – that affected polyreactivity. A handful of residues in the light chain and two in the heavy chain affected microbiota-reactivity, including the prominent light chain residue involved in polyreactivity.

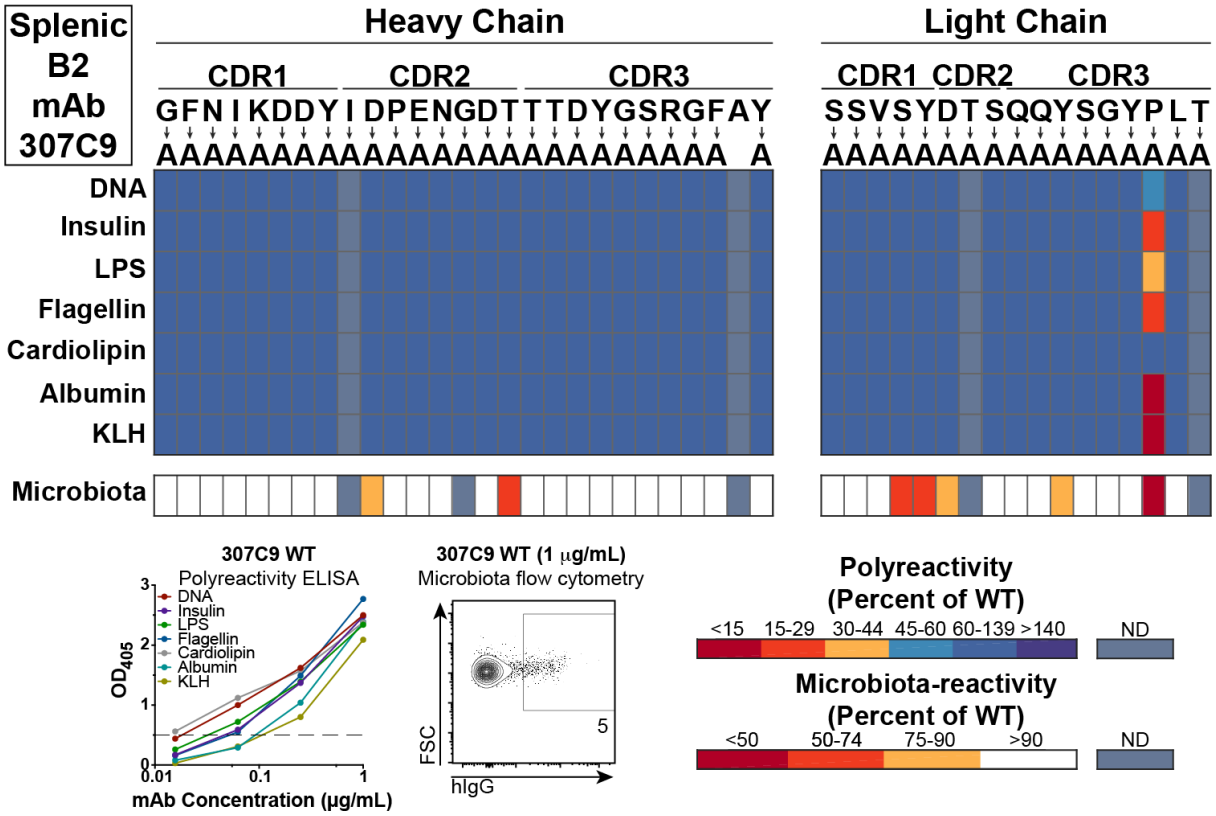

Figure 40. Polyreactivity and microbiota-reactivity of B2 mAb 307C9 alanine mutants. Indicated alanine mutants were assayed for polyreactivity by ELISA or microbiota by bacterial flow cytometry. Displayed is the reactivity for each mutant as a percent of wild-type according to the color scheme indicated.

Discussion

These data identify key residues involved in antibody polyreactivity. In particular, we commonly identified aromatic amino acids such as tyrosine and phenylalanine and arginine in polyreactive recognition. These amino acids may therefore exploit their hydrophobicity or positively charged side chains in order to mediate these promiscuous interactions. Of note, this type of reactivity may be reminiscent of hydrophobic patches used by cytokine receptors to recognize diverse cytokine ligands (*164*).

Interestingly, mutations that disrupted reactivity to one antigen on the polyreactivity ELISA panel typically affected reactivity to most or all other antigens. These data suggest that particular residues are involved in promiscuous reactivity to diverse antigens and suggest that common structural mechanisms are likely to mediate interaction with each individual antigen.

While these data have elucidated the amino acids involved in polyreactivity for a handful of antibodies, they have not revealed general trends that could be applied to unknown antibodies. It appears that many different structural mechanisms can be utilized by different antibodies to achieve polyreactive recognition.

The precise structural basis for polyreactive antibody recognition of various ligands remains unknown and will require detailed crystallographic studies. These studies are in progress and will be the subject of future research. Our future studies will include crystallographic descriptions of the antibodies individually and, if technically possible, in complex with two or more diverse ligands. Together with our mutational analyses, these studies should clarify the structural basis of antibody polyreactivity and may enable prediction of this property in unknown sequences or rational antibody engineering to either enable or disable polyreactivity.

Materials and Methods

Production of alanine mutants

CDR1, 2, and 3 regions were determined using IMGT (ww.imgt.org). Residues were individually changed to alanine and ordered as gBlock fragments from Integrated DNA Technologies (IDT) with Gibson overhangs as described in Chapter 3. Fragments were assembled into antibody expression vectors using the HiFi Assembly master mix (NEB),

transformed in to *E. coli*, miniprepped, transfected into 293T cells, and proteins were purified as described in detail in Chapter 3.

Polyreactivity ELISAs

Polyreactivity assays were performed as described (*92, 108, 109*). ELISA plates (Thermo) were coated overnight with 50 μL/well antigen diluted in carbonate buffer (Bethyl) with the exception of cardiolipin, which was coated overnight in 100% ethanol left uncovered to allow evaporation. The following antigens and concentrations were used for coating: calf thymus DNA (Life Technologies), 10 μg/mL; human insulin (Fitzgerald), 5 μg/mL; LPS from *E. coli* (Sigma), 10 μg/mL; flagellin from *S. typhimurium* (InvivoGen), 2 μg/mL; cardiolipin (Sigma), 10 μg/mL; albumin from human serum, low endotoxin (Sigma), 10 μg/mL; and KLH, endotoxin free (Millipore), 10 μg/mL. Plates were washed 4x with nanopure H_2O with an ELISA plate washer (BioTek) and blocked with 150 μL/well blocking buffer [1X TBS-T (Thermo), 1mM EDTA (Boston BioProducts)] for 1 hour at 37 ºC. Plates were washed 4x with H_2O using an ELISA plate washer (BioTek) and 50 μL/well of mAbs pre-diluted in TBS pH 7.4 were added. mAbs were assayed at 1 μg/mL and three additional 1:4 dilutions. Strongly polyreactive positive control mAb 3H9 and four TBS-only wells were included on each plate. Plates were incubated at 37 ºC for one hour then washed 4x with H_2O. 75 μL/well of goat anti-human IgG HRP (Southern Biotech) diluted in blocking buffer were added and plates were incubated one hour at 37 ºC then washed 4x with H_2O. 150 μL/well of blocking buffer was added and plates incubated 5 mins at room temperature. Plates were washed 4x with H_2O and 100 μL/well of developing reagent was added (Super AquaBlue ELISA Substrate, eBioscience). Plates were monitored at OD_{405} using an ELISA plate reader (BioTek) and reading was stopped when the 3H9 positive control reached an OD_{405} of ~3.0. Average OD_{405} of TBS-only wells was subtracted from mAb-

containing wells for analysis. mAbs were considered polyreactive if they bound two or more antigens with an OD_{405} of ≥0.5 at a concentration of ≤ 1 μg/mL. To obtain the percent of WT, OD_{405} of alanine mutants was divided by that of the WT antibody assayed side-by-side on the same plate.

Bacterial flow cytometry and antibodies

Small intestinal contents from two or more 6-to-20-week-old *Rag1*$^{-/-}$ mice were isolated by running forceps along the length of the intestinal tissue, pooled, and placed into a 2 mL Eppendorf Biopur tube on ice. 1 mL PBS (Corning) was added and samples were homogenized by taping the Eppendorf tube horizontally on a vortex and vortexing vigorously for 5 mins. Samples were centrifuged for 5 min at 400g to pellet large debris, and supernatant was filtered through a sterile 70 μm cell strainer (Fisher) and transferred to a new 2 mL tube. Samples were centrifuged at 8000g for 5 min and supernatant was removed by aspiration. The bacterial pellet was resuspended in ~3 mL per mouse PBS 0.25% BSA with SYTO BC (1:7500, Life Technologies) and incubated ~30 mins on ice. 50 μL/well of bacterial suspension was added to a 96-well V bottom plate (Fisher) and cells pelleted by centrifugation at 4700g for 15 mins. Supernatant was removed and bacteria were resuspended in 100 μL mAb pre-diluted to 10 μg/mL (or desired concentration) in PBS 0.25% BSA and incubated for 20 mins on ice. Suspensions were washed once with 100 uL PBS 0.25% BSA and cells pelleted by centrifugation at 4700g for 15 mins. Supernatant was removed and pellets were resuspended in 100 μL PBS 0.25% BSA 5% normal mouse serum (Jackson Immunoresearch) with mouse anti-human IgG-APC (1:800; HP6017, Biolegend) and incubated for 20 mins on ice. Suspensions were washed once with 100 uL PBS 0.25% BSA and cells pelleted by centrifugation at 4700g for 15 mins, then resuspended in PBS 0.25% BSA with DAPI (Life Technologies) prior to flow

cytometry. Staining of live bacteria was visualized by gating on $FSC^{+}SSC^{+}$SYTO $BC^{+}DAPI^{-}$ cells. In most experiments, samples were run using an LSRII flow cytometer (BD) equipped with a high throughput sampler (HTS). To obtain the percent of WT, %hIgG+ of alanine mutants was divided by that of the WT antibody assayed side-by-side in the same experiment.

CHAPTER 6

DISCUSSION

Mechanisms of homeostatic IgA responses that target microbiota

IgA responses to microbiota occur via both TI and TD pathways (*4, 11*), and target a taxonomically distinct subset of microbiota that we consider in detail below. Precursors to IgA^+ PCs include circulating naive follicular B2 cells and innate-like peritoneal B1b cells; peritoneal B1a cells that contribute to natural serum IgM responses are not observed within the IgA repertoire (*4, 11, 67, 138*). In classical models of systemic immunity, TI responses occur in response to polyvalent antigens such as bacterial polysaccharides and involve rapid cellular differentiation with little somatic hypermutation (SHM). By contrast, TD responses typically target protein antigens and involve iterative rounds of SHM and affinity selection in GCs based on cognate interactions with $CD4^+$ T follicular helper cells (Tfh) (*165*). However, the extent to which homeostatic mucosal IgA responses resemble these processes remains unclear, and several lines of evidence suggest distinct mechanisms and regulation.

First, specific and high-affinity recognition of individual microbial antigens by homeostatic IgA antibodies has not been demonstrated. Instead, studies of monoclonal antibodies (mAbs) indicate that IgA-derived antibodies are commonly polyreactive and show low-affinity binding to numerous microbial antigens including lipopolysaccharides, DNA, flagellin, and capsular polysaccharides (Figure 41A) (*3, 57, 101, 102, 104, 105, 131*). Moreover, a substantial number of natural SI IgA PCs differentiate in germ-free (GF) mice or GF mice fed an antigen-free diet (GF/AF) that are devoid of exogenous antigens; mAbs cloned from these IgA^+ PCs can bind to the same bacteria normally coated with IgA in specific pathogen free (SPF) mice (*3, 102, 103*).

Further, random polyreactive mAbs cloned from naïve B cells or influenza-specific responses bind the same subset of microbiota that is coated with IgA in vivo (*3*). These data suggest that antibody polyreactivity and associated self-reactivity may be the predominant drivers of IgA selection, and support a model whereby IgA polyreactivity enables low-affinity binding to multiple bacterial surface molecules (Figure 41A).

A

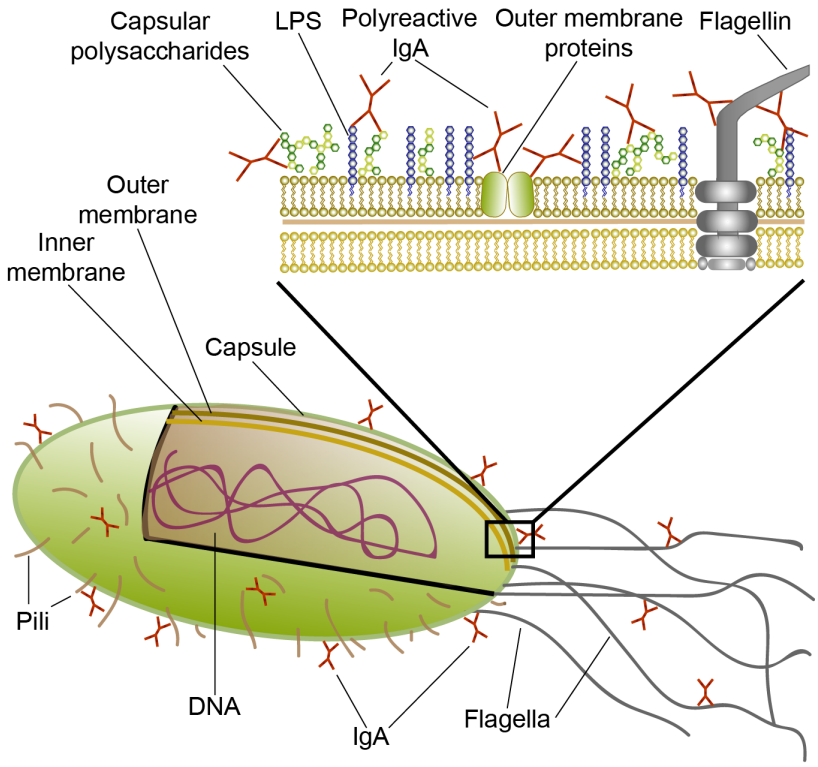

B

Bacterial taxon	Requirements for Ig coating: T cells	Tfh	SHM	Properties of coating antibodies: Polyreactive	Microbial cross-reactive	Antigen-specific
Proteobacteria	No	No	No	Frequently	Frequently	Unknown
Lactobacillus	No	No	No	Frequently	Frequently	Unknown
SFB	Yes	No	No	Yes/Unknown	Yes/Unknown	Unknown
Mucispirillum	Yes	No	No	Unknown	Unknown	Unknown
Prevotella	Yes	Unknown	Unknown	Unknown	Unknown	Unknown
Helicobacter	Yes	Unknown	Unknown	Unknown	Unknown	Unknown
Pathogens	Yes	Yes	Yes	Unknown	Unknown	Yes

Figure 41. IgA-coated bacterial taxa and mechanisms of targeting. A) The IgA repertoire is enriched in natural polyreactive IgA antibodies that can bind multiple self and bacterial antigens with low affinity. Individual antibodies can react against lipopolysaccharides (LPS), capsular polysaccharides, flagellin, DNA, and other antigens, and may target multiple surface antigens in vivo. **B)** Summary of bacterial taxa that are targeted by IgA in vivo and the humoral mechanisms that lead to their coating, as determined by IgA-seq. The requirements for IgA targeting are based on Ig-seq studies of *Tcrb*$^{-/-}$*d*$^{-/-}$, *CD4-cre Bcl-6f*$^{fl/fl}$, or *Aicda*$^{-/-}$ mice lacking T cells, Tfh, or SHM and CSR, respectively. Properties of coating antibodies are based on polyreactivity ELISAs and Ig-seq using individual mAbs.

A minor fraction of murine naive B cell precursors express polyreactive specificities and can recognize microbiota in their germline configuration (*3*). These polyreactive cells recirculate and are preferentially induced to divide in MALT such as the PPs, where they upregulate expression of the chemokine receptor CCR6 and downregulate IgD (Figure 42) (*3, 35*). CCR6 signaling directs their migration to the PP subepithelial dome (SED), where they receive TGFβ1 signals via interactions with $CD11c^{+}CD11b^{+}$ and $CD11c^{+}CD11b^{-}CD8^{-}$ DCs (*35*). This cellular pathway initiates IgA CSR in $CCR6^{+}$ cells via a mechanism that requires DC expression of integrin αvβ8, which binds to latency-associated peptide (LAP) and liberates active TGFβ1 (Figure 42) (*35*). After receiving signals in the SED, B cells downregulate CCR6 and migrate back to the PP follicle where they continue differentiation. After splenic cell transfer, virtually all dividing B cells in the PPs express CCR6 and thus this population likely contains cells that differentiate via both TI and TD pathways, although CCR6-deficient mice show more profound TD defects (*3, 35*). Of note, the relevance of this pathway in vivo has only been demonstrated in PPs; by contrast, mLN IgA responses are largely unaffected by CCR6-deficiency (*35*) suggesting additional potential contributions of CCR6-independent pathways.

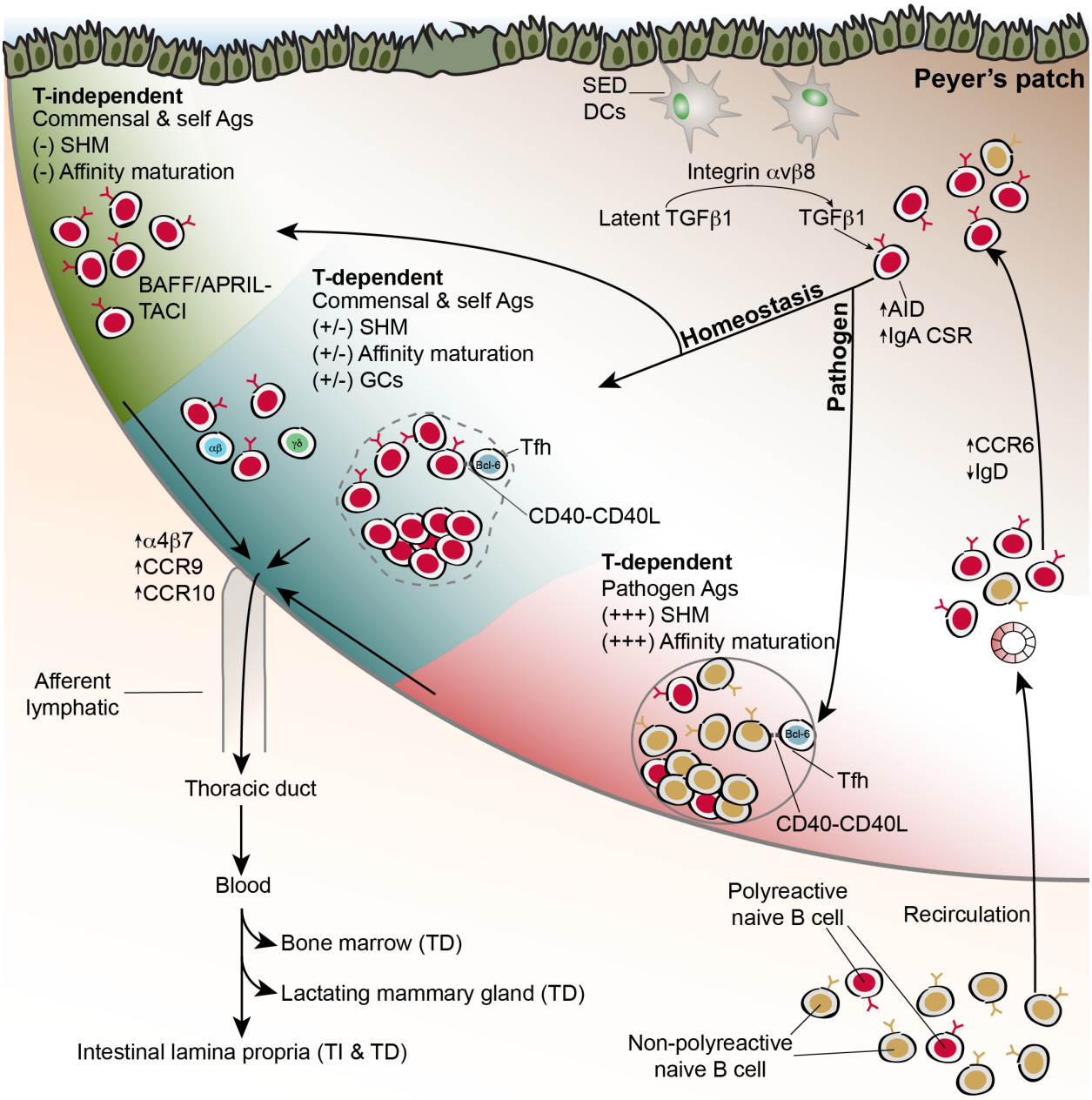

Figure 42. Mechanisms of IgA selection in Peyer's patches. Natural polyreactive antibodies arise at low frequencies in the naïve B cell repertoire and recirculate through secondary lymphoid organs including MALT such as PPs. Upon reaching PPs, polyreactive cells are preferentially induced to divide in a manner that may involve reactivity with self-antigens. Upregulation of CCR6 drives migration to the subepithelial dome (SED), where cells receive TGFβ1 signals that induce IgA CSR via a mechanism that requires SED DC activation of latent TGFβ1 through the integrin αvβ8. After initiating CSR, B cells migrate back to the follicle where they can differentiate through either TD or TI pathways. During homeostasis, polyreactive and microbiota-reactive specificities differentiate via either a TI pathway lacking SHM or affinity maturation, or a TD pathway that accumulates SHM but shows little affinity maturation and may include both GC and extrafollicular contributions. This contrasts with TD responses to

Figure 42, continued. pathogens that are typically non-polyreactive and show extensive SHM and affinity maturation in GCs. TNF-superfamily receptor-ligand interactions contribute to both TD (CD40-CD40L) and TI (BAFF/APRIL-TACI) pathways. Cells are imprinted for gut homing by induced upregulation of integrin $\alpha4\beta7$ and the chemokine receptors CCR9 and CCR10. Lymphoblasts leave the PPs via lymphatics and transit through the thoracic duct to reenter blood circulation, which facilitates their migration to mucosal effector sites such as the intestinal LP, BM, or LMG.

SHM and affinity maturation of the homeostatic IgA response in PP and mLN GCs may also differ significantly from systemic responses. Analysis of SHM distribution and of T cell-deficient mice indicates that the SI IgA^+ PC repertoire is a mixture of TI and TD specificities: in young mice and humans, ~75% of PCs are mutated and likely of TD origin, and the frequency of TD specificities increases with age (*3, 133, 166*). However, while MALT GCs are clearly dependent on T cells, affinity maturation to antigens from the microbiota has not been demonstrated (*4, 11, 71, 167*). B cells lacking a BCR but expressing the constitutively active BCR surrogate LMP2A form GCs in MALT but not extraintestinal lymphoid tissues (*71*), suggesting that GC B cell differentiation can occur in the absence of cognate antigen. Moreover, careful analysis of SHM patterns in PP GC cells suggest random mutation driven by DNA sequence-intrinsic AID hotspots rather than affinity-driven selection (*134*). Further, the amino acid replacement to silent mutation ratio in IgA PCs is approximately 2:1, also suggestive of random SHM in the absence of selection (*3*). Many mutated IgA mAbs are polyreactive, and this reactivity is typically retained upon reversion of mutations to germline (*3*). Additionally, analyses of mice lacking T cells, CD40, or GCs show largely normal IgA coating of microbiota, with the exception of a handful of rare and atypical commensals (*4, 168, 169*). Perhaps the exceptionally diverse antigen burden in MALT tissues and the scarcity of T cell help for non-protein antigens precludes affinity maturation and instead selects for polyreactivity. Thus,

although both TI and TD responses contribute to the homeostatic IgA repertoire, clear differences in specificity between these responses have not been documented. By contrast, IgA affinity maturation in PPs in response to vaccination or mucosal pathogens is well documented and may be mechanistically distinct from homeostatic responses (Figure 42) (*170*).

Although homeostatic TD and TI responses do not show major differences in specificity, T cells do influence IgA responses through other mechanisms. Notably, T cell-deficient mice show a significant decrease in intestinal IgA^+ PC abundance and a near complete lack of IgA^+ PCs in extraintestinal tissues (*3, 4, 11*). As noted previously, a significant population of SI IgA^+ PCs can differentiate in the absence of microbiota or dietary antigens; however, these IgAs are largely unmutated (*3, 166*). While $CCR6^+$ dividing cells are detectable in GF PPs, GCs are largely absent (*63*). Indeed, T cell-intrinsic sensing of microbial signals through TLRs via the universal adaptor protein myeloid differentiation primary response 88 (MyD88) may be necessary to initiate TD IgA responses (*63*). This pathway likely involves MyD88 signaling in both Tfh and forkhead box $P3^+$ ($FoxP3^+$) T follicular regulatory (Tfr) cells (*63, 171*). The origins and specificity of mucosal Tfh/Tfr remain poorly understood, and different studies have suggested that these cells may differentiate from either naïve $CD4^+$ T cells, Th17 cells, or T regulatory cells (*5, 172, 173*). Further, it remains unclear to what extent the interactions between MALT Tfh/Tfr and GC B cells depend on cognate antigen recognition. While high-affinity cognate recognition by Tfh is necessary to support affinity maturation in response to pathogens, the observation that IgA PCs show few signs of affinity maturation suggests that other mechanisms may operate in MALT during homeostasis. For example, these could involve low-affinity interactions with self-reactive T cells, sequential recognition by different T cell clones with distinct specificities due to

internalization and presentation of diverse protein and non-protein antigens by polyreactive BCRs, and/or cytokine-driven interactions. Although the extent to which Tfh specificity influences the IgA repertoire remains unclear, other T cell factors such as PD-1 can negatively regulate TD IgA responses (*42*). In summary, these observations support a model in which T cell-intrinsic sensing of microbiota promotes GC formation, which increases the magnitude of IgA responses, facilitates migration of extraintestinal IgAs, and randomly diversifies the IgA repertoire.

IgA-seq and the identification of IgA-coated microbiota

The commensal bacteria bound by IgA in vivo can be studied using bacterial flow cytometry of microbiota taken directly ex vivo and stained with anti-IgA detection reagents. Early studies of human and murine microbiota revealed that only a fraction of commensal bacteria are coated with IgA in vivo (*7, 13, 14*). Recently, new insights have emerged from the combination of bacterial flow cytometry with high-throughput 16S gene amplicon (16S) sequencing, termed IgA-seq. This technique allows relatively unbiased profiling of the complete repertoire of IgA-bound or -unbound bacteria in vivo. Several laboratories have independently developed variants of IgA-seq and these studies have universally revealed that, despite the frequent polyreactivity of IgA antibodies, a taxonomically distinct subset of microbiota is coated with IgA antibodies in mice and humans in vivo (*3-6, 16, 59, 63, 116, 141, 174*). By contrast, most microbes can become IgA-coated in monocolonized gnotobiotic mice (*175*), likely representing an artifact of monocolonization. Additionally, while some studies have suggested that IgA antibodies may interact with bacteria in a fragment antigen-binding (Fab)-independent manner via glycans on SC (*76*), such interactions have not been demonstrated in vivo and the patterns of polyclonal IgA

binding to microbiota have been largely confirmed by analysis of IgA-derived mAbs expressed with a human IgG1 constant region (*3*). Together, these observations suggest that IgA coats a particular subset of microbiota in vivo via interactions that are predominantly Fab-dependent.

The human gut microbiota exhibits substantial inter-individual variation (*176*). Murine microbiota is relatively stable in animals that are co-housed, but can differ significantly in mice with distinct environmental histories or between animal facilities (*177*). Moreover, substrains within a species can show considerable variation that is not typically resolved in 16S sequencing analyses (*178*). Thus, some caution is warranted in comparing and generalizing IgA-targeted bacteria identified in different studies in mice and/or humans. We now consider the bacterial taxa bound by IgA in vivo and the humoral mechanisms that regulate their targeting (Figure 41B).

Several studies have described substantial enrichment of multiple taxa of the phylum Proteobacteria within the IgA^+ fraction (*3, 4, 16, 116*). Although these organisms are relatively rare in the colon, they are often abundant in the SI, and this may explain the high frequency of IgA^+ bacteria typically observed in the SI lumen (*4, 13, 14*). Indeed, fecal IgA^+ bacteria preferentially colonize the SI upon transfer to GF recipients (*4*). Additionally, intestinal Proteobacteria may influence the abundance of BM IgA^+ PCs and serum IgA (*16*). Proteobacteria are targeted by both TI and TD IgA antibodies in vivo, but their recognition usually does not require SHM or T cells (*3, 4*). Moreover, individual antibodies typically bind multiple distinct Proteobacterial taxa. Polyreactive antibodies of various origins are frequently reactive to Proteobacteria and often bind these taxa in their germline configuration; as such,

Proteobacteria-reactive antibodies can arise naturally in the SI of GF or GF/AF mice. Whether IgA binding to Proteobacteria represents active expression of microbial factors that attract these antibodies or widespread binding of polyreactive specificities remains unclear; however, individual bacterial strains typically lose their reactivity to these antibodies upon culture in vitro and regain their binding after reintroduction in vivo, suggesting that antibody binding can be modulated under different growth or environmental conditions (*3*) and (JJ Bunker, unpublished observation).

IgA responses to several atypical commensals seem to uniquely require TD responses. Of these, segmented filamentous bacteria (SFB) is prototypical and is known to inhabit an unusual niche in close proximity to the ileal epithelium, where it potently stimulates IgA production as well as $CD4^+$ Th17 cell differentiation (*118, 179*). SFB induces PP GC hyperplasia, tertiary lymphoid structure formation in the LP, and substantial quantities of both SFB-reactive and SFB-non-reactive IgA (*24, 118, 180*). SFB is highly coated with IgA in both SPF and monocolonized mice (*4, 6, 181*). Studies of AID-deficient mice that lack SHM have noted PP and ILF hyperplasia in response to SFB outgrowth, though these phenotypes have not been observed in all studies (*4, 32, 182, 183*). While IgA coating of SFB is lost in T cell-deficient mice, the extent to which this response involves specific, high-affinity antibodies remains unclear, as SFB Ig-coating is unaltered in mice lacking AID (*Aicda*$^{-/-}$) or GCs (*CD4-cre Bcl-6*$^{fl/fl}$) (*4*), and polyreactive IgA mAbs that cross-react with both SFB and Proteobacterial taxa in vivo have been observed (*3*). Thus, SFB IgA coating apparently occurs via a non-canonical mechanism that is dependent upon T cells but neither GCs nor SHM.

In addition to SFB, several additional taxa seem to selectively elicit TD responses. These include *Mucispirillum* spp., *Prevotella* spp., and *Helicobacter flexispira* (*4, 6*). Similar to SFB, these bacteria seem to inhabit unconventional niches in close proximity to the intestinal epithelium (*6, 72*). While the precise humoral mechanisms that regulate the targeting of these taxa are not known, IgA coating of *Mucispirillum*, as with SFB, apparently requires T cells but neither SHM nor GCs (*4*).

Many taxa in the microbiota are not bound by IgA antibodies in vivo (*4, 6*). These include most members of the phyla Bacteroidetes and Firmicutes, which are typically abundant in the colon. It remains unclear why these bacteria are not targeted by IgA antibodies. However, it seems that polyreactive antibodies, which commonly cross react with IgA-targeted taxa, do not bind most Bacteroidetes and Firmicutes in vivo (*3*). This may be due to active expression of factors that prevent polyreactive antibody binding or may relate to intrinsic properties of bacterial cell surface molecules that preclude antibody binding, among other possibilities.

A number of other bacterial taxa are coated with IgA in vivo. While most Firmicutes are not bound by IgA antibodies, coating of Lactobacilli and some but not all Clostridial species have been observed (*4, 116*). *Akkermansia mucinophila*, a member of the phylum Verrucomicrobia, is highly enriched in the IgA^+ fraction in humans (*4, 116*). Additional taxa are likely to be identified in further studies of diverse microbiota. Moreover, as we discuss later, some pathogens or opportunistic commensals may elicit strong IgA responses in the context of inflammation or dysbiosis (*6, 59*).

Bone marrow and lactating mammary gland IgA

While the SI is the predominant site of IgA synthesis, IgA^+ PCs are also found in a number of extraintestinal tissues including the bone marrow (BM) and lactating mammary gland (LMG). BM IgA^+ PCs are presumably the source of most serum IgA antibodies, and the specificity of these antibodies has been analyzed by staining fecal bacteria with serum followed by IgA-seq (*16, 141*). These experiments have revealed that serum IgA antibodies typically react against a similar subset of microbiota to that targeted by intestinal IgA. Notably, serum IgAs bind prominently to Proteobacterial taxa, and the relative abundance of these microbes in the gut may influence the magnitude of the BM IgA^+ PC response (*3, 16*). Analysis of mAbs cloned from BM IgAs indicates that these include many polyreactive specificities that bind Proteobacterial taxa (*3*). However, in contrast to the intestinal IgA repertoire, virtually all BM IgAs arise via TD responses (*3, 16*), perhaps because T cell-derived signals are required for induction of molecules such as integrin $\alpha4\beta1$ and chemokine receptors such as CXCR4 that facilitate migration and homing to the BM (*184*).

Although few IgA^+ PCs are found in the mammary gland of nonpregnant females, there is a dramatic accumulation of these cells during pregnancy and postpartum lactation that wanes after lactation ceases (Figure 43) (*185*). These cells presumably secrete the IgAs that are found at high titers in breast milk (*52*). As intestinal IgA^+ PCs do not appear in young mice until 3-4 weeks of age (*186*), breast milk IgAs ostensibly serve to coat the intestinal microbiota of neonatal mice. Indeed, the LMG and SI IgA repertoires are highly similar within individual mice, implying a common origin (*133*). Analysis of mAbs cloned from LMG IgAs further suggests that these antibodies resemble intestinal IgAs, with frequent polyreactivity and binding to various

microbial taxa including many Proteobacteria (*3*). Similar to BM IgAs, differentiation of LMG IgAs is predominantly TD and microbiota-dependent (*3*). Migration of IgA^+ PCs to the LMG is dependent upon CCR10 and glandular expression of its ligand CCL28 (*187*).

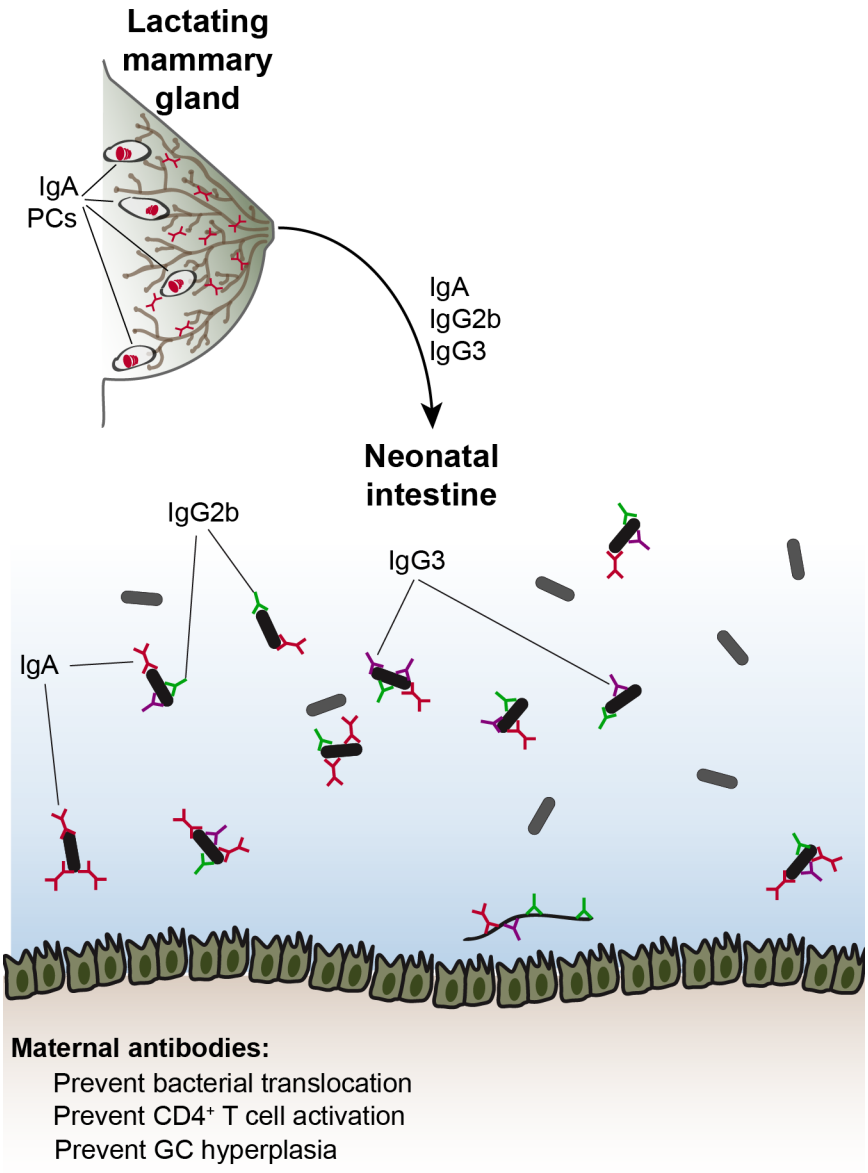

Figure 43. Maternal antibodies impact neonatal microbiota and immunity. During postpartum lactation, IgA, IgG2b, and IgG3 antibodies are transferred to neonates via breast milk. These antibodies coat the neonatal microbiota and restrain the differentiation of $CD44^+$ effector T cells, GCs, and IgA^+ PCs in the mucosa, perhaps by preventing bacterial translocation.

IgM and IgG responses to microbiota

In addition to IgA antibodies, a variety of studies have demonstrated that IgM and IgG antibodies can also react against microbiota. There are virtually no detectable PCs expressing IgM or IgG in the murine intestine, however IgM^+ and IgG^+ PCs are readily detectable in the human gut (*4, 104, 188*). IgM and IgG coating of microbiota is observable in humans but not mice, and these antibodies coat a similar subset of microbiota to that bound by IgA (*188, 189*). IgM also coats a subset of microbiota in bony fish that predominantly express mucosal IgT (*9*). While intestinal IgG^+ and IgM^+ PCs remain poorly characterized, their similar specificity to IgAs suggests these cells may all derive from similar precursors. It remains unclear why these cells do not undergo IgA CSR; however, the fact that they are present in humans but not mice may suggest that they differentiate during transient periods of inflammation during which IgA CSR is impaired by the presence of inflammatory cytokines.

While IgM^+ and IgG^+ PCs are not detectable in the murine intestine, staining of microbiota with murine serum indicates that homeostatic IgM and IgG antibodies can bind microbiota (*141, 190*). Systemic IgGs that react to microbiota are further enriched under conditions that select for self-reactive and polyreactive antibodies, such as certain genetic deficiencies that alter central tolerance or anti-HIV responses (*99, 191, 192*). In mice, homeostatic serum antibodies of the IgG2b and IgG3 isotypes are commonly reactive to microbiota and bind a similar subset to that coated with IgA; IgG1 antibodies also bind a smaller subset (*141*). IgG2b and IgG3 antibodies arise via a TI mechanism that is dependent upon signaling through TLR2 and TLR4. IgG2b and IgG3-expressing precursors are detectable at low frequencies in MALT and may derive from B1

cells. These antibodies commonly bind intestinal Proteobacteria and can limit their translocation to extraintestinal tissues under both steady-state and inflammatory conditions (*190*). Interestingly, IgG2b and IgG3 antibodies are transmitted to neonates in breast milk and coat the neonatal microbiota (Figure 43) (*141*). These antibodies may also influence the metabolites found in breast milk by an unknown mechanism, and consequently modulate neonatal intestinal ILC3 and macrophage differentiation indirectly (*140*). Mice born to mothers lacking IgG2b and IgG3 show increased effector $CD4^+$ T cell differentiation in MALT and GC hyperplasia, suggesting that these antibodies limit neonatal T cell responses (*141*). The precise mechanisms by which these antibodies affect microbiota and/or neonatal immunity remain unknown.

IgA memory

Pharmacological depletion of intestinal IgA^+ PCs leads to rapid recall of similar specificities, suggesting that IgA^+ memory B cells differentiate under homeostatic conditions (*166*), although expansion of residual PCs may also explain this observation. However, IgA responses to microbiota appear to generate an atypical memory response that differs from the classical prime-boost effect observed upon systemic immunization. Studies utilizing a "reversible" GF system involving transient colonization with an auxotrophic strain of *Escherichia coli* suggest that repeated commensal exposure results in an additive, rather than exponential, increase in IgA titers (*142*). These titers can persist for long periods in GF mice after *E. coli* exposure but are rapidly lost upon colonization with a complex microbiota. Repeated rounds of memory B cell reactivation, each resulting in low levels of random SHM, may explain the observation that the IgA repertoire accumulates SHM with little affinity maturation (*133*). Together, these studies

suggest that IgA memory cells arise under normal conditions but turn over rapidly and exhibit reduced expansion upon reactivation relative to systemic memory cells.

The cellular phenotype of IgA memory cells in MALT remains poorly defined. Memory cells are likely contained within the $IgD^{-}CCR6^{+}$ population in PPs, though this population may be heterogenous (*35*). In response to mucosal vaccination, an $\alpha4\beta7^{+}CD73^{+}PD\text{-}L2^{+}CD80^{+}$ memory population was identified (*193*). In humans, a $CD19^{+}CD27^{+}IgA^{+}$ memory population is identifiable in blood, though the relation of these cells to intestinal responses remains unclear (*194*). Further studies detailing the phenotypic and functional properties of IgA^{+} memory cells are warranted.

Functions of antibodies that bind microbiota

Functional consequences of IgA binding to microbiota are commonly invoked but remain poorly understood, and few if any definite functions have been demonstrated in vivo under homeostatic conditions with an intact microbiota. Assigning precise functions to IgA antibodies has been complicated by a lack of genetic models that are truly deficient in secretory antibody production. As mentioned previously, mice lacking pIgR display only partial loss of IgA secretion (*51*). Mice bearing a disrupted Igμ constant region (μMT) are widely used as models of B cell deficiency, yet these mice produce largely normal titers of intestinal IgA (*195*). Mice with a deletion in the Ig heavy chain J locus ($J_H^{-/-}$) lack all B cells but, due to the critical role for these cells in lymphoid organogenesis, lack most MALT and thus display numerous B cell-extrinsic deficiencies (*196*). Mice that lack IgA via disruption of the Igα constant region or deletion of AID produce a compensatory IgM response that targets the same commensal bacteria normally

coated with IgA (*4*). Of note, IgA deficiency is one of the most common human immunodeficiencies, ranging from 1:400 to 1:3000 in various populations (*55*). Similar to IgA-deficient mice, a compensatory mucosal IgM responses arises in these patients (*197-199*). Consistent with this observation, these patients generally have few clinical symptoms. However, IgA-deficient patients do show moderately enhanced susceptibility to a variety of pathologies including recurrent respiratory infections, celiac disease, and autoimmunity (*55*). In summary, genetic analyses in mice and humans have generally failed to highlight a clear functional role for homeostatic IgA antibodies.

Although its functions remain elusive, the magnitude of the IgA response and the strong evolutionary pressure to secrete mucosal antibodies both suggest functional relevance. It is possible that IgA antibodies may have either beneficial or deleterious effects on IgA-targeted microbes, yet the constitutive presence of IgA-coated commensals suggests that any detrimental effects are not generally sufficient to drive extinction. Indeed, IgA binding to capsular polysaccharides may be exploited by some microbiota species in order to form clusters anchored to the mucus layer, thereby securing a niche from invasion by competing species (Figure 44) (*200*). A number of studies have suggested possible functions for these antibodies that may or may not play a role in vivo in the context of homeostatic interactions with the microbiota (Figure 44).

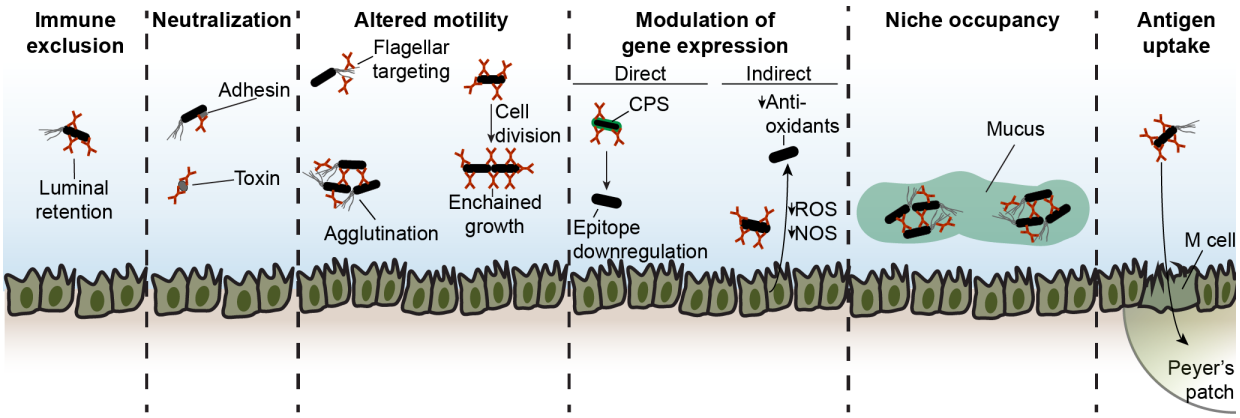

Figure 44. Potential functions of IgA antibodies. Numerous potential functions for IgA antibodies have been suggested that may or may not play a role in vivo in the context of homeostatic interactions with the commensal microbiota. These include immune exclusion, neutralization, altered motility, modulation of gene expression, niche occupancy, and enhanced antigen uptake.

The protective functions of IgG and IgM antibodies typically involve opsonization and complement recruitment or binding to fragment crystallizable (Fc) receptors (*201*). However, IgA is a poor stimulator of the classical complement pathway compared to other isotypes (*202*). An IgA Fc receptor, FcαRI, is present in humans, primates, and several other mammals but absent in mice (*203*). Ligation of this receptor can lead to either activating or inhibitory effects, depending on the monomeric or dimeric nature of the IgA stimulus (*139*). FcαRI is expressed by neutrophils, eosinophils, monocytes, and macrophages that are largely absent during homeostasis but can infiltrate the gut during inflammation (*203*). These observations suggest that Fc receptors and complement are unlikely to play a functional role during normal homeostasis with microbiota but may be relevant in inflammatory contexts.

One function of IgA may be immune exclusion of its targets, in which antibody binding retains antigen in the intestinal lumen until it is digested or eliminated and thereby precludes priming of other immune responses. This function has been demonstrated in the context of model antigens

and specific monoclonal IgA antibodies (*144*), but its relevance in vivo in the context of IgA-targeted microbiota remains untested. A second possible function is neutralization of bacterial surface antigens, such as adhesins or pili, that promote invasion and pathogenesis. While this has been demonstrated in the context of enteric pathogens (*145*), it remains unknown whether this mechanism is relevant to homeostasis with commensal microbes. Notably, B cells are required to prevent translocation of commensal bacteria to the mLN upon microbiota colonization of GF mice, although the mechanisms of protection remain undefined (*22*).

IgA binding may restrict bacterial motility through several possible mechanisms, whose relevance in vivo in the context of microbiota and natural microbiota-reactive IgA remains unclear. Studies of monoclonal IgA antibodies specific for the pathogen *Shigella flexneri* have suggested that IgA can entrap bacteria within the mucus layer overlaying the intestinal epithelium (*204*). Additionally, IgA may agglutinate pathogens and facilitate their clearance (*205*). IgA antibodies generated after oral vaccination with inactivated *Salmonella* Typhimurium were shown to enchain daughter cells of dividing bacteria and accelerate their clearance (*143*). IgA may also limit motility by binding bacterial flagellins: while specific IgA recognition of commensal flagellins has not been demonstrated, many polyreactive IgAs bind flagellin with low affinity (*3, 58*). In vitro studies of high-affinity mAbs to flagellin have demonstrated that these can limit bacterial motility (*58*). Further, increases in flagellar gene expression are observable in the microbiota of mice lacking the flagellin innate immune sensor TLR5, and a role for IgA in this process has been suggested (*58*).

Another possible function may involve direct or indirect modulation of microbial gene expression. This is supported by studies of IgA hybridomas isolated from mice monocolonized with *Bacteroides thetaiotaomicron* and subsequently administered to *B. thetaiotaomicron*-monocolonized *Rag1*$^{-/-}$ mice, which lack IgA (*57, 131*). In direct modulation, IgA binding results in changes in bacterial gene expression. For example, one IgA mAb against a capsular polysaccharide antigen downregulated epitope expression and reduced bacterial fitness relative to an epitope-deficient strain (*57*). A second mAb against an LPS O-antigen polysaccharide did not modulate antigen expression or microbial fitness, suggesting that this property may be variable (*131*). In indirect modulation, IgA binding may alter gene expression by epithelial or other cells, which in turn secrete factors that alter bacterial gene expression. Monocolonization of *Rag1*$^{-/-}$ mice with *B. thetaiotaomicron* leads to upregulation of reactive oxygen and nitrogen species synthesis in the intestinal epithelium and concomitant upregulation of bacterial antioxidant enzymes; these phenotypes were abrogated in the presence of IgA monoclonal antibody (*57*). This system is reductionist but informative; however, *B. thetaiotaomicron* is not a major target of IgA antibodies in vivo and thus it remains unclear whether these principles apply to naturally-arising IgAs in the context of an intact microbiota.

Homeostatic IgA antibodies may also play distinct functional roles in specific physiological contexts. The Proteobacteria-reactive serum IgA response that arises under normal homeostatic conditions appears to be protective against polymicrobial sepsis after intestinal injury (*16*); the mechanisms by which IgA is protective in this model remain unknown. Further, as mentioned previously, maternal antibodies transmitted in breast milk seem to attenuate intestinal immune activation in neonates (Figure 37). Mice born to B cell-deficient mothers show exaggerated

intestinal IgA responses early in life, perhaps as a result of increased commensal translocation to the mLN (*52, 186*). Maternal IgA may also influence the composition of the neonatal microbiota via unknown mechanisms (*52*). Additionally, maternal IgA may play a partially redundant role together with IgG2b and IgG3 antibodies to limit neonatal TD responses (*141*). Lastly, IgA binding to intestinal antigens may facilitate their uptake through epithelial microfold (M) cells and enhance priming of further responses (Figure 44) (*102*).

IgA antibodies can confer protective immunity in response to mucosal pathogens in a variety of additional contexts that have been reviewed extensively elsewhere (*206, 207*). Cholera toxin has been well-studied and induces a TD response that protects via neutralization (*208*). In vitro studies suggest that IgA can bind toxins in the intestinal LP and facilitate their excretion (*209*). Additionally, IgA antibodies against the HIV Envelope were strongly correlated with protection in the RV144 HIV vaccine trial (*210*). While preexisting polyreactive IgA antibodies were shown to provide early protection against *Salmonella* Typhimurium (*103*), in the vast majority of infections the relationship between protective responses and pre-existing homeostatic IgA remains unknown. In many cases, protective responses to pathogens are likely to proceed via cellular pathways that more closely resemble systemic immunity than the homeostatic IgA response; careful studies of the pre- and post-immune repertoires and cellular processes involved should shed light on these mechanisms.

Antibodies to microbiota in inflammatory bowel diseases

Mucosal antibody responses are exaggerated in inflammatory bowel diseases (IBD) including Crohn's disease and ulcerative colitis, which involve a complex interplay between host genetics,

environmental factors, and microbiota composition (*211*). Increased coating of fecal microbiota with IgA, IgG, and IgM has been observed in both human IBD and mouse models (*6, 189, 212*). IgM^+ and IgG^+ PCs accumulate in the inflamed gut and may exacerbate inflammation, though their specificity and contributions to pathology remains poorly understood (*213, 214*). IBD patients also show elevated serum IgA that reacts against flagellin and various autoantigens; whether this represents induction of specific antibodies or expansion of polyreactive specificities remains unknown (*112, 113, 215*). Mouse models of colitis induced by T cell-transfer into lymphopenic recipients suggest that B cells can protect against pathology (*216*), though the mechanisms of protection and their contributions in human IBD remain unclear. Recently, several studies have suggested that IgA coating can identify disease-associated members of the microbiota in IBD or IBD-associated spondyloarthritis (*6, 212*). These studies have generally focused on single microbes or somewhat arbitrary consortia without performing systematic analysis of both IgA^+ and IgA^- bacteria. Given the extensive IgA coating of microbiota found under normal healthy conditions, it is unlikely that all IgA-targeted microbes in IBD patients are colitogenic. A more likely scenario is that bona fide pathogens elicit IgA responses and are present alongside a wide variety of non-pathogenic commensals in the IgA^+ fraction. Therefore, IgA-seq in combination with other assays may be required for more reliable discrimination between pathogens and commensals.

Outlook and Future Directions

Two distinct types of humoral immunity coexist in the intestinal mucosa (Figure 42). The predominant pathway is intrinsically polyreactive and low affinity, largely independent of T cells and somatic mutations, and bears features of germline-encoded innate immunity; this response

seems mostly involved in homeostatic interactions that may benefit both the host and microbes. The other pathway exhibits classical features of T cell dependent, hypermutated and affinity-matured adaptive responses and is predominantly triggered by pathogens. How these radically different responses are integrated to protect the host while preserving the symbiotic relationship with complex microbiota is a major direction of future research. From an immunological viewpoint, the generation of polyreactive antibodies raises fundamental issues about self tolerance, the mechanisms of recognition, and the protection afforded in various conditions including against rapidly mutating viruses (*108, 109*). From a microbiological perspective, major questions remain regarding the molecular targets of IgA, the consequences of antibody binding on microbes, and the microbial mechanisms that lead to either attraction or evasion of antibodies. Thus, many important aspects remain to be explored, and their answers may provide wide-ranging insights from evolutionary aspects of immunity and commensalism, to new strategies to manipulate the host or microbiota in order to prevent, treat, or cure enteric pathologies.

BIBLIOGRAPHY

1. K. Honda, D. R. Littman, The microbiota in adaptive immune homeostasis and disease. *Nature* **535**, 75-84 (2016).

2. S. Fagarasan, S. Kawamoto, O. Kanagawa, K. Suzuki, Adaptive immune regulation in the gut: T cell-dependent and T cell-independent IgA synthesis. *Annu Rev Immunol* **28**, 243-273 (2010).

3. J. J. Bunker *et al.*, Natural polyreactive IgA antibodies coat the intestinal microbiota. *Science* **358**, (2017).

4. J. J. Bunker *et al.*, Innate and Adaptive Humoral Responses Coat Distinct Commensal Bacteria with Immunoglobulin A. *Immunity* **43**, 541-553 (2015).

5. S. Kawamoto *et al.*, Foxp3(+) T cells regulate immunoglobulin a selection and facilitate diversification of bacterial species responsible for immune homeostasis. *Immunity* **41**, 152-165 (2014).

6. N. W. Palm *et al.*, Immunoglobulin A coating identifies colitogenic bacteria in inflammatory bowel disease. *Cell* **158**, 1000-1010 (2014).

7. L. A. van der Waaij, P. C. Limburg, G. Mesander, D. van der Waaij, In vivo IgA coating of anaerobic bacteria in human faeces. *Gut* **38**, 348-354 (1996).

8. M. F. Flajnik, M. Kasahara, Origin and evolution of the adaptive immune system: genetic events and selective pressures. *Nat Rev Genet* **11**, 47-59 (2010).

9. Y. A. Zhang *et al.*, IgT, a primitive immunoglobulin class specialized in mucosal immunity. *Nat Immunol* **11**, 827-835 (2010).

10. R. Mussmann, L. Du Pasquier, E. Hsu, Is Xenopus IgX an analog of IgA? *Eur J Immunol* **26**, 2823-2830 (1996).

11. A. J. Macpherson *et al.*, A primitive T cell-independent mechanism of intestinal mucosal IgA responses to commensal bacteria. *Science* **288**, 2222-2226 (2000).

12. B. He *et al.*, Intestinal bacteria trigger T cell-independent immunoglobulin A(2) class switching by inducing epithelial-cell secretion of the cytokine APRIL. *Immunity* **26**, 812-826 (2007).

13. F. G. Kroese, R. de Waard, N. A. Bos, B-1 cells and their reactivity with the murine intestinal microflora. *Semin Immunol* **8**, 11-18 (1996).

14. T. Tsuruta *et al.*, The amount of secreted IgA may not determine the secretory IgA coating ratio of gastrointestinal bacteria. *FEMS Immunol Med Microbiol* **56**, 185-189 (2009).

15. L. Moro-Sibilot *et al.*, Mouse and Human Liver Contain Immunoglobulin A-Secreting Cells Originating From Peyer's Patches and Directed Against Intestinal Antigens. *Gastroenterology* **151**, 311-323 (2016).

16. J. R. Wilmore *et al.*, Commensal Microbes Induce Serum IgA Responses that Protect against Polymicrobial Sepsis. *Cell Host Microbe*, (2018).

17. S. W. Craig, J. J. Cebra, Peyer's patches: an enriched source of precursors for IgA-producing immunocytes in the rabbit. *J Exp Med* **134**, 188-200 (1971).

18. H. Hamada *et al.*, Identification of multiple isolated lymphoid follicles on the antimesenteric wall of the mouse small intestine. *J Immunol* **168**, 57-64 (2002).

19. K. Masahata *et al.*, Generation of colonic IgA-secreting cells in the caecal patch. *Nat Commun* **5**, 3704 (2014).

20. M. McWilliams, J. M. Phillips-Quagliata, M. E. Lamm, Mesenteric lymph node B lymphoblasts which home to the small intestine are precommitted to IgA synthesis. *J Exp Med* **145**, 866-875 (1977).

21. M. Tsuji *et al.*, Requirement for lymphoid tissue-inducer cells in isolated follicle formation and T cell-independent immunoglobulin A generation in the gut. *Immunity* **29**, 261-271 (2008).

22. A. J. Macpherson, T. Uhr, Induction of protective IgA by intestinal dendritic cells carrying commensal bacteria. *Science* **303**, 1662-1665 (2004).

23. S. Fagarasan, K. Kinoshita, M. Muramatsu, K. Ikuta, T. Honjo, In situ class switching and differentiation to IgA-producing cells in the gut lamina propria. *Nature* **413**, 639-643 (2001).

24. E. Lecuyer *et al.*, Segmented filamentous bacterium uses secondary and tertiary lymphoid tissues to induce gut IgA and specific T helper 17 cell responses. *Immunity* **40**, 608-620 (2014).

25. M. Yamamoto *et al.*, Alternate mucosal immune system: organized Peyer's patches are not required for IgA responses in the gastrointestinal tract. *J Immunol* **164**, 5184-5191 (2000).

26. H. S. Kang *et al.*, Signaling via LTbetaR on the lamina propria stromal cells of the gut is required for IgA production. *Nat Immunol* **3**, 576-582 (2002).

27. A. A. Kruglov *et al.*, Nonredundant function of soluble LTalpha3 produced by innate lymphoid cells in intestinal homeostasis. *Science* **342**, 1243-1246 (2013).

28. A. Cerutti, The regulation of IgA class switching. *Nat Rev Immunol* **8**, 421-434 (2008).

29. C. S. Kaetzel, The polymeric immunoglobulin receptor: bridging innate and adaptive immune responses at mucosal surfaces. *Immunol Rev* **206**, 83-99 (2005).

30. A. Phalipon, B. Corthesy, Novel functions of the polymeric Ig receptor: well beyond transport of immunoglobulins. *Trends Immunol* **24**, 55-58 (2003).

31. P. Tuma, A. L. Hubbard, Transcytosis: crossing cellular barriers. *Physiol Rev* **83**, 871-932 (2003).

32. S. Fagarasan *et al.*, Critical roles of activation-induced cytidine deaminase in the homeostasis of gut flora. *Science* **298**, 1424-1427 (2002).

33. M. B. Litinskiy *et al.*, DCs induce CD40-independent immunoglobulin class switching through BLyS and APRIL. *Nat Immunol* **3**, 822-829 (2002).

34. B. B. Cazac, J. Roes, TGF-beta receptor controls B cell responsiveness and induction of IgA in vivo. *Immunity* **13**, 443-451 (2000).

35. A. Reboldi *et al.*, IgA production requires B cell interaction with subepithelial dendritic cells in Peyer's patches. *Science* **352**, aaf4822 (2016).

36. K. Watanabe *et al.*, Requirement for Runx proteins in IgA class switching acting downstream of TGF-beta 1 and retinoic acid signaling. *J Immunol* **184**, 2785-2792 (2010).

37. K. Suzuki *et al.*, The sensing of environmental stimuli by follicular dendritic cells promotes immunoglobulin A generation in the gut. *Immunity* **33**, 71-83 (2010).

38. H. Tezuka *et al.*, Prominent role for plasmacytoid dendritic cells in mucosal T cell-independent IgA induction. *Immunity* **34**, 247-257 (2011).

39. J. R. Mora *et al.*, Generation of gut-homing IgA-secreting B cells by intestinal dendritic cells. *Science* **314**, 1157-1160 (2006).

40. E. J. Kunkel *et al.*, CCR10 expression is a common feature of circulating and mucosal epithelial tissue IgA Ab-secreting cells. *J Clin Invest* **111**, 1001-1010 (2003).

41. C. A. Mattioli, T. B. Tomasi, Jr., The life span of IgA plasma cells from the mouse intestine. *J Exp Med* **138**, 452-460 (1973).

42. S. Kawamoto *et al.*, The inhibitory receptor PD-1 regulates IgA selection and bacterial composition in the gut. *Science* **336**, 485-489 (2012).

43. O. J. Landsverk *et al.*, Antibody-secreting plasma cells persist for decades in human intestine. *J Exp Med* **214**, 309-317 (2017).

44. V. T. Chu *et al.*, Eosinophils promote generation and maintenance of immunoglobulin-A-expressing plasma cells and contribute to gut immune homeostasis. *Immunity* **40**, 582-593 (2014).

45. E. K. Ng *et al.*, Human intestinal epithelial and smooth muscle cells are potent producers of IL-6. *Mediators Inflamm* **12**, 3-8 (2003).

46. A. J. Ramsay *et al.*, The role of interleukin-6 in mucosal IgA antibody responses in vivo. *Science* **264**, 561-563 (1994).

47. B. Huard *et al.*, APRIL secreted by neutrophils binds to heparan sulfate proteoglycans to create plasma cell niches in human mucosa. *J Clin Invest* **118**, 2887-2895 (2008).

48. R. Di Niro *et al.*, Rapid generation of rotavirus-specific human monoclonal antibodies from small-intestinal mucosa. *J Immunol* **185**, 5377-5383 (2010).

49. M. E. Koshland, The coming of age of the immunoglobulin J chain. *Annu Rev Immunol* **3**, 425-453 (1985).

50. R. Iversen *et al.*, Strong Clonal Relatedness between Serum and Gut IgA despite Different Plasma Cell Origins. *Cell Rep* **20**, 2357-2367 (2017).

51. F. E. Johansen *et al.*, Absence of epithelial immunoglobulin A transport, with increased mucosal leakiness, in polymeric immunoglobulin receptor/secretory component-deficient mice. *J Exp Med* **190**, 915-922 (1999).

52. E. W. Rogier *et al.*, Secretory antibodies in breast milk promote long-term intestinal homeostasis by regulating the gut microbiota and host gene expression. *Proc Natl Acad Sci U S A* **111**, 3074-3079 (2014).

53. C. M. Van Itallie, J. M. Anderson, Claudins and epithelial paracellular transport. *Annu Rev Physiol* **68**, 403-429 (2006).

54. O. Pabst, New concepts in the generation and functions of IgA. *Nat Rev Immunol* **12**, 821-832 (2012).

55. C. Cunningham-Rundles, Physiology of IgA and IgA deficiency. *J Clin Immunol* **21**, 303-309 (2001).

56. C. Moon *et al.*, Vertically transmitted faecal IgA levels determine extra-chromosomal phenotypic variation. *Nature*, (2015).

57. D. A. Peterson, N. P. McNulty, J. L. Guruge, J. I. Gordon, IgA response to symbiotic bacteria as a mediator of gut homeostasis. *Cell Host Microbe* **2**, 328-339 (2007).

58. T. C. Cullender *et al.*, Innate and adaptive immunity interact to quench microbiome flagellar motility in the gut. *Cell host & microbe* **14**, 571-581 (2013).

59. A. L. Kau *et al.*, Functional characterization of IgA-targeted bacterial taxa from undernourished Malawian children that produce diet-dependent enteropathy. *Sci Transl Med* **7**, 276ra224 (2015).

60. T. Tsuruta, R. Inoue, T. Iwanaga, H. Hara, T. Yajima, Development of a method for the identification of S-IgA-coated bacterial composition in mouse and human feces. *Bioscience, biotechnology, and biochemistry* **74**, 968-973 (2010).

61. W. Z. Stephens, J. L. Round, IgA targets the troublemakers. *Cell host & microbe* **16**, 265-267 (2014).

62. E. Slack, M. L. Balmer, J. H. Fritz, S. Hapfelmeier, Functional flexibility of intestinal IgA - broadening the fine line. *Frontiers in immunology* **3**, 100 (2012).

63. J. L. Kubinak *et al.*, MyD88 signaling in T cells directs IgA-mediated control of the microbiota to promote health. *Cell Host Microbe* **17**, 153-163 (2015).

64. N. Baumgarth, The double life of a B-1 cell: self-reactivity selects for protective effector functions. *Nat Rev Immunol* **11**, 34-46 (2011).

65. F. G. Kroese *et al.*, Many of the IgA producing plasma cells in murine gut are derived from self-replenishing precursors in the peritoneal cavity. *International immunology* **1**, 75-84 (1989).

66. M. C. Thurnheer, A. W. Zuercher, J. J. Cebra, N. A. Bos, B1 cells contribute to serum IgM, but not to intestinal IgA, production in gnotobiotic Ig allotype chimeric mice. *Journal of immunology* **170**, 4564-4571 (2003).

67. B. Roy *et al.*, An intrinsic propensity of murine peritoneal B1b cells to switch to IgA in presence of TGF-beta and retinoic acid. *PLoS One* **8**, e82121 (2013).

68. K. R. Alugupalli *et al.*, B1b lymphocytes confer T cell-independent long-lasting immunity. *Immunity* **21**, 379-390 (2004).

69. C. Gil-Cruz *et al.*, The porin OmpD from nontyphoidal Salmonella is a key target for a protective B1b cell antibody response. *Proceedings of the National Academy of Sciences of the United States of America* **106**, 9803-9808 (2009).

70. K. M. Haas, J. C. Poe, D. A. Steeber, T. F. Tedder, B-1a and B-1b cells exhibit distinct developmental requirements and have unique functional roles in innate and adaptive immunity to S. pneumoniae. *Immunity* **23**, 7-18 (2005).

71. S. Casola *et al.*, B cell receptor signal strength determines B cell fate. *Nat Immunol* **5**, 317-327 (2004).

72. B. R. Robertson *et al.*, Mucispirillum schaedleri gen. nov., sp. nov., a spiral-shaped bacterium colonizing the mucus layer of the gastrointestinal tract of laboratory rodents. *Int J Syst Evol Microbiol* **55**, 1199-1204 (2005).

73. K. Hollister *et al.*, Insights into the role of Bcl6 in follicular Th cells using a new conditional mutant mouse model. *Journal of immunology* **191**, 3705-3711 (2013).

74. R. Mathew *et al.*, A negative feedback loop mediated by the Bcl6-cullin 3 complex limits Tfh cell differentiation. *The Journal of experimental medicine* **211**, 1137-1151 (2014).

75. J. Mestecky, *Mucosal immunology*. (Elsevier Academic Press, Amsterdam ; Boston, ed. 3rd, 2005).

76. A. Mathias, B. Corthesy, Recognition of gram-positive intestinal bacteria by hybridoma- and colostrum-derived secretory immunoglobulin A is mediated by carbohydrates. *J Biol Chem* **286**, 17239-17247 (2011).

77. J. G. Caporaso *et al.*, QIIME allows analysis of high-throughput community sequencing data. *Nat Methods* **7**, 335-336 (2010).

78. F. Meyer *et al.*, The metagenomics RAST server - a public resource for the automatic phylogenetic and functional analysis of metagenomes. *BMC Bioinformatics* **9**, 386 (2008).

79. S. T. Bates *et al.*, Examining the global distribution of dominant archaeal populations in soil. *ISME J* **5**, 908-917 (2011).

80. J. G. Caporaso *et al.*, Global patterns of 16S rRNA diversity at a depth of millions of sequences per sample. *Proc Natl Acad Sci* **108**, 4516-4522 (2011).

81. J. G. Caporaso *et al.*, Ultra-high-throughput microbial community analysis on the Illumina HiSeq and MiSeq platforms. *ISME J* **6**, 1621-1624 (2012).

82. J. Zhang, K. Kobert, T. Flouri, A. Stamatakis, PEAR: a fast and accurate Illumina Paired-End reAd mergeR. *Bioinformatics* **30**, 614-620 (2014).

83. J. G. Caporaso *et al.*, PyNAST: a flexible tool for aligning sequences to a template alignment. *Bioinformatics* **26**, 266-267 (2010).

84. R. C. Edgar, Search and clustering orders of magnitude faster than BLAST. *Bioinformatics* **26**, 2460-2461 (2010).

85. D. McDonald *et al.*, An improved Greengenes taxonomy with explicit ranks for ecological and evolutionary analyses of bacteria and archaea. *ISME J* **6**, 610-618 (2012).

86. M. Hamady, C. Lozupone, R. Knight, Fast UniFrac: facilitating high-throughput phylogenetic analyses of microbial communities including analysis of pyrosequencing and PhyloChip data. *ISME J* **4**, 17-27 (2009).

87. C. Lozupone, M. E. Lladser, D. Knights, J. Stombaugh, R. Knight, UniFrac: an effective distance metric for microbial community comparison. *ISME J* **5**, 169-172 (2011).

88. C. A. Lozupone, M. Hamady, S. T. Kelley, R. Knight, Quantitative and qualitative β diversity measures lead to different insights into factors that structure microbial communities. *Appl Environ Microbiol* **73**, 1576-1585 (2007).

89. T. Tiller, C. E. Busse, H. Wardemann, Cloning and expression of murine Ig genes from single B cells. *J Immunol Methods* **350**, 183-193 (2009).

90. K. Smith *et al.*, Rapid generation of fully human monoclonal antibodies specific to a vaccinating antigen. *Nat Protoc* **4**, 372-384 (2009).

91. T. Tiller *et al.*, Efficient generation of monoclonal antibodies from single human B cells by single cell RT-PCR and expression vector cloning. *J Immunol Methods* **329**, 112-124 (2008).

92. H. Wardemann *et al.*, Predominant autoantibody production by early human B cell precursors. *Science* **301**, 1374-1377 (2003).

93. D. Corti *et al.*, A neutralizing antibody selected from plasma cells that binds to group 1 and group 2 influenza A hemagglutinins. *Science* **333**, 850-856 (2011).

94. C. J. Henry Dunand *et al.*, Both Neutralizing and Non-Neutralizing Human H7N9 Influenza Vaccine-Induced Monoclonal Antibodies Confer Protection. *Cell Host Microbe* **19**, 800-813 (2016).

95. M. F. Muellenbeck *et al.*, Atypical and classical memory B cells produce Plasmodium falciparum neutralizing antibodies. *J Exp Med* **210**, 389-399 (2013).

96. J. F. Scheid *et al.*, Broad diversity of neutralizing antibodies isolated from memory B cells in HIV-infected individuals. *Nature* **458**, 636-640 (2009).

97. J. J. Trombetta *et al.*, Preparation of Single-Cell RNA-Seq Libraries for Next Generation Sequencing. *Curr Protoc Mol Biol* **107**, 4 22 21-17 (2014).

98. D. G. Gibson *et al.*, Enzymatic assembly of DNA molecules up to several hundred kilobases. *Nat Methods* **6**, 343-345 (2009).

99. E. Slack *et al.*, Innate and adaptive immunity cooperate flexibly to maintain host-microbiota mutualism. *Science* **325**, 617-620 (2009).

100. J. L. Kubinak, J. L. Round, Do antibodies select a healthy microbiota? *Nat Rev Immunol* **16**, 767-774 (2016).

101. C. P. Quan, A. Berneman, R. Pires, S. Avrameas, J. P. Bouvet, Natural polyreactive secretory immunoglobulin A autoantibodies as a possible barrier to infection in humans. *Infect Immun* **65**, 3997-4004 (1997).

102. F. Fransen *et al.*, BALB/c and C57BL/6 Mice Differ in Polyreactive IgA Abundance, which Impacts the Generation of Antigen-Specific IgA and Microbiota Diversity. *Immunity* **43**, 527-540 (2015).

103. O. L. Wijburg *et al.*, Innate secretory antibodies protect against natural Salmonella typhimurium infection. *J Exp Med* **203**, 21-26 (2006).

104. J. Benckert *et al.*, The majority of intestinal IgA+ and IgG+ plasmablasts in the human gut are antigen-specific. *J Clin Invest* **121**, 1946-1955 (2011).

105. M. Shimoda, Y. Inoue, N. Azuma, C. Kanno, Natural polyreactive immunoglobulin A antibodies produced in mouse Peyer's patches. *Immunology* **97**, 9-17 (1999).

106. I. Y. Ho *et al.*, Refined protocol for generating monoclonal antibodies from single human and murine B cells. *J Immunol Methods* **438**, 67-70 (2016).

107. H. Mouquet, M. C. Nussenzweig, Polyreactive antibodies in adaptive immune responses to viruses. *Cell Mol Life Sci* **69**, 1435-1445 (2012).

108. S. F. Andrews *et al.*, Immune history profoundly affects broadly protective B cell responses to influenza. *Sci Transl Med* **7**, 316ra192 (2015).

109. H. Mouquet *et al.*, Polyreactivity increases the apparent affinity of anti-HIV antibodies by heteroligation. *Nature* **467**, 591-595 (2010).

110. A. L. Notkins, Polyreactivity of antibody molecules. *Trends Immunol* **25**, 174-179 (2004).

111. Y. Cong, T. Feng, K. Fujihashi, T. R. Schoeb, C. O. Elson, A dominant, coordinated T regulatory cell-IgA response to the intestinal microbiota. *Proc Natl Acad Sci U S A* **106**, 19256-19261 (2009).

112. M. J. Lodes *et al.*, Bacterial flagellin is a dominant antigen in Crohn disease. *J Clin Invest* **113**, 1296-1306 (2004).

113. S. V. Sitaraman *et al.*, Elevated flagellin-specific immunoglobulins in Crohn's disease. *Am J Physiol Gastrointest Liver Physiol* **288**, G403-406 (2005).

114. E. Lullau *et al.*, Antigen binding properties of purified immunoglobulin A and reconstituted secretory immunoglobulin A antibodies. *J Biol Chem* **271**, 16300-16309 (1996).

115. G. Sigounas, N. Harindranath, G. Donadel, A. L. Notkins, Half-life of polyreactive antibodies. *J Clin Immunol* **14**, 134-140 (1994).

116. J. D. Planer *et al.*, Development of the gut microbiota and mucosal IgA responses in twins and gnotobiotic mice. *Nature* **534**, 263-266 (2016).

117. J. Mirpuri *et al.*, Proteobacteria-specific IgA regulates maturation of the intestinal microbiota. *Gut Microbes* **5**, 28-39 (2014).

118. H. L. Klaasen *et al.*, Apathogenic, intestinal, segmented, filamentous bacteria stimulate the mucosal immune system of mice. *Infect Immun* **61**, 303-306 (1993).

119. K. Atarashi *et al.*, Th17 Cell Induction by Adhesion of Microbes to Intestinal Epithelial Cells. *Cell* **163**, 367-380 (2015).

120. C. M. Krinos *et al.*, Extensive surface diversity of a commensal microorganism by multiple DNA inversions. *Nature* **414**, 555-558 (2001).

121. J. C. Lee, S. Takeda, P. J. Livolsi, L. C. Paoletti, Effects of in vitro and in vivo growth conditions on expression of type 8 capsular polysaccharide by Staphylococcus aureus. *Infect Immun* **61**, 1853-1858 (1993).

122. S. Lebeer *et al.*, Identification of a Gene Cluster for the Biosynthesis of a Long, Galactose-Rich Exopolysaccharide in Lactobacillus rhamnosus GG and Functional Analysis of the Priming Glycosyltransferase. *Appl Environ Microbiol* **75**, 3554-3563 (2009).

123. S. M. Logan, Flagellar glycosylation - a new component of the motility repertoire? *Microbiology* **152**, 1249-1262 (2006).

124. I. Gryllos *et al.*, Induction of group A Streptococcus virulence by a human antimicrobial peptide. *Proc Natl Acad Sci U S A* **105**, 16755-16760 (2008).

125. N. Kamada *et al.*, Regulated virulence controls the ability of a pathogen to compete with the gut microbiota. *Science* **336**, 1325-1329 (2012).

126. B. D. Needham, M. S. Trent, Fortifying the barrier: the impact of lipid A remodelling on bacterial pathogenesis. *Nat Rev Microbiol* **11**, 467-481 (2013).

127. M. J. Coyne, B. Reinap, M. M. Lee, L. E. Comstock, Human symbionts use a host-like pathway for surface fucosylation. *Science* **307**, 1778-1781 (2005).

128. S. van Houte, A. Buckling, E. R. Westra, Evolutionary Ecology of Prokaryotic Immune Mechanisms. *Microbiol Mol Biol Rev* **80**, 745-763 (2016).

129. S. Lebeer, J. Vanderleyden, S. C. De Keersmaecker, Host interactions of probiotic bacterial surface molecules: comparison with commensals and pathogens. *Nat Rev Microbiol* **8**, 171-184 (2010).

130. S. R. Stowell *et al.*, Microbial glycan microarrays define key features of host-microbial interactions. *Nat Chem Biol* **10**, 470-476 (2014).

131. D. A. Peterson *et al.*, Characterizing the interactions between a naturally primed immunoglobulin A and its conserved Bacteroides thetaiotaomicron species-specific epitope in gnotobiotic mice. *J Biol Chem* **290**, 12630-12649 (2015).

132. T. Tiller *et al.*, Autoreactivity in human IgG+ memory B cells. *Immunity* **26**, 205-213 (2007).

133. C. Lindner *et al.*, Diversification of memory B cells drives the continuous adaptation of secretory antibodies to gut microbiota. *Nat Immunol* **16**, 880-888 (2015).

134. L. S. Yeap *et al.*, Sequence-Intrinsic Mechanisms that Target AID Mutational Outcomes on Antibody Genes. *Cell* **163**, 1124-1137 (2015).

135. J. Mestecky, *Mucosal immunology*. (Elsevier/AP, Academic Press is an imprint of Elsevier, Amsterdam, ed. Fourth edition., 2015), pp. volumes.

136. K. S. Kim *et al.*, Dietary antigens limit mucosal immunity by inducing regulatory T cells in the small intestine. *Science* **351**, 858-863 (2016).

137. J. R. Pleasants, M. H. Johnson, B. S. Wostmann, Adequacy of chemically defined, water-soluble diet for germfree BALB/c mice through successive generations and litters. *J Nutr* **116**, 1949-1964 (1986).

138. A. E. Reynolds, M. Kuraoka, G. Kelsoe, Natural IgM is produced by CD5- plasma cells that occupy a distinct survival niche in bone marrow. *J Immunol* **194**, 231-242 (2015).

139. B. Pasquier *et al.*, Identification of FcalphaRI as an inhibitory receptor that controls inflammation: dual role of FcRgamma ITAM. *Immunity* **22**, 31-42 (2005).

140. M. Gomez de Aguero *et al.*, The maternal microbiota drives early postnatal innate immune development. *Science* **351**, 1296-1302 (2016).

141. M. A. Koch *et al.*, Maternal IgG and IgA Antibodies Dampen Mucosal T Helper Cell Responses in Early Life. *Cell* **165**, 827-841 (2016).

142. S. Hapfelmeier *et al.*, Reversible microbial colonization of germ-free mice reveals the dynamics of IgA immune responses. *Science* **328**, 1705-1709 (2010).

143. K. Moor *et al.*, High-avidity IgA protects the intestine by enchaining growing bacteria. *Nature* **544**, 498-502 (2017).

144. C. R. Stokes, J. F. Soothill, M. W. Turner, Immune exclusion is a function of IgA. *Nature* **255**, 745-746 (1975).

145. R. C. Williams, R. J. Gibbons, Inhibition of bacterial adherence by secretory immunoglobulin A: a mechanism of antigen disposal. *Science* **177**, 697-699 (1972).

146. Y. Ichiyoshi, P. Casali, Analysis of the structural correlates for antibody polyreactivity by multiple reassortments of chimeric human immunoglobulin heavy and light chain V segments. *J Exp Med* **180**, 885-895 (1994).

147. H. Wardemann, J. Hammersen, M. C. Nussenzweig, Human autoantibody silencing by immunoglobulin light chains. *J Exp Med* **200**, 191-199 (2004).

148. C. Martinoli, A. Chiavelli, M. Rescigno, Entry route of Salmonella typhimurium directs the type of induced immune response. *Immunity* **27**, 975-984 (2007).

149. V. J. Craig *et al.*, Gastric MALT lymphoma B cells express polyreactive, somatically mutated immunoglobulins. *Blood* **115**, 581-591 (2010).

150. I. Isnardi *et al.*, IRAK-4- and MyD88-dependent pathways are essential for the removal of developing autoreactive B cells in humans. *Immunity* **29**, 746-757 (2008).

151. S. Yurasov *et al.*, Defective B cell tolerance checkpoints in systemic lupus erythematosus. *J Exp Med* **201**, 703-711 (2005).

152. J. F. Scheid *et al.*, Sequence and structural convergence of broad and potent HIV antibodies that mimic CD4 binding. *Science* **333**, 1633-1637 (2011).

153. B. F. Haynes *et al.*, Cardiolipin polyspecific autoreactivity in two broadly neutralizing HIV-1 antibodies. *Science* **308**, 1906-1908 (2005).

154. X. Brochet, M. P. Lefranc, V. Giudicelli, IMGT/V-QUEST: the highly customized and integrated system for IG and TR standardized V-J and V-D-J sequence analysis. *Nucleic Acids Res* **36**, W503-508 (2008).

155. V. Giudicelli, X. Brochet, M. P. Lefranc, IMGT/V-QUEST: IMGT standardized analysis of the immunoglobulin (IG) and T cell receptor (TR) nucleotide sequences. *Cold Spring Harb Protoc* **2011**, 695-715 (2011).

156. Q. Wang, G. M. Garrity, J. M. Tiedje, J. R. Cole, Naive Bayesian classifier for rapid assignment of rRNA sequences into the new bacterial taxonomy. *Appl Environ Microbiol* **73**, 5261-5267 (2007).

157. W. Walters *et al.*, Improved Bacterial 16S rRNA Gene (V4 and V4-5) and Fungal Internal Transcribed Spacer Marker Gene Primers for Microbial Community Surveys. *mSystems* **1**, (2016).

158. J. G. Caporaso *et al.*, Ultra-high-throughput microbial community analysis on the Illumina HiSeq and MiSeq platforms. *ISME J* **6**, 1621-1624 (2012).

159. J. G. Caporaso *et al.*, QIIME allows analysis of high-throughput community sequencing data. *Nat Methods* **7**, 335-336 (2010).

160. J. Zhang, K. Kobert, T. Flouri, A. Stamatakis, PEAR: a fast and accurate Illumina Paired-End reAd mergeR. *Bioinformatics* **30**, 614-620 (2014).

161. J. G. Caporaso *et al.*, PyNAST: a flexible tool for aligning sequences to a template alignment. *Bioinformatics* **26**, 266-267 (2010).

162. R. C. Edgar, Search and clustering orders of magnitude faster than BLAST. *Bioinformatics* **26**, 2460-2461 (2010).

163. D. McDonald *et al.*, An improved Greengenes taxonomy with explicit ranks for ecological and evolutionary analyses of bacteria and archaea. *ISME J* **6**, 610-618 (2012).

164. J. L. Mendoza *et al.*, The IFN-lambda-IFN-lambdaR1-IL-10Rbeta Complex Reveals Structural Features Underlying Type III IFN Functional Plasticity. *Immunity* **46**, 379-392 (2017).

165. G. D. Victora, M. C. Nussenzweig, Germinal centers. *Annu Rev Immunol* **30**, 429-457 (2012).

166. C. Lindner *et al.*, Age, microbiota, and T cells shape diverse individual IgA repertoires in the intestine. *J Exp Med* **209**, 365-377 (2012).

167. D. Guy-Grand, C. Griscelli, P. Vassalli, Peyer's patches, gut IgA plasma cells and thymic function: study in nude mice bearing thymic grafts. *J Immunol* **115**, 361-364 (1975).

168. P. Bergqvist, E. Gardby, A. Stensson, M. Bemark, N. Y. Lycke, Gut IgA class switch recombination in the absence of CD40 does not occur in the lamina propria and is independent of germinal centers. *J Immunol* **177**, 7772-7783 (2006).

169. P. Bergqvist, A. Stensson, N. Y. Lycke, M. Bemark, T cell-independent IgA class switch recombination is restricted to the GALT and occurs prior to manifest germinal center formation. *J Immunol* **184**, 3545-3553 (2010).

170. P. Bergqvist *et al.*, Re-utilization of germinal centers in multiple Peyer's patches results in highly synchronized, oligoclonal, and affinity-matured gut IgA responses. *Mucosal Immunol* **6**, 122-135 (2013).

171. S. Wang *et al.*, MyD88 Adaptor-Dependent Microbial Sensing by Regulatory T Cells Promotes Mucosal Tolerance and Enforces Commensalism. *Immunity* **43**, 289-303 (2015).

172. K. Hirota *et al.*, Plasticity of Th17 cells in Peyer's patches is responsible for the induction of T cell-dependent IgA responses. *Nat Immunol* **14**, 372-379 (2013).

173. M. Tsuji *et al.*, Preferential generation of follicular B helper T cells from Foxp3+ T cells in gut Peyer's patches. *Science* **323**, 1488-1492 (2009).

174. M. Dzidic *et al.*, Aberrant IgA responses to the gut microbiota during infancy precede asthma and allergy development. *J Allergy Clin Immunol* **139**, 1017-1025 e1014 (2017).

175. N. Geva-Zatorsky *et al.*, Mining the Human Gut Microbiota for Immunomodulatory Organisms. *Cell* **168**, 928-943 e911 (2017).

176. M. Arumugam *et al.*, Enterotypes of the human gut microbiome. *Nature* **473**, 174-180 (2011).

177. T. S. Stappenbeck, H. W. Virgin, Accounting for reciprocal host-microbiome interactions in experimental science. *Nature* **534**, 191-199 (2016).

178. S. Greenblum, R. Carr, E. Borenstein, Extensive strain-level copy-number variation across human gut microbiome species. *Cell* **160**, 583-594 (2015).

179. Ivanov, II *et al.*, Induction of intestinal Th17 cells by segmented filamentous bacteria. *Cell* **139**, 485-498 (2009).

180. G. L. Talham, H. Q. Jiang, N. A. Bos, J. J. Cebra, Segmented filamentous bacteria are potent stimuli of a physiologically normal state of the murine gut mucosal immune system. *Infect Immun* **67**, 1992-2000 (1999).

181. H. Q. Jiang, N. A. Bos, J. J. Cebra, Timing, localization, and persistence of colonization by segmented filamentous bacteria in the neonatal mouse gut depend on immune status of mothers and pups. *Infect Immun* **69**, 3611-3617 (2001).

182. K. Suzuki *et al.*, Aberrant expansion of segmented filamentous bacteria in IgA-deficient gut. *Proc Natl Acad Sci U S A* **101**, 1981-1986 (2004).

183. M. Wei *et al.*, Mice carrying a knock-in mutation of Aicda resulting in a defect in somatic hypermutation have impaired gut homeostasis and compromised mucosal defense. *Nat Immunol* **12**, 264-270 (2011).

184. J. R. Mora, U. H. von Andrian, Differentiation and homing of IgA-secreting cells. *Mucosal Immunol* **1**, 96-109 (2008).

185. P. Weisz-Carrington, M. E. Roux, M. E. Lamm, Plasma cells and epithelial immunoglobulins in the mouse mammary gland during pregnancy and lactation. *J Immunol* **119**, 1306-1307 (1977).

186. N. L. Harris *et al.*, Mechanisms of neonatal mucosal antibody protection. *J Immunol* **177**, 6256-6262 (2006).

187. E. Wilson, E. C. Butcher, CCL28 controls immunoglobulin (Ig)A plasma cell accumulation in the lactating mammary gland and IgA antibody transfer to the neonate. *J Exp Med* **200**, 805-809 (2004).

188. G. Magri *et al.*, Human Secretory IgM Emerges from Plasma Cells Clonally Related to Gut Memory B Cells and Targets Highly Diverse Commensals. *Immunity* **47**, 118-134 e118 (2017).

189. L. A. van der Waaij *et al.*, Immunoglobulin coating of faecal bacteria in inflammatory bowel disease. *Eur J Gastroenterol Hepatol* **16**, 669-674 (2004).

190. M. Y. Zeng *et al.*, Gut Microbiota-Induced Immunoglobulin G Controls Systemic Infection by Symbiotic Bacteria and Pathogens. *Immunity* **44**, 647-658 (2016).

191. J. N. Schickel *et al.*, Self-reactive VH4-34-expressing IgG B cells recognize commensal bacteria. *J Exp Med* **214**, 1991-2003 (2017).

192. W. B. Williams *et al.*, HIV-1 VACCINES. Diversion of HIV-1 vaccine-induced immunity by gp41-microbiota cross-reactive antibodies. *Science* **349**, aab1253 (2015).

193. M. Bemark *et al.*, Limited clonal relatedness between gut IgA plasma cells and memory B cells after oral immunization. *Nat Commun* **7**, 12698 (2016).

194. J. Prigent *et al.*, Scarcity of autoreactive human blood IgA(+) memory B cells. *Eur J Immunol* **46**, 2340-2351 (2016).

195. A. J. Macpherson *et al.*, IgA production without mu or delta chain expression in developing B cells. *Nat Immunol* **2**, 625-631 (2001).

196. T. V. Golovkina, M. Shlomchik, L. Hannum, A. Chervonsky, Organogenic role of B lymphocytes in mucosal immunity. *Science* **286**, 1965-1968 (1999).

197. M. D. Barros, M. H. Porto, P. G. Leser, A. S. Grumach, M. M. Carneiro-Sampaio, Study of colostrum of a patient with selective IgA deficiency. *Allergol Immunopathol (Madr)* **13**, 331-334 (1985).

198. T. Klemola, Immunohistochemical findings in the intestine of IgA-deficient persons: number of intraepithelial T lymphocytes is increased. *J Pediatr Gastroenterol Nutr* **7**, 537-543 (1988).

199. J. Fadlallah *et al.*, Microbial ecology perturbation in human IgA deficiency. *Sci Transl Med* **10**, (2018).

200. G. P. Donaldson *et al.*, Gut microbiota utilize immunoglobulin A for mucosal colonization. *Science*, (2018).

201. J. V. Ravetch, J. P. Kinet, Fc receptors. *Annu Rev Immunol* **9**, 457-492 (1991).

202. K. Murphy, C. Weaver, *Janeway's immunobiology*. (Garland Science/Taylor & Francis Group, LLC, New York, NY, ed. 9th edition., 2016), pp. xx, 904 pages.

203. J. E. Bakema, M. van Egmond, The human immunoglobulin A Fc receptor FcalphaRI: a multifaceted regulator of mucosal immunity. *Mucosal Immunol* **4**, 612-624 (2011).

204. S. Boullier *et al.*, Secretory IgA-mediated neutralization of Shigella flexneri prevents intestinal tissue destruction by down-regulating inflammatory circuits. *J Immunol* **183**, 5879-5885 (2009).

205. A. P. Hendrickx *et al.*, Antibiotic-Driven Dysbiosis Mediates Intraluminal Agglutination and Alternative Segregation of Enterococcus faecium from the Intestinal Epithelium. *MBio* **6**, e01346-01315 (2015).

206. N. Lycke, Recent progress in mucosal vaccine development: potential and limitations. *Nat Rev Immunol* **12**, 592-605 (2012).

207. A. J. Macpherson, L. Hunziker, K. McCoy, A. Lamarre, IgA responses in the intestinal mucosa against pathogenic and non-pathogenic microorganisms. *Microbes Infect* **3**, 1021-1035 (2001).

208. C. E. Hornquist, L. Ekman, K. D. Grdic, K. Schon, N. Y. Lycke, Paradoxical IgA immunity in CD4-deficient mice. Lack of cholera toxin-specific protective immunity despite normal gut mucosal IgA differentiation. *J Immunol* **155**, 2877-2887 (1995).

209. M. I. Fernandez *et al.*, Anti-inflammatory role for intracellular dimeric immunoglobulin a by neutralization of lipopolysaccharide in epithelial cells. *Immunity* **18**, 739-749 (2003).

210. B. F. Haynes *et al.*, Immune-correlates analysis of an HIV-1 vaccine efficacy trial. *N Engl J Med* **366**, 1275-1286 (2012).

211. S. R. Dalal, E. B. Chang, The microbial basis of inflammatory bowel diseases. *J Clin Invest* **124**, 4190-4196 (2014).

212. M. Viladomiu *et al.*, IgA-coated E. coli enriched in Crohn's disease spondyloarthritis promote TH17-dependent inflammation. *Sci Transl Med* **9**, (2017).

213. T. Kanai *et al.*, TH1/TH2-mediated colitis induced by adoptive transfer of CD4+CD45RBhigh T lymphocytes into nude mice. *Inflamm Bowel Dis* **12**, 89-99 (2006).

214. M. Uo *et al.*, Mucosal CXCR4+ IgG plasma cells contribute to the pathogenesis of human ulcerative colitis through FcgammaR-mediated CD14 macrophage activation. *Gut* **62**, 1734-1744 (2013).

215. C. J. Landers *et al.*, Selected loss of tolerance evidenced by Crohn's disease-associated immune responses to auto- and microbial antigens. *Gastroenterology* **123**, 689-699 (2002).

216. A. J. Gerth, L. Lin, M. F. Neurath, L. H. Glimcher, S. L. Peng, An innate cell-mediated, murine ulcerative colitis-like syndrome in the absence of nuclear factor of activated T cells. *Gastroenterology* **126**, 1115-1121 (2004).